FATE OF NATURAL AND ANTHROPOGENIC PARTICLES IN PEAT BOGS

INAUGURAL – DISSERTATION

Zur
Erlangung der Doktorwürde
der
Naturwissenschaftlich- Mathematischen
Gesamtfakultät
der
Ruprecht-Karls-Universität
Heidelberg

Vorgelegt von

Gaël Le Roux (MSc. Environmental Geosciences)
aus Paris, Frankreich

Tag der mündlichen Prüfung : 09.05.2005

FATE OF NATURAL AND ANTHROPOGENIC PARTICLES IN PEAT BOGS

Gutachter:
Prof. Dr. William Shotyk
Institute of Environmental Geochemistry
Im Neuenheimer Feld 234
D.69120 Heidelberg
Deutschland

HD Dr. Alain Véron
CEREGE-UMR6635
Europôle Med Arbois – BP80
13545 Aix en Provence Cedex 4
Frankreich

“Objectivity cannot be equated with mental blankness; rather, objectivity resides in recognizing your preferences and then subjecting them to especially harsh scrutiny and also in a willingness to revise or abandon your theories when the tests fail (as they usually do).“

Stephen Jay Gould (1941-2002); *The Lying Stones of Marrakech*

-Table of contents-

Table of Contents 1

Abstract 3

Zusammenfassung 5

Résumé 7

Introduction and Objectives ***9***

1.Introduction and background ***9***

2.Objectives ***16***

3.Results ***17***

4.Studied sites ***19***

PART 1: Sampling and Analytical Techniques 27

1.1 Suggested protocol for collecting, handling and preparing peat cores and peat samples for physical, chemical, mineralogical and isotopic analyses ***29***

1.2 Accurate and precise Pb isotope ratio measurements in environmental samples by MC-ICP-MS ***49***

1.3 *Optimising accuracy and precision of lead isotope measurement (^{206}Pb, ^{207}Pb, ^{208}Pb) in acid digests of peat using individual mass discrimination correction* ***65***

PART 2: Investigating Pb atmospheric deposition using peat bogs 79

2.1 Biogeochemistry and cycling of Pb ***81***

2.2 Recent atmospheric Pb deposition at a rural site in Southern Germany assessed using a peat core and snow pack, and comparison with other archives ***111***

2.3 Identifying the sources and timing of ancient and medieval atmospheric lead pollution in England using a peat profile from Lindow bog, Manchester ***125***

PART 3: Fate of minerals in peat bogs **143**

3.1 Alteration of inorganic matter in peat bogs ***145***

3.2 Fate of minerals in the upper part of a peat bog ***159***

Appendixes **169**

A.1 REE compositions of atmospheric deposition entering an ombrotrophic peat bog in Black Forest (SW Germany): evidence from snow, lichens and mosses ***171***

A.2 Accumulation rates and predominant atmospheric sources of natural and anthropogenic Hg and Pb on the Faroe Islands ***177***

A.3 Comparison of atmospheric deposition of copper, nickel, cobalt, zinc and cadmium recorded by peat cores from three ombrotrophic bogs in Finland with monitoring data and emissions records ***195***

A.4 Surface distribution of ^{137}Cs in the Kohlhütte Moor ***213***

A.5 Microbial investigations in the KM bog ***215***

Acknowledgements **217**

-Abstract-

Investigating atmospheric deposition over a scale of millennial period is crucial because humans are emitting more and more synthetic and natural compounds (i.e.: pollutants and/or dust) to the environment through the atmosphere. It is therefore necessary *to determine the background deposition rate of these compounds, to assess their natural variations (ie.: temporal and/or spatial)* and *to understand the effects of the increased atmospheric depositions induced by humans on the environment.*

The primary aim of this work was to improve the understanding of the processes affecting the fate of anthropogenic and natural particles in peat bogs, to see which geochemical processes can affect the suitability and accuracy of peat bogs as archives of atmospheric deposition, and also the effects of these inputs on the bog ecosystem.

To test whether peat bogs are accurate archives of Pb atmospheric deposition, Pb distribution was investigated in Kohlhütte Moor (KM), a bog in Southern Germany. Pb is a toxic element extensively dispersed by human activities **(Chap.2.1)**. The atmospheric Pb record assessed using a peat core was compared with other archives, including a snow pack and previously studied Swiss peat cores **(Chap.2.2)**. To this end, new improved methods both methodically **(Chap.1.1)** and analytically **(Chap.1.2 and Chap.1.3)** were developed. Also particular attention was given to age dating using ^{210}Pb and ^{14}C and the estimation of the Pb accumulation rate (AR) based on these ages. The most recent Pb AR in KM (2.5 mg m^{-2} y^{-1}) is similar to that obtained from the snow pack on the bog surface (1 to 4 mg m^{-2} y^{-1}). The isotopic composition of Pb was measured in both the modern and ancient peat samples as well as in the snow samples, and clearly shows that recent inputs are dominated by anthropogenic Pb. The chronology and isotopic composition of atmospheric Pb accumulation recorded by the peat from the Black Forest is similar to the chronologies reported earlier using peat cores from various Swiss peat bogs and point to *a common Pb source to the region for the past 200 years.* Taken together, the results show that peat cores from ombrotrophic bogs can yield accurate records of atmospheric Pb deposition, provided that the cores are carefully collected, handled, prepared, and analysed using appropriate methods.

In addition, the rates of atmospheric Pb accumulation at least for the last 6000 years were quantified using peat cores from KM and Lindow Bog (LDW), England.

In KM, the most recent Pb accumulation rate (2.5 mg m^{-2} y^{-1}) is 50 to 200 times greater than the "natural" average background rate of atmospheric Pb accumulation (~20 µg m^{-2} y^{-1}) calculated using "pre-anthropogenic" samples from the same site.

The core from LDW **(Chap.2.3)** shows the potential of carefully studying Pb distribution in a peat profile for regional paleo-ecology and archaeology. Using the Pb/Ti ratio to calculate the rates of anthropogenic, atmospheric Pb deposition, the core reveals Pb contamination first appearing in peat samples dating from ca. 900 B.C. which clearly pre-date Roman mining activities. The timing of the ancient and medieval Pb pollution is also directly related to socio-economical events. ^{208}Pb/^{206}Pb and ^{206}Pb/^{207}Pb data indicate that *English ores were the predominant sources for atmospheric deposition in England* during the pre-Roman, Roman, and medieval periods.

To test whether peat bogs are suitable archives of atmospheric deposition of minerals and after a review of the different possible dissolution mechanisms influencing inorganic particles **(Chap.3.1)**, mineral distributions in the upper part of KM were investigated **(Chap.3.2)**. Similar minerals to the local granite were identified using X-Ray-Diffraction: most of the minerals are therefore of local origin. The distribution of quartz and feldspars is unaffected by the low pH and the abundance of organic acids, possibly due to the early formation of a siliceous layer and/or coating by humic acids. Therefore the preservation of quartz and feldspars in ombrotrophic peat might make bogs useful archives of the changing rates of atmospheric dust since the Last Glacial.

In addition, other minerals, calcite and apatite, were identified but only in the topmost samples of the bog. They probably dissolve comparatively quickly and thereby influence the chemistry of the surface of the bog releasing nutrients and therefore influencing the botanical composition of the bog and the rates of plant growth.

-Zusammenfassung-

Die Untersuchung der atmosphärischen Deposition über eine Zeitspanne von 1000 Jahren ist von großer Bedeutung, da der Mensch mehr und mehr synthetische und natürliche Komponenten (z.B. Schadstoffe und/oder Staub) in die Atmosphäre emittiert. Es ist folglich notwendig, die natürliche Belastung sowie ihre zeitliche und räumliche Veränderung festzustellen, und die Auswirkungen der durch den Menschen erhöhten Deposition auf die Umwelt zu verstehen.

Ziel dieser Arbeit war es, tiefere Einblicke in die Prozesse zu erhalten, die den Verbleib der anthropogenen und natürlichen Partikel in ombrotrophen Mooren beeinflussen. Es galt die geochemischen Prozesse herauszufinden, die die Eignung ombrotropher Moore als Archiv der atmosphärischen Einträge beeinflussen können und welche Auswirkungen diese Einträge auf das Moor-Ökosystem haben.

Untersucht wurde das Hochmoor „Kohlhütte" in Süddeutschland. Blei ist ein giftiges Element, das überwiegend durch menschliche Tätigkeiten **(Kap. 2.1)** in die Umwelt gelangt. Der Eintrag atmosphärischen Bleis, der mit Hilfe des Torfkerns rekonstruiert wurde, wurde mit anderen Archiven, einschließlich eines Schneeprofils und zuvor untersuchter Torfkerne aus der Schweiz verglichen **(Kap. 2.2)**. Zu diesem Zweck wurden neue, verbesserte methodische **(Kap. 1.1)** und analytische **(Kap. 1.2 und Kap. 1.3)** Verfahren entwickelt. Ein weiterer Schwerpunkt bildete die Altersbestimmung mittels ^{210}Pb und ^{14}C und die daraus ermittelten Bleidepositionsraten (AR). Die jüngste Blei AR im Kohlhütte Moor (2,5 mg m^{-2} y^{-1}) entsprach den Werten, die in den heutigen Schneeproben auf der Mooroberfläche ermittelt wurden (1 bis 4 mg m^{-2} y^{-1}). Die Bleiisotopen-Verhältnisse wurden in den modernen und älteren Torfproben sowie in den Schneeproben gemessen. Die Ergebnisse zeigten deutlich, dass die aktuellen Einträge durch anthropogenes Blei dominiert werden. Die anhand dieses Hochmoores rekonstruierten Blei-Einträge sowie die jeweiligen Isotopenverhältnisse entsprachen den Ergebnissen der Schweizer Torfkerne. Dies legte den Schluss nahe, dass es im Zeitraum der letzen 200 Jahre eine gemeinsame Bleiquelle gegeben haben muss. Zusammen genommen zeigten die Ergebnisse, dass Torfkerne aus ombrotrophen Mooren die Geschichte der atmosphärischen Bleideposition aufzeichnen können, sofern die Kerne sorgfältig genommen, Proben sorgfältig aufbereitet und geeignete Analysenmethoden ausgewählt wurden. Zusätzlich wurde die Rate der atmosphärischen Bleideposition für mindestens die letzten 6000 Jahre anhand der Torfkerne aus Kohlhütte Moor und Lindow Bog (LDW), England, quantitativ bestimmt.

In Kohlhütte Moor war die aktuelle atmosphärische Bleidepositionsrate (2,5 mg m^{-2} y^{-1}) 50 bis 200 mal größer als die durchschnittliche „natürliche" Hintergrundrate (~ 20 µg m^{-2} y^{-1}), die in tieferen, „vor-anthropogenen" Schichten des Kernes ermittelt wurde. Der Kern aus LDW **(Kap. 2.3)** zeigte, wie wichtig die Untersuchung der Bleiverteilung in einem Torfprofil für die regionale Paläoökologie und Archäologie sein kann. Anhand der Blei – Titan Verhältnisse konnten die Raten des anthropogenen atmosphärischen Blei-eintrags berechnet werden. Die Ergebnisse zeigten, dass eine Bleiverschmutzung erstmalig in den Jahren um 900 B.C. auftrat, also deutlich vor der Römischen Bergbautätigkeit. Diese frühe sowie die mittelalterliche Bleiverschmutzung war auch direkt mit soziologisch-ökonomischen Ereignissen verknüpft. Die ^{208}Pb/^{206}Pb und ^{206}Pb/^{207}Pb Verhältnisse zeigten, dass englische Erze die Hauptquelle für die atmosphärische Bleibelastung in England während der vor-römischen, römischen und mittelalterlichen Perioden waren.

Anhand der Mineralverteilung in den oberen Lagen des Kohlhütte Moores **(Kap. 3.2)** wurde untersucht, ob Hochmoore auch den Eintrag einzelner Mineralpartikel konservieren. Zuvor wurden unterschiedliche Mechanismen beschrieben **(Kap. 3.1)**, die zur Auflösung der abgelagerten anorganischen Partikel geführt haben könnten. Mittels Röntgendiffraktometrie wurden Minerale nachgewiesen, die auch in den lokalen Graniten vorhanden sind; die meisten im Torf vorhandenen Mineralpartikel stammten also aus den Gesteinen der nahen Umgebung. Die vorhandenen Quarze und Feldspäte wurde durch den niedrigen pH Wert und den Einfluss organischer Säuren nicht aufgelöst, eventuell aufgrund der Ausbildung einer schützenden Schicht aus Si-Lagen und/oder Huminsäuren um die einzelnen Partikel. Da die Quarze und Feldspäte im ombrotrophen Moor erhalten bleiben, könnten Torfkerne als Archiv für die veränderten Einträge des atmosphärischen Staubs seit der letzten Eiszeit verwendet werden. Zusätzlich wurde Calcit und Apatit nachgewiesen, jedoch nur in den obersten Lagen des Moores. Vermutlich lösen sie sich vergleichsweise schnell auf und setzen Nährstoffe frei, die die botanische Zusammensetzung des Moores und die Wachstumsgeschwindigkeit der Pflanzen verändern können.

-Résumé-

Savoir reconstruire les flux atmosphériques passés sur des périodes de l'ordre du millénaire est essentiel car les humains émettent de plus en plus de composants synthétiques ou naturels (polluants et/ou poussière) dans l'environnement par l'intermédiaire de l'atmosphère. Il est donc nécessaire *d'évaluer les taux de dépôt atmosphérique naturel de ces composants, d'évaluer leurs variations naturelles (temporelles et/ou spatiales) et de comprendre les effets d'une augmentation des dépôts atmosphériques d'origine humaine.*

L'objectif principal de ce travail est d'améliorer la compréhension des processus affectant les dépôts d'origine anthropique et naturelle dans la tourbe, de voir quels processus géochimiques peuvent affecter la pertinence et la précision des tourbières bombées comme archives des flux atmosphériques, et comment ces apports peuvent influencer l'écosystème de la tourbière.

Pour tester la précision des tourbières bombées en tant qu'archives des flux atmosphériques en plomb, la distribution de celui-ci a été étudiée dans une tourbière bombée du Sud de l´Allemagne : Kohlhütte Moor. Le plomb est un élément toxique largement dispersé par les activités humaines **(Chap.2.1.)** L'histoire des flux de plomb atmosphérique estimés grâce à une carotte de tourbe a été comparée avec d´autres archives, dont un dépôt de neige et des carottes de tourbière déjà étudiées auparavant **(Chap.2.2)**. À cette fin, de nouvelles méthodes techniques **(Chap.1.1)** et analytiques **(Chap.1.2 et Chap.1.3)** ont été développées. Une attention particulière a été donnée aux datations par ^{210}Pb et ^{14}C et l'estimation du taux d'accumulation en plomb. Le plus récent taux d'accumulation en plomb à Kohlhütte Moor (2.5 mg m^{-2} y^{-1}) est identique à celui obtenu à l'aide du dépôt neigeux à la surface de la tourbière (1 à 4 mg m^{-2} y^{-1}). La composition isotopique du plomb mesurée dans des échantillons de tourbe récents et plus âgés et dans la neige montre clairement que les apports récents sont dominés par du plomb d'origine humaine.

La chronologie et la composition isotopique du flux de plomb enregistré par la tourbière de Forêt Noire sont identiques aux chronologies de tourbières suisses et mettent en évidence une source de plomb commune pour la région ces 200 dernières années. Pris ensemble, ces résultats montrent que des carottes de tourbières hautes dites ombrotrophiques peuvent donner des enregistrements des dépôts du plomb atmosphérique à condition d'utiliser des méthodes appropriées d'échantillonnage et d'analyse.

De plus, les taux d'accumulation en plomb pour ces derniers 6000 ans ont été quantifiés avec des carottes de Kohlhütte Moor et de Lindow Bog, en Angleterre. À Kohlhütte Moor, le taux d'accumulation du plomb (2.5 mg m^{-2} y^{-1}) est de 50 à 100 fois plus important que le taux naturel (~20 µg m^{-2} y^{-1}) estimé à l'aide d'échantillons du même site mais plus anciens pré-datant le début de la métallurgie.

Le profile de Lindow Bog **(Chap.2.3)** montre les possibilités offertes par une étude précautionneuse du plomb dans un profile de tourbe pour la paléoécologie et l'archéologie. En utilisant le rapport Pb/Ti pour calculer les taux de dépôt de plomb anthropogénique, la carotte révèle que la contamination au plomb date de 900 B.C. et est donc bien antérieure à l'occupation romaine. La chronologie de la pollution antique et médiévale est aussi directement en relation avec des événements socio-économiques. Les rapports isotopiques ^{208}Pb/^{206}Pb et ^{206}Pb/^{207}Pb indiquent que les minerais anglais sont les sources prédominantes pour les dépôts atmosphériques en plomb durant l'Age du Fer, l'occupation romaine et le Moyen-Âge.

Pour tester si les tourbières peuvent enregistrer le flux de poussière atmosphérique et après une revue des différents mécanismes influençant la dissolution des particules inorganiques **(Chap.3.1)**, la distribution des minéraux dans la partie supérieure de Kohlhütte Moor a été étudiée **(Chap.3.2)**. Des minéraux identiques au granite local ont été identifiés en utilisant la diffraction de rayons X : la plupart des minéraux sont donc d'origine locale. La distribution en profondeur du quartz et feldspaths n'est pas affectée par le faible pH et l'abondance en acides organiques, peut-être due à la formation précoce d´une couche enrichie en silice et/ou d'un enrobage par des acides humiques. Par conséquent, la préservation du quartz et des feldspaths dans les profils de tourbe ombrotophique indique que les tourbières bombées peuvent être des archives du dépôt atmosphérique de poussière depuis la dernière période glaciaire.

De plus, d´autres minéraux, la calcite et l´apatite, ont été identifiés mais seulement dans les échantillons de surface de la tourbière. Probablement s´altèrent-ils comparativement rapidement, influencent la chimie de la surface de la tourbière en relarguant des nutriments et conditionnent la composition botanique de la tourbière et les taux de croissance des plantes.

- Introduction and objectives -

This doctoral dissertation consists of an introduction, a description of the objectives and eight articles (cumulative thesis). The eight articles are in the form of manuscripts, which have either been published, accepted for publication or are in review. The first three papers are methodological papers describing sampling and analytical techniques developed during the PhD of the candidate. Two of these chapters are book chapters reviewing the scientific state of the art on Pb in the environment and on the alteration of particles in peat bogs; those introduce the research articles, which follow.
The appendixes consist of supplement data and two co-authored papers.

1. Introduction and Background

1.1 Environmental Geochemistry // Biogeochemistry

Humans strongly modified their environment since the discovery of fire, the beginning of agriculture and metallurgy and industrialization. They have "an enormous impact on the global movement of chemical material" (Schlesinger, 2004). Hooke (1994; 2000) has even argued that human earthmoving activity is the most volumetrically significant process currently shaping the surface of the Earth.
One major goal of the Geochemistry[1] is to evaluate the magnitude of the fluxes between Earth reservoirs and their fluctuations over relevant time scales (Staudigel et al., 1998). Particularly, Environmental Geochemistry and/or Biogeochemistry use the tools of chemistry to understand environmental, Earth surface processes induced either naturally or from human origin and to estimate natural and anthropogenic fluxes between the different surface reservoirs of the Earth.
Peat bogs are more widely distributed across the globe than glacial ice and, unlike lake sediments, their surface layers are fed solely by atmospheric deposition. Thus peat bogs have the potential to provide detailed records of *atmospheric fluxes*.

In this introduction, peat bogs are first briefly described for their main characteristics. Then it is shown how the studies of peat bog are related to some major questions and challenges for biogeochemistry (Table 1) (Likens, 2004) such as the quantification of the atmospheric fluxes of pollutants or the increasing concentration of CO_2 in the atmosphere.

1.2 What is an ombrotrophic peat bog?

A peat bog is a domed accumulation of peat, which receives all its surface inputs from the atmosphere. That is why it is called ombrotrophic. The different names of bogs in German, French and English are given in Table 2. Most recent reference books about peatlands including bogs are "Moor und Torfkunde" (Göttlich, 1990) and "Moore" (Dierssen and Dierssen, 2001) in German, "Mires" in English, which is the updated English translation of the previously cited book (Heathwaite et al., 1993) and "Le monde des tourbières et des marais" (Manneville et al., 1999) in French.

1.2.1 Development of peat bogs

A bog is often the last stadium of a succession of humid environments (wetlands) concluded by the final invasion by *Sphagnum* mosses.

[1] Geochemistry is the discipline using the tools of chemistry to solve geological problems (Albarède F. (2001) *La Géochimie*. Gordon & Breach Science Publishers.)

1. What are the specific effects and relationships of the increase size of the human population on flux and cycling of elements, and what are the biogeochemical effects of forcing functions often incongruent in space and time associated with these changes?
2. What controls fluxes of N and P to and from natural and human-dominated (cities, agricultural) ecosystems?
3. What is and what controls C sequestration in diverse ecosystems (e.g., forest, ocean, lakes, wetlands) on variable temporal and spatial scales?
4. What controls weathering rates, and what are the fates of weathered products, including nutrient loss in terrestrial ecosystems?
5. What is the qualitative and quantitative role of non-human animals in the flux and cycling of nutrients, and what is the long-term effect of these fluxes (e.g. Guano and other waste products).
6. How do the flux and cycling of antibiotics, steroids, hormones and pharmaceuticals affect element flux and cycling?
7. What is the quantitative linkage between biogeochemistry and species richness, species extinction and invasion of alien species?
8. What are the effects of lags and legacies on current and future biogeochemical fluxes and cycles?
9. What are the quantitative interrelationships between hydrology and biogeochemistry?
10. How can a better synoptic understanding of the biogeochemical flux, cycling and interaction of elements among air, land and water (including oceans) systems be achieved?
11. What are the critical linkages and feedbacks among major nutrient and toxic element fluxes and cycles?
12. What are the potential impacts of bioterrorism on biogeochemical fluxes and cycles, and human welfare that depends on these cycles?

Table 1: Some major questions and challenges for biogeochemistry (Likens, 2004). In bold are questions related to bog studies.

The typical development of a mountainous bog is show in Figure 1. As it is later shown in the paragraph describing specifically the peat bogs studied in this work, variations of this development could occur. This is especially the case in the Southern Black Forest where climatic conditions favoured peat bog development on different types of landscapes after the retreat of the local glacier (Lang et al., 1984). It must be emphasized that the peat profile in a bog not only represents its last stadium where all its inputs are coming from the atmosphere (Figure 2) but also deeper older stadiums when inputs were provided both from the atmosphere and surface runoff. A review of published studies on European peat bogs (Table 3) shows that the peat bog that has the longest ombrotrophic stadium is Étang de la Gruère with the last 7000 years of peat accumulation under an ombrotrophic status (Shotyk, 2001).

1.2.2 General characteristic of peat bogs

As shown in the Figure 2, peat bogs are ombrotrophic ecosystems, fed only by atmospheric inputs. They are commonly dominated by *Sphagnum* mosses, which have a high cation exchange capacity (CEC) in order to better remove cations in the oligotrophic pore waters.

English	German	French
Raised mire, bog	Regenmoor, Hochmoor	Tourbière bombée, Haut Marais
Blanket bog or mire	Decken (hoch-) moor	Tourbière de couverture

Table 2: Bogs terminology in English, German, French (Manneville et al., 1999)

A typical peat bog can be divided in two layers:

- the surface layer (acrotelm) is an active oxic layer, where plant decay occurs rapidly,
- the deepest layer (catotelm) is an anoxic layer, where plant decay occurs very slowly.

The main chemical characteristics of peat bogs are summarized in Chapter 3.1 of this work.

Name and Location of the bog	Calendar year (AD/BC) marking the beginning of peat accumulation (ash content <25%)	Calendar year marking the beginning of the bog formation (*Sphagnum*-dominated bog)
Kohlhütte Moor (this study)	-7000	-3600
Lindow Bog (this study)	Older than -6600	-500
Étang de la Gruère (Jura, Switzerland) (Shotyk, 2001)	-13000	-7000
Luther Bog (Ontario, Canada) (Givelet et al., 2003)	-7700	-3300

Table 3: Calendar ages marking the beginning of peat formation and Sphagnum-bog development for 4 peat bogs including the bogs investigated in this study

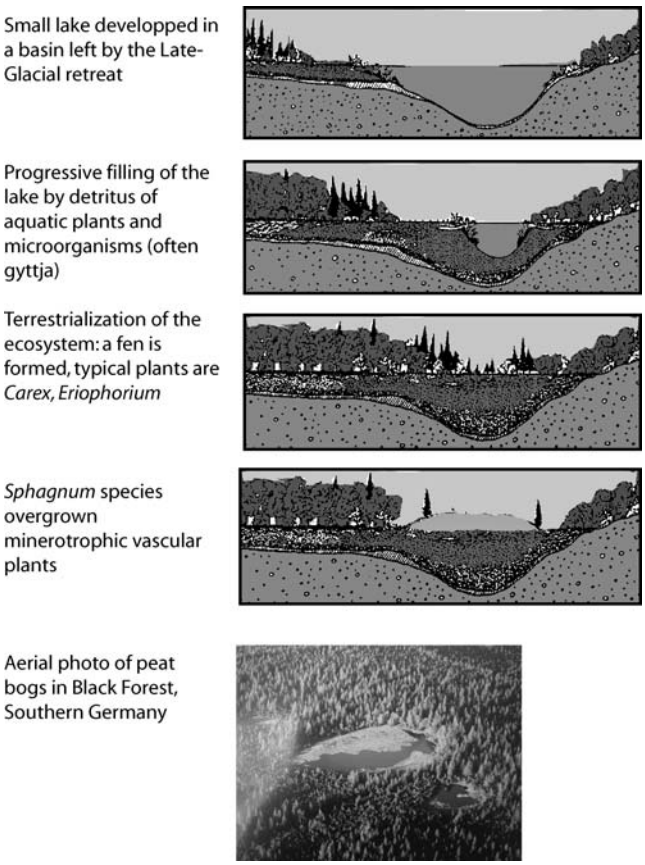

Figure 1: Development of a peat bog after the ice retreat at the end of the last glaciation + Aerial Photo of a peat bog from Black Forest, Southern Germany. In Black Forest, the distribution of large hollows is very climatic dependent. Dried peat in summer could form crevasses, which in autumn turned into free water areas (personal observations)

1.3 Peat bogs as biogeochemical objects

The Figure 3 demonstrates how the study of a peat bog ecosystem is related to the study of natural and human-accelerated environmental changes.

1.3.1 Peat bogs as archives of environmental change:

Because peat bogs trap various environmental signals (biota, atmospheric deposition) and are readily[2] age-dated, they are archives of many environmental changes (Chambers and Charman, 2004).

Peat bogs are mainly used as archives in palynology (e.g. Woillard, 1978). In comparison with lake sediments, peat bogs are valuable archives because there is no "catchment effect" and the pollen distribution reflects the atmospheric input of pollen. They are also archives of the plants and fauna (i.e. insects) living on the surface of the bog (e.g. Ponel and Coope, 1990). Using transfer functions, it is possible to use these proxies as record of past vegetation and past climate[3].

Peat bogs are also used as archives of atmospheric dust, especially pollutants such as heavy metals (cf. Chap.1.1 and references therein) or anthropogenic particles (Punning and Alliksaar, 1997). *However to date only studies of Pb have demonstrated strong arguments of the preservation of its atmospheric signal in peat cores*. It was shown that different sediment deposits, including bogs, yields the same Pb chronology although they have different sedimentation accumulation rates (Renberg et al., 2001 and references therein).

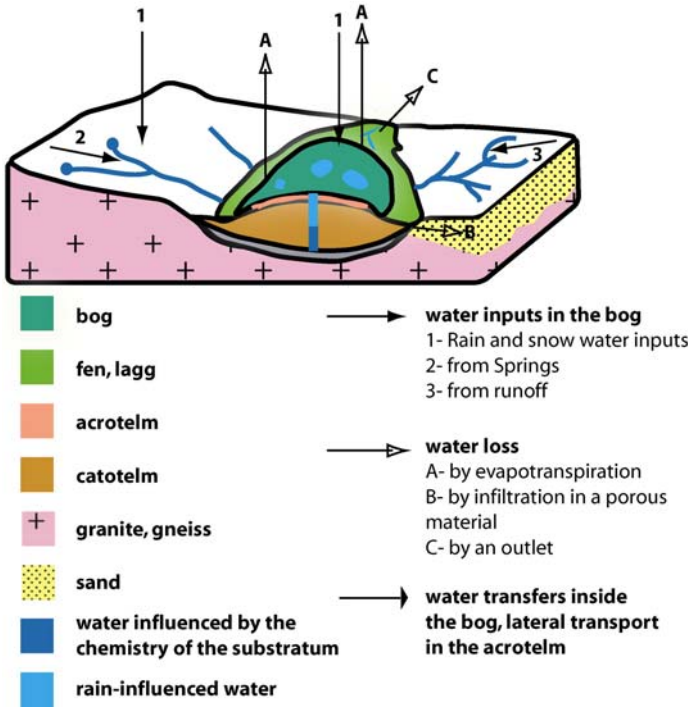

Figure 2: Inputs, transfers and losses of water in a peat bog

[2] Age dating of peat bogs is discussed in Chapter 2.2; 2.3 and Appendix A3.

[3] Cf. the electronic database from the NOAA: http://www.ngdc.noaa.gov/paleo/pollen.html

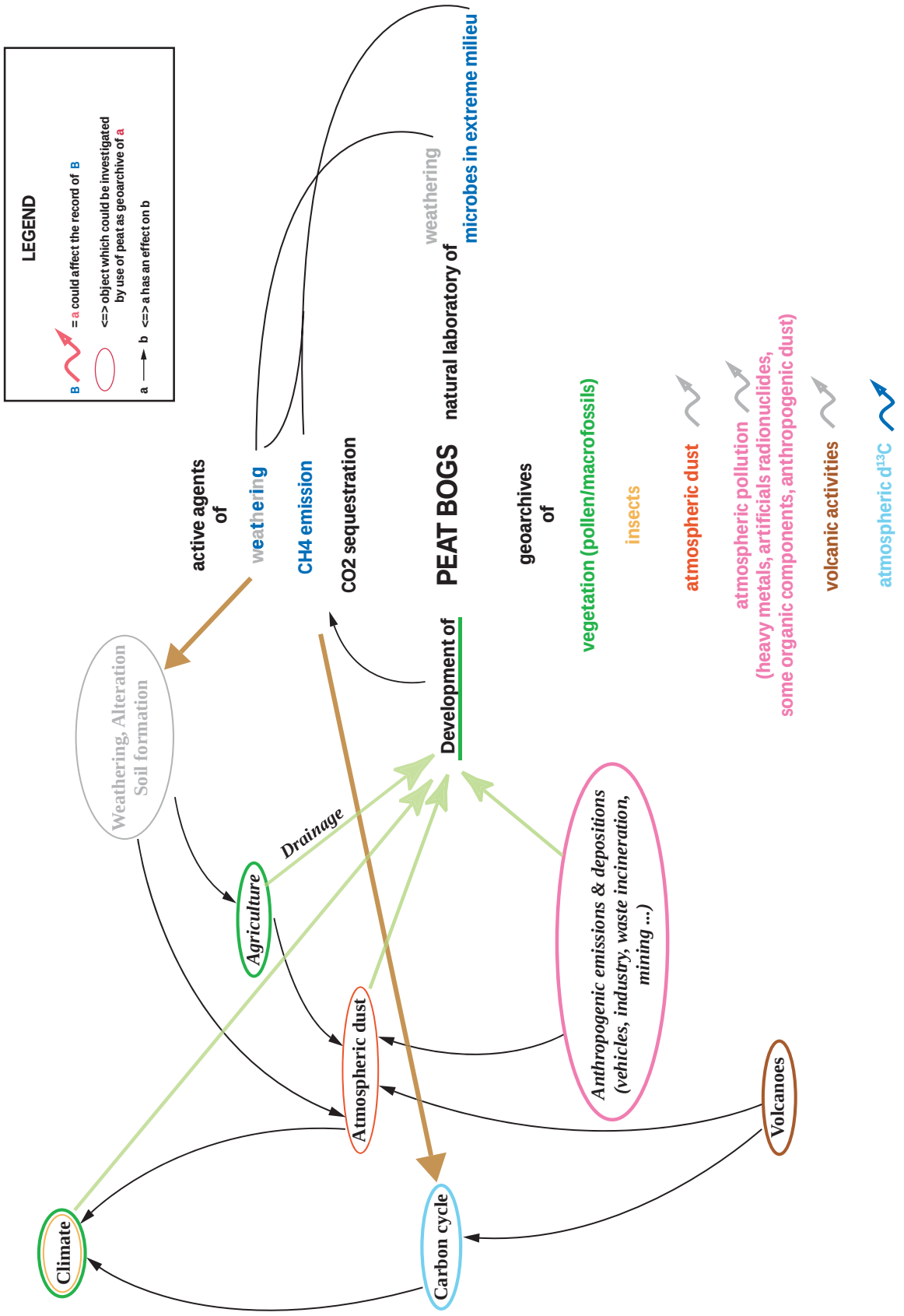

Figure 3: implication of peat bog studies on global environmental concerns

Indeed there is an increase of the Pb concentration in the peat layers dated from historical periods of recorded enhanced Pb production (Figure 4 and Chap.1.3).

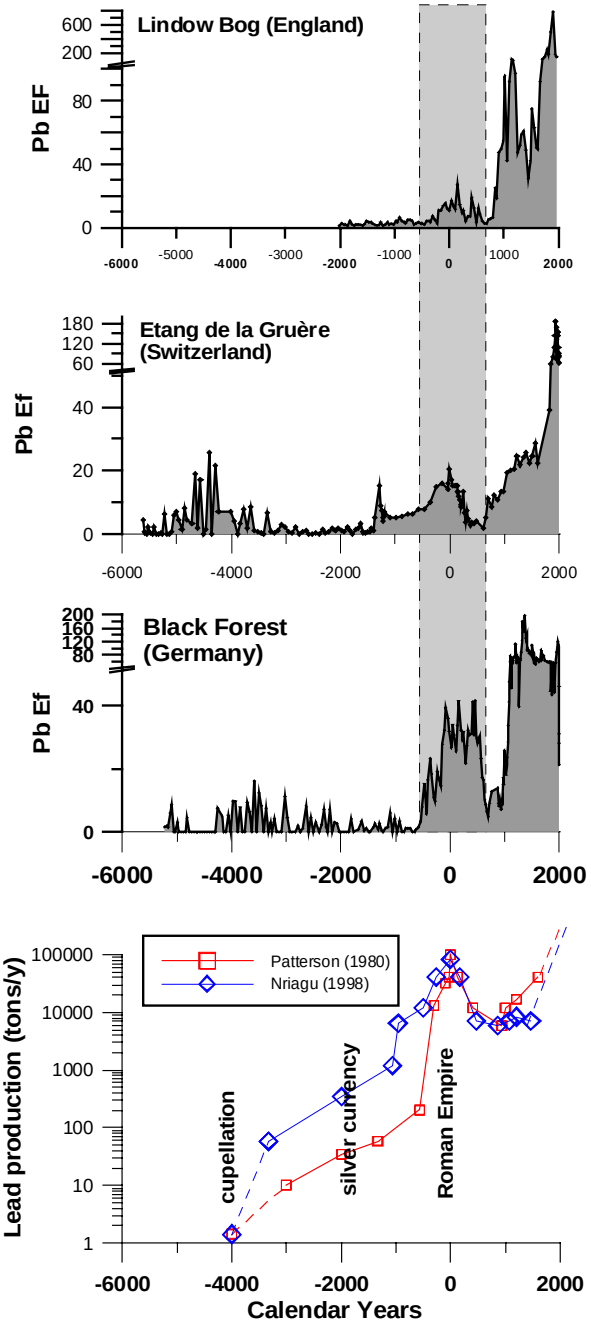

Figure 4: Comparison of Pb enrichment factor[4] in three European peat profiles with estimations of Pb production by Patterson (1980) and Nriagu (1998)

Secondly in comparison with other metals (Hg, Cu or Zn), Pb has a very variable isotopic composition because three of its isotopes, ^{208}Pb, ^{207}Pb, ^{206}Pb, are radiogenic and derived from the decay chains of ^{232}Th, ^{235}U, ^{238}U respectively. Depending on the initial U-Th concentration and age, rocks will display different isotopic signatures (Chap.1.1). Weiss et al. (1999) showed that the chronology of the Pb isotopic composition in herbarium *Sphagnum* samples from Swiss and Southern Germany was the same than the chronology of Pb isotopic compositions in peat samples age dated using ^{210}Pb. The distribution of ^{210}Pb (1/2 life: 22.26 years) in the peat core was the third argument for the preservation of the Pb atmospheric signal in peat cores. The ^{210}Pb CRS age model (Appleby, 2001; Appleby and Oldfield, 1978) is in good agreement with pollen chronological markers (Appleby et al., 1997). Figure 5 also gives a comparison between age dating made using the ^{210}Pb CRS model and ^{14}C Bomb Pulse Curve (Goodsite et al., 2001) in a peat core from Sifton Bog, Ontario, Canada (Givelet et al., 2003). In this fast-growing bog, there is also a very good agreement between the two age dating methods.

Despite this strong evidence of preservation of the atmospheric Pb signal, accurate record of recent atmospheric Pb deposition using a single peat core was questioned by Bindler et al. (2004). He claimed that one single Pb record using a peat core is not representative of the atmospheric Pb flux and that more cores are needed to really assess the atmospheric flux. In other words, Bindler et al. questioned the validity of the regional Pb atmospheric fluxes obtained using single peat cores (Chap.2.2).

Despite large decreases in anthropogenic Pb contributions to the environment mainly due to the banish on leaded gasoline and other clean-air acts, studying anthropogenic Pb pathways is always of importance because this metal has no physiological function, is toxic and always highly enriched in the environment (Chap.1.1).

The validity of peat bogs as valuable and precise archives should therefore be further tested because they can be unique *local and*

[4] The enrichment factor is defined here as Pb EF(Ti)= ($[Pb]_{peat}$ x $[Ti]_{continental\ crust}$)/($[Pb]_{continental\ crust}$ x $[Ti]_{peat}$); Pb and Ti were measured by XRF

regional archives of recent and past atmospheric deposition of Pb (Chap.2.2 and 2.3). Indeed when compared to ice caps, they are distributed worldwide (Figure 6) and when compared to lakes, they receive in their ombrotrophic part, Pb only from the atmospheric deposition.

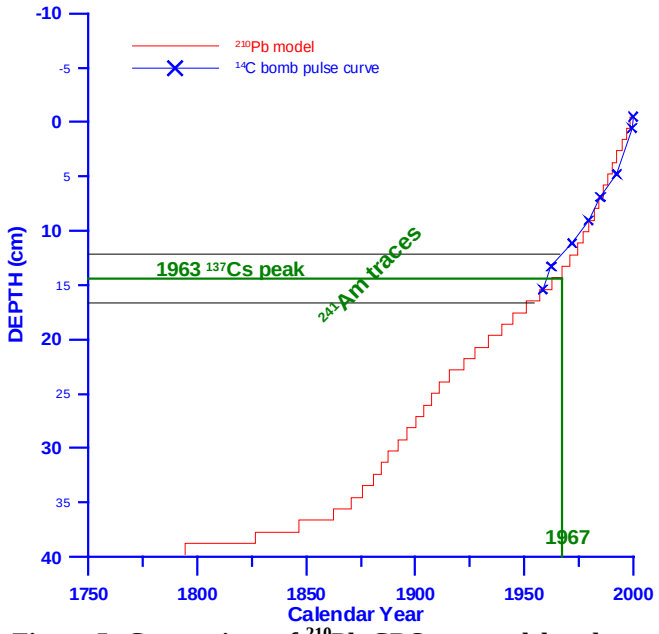

Figure 5: Comparison of ^{210}Pb CRS age model and ^{14}C Bomb-pulse curve age dating. Also are indicated peaks of ^{137}Cs and ^{241}Am, which are derived from atmospheric nuclear tests (maximum in 1963).

1.3.2 Peat bog as a significant biomass

Peat bogs also play an essential role in the carbon cycle (Figure 3). Peatlands in the Northern Hemisphere have sequestered 455 Pg of carbon since the last Glaciation (Gajewski et al., 2001). Climatic changes (Freeman et al., 2004; Gorham, 1991), atmospheric pollution (Gorham et al., 1984; Limpens et al., 2003) and change in the intensity and/or composition of atmospheric deposition (Gorham and Tilton, 1978) have a strong impact on the development of peat bogs and therefore on the storage of C by peatlands. For example, with the increase in N deposition, Limpens et al. (2003) showed that plant species change and therefore also affect the development of the bog. On a larger scale, Turunen et al. (2004) show that increased of the recent rate of carbon accumulation in peat bogs in eastern Canada were found in regions with higher N deposition.

Since the last glaciation, peatlands were a sink of atmospheric C. However, with changing conditions, peatlands could become an emission source of greenhouse gases such as CO_2 and CH_4 (Freeman et al., 2004). The production of CH_4 in peat bogs is mainly due to microbial activity (Figure 3 + Appendix 5).

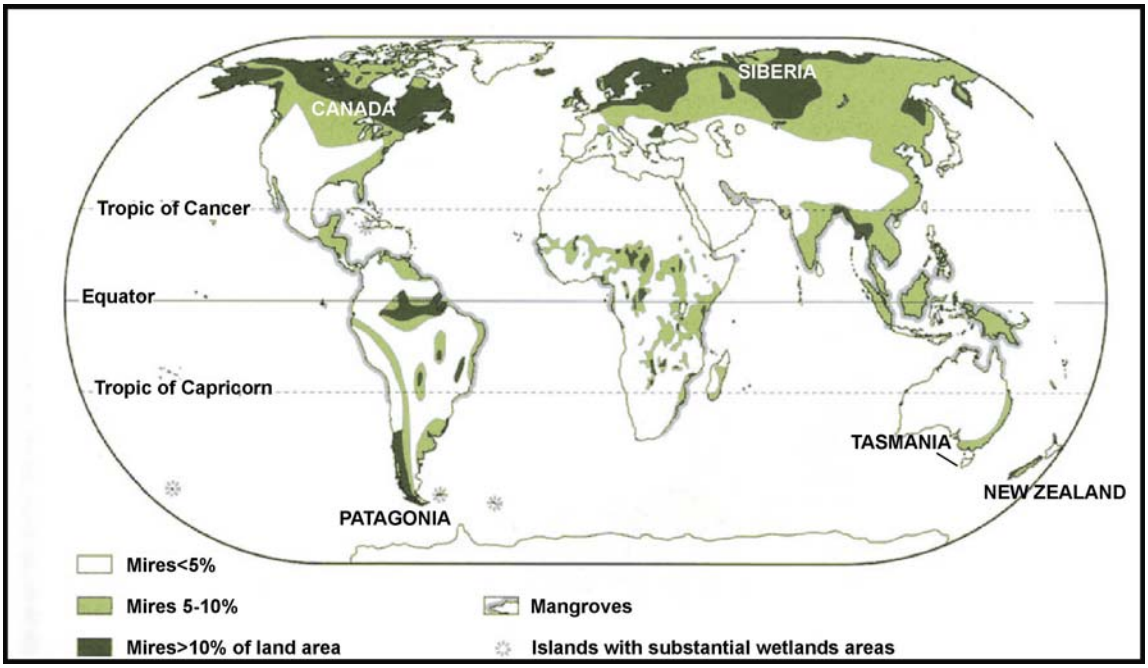

Figure 6: Distribution of peatlands expressed as a proportion of the land surface of the world and location of the most cited bogs in the text. (map redrawn from Lappalainen by permission of the International Peat Society in Charman (2002))

In addition to representing a significant carbon pool, peatlands could have a large impact on the weathering cycle. However, the global significance of these processes is poorly understood (Chap.3.1). This effect should not be underestimated because boreal peatlands cover large areas (Figure 6) of Canada and Russia, which are situated mainly on previously "glaciated" crystalline rocks (Canadian and Siberian Cratons). Indeed, chemical weathering of silicate minerals produces HCO_3^-, which is then transported by rivers to the oceans. HCO_3^- precipitates in the oceans to form carbonates, the net result being the removal of CO_2 from the atmosphere[5].

[5] This is summarized by the Urey´s equation (Urey H. (1952) *The planets, their origin and development.* Yale University Press.): $\mathbf{CO_2 + CaSiO_3 \rightarrow CaCO_3 + SiO_2}$

2. Objectives

The work done during this thesis aims primarily to improve the understanding of the processes affecting anthropogenic and natural deposition, especially particles, in peat bogs. This is crucial because:

- peat bogs receive only atmospheric inputs (Fig. 3) and any variations of these inputs could have large effects on these very fragile ecosystems,
- reactions and processes in the peat column influence the ability of peat bogs to preserve records of atmospheric dust, volcanic emissions and anthropogenic deposition.

The first objective was to understand the relationship between the record of Pb in a peat bog and *the actual atmospheric Pb deposition*, its intensity, timing and sources. If Pb is quantitatively retained, what are the potential applications to archaeology, history and paleoenvironment?

Specifically

1) robust and valuable techniques of sampling and analyses of peat material were developed,

2) peat archives of Pb deposition were compared with historical data, previous studies and other archives of atmospheric deposition in order to test the quality of the peat archive,

3) the changing rates of atmospheric Pb in England and Germany prior to the beginning of large human impacts until the present were quantified, using robust age-dating procedures. The relative importance of local and regional human sources of Pb since the Iron Age was determined using the Pb isotopes.

A second objective of this thesis was to understand the behaviour of dust particles at the contact with “aggressive” anoxic, acidic pore waters of the peat.

Specifically

1) the mechanisms altering inorganic particles in peat bog were reviewed, and

2) the distribution of minerals in the upper ombrotrophic part of a bog was studied. The implications for bog ecology and the suitability of peat bogs as archives of dust deposition are discussed.

3. Results

This work first emphasizes the need for robust sampling and appropriate analytical techniques (Chap.1.1). The present work emphasizes the need to improve the sampling and dating techniques to obtain better and valuable peat record (Chap.1.1 Fig.5, Chap.2.2). For deeper samples, the use and comparison of different ^{14}C age-depth models are necessary and a statistical approach is required to assess the accuracy of the Pb chronology given by the bog (Chap.2.3). For peat samples younger than 200 y, ^{210}Pb CRS age model (Appleby and Oldfield, 1978) appears to be the method of choice: it is quicker and less expensive than the "Bomb-pulse" curve age-depth model (Goodsite et al., 2001). Several peat cores were dated using the ^{210}Pb CRS Age Model and using the Bomb Pulse ^{14}C Model for the last 50 years. It appears that the two models are in good agreement especially when the peat is rapidly accumulating in undisturbed bogs (Figure 5 and Appendix 3).

Analytical protocols were developed to determine the isotopic composition of natural samples, including peat and snow, with thermal ionisation mass spectrometry (TIMS), multi-collector inductively-coupled-plasma spectrometry (MC-ICP-MS) and sector field ICP-MS (SF-ICP-MS) (Chap.1.2 and Chap.1.3). The correction of mass bias/discrimination was investigated using Pb and/or Tl spike and external standards both for MC-ICP-MS and SF-ICP-MS. For example, on the SF-ICP-MS instrument, mass discrimination was found to be non-systematic, and to vary among the masses both with respect to magnitude and direction. This new result shows that only an individual mass discrimination correction will lead to accurate Pb isotope ratios measured using SF-ICP-MS (Chap.1.3).

Secondly, using the results cited above and after a review of the Pb biogeochemical cycle (Chap.2.1), the timing, sources and intensity of atmospheric Pb deposition were analysed in a cutover bog (Lindow Bog, England) and a German bog located in the Black Forest, Southern Germany: Kohlhütte Moor (Chap.2.2 and Chap.2.3).

The main results of these two studies are:

1) that good agreement with other archives (snow and other peat cores) in Germany and with archaeological and historical evidences in England shows that peat cores are accurate archives of the real atmospheric Pb flux;

2) a recent record of Pb deposition in South-West Germany using a core representing more than 9000 years of peat accumulation. As evidenced by the Pb concentrations as well as the isotopic composition, snow, moss, and peat are dominated by anthropogenic Pb, even today. The present Pb flux is ~ 2.5 mg m^{-2} y^{-1} assessed with the peat core age-dated using ^{210}Pb. This is seven times lower than during the period 1970-1980 as assessed by the same peat core and Swiss peat cores, but it is still at least one hundred times higher than natural pre-anthropogenic Pb flux.

3) a record of the local Pb atmospheric deposition evidenced by Pb concentration and isotope measurements in Mid-West England is linked to technological improvements and socio-economical changes since 2000 B.C. Atmospheric Pb contamination in England pre-date Roman occupation by 900 years and until the industrial period, was of local origin.

After the validity and the relevance of using peat cores as archive of Pb deposition was reinforced, the fate of other elements in the peat bog was investigated. These major and trace elements are deposited by wet deposition but also by dry deposition. The behaviour of the inorganic dry matter in the, acid, anoxic and rich in dissolved organic carbon (DOC), peat is critical to understand if the dust signal is preserved in the bog.

After a review of the different mechanisms of alteration of inorganic matter in peat bogs (Chap.3.1), the fate and distribution of the minerals in the upper ombrotrophic part of the bog was studied. Using X-Ray Diffraction (XRD), it was found that the distribution of

the silicates and alumino-silicates has a large effect on the geochemical distribution of minor and major elements in the bog because there is no detectable dissolution of these minerals. The lack of alteration of these minerals is promising for the study of the composition and fluxes of dust to the bog.
The dissolution of other minerals such as calcite and apatite is also slower than expected from laboratory studies under the same chemical conditions. However these inputs, whether they are natural or anthropogenic (liming of the surrounding forest), could have a large impact on the development of the bog because the dissolution of apatite releases bioavailable-P, a limiting nutrient for bog plants (Chap.3.2).

4. Studied Sites

Two sites were investigated during this work:

1) Lindow Bog (LDW) is located in Mid-West England near Manchester. It is a cutover bog and well documented (Birks, 1965; Lageard, 1998; Stead et al., 1986; Turner and Scaife, 1995) because two bog bodies were found during peat extraction. The bog bodies were age-dated from the Iron Age-Roman Period with ^{14}C age dating on the tissues and the surrounding peat. Investigations of the skin of one of the bodies suggested that the body might have been painted (Pyatt et al., 1991). As a part of an informal project trying to confirm this hypothesis, a monolith of peat collected by John Grattan (University of Wales) was investigated. In 2002, complementary samples were collected to investigate the complete Pb chronology in England[6].

2) Whereas the Lindow Bog is a well-documented peat bog, Kohlhütte Moor (KM), the bog investigated in Black Forest, was never the subject, to our knowledge, of a complete scientific investigation. Also despite the fact that the development and palynology of numerous peat bogs in Southern Black Forest have already been published (Lang, 1954; Lang et al., 1984; Lotter and Birks, 1993; Lotter and Holzer, 1989; Rösch, 2000), there is no published study of the KM bog. Therefore this paragraph reviews briefly the geological and botanical contexts and presents new insights on the KM bog based on sedimentological observations and REE measurements[7].

The KM bog (called also Torfstich Kohlhütte or Kohlhüttenmoos[8]) is an asymmetric raised bog (Dierssen and Dierssen, 1984). Kohlhütte Moor is the deepest peat bog in the Hotzenwald Plateau, the Hotzenwald plateau being the South-East part of the Oberbadischer Schwarzwald (Litzelmann and Litzelmann, 1967).

4.1 Geology (Metz, 1980; Sawatzki, 1992)

KM is lying indirectly on the Albtal granite, near an end-moraine and on the side of an ice marginal channel[9] (Hantke and Rahm, 1977). In the proximity of the bog, there are also two other types of rocks: the St. Blasien granite and the Todmoos Gneiss (Figure 7). The Albtal Granite is a grey rock characterised by large (20-40, max. 100 mm) macro-crystals of K-feldspar (white-pink). The matrix is made of quartz, plagioclase (An_{15-35}), some K-feldspars and brilliant black biotite rich in Ti. Accessory minerals are apatite, zircon, opaque minerals, and monazite. The Albtal granite is commonly weathered to a sandy grus over a thickness of a few metres.

Despite their different textures, the St-Blasien and the Albtal granites are very similar with respect to their chemistry. The St-Blasien granite is a white to lightly red stone made of plagioclase, quartz, biotite, and small K-feldspars. The main minerals of the Todtmoos Gneiss include quartz, plagioclase (anorthite), biotite, more or less garnet and sillimanite. Accessory minerals are apatite, zircon, rutile, magnetite, hematite, and some pyrites.

4.2 Botany and status of the bog at the surface

The main plant species were identified after personal observations and Dierssen &Dierssen (1984): *Sphagnum* Angustifolium, *Sphagnum* Cuspidatum, *Sphagnum* Magellanicum, *Carex* Limosa, *Eriophorum* Vaginatum. These species, especially the *Sphagnum,* are typical of peat bogs. Waters at the surface of most of the bog are acidic[10] (pH = 3.5-4). Precipitation is between 1300 and 1800 mm per year, and the annual temperature around 6°C (Sawatzki, 1992).

[6] http://cf.geocities.com/gwanach/Lindowmossfieldreport.pdf

[7] 10 g of the samples described here were powdered in an agate mortar and measured using an ICP-MS by ACME Lab, Canada, after Li-fusion.

[8] See discussion on the bog name in the part "history of the bog"

[9] marginal channel: a channel cut by flowing water along the ice margin

[10] Le Roux G. & Rausch N. (Unpublished data)

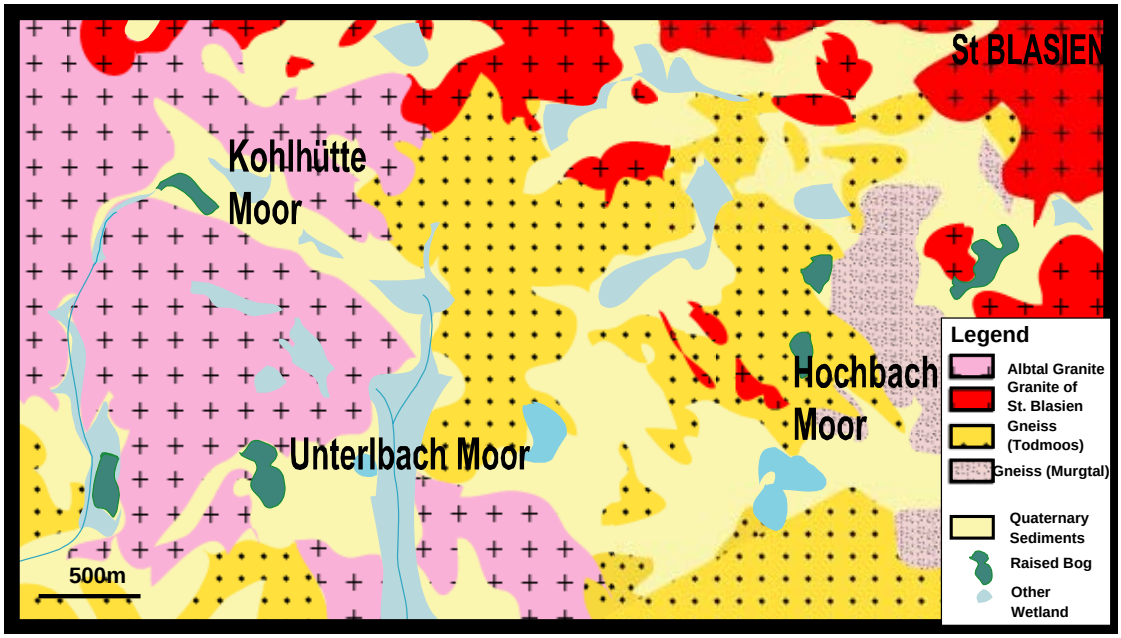

Figure 7: Geological map of KM surrounding area

Despite the oligotrophic status of the bog, it seems that the bog has been invaded by pines as shown by Figure 8, which compares a photo taken before 1984 (Dierssen and Dierssen, 1984) with one taken in 2002.

4.3 Stratigraphy of the bog and its substratum

Litzelmann and Litzelmann (1967) wrote that peat bogs in the Hotzenwald Plateau are lying on silicate soils. From Figure 9.a showing the stratigraphy of the bog, this description is possible because the accumulation of "sediments or soil" is very thin without a gyttja[11] stadium.

From the stratigraphy of the bog profile, a summary of the development can be made:

1) An end moraine was formed by the retreat of the Feldberg glacier during the Falkau stadium (Hantke and Rahm, 1977) and formed a side-basin where some plastic clay sediments (milky clay, glacial flour) and pieces of local but also allochtonous rocks were deposited. Figure 9.d shows the REE pattern of the local granite Albtal compared to some stones found in the clays under the peat.

Figure 8: Comparison between 2 photos of the site taken respectively in spring 2002 and before 1984 (cf. text for explanation)

[11] Gyttja: lake muds composed of organic remains of aquatic plants

Whereas the sample "Granite Stone n°2 bis" has a similar pattern to that of the Albtal Granite, other stones ("Granite Stone n°2" and "Stone in clay 15") have a different pattern and are derived from further locations. "Granite Stone n°2" has the same petrology as the St Blasien Granite, however, the REE pattern is different. Further investigations of REE patterns of rocks, which were under the glacier, will be needed to trace the exact provenance of these two stones.

2) Unlike neighbouring bogs (Lang, 1954; Rösch, 2000), no distinct Laacher See tephra horizon (Hadjas et al., 1995; Juvigné, 1991) was found in the Kohlhütte Moor. However, reworked titanite (or sphene), a mineral typical for the Laacher See tephra (E. Juvigné and F. De Vleeschouwer, personal communication and Lang, 1954) was found in the clays[12]. Because the tephra layer is younger (10300 ± 300 cal. B.C) than the presupposed retreat of the glacier in Black Forest (Lang et al., 1984), the clays (at least the upper part) are of postglacial origin and deposited contemporaneously or after the Laacher See explosion.

3) Above the clays, there is a layer of organic sediment (~50% ash content). Litzelmann and Litzelmann (1967) speculated that peat bogs in this area (the "Hotzenwald Plateau) are lying on silicate soils. However it is not clear if these are soils or sediments. A botanical study is the most appropriate way to identify this formation and will show if it is derived from aquatic or terrestrial plants. No large and easy-to-identify macrofossils were found and further botanical studies are required. It is however possible to call them sediments because they formed an accumulation of 1 meter in 500 years and they are not directly derived from the clays underneath (Figure 9. b).

4) A fen[13] formed above these sediments. The sedimentology (50% ash to <2% ash) and the chemistry changed abruptly at the limit between the sediments and the fen peat (Figure 9 a).

5) Accumulation of fen plants was brief and a *Sphagnum*-dominated bog followed. The accumulation of peat is linear, showing that the peat bog was undisturbed where the peat core was taken at least until the industrial period. The peat bog is also called "Torfstich" by Dierssen and Dierssen (1984), which would mean that there was peat cutting[14] in this place. However the nomenclature of the bogs in this area is quite unclear with similar names used for different bogs (Dierssen and Dierssen, 1984; Metz, 1980). Also a former fen is present 100 m east from the bog. This is possibly the "Torfstich". Finally the bog do not show any "cutting lines" as it is possible to see in neighbouring "farmed" peatlands in Black Forest. Therefore there is strong evidence that at least the spot, where the core was collected, was undisturbed until present.

6) Despite no indication of strong human perturbations on the peat accumulation, there are, following the interpretation of Rösch (2000), peaks of ash correlated with human development. Especially the peak at – 450 cm is correlated with a similar peak of ash at the same age (~5000 B.C.) in a bog (Steerenmoos, 5 km to the North) investigated by Rösch (2000) (Figure 9.e). In KM, no charcoal was found at the same depth despite the collection of four cores of the same mineral horizon. At this time, the most probable interpretation is that a flooding event, possibly human-induced, transported soil minerals into the two bogs. Further investigations on samples from Steerenmoos bog will be necessary to test this hypothesis. Ancient environmental human induced impacts in Black Forest are reviewed by Kalis et al. (2003) and are significant since the Early Neolithic (4300 cal. B.C).

7) Recent peat accumulation evidenced by ^{210}Pb age dating is low (Figure 9.c). If the

[12] Using a petrological microscope on the clay samples after granulometric separation. Further investigations on other minerals (augite for example) will be needed to confirm this hypothesis.

[13] *Carex* and *Eriophorium* rests were identified by Prof. H.J. Küster, Hannover

[14] The author of this thesis was not present when the choice of this site was taken. It appears that no real geological and historical background bibliographical studies were done. Fortunately, the core collected in this study shows that the bog was undisturbed.

core is representative of the bog, low peat accumulation rate and invasion by pines are good evidence that the peat bog is surely reaching its terminal stadium with a natural pine afforestation (Manneville et al., 1999).

Figure 9: sketch summary of the bog development

Fig. 9A: Stratigraphy of the bog + Ca and S concentration in the bulk peat. Like Sulphur, other elements such as Hg, Pb or Cu are also enriched in the mineral horizon.

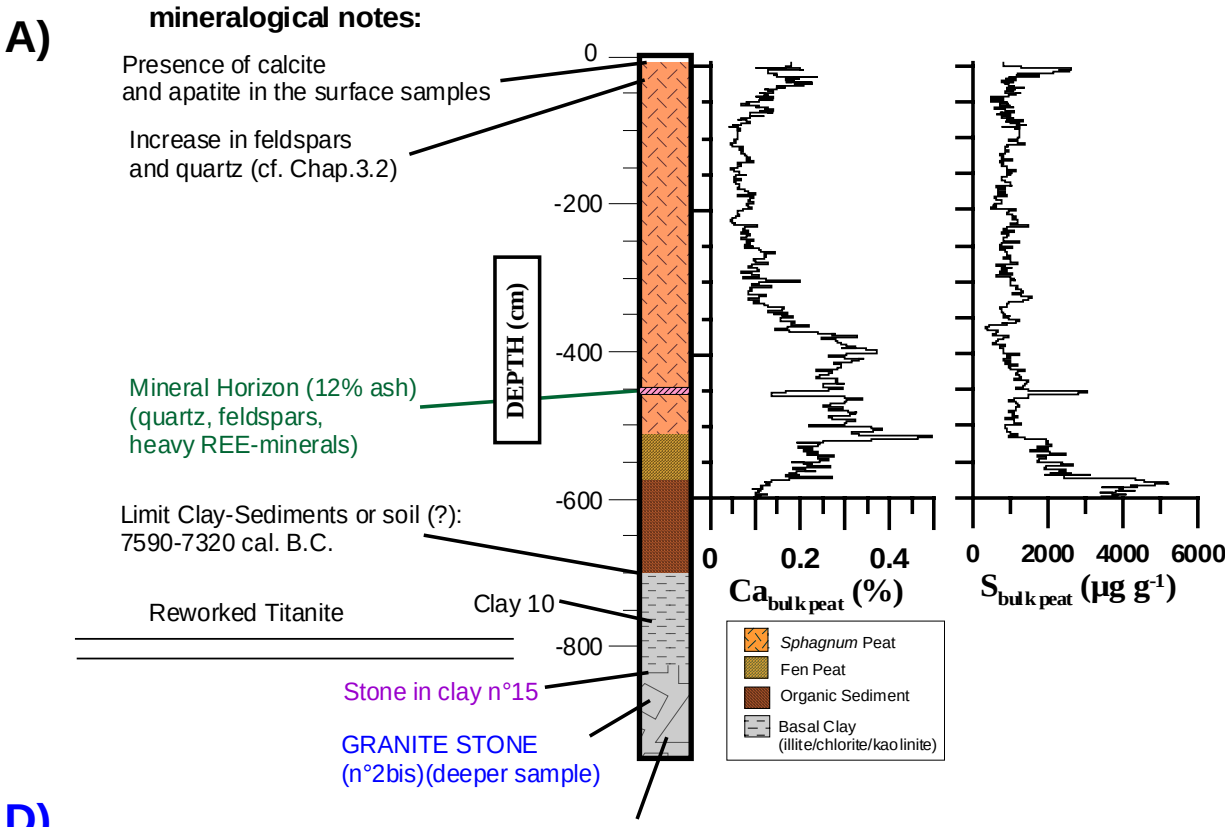

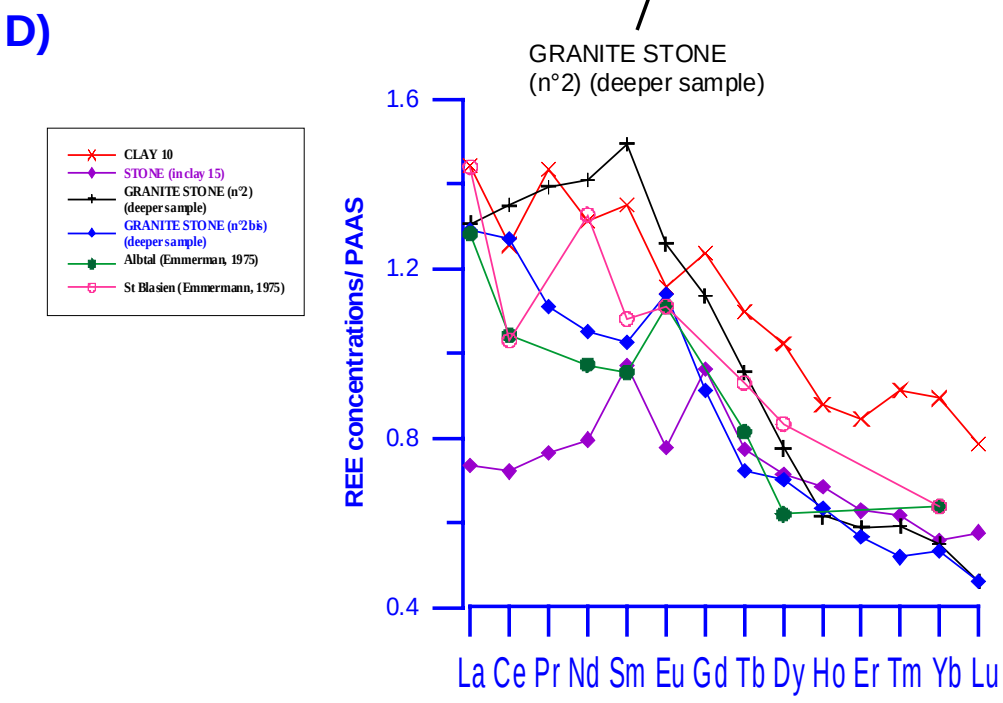

Fig. 9D: REE patterns of stones and clay found under the bog compared to the REE patterns of local rocks (Emmermann et al., 1975)

Fig 9B: ^{14}C linear age-depth model
Fig 9C: ^{210}Pb CRS model compared to the top part of the ^{14}C age depth model (circles)
Fig.9E: Comparison of the ash content in the peat bog analysed by Rösch (2000): Steerenmoos and the Kohlhütte Moor (KM, this study). In yellow-shaded, the mineral horizon in the bogs; the older (and deeper) samples are sediments.

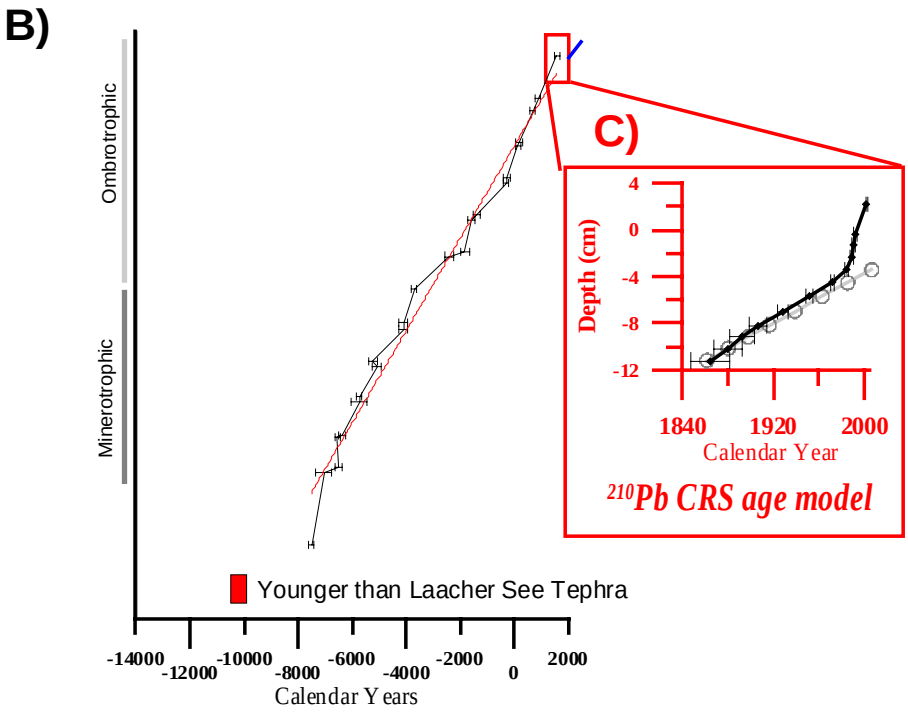

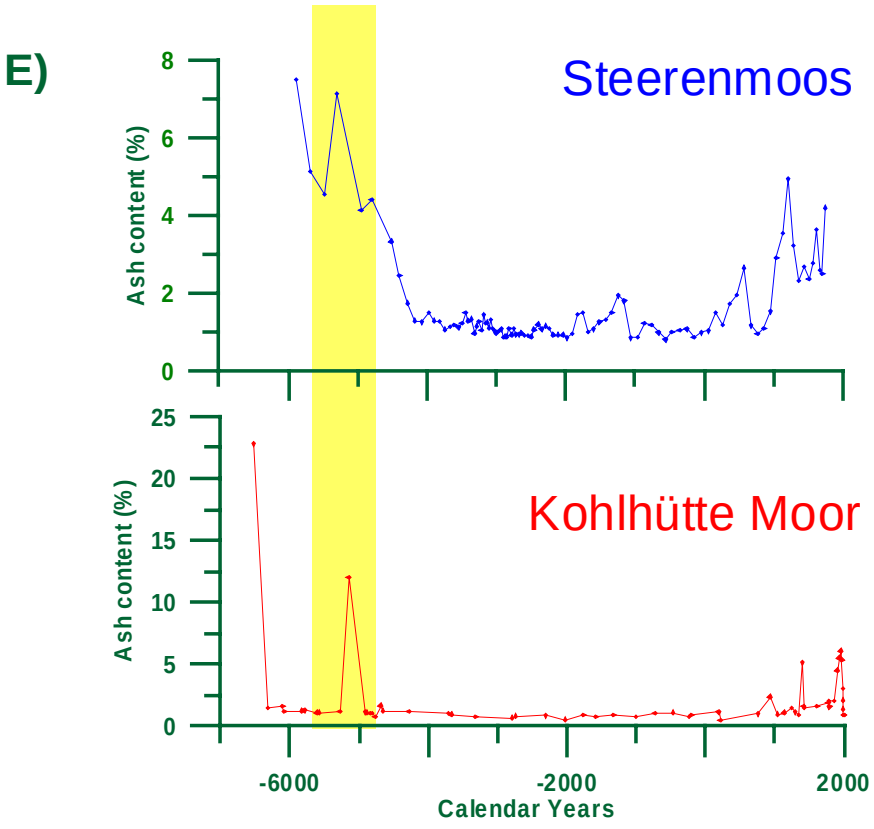

REFERENCES

Albarède F. (2001) *La Géochimie*. Gordon & Breach Science Publishers.

Appleby P. G. (2001) Chronostratigraphic techniques in recent sediments. In *Tracking Environmental Change Using Lake Sediments: Basin Analysis, coring, and chronological techniques*, Vol. 1 (ed. W. M. Last and J. P. Smol), pp. 171-203. Kluwer Academics.

Appleby P. G. and Oldfield F. (1978) The calculation of lead-210 dates assuming a constant rate of supply of unsupported 210Pb to the sediments. *Catena* **5**, 1-8.

Appleby P. G., Shotyk W., and Fankauser A. (1997) Lead-210 Age Dating of Three Peat Cores in the Jura Mountains, Switzerland. *Water Air Soil Pollution* **100**(3/4), 223-231.

Bindler R., Klarqvist M., Klaminder J., and Förster J. (2004) Does within-bog spatial variability of mercury and lead constrain reconstructions of absolute deposition rates from single peat records? The example of Store Moss, Sweden. *Global Biogeochemical Cycles* **18**(GB3020).

Birks H. J. B. (1965) Pollen analytical investigations at Holcroft Moss, and Lindow Moss, Cheshire. *The Journal of Ecology* **53**(2), 299-314.

Chambers F. M. and Charman D. J. (2004) Holocene environmental change: contributions from the peatland archives. *The Holocene* **14**(1), 1-6.

Charman D. (2002) *Peatland and Environmental Change*. John Wiley & Sons.

Dierssen B. and Dierssen K. (1984) *Vegetation und Flora der Schwarzwaldmoore*. Landesanstalt für Umweltschutz Baden-Württemberg.

Dierssen K. and Dierssen B. (2001) *Moore*. Ulmer.

Emmermann R., Daieva L., and Schneider J. (1975) Petrologic significance of Rare Earth Distribution in Granites. *Contribution to Mineralogy and Petrology* **52**, 267-328.

Freeman C., Fenner N., Ostle N. J., Kang H., Dowrick D. J., Reynolds B., Lock M. A., Sleep D., Hughes S., and Hudson J. (2004) Export of dissolved organic carbon from peatlands under elevated carbon dioxide levels. *Nature* **430**, 195-198.

Gajewski K., Viau A., Sawada M., Atkinson D., and Wilson S. (2001) Sphagnum peatland distribution in North America and Eurasia during the past 21,000 years. *Global Biogeochemical Cycles* **15**(2), 297-310.

Givelet N., Roos-Barraclough F., and Shotyk W. (2003) Predominant anthropogenic sources and rates of atmospheric mercury accumulation in southern Ontario recorded by peat cores from three bogs: comparison with natural "background" values (past 8,000 years). *Journal of Environmental Monitoring* **5**(6), 935-949.

Goodsite M. E., Rom W., Heinemeier J., Lange T., Ooi S., Appleby P. G., Shotyk W., Van der Knapp W. O., Lohse C., and Hansen T. S. (2001) High-resolution AMS 14C dating of post-bomb peat archives of atmospheric pollutants. *Radiocarbon* **43**(3), 453-473.

Gorham E. (1991) Northern Peatlands: Role in the Carbon Cycle and Probable Responses to Climatic Warming. *Ecological Applications* **1**(2), 182-195.

Gorham E., Bayley S. E., and Schindler D. W. (1984) Ecological effects of acid deposition upon peatlands: a neglected field in "acid rain" research. *Canadian Journal of Fisheries and Aquatic Science* **41**, 1256-1268.

Gorham E. and Tilton D. L. (1978) The mineral content of Sphagnum fuscum as affected by human settlement. *Canadian Journal of Botany* **56**, 2755-2759.

Göttlich K. (1990) Moor-und Torf-Kunde, pp. 529. E.Schweizerbart´sche Verlagsbuchhandlung.

Hadjas I., Ivy-Ochs S. D., Bonani G., Lotter A. F., Zolitschka B., and Schlüchter C. (1995) Radiocarbon age of the laacher see tephra: 11,230+-40 BP. *Radiocarbon* **37**(2), 149-154.

Hantke R. and Rahm G. (1977) Die wurmzeitlichen Rückzugsstände in den Tälern Ibach und Schwarzenbäcle im Hotzenwald (Südschwarzwald). *Jahrbuch geol. Landesamt Baden-Württemberg* **19**, 143-150.

Heathwaite A. L., Göttlich K., and Cooke J. (1993) Mires: process, exploitation and conservation, pp. 516. John Wiley & Sons.

Hooke R. L. (1994) On the efficacy as human as geomorphic agents. *GSA Today* **4**(9), 224-225.

Hooke R. L. (2000) On the history of humans as geomorphic agents. *Geology* **28**(9), 843-846.

Juvigné E. (1991) Distribution de vastes retombées volcaniques originaires de l´Eifel et du Massif Central aux temps post-glaciaires dans le NE de la France et les régions voisines. *Comptes-rendus de l´Académie des Sciences* **312 (II)**, 415-420.

Kalis A. J., Merkt J., and Wunderlich J. (2003) Environmental changes during the Holocene climatic optimum in central Europe- human impact and natural causes. *Quaternary Science Reviews* **22**, 33-79.

Lageard J. G. A. (1998) Dendochronological analysis and dating of subfossil Pinus sylvestris at Lindow Moss, Cheshire. *Bulletin of the British Ecological Society* **29**(2), 31-32.

Lang G. (1954) Neue Untersuchungen über die spät- und nacheiszeitliche Vegetation Geschichte des Schwarzwaldes. I. Der Hotzenwald im Südschwarzwald. *Beiträge zur Naturkundlichen Forschung in Südwestdeutschland* **13**, 3-42.

Lang G., Merkt J., and Streif H. (1984) Spätglazialer Gletscherrückzug und See- und Moorentwicklung im Südschwarzwald, Südwestdeutschland. *Dissertation Botanicae* **72**, 213-234.

Likens G. E. (2004) Biogeochemistry: some opportunities and challenges for the future. *Water Air Soil Pollution: Focus* **4**(5-24), 2004.

Limpens J., Tomassen H. B. M., and Berendse F. (2003) Expansion of Sphagnum fallix in bogs: striking the balance between N and P availability. *Journal of Bryology* **25**, 1-8.

Litzelmann E. and Litzelmann M. (1967) Die Moorgebiete auf der vormals vereist gewesenen Plateaulandschaft des Hotzenwald. *Mitteilungen der Naturforschenden Gesellschaft Schaffhausen* **28**, 21-77.

Lotter A. F. and Birks H. J. B. (1993) The impact of the Laacher See Tephra on terrestrial and aquatic ecosystems in the Black Forest, Southern Germany. *Journal of Quaternary Science* **8**(3), 263-276.

Lotter A. F. and Holzer A. (1989) Spätglaziale Umweltverhältnisse im Südschwarzwald: Erste Ergebnisse paläolimnologischer und paläoökologischer Untersuchungen an Seesedimenten des Hirschenmoores. *Carolinea* **47**, 7-14.

Manneville O., Vergne V., Villepoux O., Blanchard F., Bremer K., Dupieux N., Feldmeyer-Christe E., Francez A.-J., Hervio J.-M., Julve P., Laplace-Dolonde A., Paelinckx D., and Schumaker R. (1999) *Le monde des tourbières et des marais*. Delachaux et Niestlé.

Metz R. (1980) *Geologische Landeskunde des Hotzenwalds*. Moritz Schauenburg.

Nriagu J. O. (1998) Tales Told in Lead. *Science* **281**, 1622-1623.

Patterson C. C. (1980) An alternative Perspective-Lead Pollution in the Human Environment: Origin, Extent, and Significance. In *Lead in the Human Environment. A report prepared by the Committee on Lead in the Human Environment*, pp. 265-349. Environmental Studies Board, Commission of Natural Resources Research Council.

Ponel P. and Coope G. R. (1990) Lateglacial and Early Flandrian Coleoptera from La Taphanel, Massif Central, France: Climatic and Ecological Implications. *Journal of Quaternary Science* **5**(3), 235-249.

Punning J.-M. and Alliksaar T. (1997) The trapping of fly-ash particles in the surface layers of Sphagnum-dominated peat. *Water, Air and Soil Pollution* **94**, 59-69.

Pyatt F. B., Beaumont E. H., Lacy D., Magilton J. R., and Buckland P. C. (1991) Non isatis sed vitrum or, the colour of Lindow Man. *Oxford Journal of Archeology* **10**(1).

Renberg I., Bindler R., and Brännvall M.-L. (2001) Using the historical atmospheric lead-deposition record as a chronological marker in sediments deposits in Europe. *The Holocene* **11**(07), 511-516.

Rösch M. (2000) Long-term human impacts as registered in an upland pollen profile from the Southern Black Forest, south-western Germany. *Vegetation history and archaeobotany* **9**, 205-218.

Sawatzki G. (1992) *Erläuterung zu Blatt 8214 St. Blasien*. Geologischen Landesamt Baden-Württemberg.

Schlesinger W. H. (2004) Better living through biogeochemistry. *Ecology* **85**(9), 2402-2407.

Shotyk W. (2001) Geochemistry of the peat bog at Étang de la Gruère, Jura Mountains, Switzerland, and its record of atmospheric Pb and lithogenic trace metals (Sc, Ti, Y, Zr, and REE) since 12,370 14C BP. *Geochimica et Cosmochimica Acta* **65**(14), 2337-2360.

Staudigel H., Albarède F., Blichert-Toft J., Edmond J., Mc Donough B., Jacobsen S. B., Keeling R., Langmuir C. H., Nielsen R. L., Plank T., Rudnick R., Shaw H., Shirey S., Veizer J., and White W. (1998) Geochemical Earth Reference Model (GERM), description of the initiative. *Chemical Geology* **145**, 153-160.

Stead I. M., Bourke J. B., and Brothwell D. (1986) Lindow Man, the body in the bog, pp. 206. British Museum.

Turner R. C. and Scaife R. G. (1995) Bog bodies, new discoveries and perspectives, pp. 256. British Museum.

Turunen J., Roulet N. T., and Moore T. R. (2004) Nitrogen deposition and increased carbon accumulation in ombrotrophic peatlands in eastern Canada. *Global Biogeochemical Cycles* **18**(GB3002), 1-12.

Urey H. (1952) *The planets, their origin and development*. Yale University Press.

Weiss D., Shotyk W., Kramers J. D., and Gloor M. (1999) Sphagnum mosses as archives of recent and past atmospheric lead deposition in Switzerland. *Atmospheric Environment* **33**, 3751-3763.

Woillard G. M. (1978) Grande Pile Peat Bog: a continuous pollen record for the last 140,000 years. *Quaternary Research* **9**, 1-21.

PART 1
SAMPLING AND ANALYTICAL TECHNIQUES

- Chapter 1.1 -

Suggested protocol for collecting, handling and preparing peat cores and peat samples for physical, chemical, mineralogical and isotopic analyses

Nicolas Givelet[a‡], Gaël Le Roux[b], Andriy Cheburkin[b], Bin Chen[b], Jutta Frank[b], Michael E. Goodsite[c], Heike Kempter[b], Michael Krachler[b], Tommy Noernberg[c], Nicole Rausch[b], Stefan Rheinberger[b], Fiona Roos-Barraclough[#a], Atindra Sapkota[b], Christian Scholz[b], and William Shotyk[b*]

[a] Institute of Geological Sciences, University of Berne, Baltzerstrasse 1-3, CH-3012 Berne, Switzerland.
[b]Institute of Environmental Geochemistry, University of Heidelberg, Im Neuenheimer Feld 236, D-69120 Heidelberg, Germany. E-mail: shotyk@ugc.uni-heidelberg.de; Tel: +49 (6221) 54 4803; Fax: +49 (6221) 54 5228
[c]Department of Chemistry, University of southern Denmark, Campusvej 55, DK-5230 Odense M.
[‡]*Present affiliation: Institute of Environmental Geochemistry, University of Heidelberg, Germany. E-mail: givelet@ugc.uni-heidelberg.de*
[#]*Present affiliation: Chemical Analytical R&D, Cilag, Switzerland.*
* To whom correspondence should be addressed

Journal of Environmental Monitoring 6, 481-492 (2004)

Abstract

For detailed reconstructions of atmospheric metal deposition using peat cores from bogs, a comprehensive protocol for working with peat cores is proposed. The first step is to locate and determine suitable sampling sites in accordance with the principal goal of the study, the period of time of interest and the precision required. Using the state of the art procedures and field equipment, peat cores are collected in such a way as to provide high quality records for paleoenvironmental study. Pertinent field observations gathered during the fieldwork are recorded in a field report. Cores are kept frozen at -18 °C until they can be prepared in the laboratory. Frozen peat cores are precisely cut into 1 cm slices using a stainless steel band saw with stainless steel blades. The outside edges of each slice are removed using a titanium knife to avoid any possible contamination, which might have occurred during the sampling and handling stage. Each slice is split, with one-half kept frozen for future studies (archived), and the other half further subdivided for physical, chemical, and mineralogical analyses. Physical parameters such as ash and water contents, the bulk density and the degree of decomposition of the peat are determined using established methods. A subsample is dried overnight at 105 °C in a drying oven and milled in a centrifugal mill with titanium sieve. Prior to any expensive and time consuming chemical procedures and analyses, the resulting powdered samples, after manual homogenisation, are measured for more than twenty-two major and trace elements using non-destructive X-Ray fluorescence (XRF) methods. This approach provides lots of valuable geochemical data, which documents the natural geochemical processes, which occur in the peat profiles and their possible effect on the trace metal profiles. The development, evaluation and use of peat cores from bogs as archives of high-resolution records of atmospheric deposition of mineral dust and trace elements have led to the development of many analytical procedures which now permit the measurement of a wide range of elements in peat samples such as lead and lead isotopes ratios, mercury, arsenic, antimony, silver, molybdenum, thorium, uranium, rare earth elements. Radiometric methods (the carbon bomb pulse of ^{14}C, ^{210}Pb and conventional ^{14}C dating) are combined to allow reliable age-depth models to be reconstructed for each peat profile.

Introduction

The use of peat cores from bogs in paleoenvironmental studies has increased dramatically during the last decade.[1-6] The reasons for this are not only that peat cores from ombrotrophic bogs are excellent archives of many kinds of atmospheric particles: soil dust, volcanic ash, phytoliths, anthropogenic aerosols, and many trace elements but peat bogs are also economically attractive archives because the concentrations of trace elements such as mercury (Hg) and lead (Pb), are sufficiently high that they are much more accessible by conventional methods of analysis than other archives of atmospheric deposition such as ice cores. Unlike glacial ice which is restricted to Alpine and Polar regions, peatlands are widely distributed across the globe, accounting perhaps 5% of the land area of the Earth.[7] There is growing evidence that undisturbed bogs have faithfully preserved the historical records of a wide range of trace metals, despite the low pH and abundance of dissolved organic acids in the waters, and the seasonal variations in water table (and impact which this may have on redox state). In the case of a metal such as lead, for example, the historical record of atmospheric Pb deposition is so well preserved in undisturbed bogs[8] that our ability to read and interpret the peat bog records is largely independent of chemical processes taking place within the bog itself, but can depend to a large extent on the methods used to collect, handle, and prepare the samples for analysis.[9] Moreover, the lack of a commonly used, validated protocol has hindered the interpretation and comparison of peat core metal profiles from different laboratories within the international community. Therefore, to compare the published peat bog records with one another or to other archives (e.g. lake sediments, ice cores, tree rings), and for detailed reconstructions of atmospheric metal deposition, a comprehensive protocol for working with peat cores is warranted.

Since the first cores for chemical analysis were collected at Etang de la Gruère in the Jura Mountains, Switzerland, in the autumn of 1990,[10] many changes and developments have been made with respect to the practical aspects of this work. The present paper shows that the effects of core compression during sampling, the spatial resolution obtained by core cutting, as well as the accuracy and precision of peat core slicing can very much affect the measured record of trace element concentrations and enrichment factors (EF). Moreover, in this paper we have summarized the refinements made to the methodological procedures and analyses, which have been developed by our research group over the years, to share these with the international community. We hope that the protocol described here can serve as a guideline for future paleoenvironmental studies using peat cores from bogs. Improvements to the description of the coring sites and the cores themselves, the accuracy and precision of slicing techniques and sub-sampling, as well as the physical and chemical analytical methods employed and the dating methods used to model the age-depth relationship, will help to ensure that the results obtained by different research teams are directly comparable.

Background to the problem

Comparison of two peat bog records of atmospheric lead pollution from Étang de la Gruère in Switzerland (EGR) have shown that while the general agreement between the two cores (EGR, cores 2F and 2K) is very good, there are also some differences.[9] One difference is revealed by the concentration profiles of anthropogenic Pb. The 2F core reveals two pronounced peaks of nearly identical Pb EF during the 20th century, but in the 2K core the more recent of these two is less pronounced (Fig. 1). Here, possible reasons for this difference are explored: differential core compression during sample collection, the relative thick peat slices (3 cm) used to represent the individual samples, and from the imprecision of the cutting technique used to section the cores.

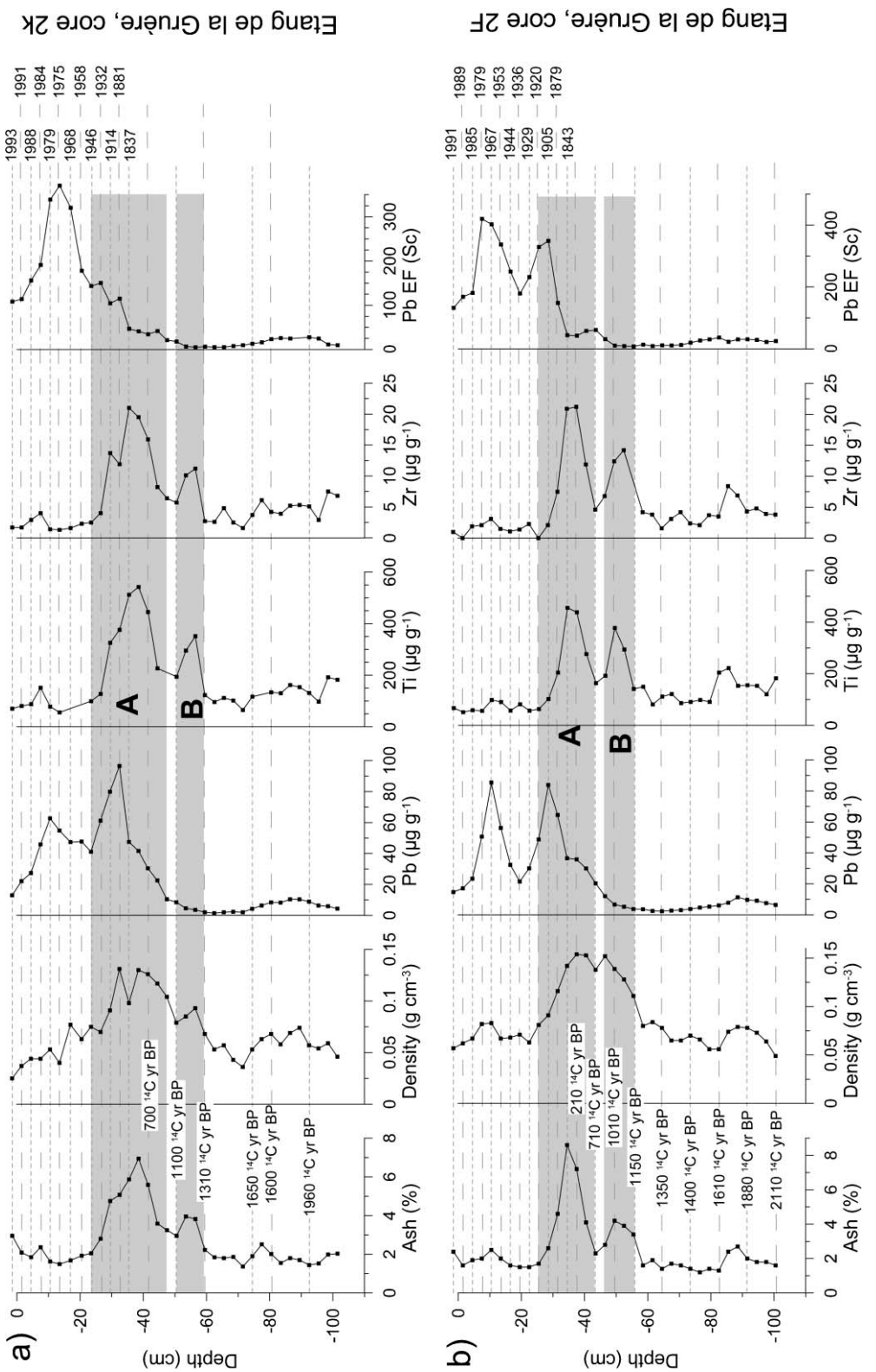

Figure 1 : a) Ash content, bulk density, concentrations of Pb, Ti, Zr, and Pb EF in the 2K core. b) ash content, bulk density, concentrations of Pb, Ti, Zr, and Pb EF in the 2F core. Maximum concentrations of Ti and Zr are indicated beside the peaks identified by the shaded bars. Pb EF calculated using Sc (relative to Earth's Crust). Age dates shown on the right hand side of box b) were obtained using ^{210}Pb, age dates within box b) are radiocarbon ages, expressed as conventional radiocarbon years Before Present.

1. Effects of core compression on anthropogenic Pb concentrations

A summary of some physical and chemical properties of the two peat cores is given in Figure 1. In general, both profiles contain a zone of enhanced peat humification from ca. 20 to 60 cm, which is visible upon inspection of the cores in the field (darker colour, finer texture, fewer visible plant remains). This zone is also revealed in each core by the elevated bulk density values at these depths, as well as reduced pH values and lower yields of extractable porewater (Fig. 2). However, there are some discernible differences between the two cores. First, the ash content profile shows significantly higher maximum ash content in the 2F core (8.6 %) compared with 2K (6.9 %). Second, the maximum bulk density in the 2F core (0.15 g cm^{-3}) exceeds that of 2K (0.13 g cm^{-3}). Both of these changes suggest that the 2F core experienced compression in the vertical direction, relative to the 2K core. At the time which core 2F was collected (26. August, 1991), the bog surface was very dry; with the depth to water table approximately 70 cm below the peat surface. During these conditions, it is very difficult to obtain a peat monolith without compressing the core, especially with the abundance of roots of *Ericaceous* shrubs and *Eriphorum* fibres, which dominate the near surface layers of the peat, profile. Comparison of the ash content and bulk density profiles introduces (Fig. 1) the suspicion that the 2F core was compressed, relative to 2K, during core retrieval.

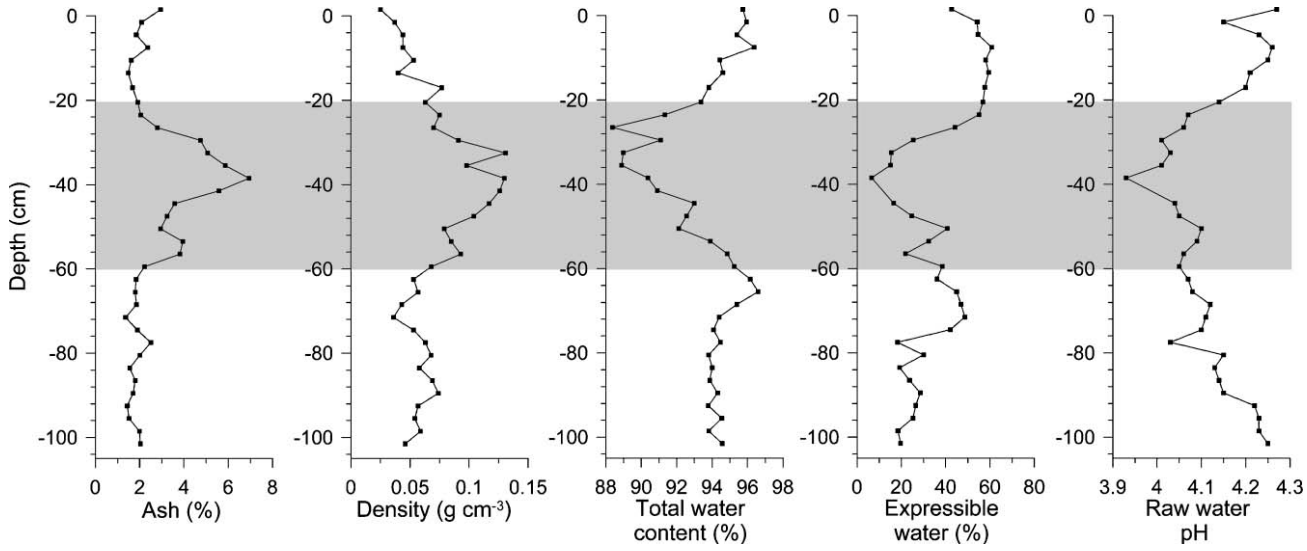

Figure 2 : Ash concentration, bulk density, total water content, expressible water, and raw water pH, 2K core.

The abundance and distribution of total Pb concentrations exhibit striking differences: in 2F, there are two nearly identical peaks in Pb concentration, whereas in the 2K core the deeper, older peak is clearly superior (Fig. 1). The concentrations of Pb at these depths exceed the LLD (0.4 µg g^{-1}) by more than two orders of magnitude, and in this concentration range the accuracy and precision of the Pb measurements using EMMA XRF are better than 5 %.[11] Thus, the difference in the abundance and distribution of Pb cannot be explained in terms of analytical error. Titanium and Zr both show two pronounced peaks in each core, but the ratios between the two peaks differ (Fig. 1): in the 2K core, the ratio of Ti and Zr in peak A to peak B are 1.5 and 1.9, respectively; the corresponding ratios in 2F are 1.2 and 1.5, respectively. Thus, soil-derived mineral material is relatively more abundant in the A peak of the 2K core than the A peak of the 2F core. To say it another way, Pb, Ti, and Zr are relatively more abundant in the B peak of core 2F compared with core 2K. This difference may simply reflect the extent of natural variation with a

given area at a given time, as observed previously using *Sphagnum* mosses collected from a given bog during a single year.[12] However, if both Pb and Ti have been accidentally increased at any point in the 2F peat core by vertical compression while coring, then both elements would increase in concentration to the same extent, and this would have no net effect on anthropogenic Pb calculated as described earlier. Thus, the direct effect of compression in the 2F peat core on the concentrations of Pb and Ti cannot explain the differences in the relative abundance of anthropogenic Pb between the two cores.

2. Effects of core compression on the age-depth relationship

To further evaluate the possibility that the 2F core may have been compressed and to try to understand the possible importance of this process, the age depth relationship has been plotted for the entire length of both cores (Fig. 3a) and for only the uppermost layers, which were dated using ^{210}Pb (Fig. 3b). Both graphics show clearly that there has been some vertical displacement of the 2F core, relative to 2K. First, the arrows in Fig. 3a show an inflection point where age does not measurably change with depth; in the 2F core, this is found between 64 and 74 cm, but in the 2K core from 74 to 81 cm. The change in ^{210}Pb age with depth shows that the 2F core has certainly been compressed, relative to 2K, in particular in the range ca. 10 to 30 cm (Fig. 3b).

Also shown in Fig. 3c is the incremental age, in calendar years, for the individual slices of 2K samples pre-dating ca. 1980. This information is included to emphasize the increase in age of each peat slice with increasing depth. In the range where the 2F core was compressed, the individual peat slices represent from 4 to 33 years of peat accumulation. The effect of compression on age therefore becomes increasingly important with depth, as a greater proportion of older material becomes compressed into a given volume. The extent of compression can be estimated by assuming that any given ^{210}Pb age should be found at the same depth in each core. Assuming this ideal case, the vertical difference between the two cores is approximately 3 cm at 1920, 6 cm at 1940, 12 cm at 1960, and 4 cm at 1980 (Fig. 3c).

Despite these differences and the causes to which they are due, compression of the peat core will affect the activity of ^{210}Pb and the concentrations of Pb and Sc. Compression of the peat core alone, therefore will not affect the chronology or intensity of the changes in anthropogenic Pb concentrations.

3. Effects of hand slicing of peat cores on the chronology of anthropogenic Pb

When the two peat cores were sectioned, they had been removed from the bog and were cut fresh, at ambient temperature, by hand using a bread knife. A measuring tape was attached to the cutting board and used to guide the eye while positioning the knife blade. While the intended thickness of each slice was 3 cm, no effort was made to determine the accuracy or precision of the cuts. Using the green plant material as a guide to the location of the living, biologically active layer, this section was cut away first, and is the first sample of each core. Strictly speaking, however, this material is living plant matter, and not peat. After cutting away the living layer, the top of the core became the “zero” depth, and all subsequent cuts, in increments of ca. 3 cm, were made relative to this point. Given the differential compression between the two cores and the differences in age-depth relationship, modelling of curve smoothing and combined smoothing plus compression scenarios indicates that the thickness and position of peat core slicing can significantly affect the intensity of a peak in anthropogenic Pb (Fig. 4) by incorporating overlying and underlying material of lower anthropogenic Pb concentration. Not only could this process affect the calculated concentration of anthropogenic Pb per slice, but also the chronology of the enrichment, as determined using ^{210}Pb, as material of younger and older age becomes incorporated into any given slice.

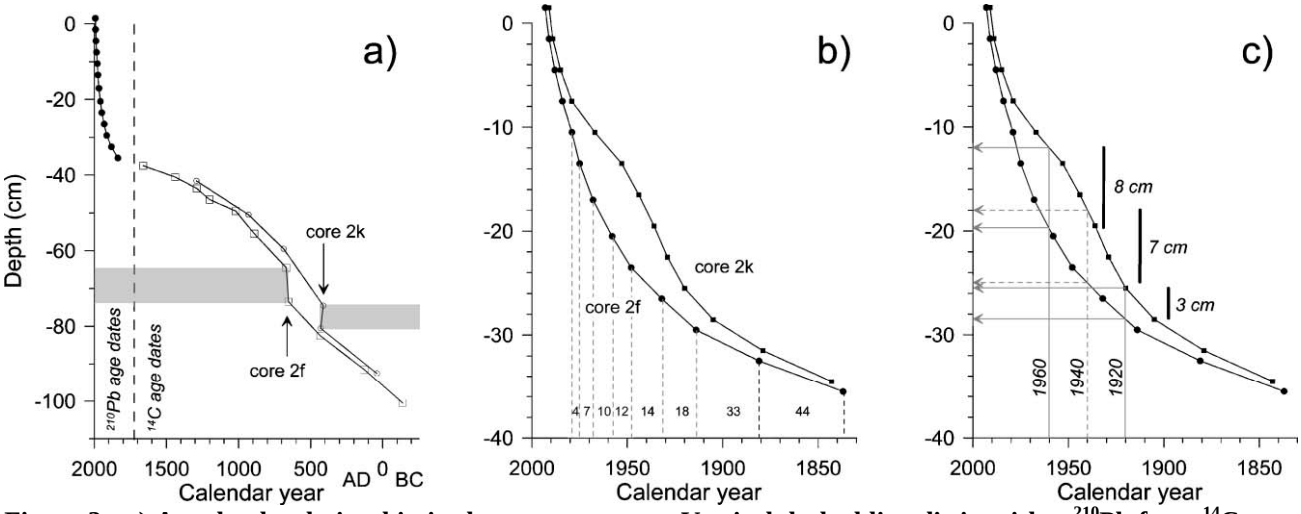

Figure 3 : a) Age-depth relationship in the two peat cores. Vertical dashed line distinguishes ^{210}Pb from ^{14}C age dates. Notice that both ^{14}C curves show an inflection, indicated by the arrows, but that this section is deeper in the 2K core (shaded bar on right) compared to 2F (shaded bar on left). b) ^{210}Pb age dates of the two peat profiles. Numerical values between vertical dotted lines indicate the number of calendar years represented by each slice. c) Assuming that the ^{210}Pb age should represent the same depth in each peat core, the dotted line indicates the vertical displacement (cm) between the two cores at AD 1920, the dashed line at AD 1940, and the solid line at AD 1960.

4. Effect of the thickness of a peat slice on the signal resolution

The resolution and magnitude of any given peak depends on the thickness of the slice. The thinner the slice is, the better will be the resolution of the record. Moreover, as shown in Figure 1, over a small vertical distance (ca. 50 cm), there are extreme changes in Pb concentration, as well as significant changes in ash content and bulk density. Therefore the thickness of the slices is of greatest importance in the uppermost peat layers, which represent the most critical time period in terms of pollution reconstruction (i.e. the past two centuries since the start of industrialisation). However, even in the lower peat layers, the thickness of the slices is also important. For example, short-lived events such as the deposition of volcanic ash can be clearly resolved using 1 cm slices (Fig. 5). Thicker slices, however, not only provide poorer resolution (Fig. 5), but they also prevent the event from being accurately age-dated. Taken together, the available evidence suggested that the protocol used during the past decade had to be improved. Specifically, cutting the cores very precisely into 1 cm slices will maximize the signal/noise ratio of the peaks in metal concentration and therefore greatly contribute to improving the accuracy, reproducibility and reliability of peat bog archives (Figure 6).

Improvements and proposed protocol

Since EGR 2F and 2K cores were collected in 1991 and 1993, respectively, several changes have been made in the collection, handling and preparation of peat cores to improve the accuracy and precision of peat bog records of atmospheric dust and trace metal deposition. The most important changes are summarised below.

1. Field sampling strategy

The success of paleoenvironmental studies using peat cores as archives largely depends on the ability to select appropriate peatlands, which have preserved high-quality paleoenvironmental records. Therefore careful selection of sites and coring locations within the sites are critical elements of field research. Although, the strategy will vary depending on the purpose of the study and the site itself, several general considerations can be helpful to design suitable field sampling strategies and for retrieving peat cores. Since comprehensive field observations are a very valuable aspect of the survey, pertinent information that should be recorded are listed and discussed below.

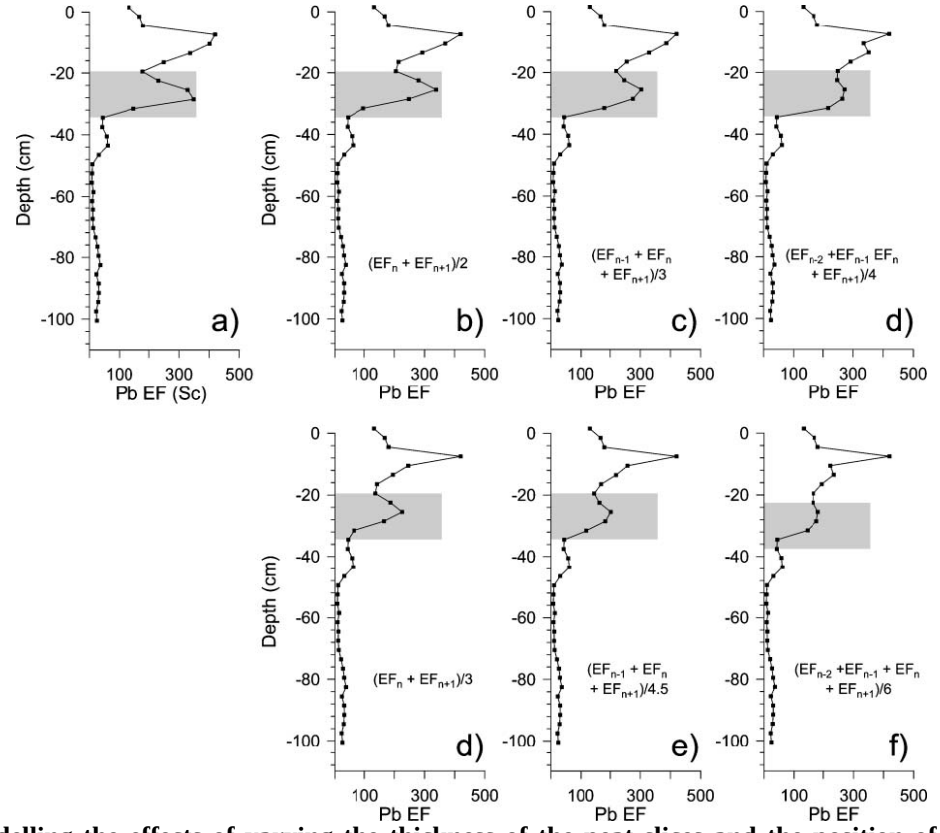

Figure 4 : Modelling the effects of varying the thickness of the peat slices and the position of the cut on the vertical distribution of Pb EF, from 10.5 cm to 32.5 cm in the EGR 2F core. The original data set is given in a) where the Pb EF (calculated using Sc as the reference element and the Earth's Crust as reference point) is plotted versus depth. b) to d) simulate the effect of varying the position of the cut, but not the thickness of the peat slice. e) to g) simulate the effect of varying both the position of the cut and the thickness of the slice.

1.1. Site selection

To reconstruct the deposition history of atmospheric particles using peat cores, selection criteria should include the morphology of the peatland (topography and depth of peat accumulation), character of peat (visual inspection of the botanical composition, degree of decomposition, moisture content and abundance of mineral matter), possible damages to the peatland and to the peatland hydrology (peat cutting, drainage, dams), possible use of the peatland for forestry or agriculture, and distance from human activities.

Not all peatlands are appropriate for the reconstruction of the changing rates of atmospheric metal deposition and it is worthwhile to pay particular attention on the selection of the peatland.

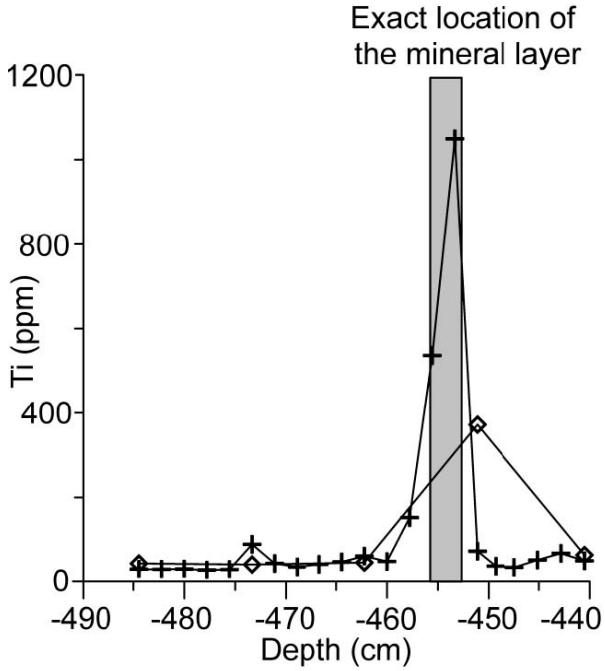

Figure 5 : Concentration of Ti (ppm) between 440 and 490 cm depth from a peat core from the Black Forest, Germany.[28] Titanium concentrations were measured in every second sample, cut into 1 cm slices; those are reported as crosses (+) whereas average Ti concentrations for five samples (10 cm peat section) are indicated by diamonds (◇).

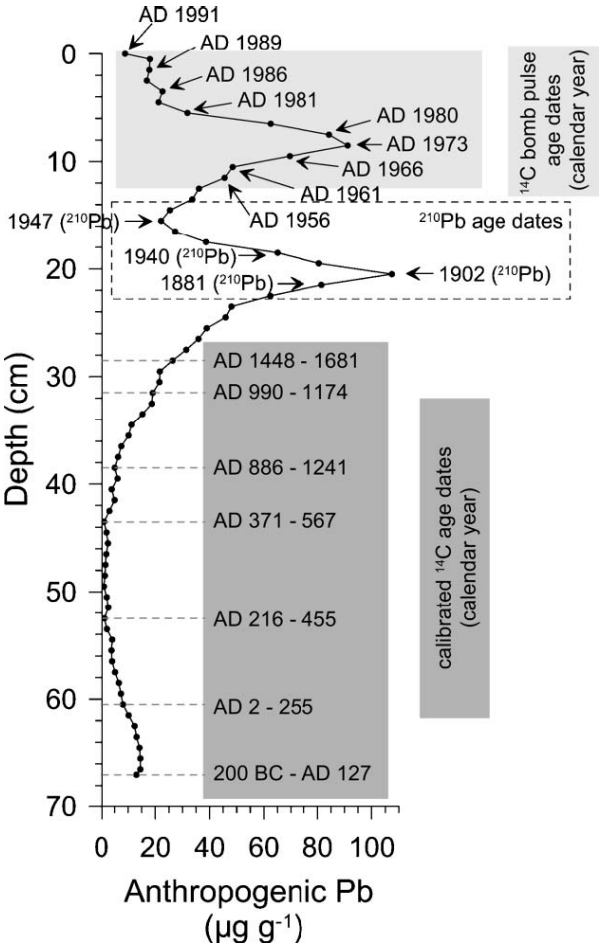

Figure 6 : Concentration of Pb (ppm) for the Wardenaar peat profile 2G from Étang de la Gruère, Switzerland (Shotyk, unpublished). This core was collected the same year as the EGR 2F core (i.e. 1991). It shows the kind of resolution, which can be obtained using 1 cm slices (compare the 2F and 2K cores (Fig. 1) which were cut into 3 cm slices) and accurate age dating. The upper layer age dates have been calculated using the ^{14}C "atmospheric bomb pulse curve" (Goodsite et al., Radiocarbon 42(2B): 495 (2001)).

The quality of the paleoenvironmental record for many trace elements is mainly controlled by the trophic status of the peatland as revealed by e.g. the botanical composition and abundances of mineral matter. Ombrotrophic ("rain-fed") bogs should be favored over other types of peatlands, as they receive water solely from atmospheric precipitation (rain, snow) falling onto their surface. Ideally, the most valuable part of a bog is the raised dome. Neither groundwater nor surface water runoff from other areas can reach the raised part of the bog, as it is above the level of the local groundwater table. Moreover, ombrotrophic bogs provide records with better time resolution than minerotrophic deposits, mainly due to the lower degree of organic decomposition. Both biological and chemical characteristics that can be used in the field and in the lab to establish the existence of an ombrotrophic zone are presented elsewhere in detail.[13] The mineralogical and chemical composition of the basal sediment on which the peatland is resting should be also considered. Weathering of minerals from the underlying rocks and sediments could be an important source of ions which migrate upward into the peat by diffusion.[10] There is a great difference between the trophic status of peat profile in a bog forming on calcareous versus granitic substratum, with carbonate weathering clearly supplying more metals to the basal peat layers. Therefore, ombrotrophic bogs underlain by granites are chemically less affected by upward diffusion of ions and should be favoured over bogs growing on carbonate rocks.

If ombrotrophic bogs are common in temperate and boreal latitudes, they are scarce in sub-Arctic and Arctic latitudes.[7] Therefore at high latitudes, minerotrophic peat deposits may have to be used as archives of atmospheric metals even though they are fed both by atmospheric and terrestrial inputs. Recent studies have shown that at some predominantly minerotrophic peatlands, mercury and lead may be supplied exclusively by the atmosphere and therefore can still provide a record of the changing rates of atmospheric deposition of those elements.[14-17] Such reconstructions, however, must be interpreted with great caution and on an element by element basis because some metals of interest e.g. nickel[18] and uranium[19] are certainly enriched in minerotrophic peat due to weathering inputs.

Before selecting the exact site for collecting peat profiles at a peatland, the site morphology must be known. If this is not the case, it could be established by depth profiling at least two transects at 90°. This

process will help selecting the deepest ombrotrophic part of a bog or the deepest organic accumulation of a minerotrophic peat deposit. Comparison of mercury and lead fluxes to hummocks and hollows of ombrotrophic bogs suggest that cores from both locations are recording trends in atmospheric deposition of Hg and Pb, but that hollow cores are recording lower input values than hummock cores, apparently due to a larger component of dry and occult (fog) deposition at hummocks than at hollows.[20] Therefore sampling sites located in "lawns", or at the transition between hollow and hummock are considered to be optimal and therefore recommended.

Prior to peat core collection, permission to retrieve geologic and environmental samples should be secured from the owner of the land if necessary. This is especially important in the case of nature reserves and other protected areas where many of the remaining central European raised bogs are found.

1.2. Core collection

The low density and the unsaturated environment of the topmost layers of a peat bog make the collection of good quality peat cores challenging. It is difficult to cut these layers as they are easily trampled and compressed. Moreover, the upper layers of a peat bog represent the past decades, which is the most critical and interesting period in terms of atmospheric pollution, not only for trace metals and organic contaminants, but also for fallout radionuclides. The main concern about this section is to collect surface layers as an undisturbed continuous peat profile extending as far back in time as possible in an effort to reach "natural background" values. By using procedures developed by our research group, all fieldwork is completed in such a way as to minimize the impact on the environment, utilizing the latest techniques and best available technology for sampling, handling and preparing the materials.

Modified Wardenaar corer

The topmost layers of peat can be collected using a 10 cm × 10 × 100 cm Wardenaar peat profile cutter[21] which is commercially available. Our 1 m Wardenaar corer with XY dimensions 15 cm × 15 cm, was home-made using a Ti-Al-Mn alloy and includes a serrated cutting edge; this new cutting edge cuts more easily through dwarf shrubs (e.g. *Ericaceous* shrubs) and *Eriphorum* root fibres. This feature, combined with the larger cross sectional area means that any given slice undergoes less compression in the Z (vertical) dimension. Moreover, the enlargement of the XY dimensions to 15 cm of the new Wardenaar corer compared to the older version (10 cm) provides enough peat sample material to conduct a wide range of analyses and still to be able to preserve part of the material as an archive for futures work, even using thin slices (i.e. 1 cm). The state of the art of the modified Wardenaar corer and the best way to collect a good quality peat core from the surface layers of a bog are described in detail elsewhere.[22]

During extraction, some compression of the peat core is unavoidable. However, the compression can be measured, using the bog surface as a reference. After extraction, the Wardenaar corer is laid horizontally on the bog surface, on a large sheet of plastic; the top half of the Wardenaar corer is removed, exposing the peat monolith. This core is described visually in the field (length, colour, texture, plant remains, moisture, special layers) and photographed. The core is inspected for modern plants of the bog surface, which may have "contaminated" the outside of the core; these are carefully removed using a small knife. The exposed surface and two sides of the core are wrapped in polyethylene cling film. A wooden core box built specifically for the Wardenaar core is lined with plastic (a large sheet, or two large sheets, is made using plastic garbage bags). The plastic-lined wooden core box is placed over the peat core. Two people lift the bottom half of the Wardenaar corer, flip it carefully backward 180°, allowing the peat core to slide down into the box. The surface

of the core is wrapped in polyethylene cling film, with the film pressed down around the sides of the core and ends using a plastic spatula.
The core is covered with plastic, labelled and the lid attached using screws. In this way, handling of the core in the field is kept to a minimum.

Belarus corer
A Belarus (Macaulay) peat sampler is used for deeper peat layers.[21] Two versions of this corer are actually used: stainless steel and titanium (Ti). The titanium corer, which is much lighter, was constructed using the same alloy as for the Wardenaar corer.
Cores are removed from two holes adjacent to the hole from the Wardenaar core, approximately 20 cm apart, in parallel overlapping design. Peat cores are carefully packed onto plastic-semi tubes which are lined with polyethylene cling film: while still in the peat corer, the peat sample (a semi-cylinder ca. 50 cm long and 10 cm wide) is wrapped with polyethylene cling film and a plastic semi-tube is placed on top; the corer is gently flipped backwards 180°, and holding the semi-tube, the core is carefully slid away from the corer. Again, the cores are described and photographed without touching them. The core is wrapped with polyethylene cling film, labelled, and packed in rows in a transport aluminium box.

Motorized corer for frozen peat
A unique peat sampler was designed and built by Mr. Tommy Nørnberg for obtaining continuous samples of frozen peat in the Arctic. Up to 10 meters of frozen peat in 70 cm sections can be removed using this corer. The sampler and the coring technique is described in detail elsewhere.[23]

Cores are kept cool until they can be frozen: this is done soon as possible after collection, and kept frozen at -18 °C until they can be prepared in the laboratory. Cores collected from frozen peat deposits are shipped frozen back to the laboratory.

1.3. Field observations

Pertinent field observations that should be gathered during the fieldwork include sampling date and time, sampling site significance and location. The precise location of the core collection should be indicated on a topographical map and the GPS coordinates recorded. Because it may be very useful to return to the coring site at some future date, burying a plastic soda pop bottle containing a handful of steel just below the surface of the coring site will allow the exact site of core collection to be found later, using a metal detector. This also helps to avoid possible further peat collection at the same location, as the peat stratigraphy may have been affected by the coring session. Notes on colour, component, length, depth, core compression and other details (e.g. layers of wood, charcoal) are also information that should be recorded. As noted earlier, core compression during sample collection can be a problem, because of secondary effects on the metal concentration profiles and/or the age-depth relationship. Therefore, coring in spring or early summer when the peatland is at its wettest is recommended. Additional pertinent information that should be recorded includes maximum depth of peat accumulation at the collection site and possible disturbance. Collection of representative surface plant species may serve as a valuable reference for the plant material, which constitutes the fossil botanical assemblage of the peat cores.
In order to achieve consistency in recording such data, a field report should be written. This primarily provides a public report of the fieldwork, detailing how and where peat and other geologic or environmental samples were taken for subsequent dating and analysis. The Field Report format developed by M.E. Goodsite is highly recommended[24] and is available for downloading for free use at http://www.rzuser.uni-heidelberg.de/~i12/eergebnisse.htm.

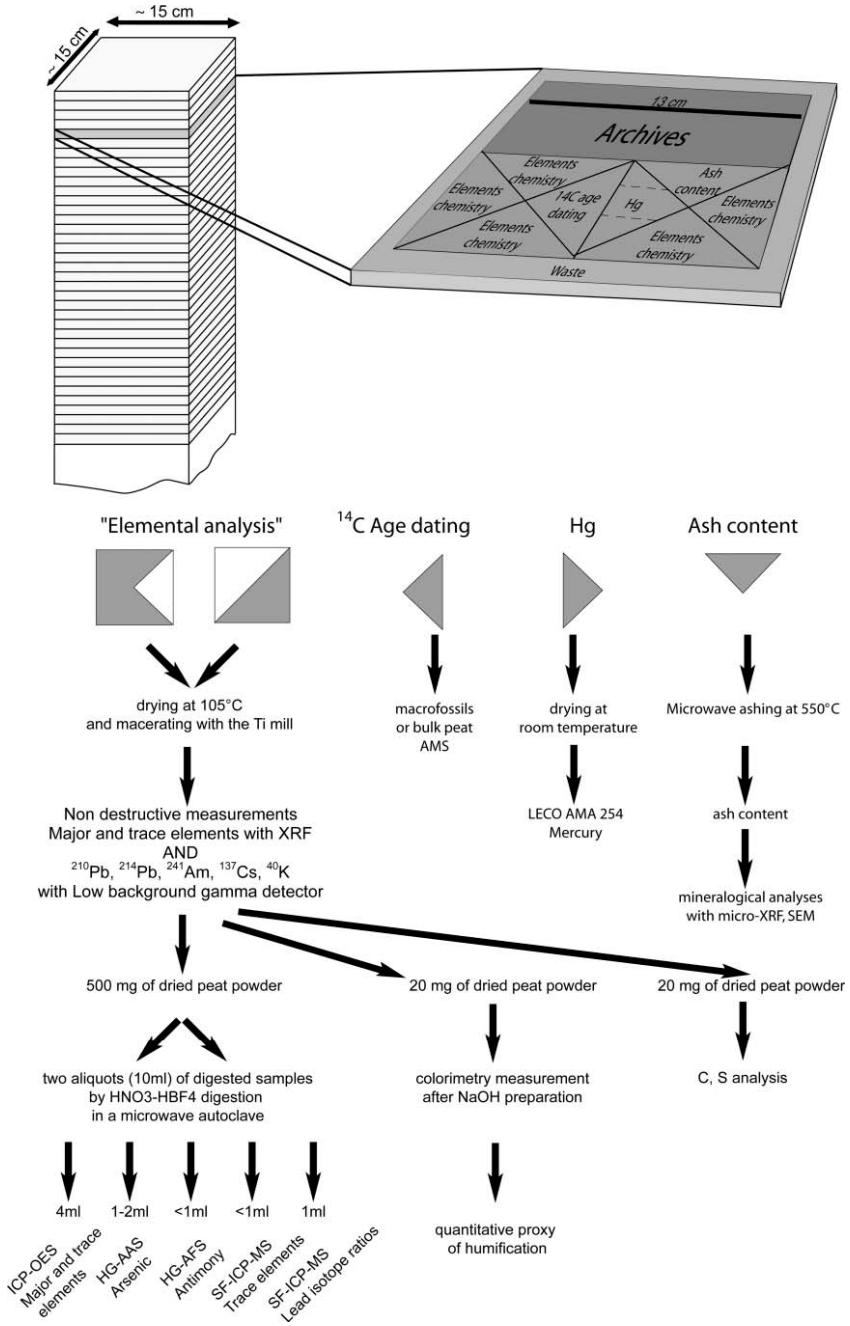

Figure 7 : Analytical flow chart and sub-sampling strategy for a peat slice from a Wardenaar core. The outside edges of the slices are systematically removed to waste to ensure that only the uncontaminated part of each sample is used for study. Part of the slice is archived for possible future studies. Peat triangles are sub-sampled, oriented to ensure that, for any given analysis, the sub-samples are taken from the same position in each slice.

2. Samples preparation

To have a rapid, approximate description of the geochemistry of a peat core, a sacrificial core may be sliced immediately in the field using a serrated stainless steel knife into 3 cm slices. Using plastic gloves, each slice is placed in a plastic bag and the bag squeezed by hand to express the pore water. The pore waters may be analyzed for pH, major element cations and anions, and DOC.[10] Slicing the core by hand with a knife has some advantages, as it can provide a rapid survey of the geochemistry of the peat profile if the pore waters are analyzed. However it only provides an approximate description of the geochemistry, and this preparation

procedure is not suitable to reconstruct high-resolution records of atmospheric metal contamination.

2.1. Slicing the cores

With respect to high-resolution records, Wardenaar, Belarus and Nørnberg peat cores are cut frozen in the lab into 1 cm increments using a stainless steel band saw with stainless steel blades. The width of the blade is 1 mm, so ca. 10% of each slice is lost during cutting. The accuracy of the thickness of theses slices is better than ± 1 mm. For Belarus and Nørnberg cores, a slicing system was designed and constructed as described elsewhere.[23] A similar system made of an Omega SO 200a band saw and a precision cutting table is used to slice the Wardenaar cores. Because the cores are large and long, they are heavy (~23 kg) and the cutting table is necessary for precise cutting. The individual slices are subsequently placed on a polyethylene cutting board and the outer 1 cm of each slice is trimmed away using a 13 × 13 cm polyethylene plate and either an acid rinsed ceramic knife or a Ti knife (Fig. 7). The outside edges are systematically discarded, as those could have been contaminated during the sampling and preparation procedures by layers enriched in mineral matter such as tephra layers (e.g. Faroe Island cores), or where there are very high metal concentrations (due to intense atmospheric pollution). The cutting board and knife are rinsed with deionised water three times between each slice. Then slices are packed into labelled zip-lock plastic bags for storage and further preparation.

2.2. Sub-sampling Strategy

Great care has to be focused on the orientation of each slice during the slicing session with respect to its original position when it was in the peat monolith. To guarantee the reconstruction of high-resolution records, peat material for a given analysis should be sub-sampled along a conceptual micro-core within the Wardenaar core and therefore at a similar location within the oriented slices.

A sub-sampling strategy is defined for each individual core depending of the main objective of the study. An example of the approach we use is shown in Figure 7. Two 6 × 6 cm squares are removed using a polyethylene plate. The squares are divided into four triangles by cutting each square along its diagonal. Each triangle is identified with respect to its position within the peat slice, packed into labeled bags and reserved for previously defined analyses (Fig. 7). Part of the material is archived at -18 °C for possible future studies, and the remainder of the sub-samples will be processed for physical, chemical, mineralogical and isotopic analyses.

2.3. Drying and milling

The peat samples are dried at 105 °C in acid-washed Teflon bowls, and macerated in a centrifugal mill equipped with a Ti rotor and 0.25 mm Ti sieve (Ultra centrifugal Mill ZM 1-T, F.K. Retsch GmbH and Co., Haan, Germany). This yields a very fine, homogeneous powder with average particle size of ca. 100 µm (and Gaussian particle size distribution). For finer powder (e.g. for slurry sampling AAS), the direction of the sieve can be reversed. For samples rich in mineral matter (e.g. tephra layers) and for organic-rich sediments, an agate ball mill is used instead. The powdered samples are manually homogenised and stored in airtight plastic beakers. The milling is carried out in a Class 100 laminar flow clean air cabinet to prevent possible contamination of the peat samples by lab dust. In the laboratory, all of the sample handling and preparation is carried out using clean laboratory techniques. Peat powder stored for longer than one year in humid conditions should be re-dried prior to analysis following similar procedures for certified standard reference materials (e.g. plant SRMS from NIST, BCR, or IAEA).

3. Analyses

3.1. Physical analyses

The precision of the bulk density measurements is of great importance for the reconstruction of records of metal contamination as the bulk density data is used to calculate the rates of metal accumulation. Until recently, the centers of the peat slices were sub-sampled using a sharpened stainless steel tube (16 mm diameter) and these plugs used to determine the dry bulk density. The height of each plug was measured to an accuracy of 0.1 mm and the volume calculated. After recording wet weights, plugs were dried at 105 °C overnight and the dry mass was weighed to 1 mg. Later, in order to decrease the discrepancy of the diameter of the plugs induced by the operator, a hand-operated stainless steel press was used to recover plugs of 20 mm diameter with an accuracy of 0.1 mm.[23] However, with respect to the heterogeneity of peat material within a slice, especially the upper layers of modern accumulation, and the unknown, possibly important uncertainties in the measurement of the volume and weight of a small plug of peat material, we found that the determination of bulk density was an important source of error in the calculation of rates of metal accumulation. For example, the calculation of Hg accumulation rates in a peat core from southern Ontario using the minimum and the maximum value of bulk density determined using four plugs for each slice show the calculated Hg accumulation rates of mercury may be ± 10 % of the accumulation rate value calculated using the average bulk density value of the four plugs (Fig. 8). This is mainly explained by the heterogeneity of the peat material within a given slice, especially in the surface peat layers which are poorly decomposed. Therefore the use of larger volume samples, such as the 6 × 6 cm rectangle as recommended in the previous section, should improve the quality of the bulk density measurement because they are more representative of the slice, thereby also improving the accuracy of the rate of metal accumulation calculation.

The degree of decomposition of the peat is measured by colorimetry on alkaline peat extracts at 550 nm using a Cary 50 UV-visible spectrophotometer. The powdered peat samples (0.02g) are placed in test tubes and 8 % NaOH soln. (10 ml) is added. The samples are shaken then heated 95 ± 5 °C for 1 hour, then made up to 20 ml with deionised water, shaken and left to stand for 1 hour before being re-shaken and filtered through Whatman no. 1 filter papers. Samples are diluted with an equal quantity of deionised water directly before colorimetric measurement. The percentage of light absorption (% absorbance) in these extracts may be used as a proxy of peat humification.[25]

3.2. Chemical analyses

The development, evaluation and use of peat cores from ombrotrophic bogs as archives of high-resolution reconstructions of atmospheric deposition of mineral dust and trace elements have led to the development of many analytical procedures which now permit the measurement of a wide range of elements in peat samples.

Prior to any expensive and time consuming chemical procedure and analysis, measurement of major and trace elements in peat samples using the non-destructive and relatively inexpensive X-Ray Fluorescence (XRF) method is performed on all peat samples first. This method provides invaluable geochemical data that helps to document the natural geochemical processes, which occur in the peat profiles and their possible effect on the distribution of trace elements. Calcium (Ca) and strontium (Sr), for example, can be used to identify mineral weathering reactions in peat profiles, manganese (Mn) and iron (Fe) redox processes, bromine (Br) and selenium (Se) atmospheric aerosols of marine origin. Titanium (Ti) and zirconium (Zr) are conservative, lithogenic elements whose abundance and distribution reflects the variation in mineral matter concentration in the peat core.[26] One gram of dried, milled peat may be analysed for these and other

major and trace elements simultaneously (Y, K, Rb, Cr, Ni, Cu, Zn, As and Pb) using the EMMA XRF.[11,27] Titanium (Ti) may be analysed precisely using the new TITAN XRF spectrometer, which provides a lower limit of detection for Ti of only 1 μg g^{-1}. Both instruments measure the sample in powder form. Because the method is non-destructive, these same samples can be used again for other measurements (Fig. 7). Complete details about the design and construction of this instrument are presented in a separate publication.[28]

Mercury

Solid peat samples can be analysed for Hg using a direct mercury analyser (LECO AMA 254).[29] The main advantage of this approach is that no acid digestion of the peat sample is necessary. After air-drying overnight in a Class 100 laminar flow clean air cabinet, three subsamples, previously removed from a pre-selected, fresh portion of each slice, are analysed for total Hg, and the results of the three subsamples are averaged (Fig. 7). The detection limit of the instrument is 0.01 ng Hg and the working range is 0.05 to 600 ng Hg, with reproducibility better than 1.5%.

Acid digestion procedures

Other elements in solid peat samples can be quantified for a wide selection of trace elements using instrumental neutron activation analysis (INAA). As no certified reference material for trace elements in ombrotrophic peat was available until recently, INAA data served as a reasonable benchmark for the development of other analytical procedures requiring dissolution of peat samples. In this context, several digestion procedures for the acid dissolution of peat have been developed and evaluated using open vessel digestion as well as closed vessel digestion procedures on a hot plate or using microwave energy. No matter which digestion approach is considered, it is essential to completely destroy the silicate fraction of peat in order to release the trace elements that are hosted in the silicates. This can be achieved by the addition of HF or HBF_4 to the acid mixture, whereas the use of HBF_4 provides many advantages in that context and thus is highly recommended.[30,31]

Quantification of trace elements

Trace elements in these digestion solutions have been determined using ICP-MS, ICP-OES, HG-AAS and HG-AFS.[32-37] The large variety of analytical instruments available allowed several inter-method comparisons, which greatly benefit the quality of the analytical results (Fig. 7). Both ICP-MS and ICP-OES were used to analyse more than 25 elements, whereas work to date with HG-AAS and HG-AFS mainly focused on the determination of low concentrations of arsenic and antimony in peat.[37,38] Using ICP-MS, a powerful multi-element technique with low detection limits, it has been possible to establish complete chronologies of Ag, Tl, Pb, Cd;[39] Mo, U, Th;[19], the REE[30] and V, Cr, Ni.[18] A method has also been developed to determine major elements in acid digested peat samples using ICP-OES and this has been successfully applied to the determination of Al, Ca, K, Mn, Ti, Fe, Na, Sr, Mg concentrations. Again, measurements of international, certified, standard reference materials yielded results, which are in good agreement with the certified values.

Lead isotope measurements

Lead isotope ratios in peat can largely help to identify the predominant anthropogenic sources of Pb. Lead isotopes measurements can be performed using ICP-MS. We recently developed a method using sector field inductively coupled mass spectrometry (SF-ICP-MS) after acid digestion of peat powders using a high-pressure and high-temperature microwave autoclave.[40] The accuracy and precision of the ICP-SMS protocol was further evaluated using thermal ionisation mass spectrometry (TIMS) of selected samples and an in-house peat reference material. In general, the Pb isotope ratios determined using ICP-SMS deviated from the

TIMS values by less than < 0.1%. Given the throughput of the ICP-SMS compared to the TIMS (which requires chemical separation of Pb), the ICP-SMS approach offers great promise for environmental studies to fingerprint the predominant sources of anthropogenic Pb. In a few cases when improved accuracy and precision are needed, the Pb isotopes ratios in these selected samples may also be measured using thermal ionisation mass spectrometry (TIMS).

Quality control

Decreasing limits and thresholds require accuracy, comparability and traceability of analytical measurements for the determination of elemental content in peat material. Certified Standard Reference Materials of coals and plants from the National Institute of Science and Technology (USA), the International Atomic Energy Agency (Vienna), South Africa, the European Community, Poland, the Czech Republic, and China are analysed in triplicate as blind standards. However, to guarantee accuracy, quality control, quality assurance or validation of a measurement by means of certified reference material, the assessment of analytical results in certified reference materials must be as accurate as possible and every single step has to be fully evaluated. To date, the lack of a common certified peat reference material has hindered the quality assurance of the generated analytical data from different laboratories in the international community. There are ongoing efforts to fill the lack of a common certified peat reference material for working with peat material by developing a multi-element reference material for low-ash peat to be used by the international community.[41,42]

3.3. Mineralogical analyses

Mineralogical analyses of the inorganic fraction could be of particular importance to identify the origin and type of anthropogenic and natural particles deposited on the surface of the peat bog. However because of the very low inorganic content in ombrotrophic peat, it is very difficult to extract the deposited atmospheric particles. Moreover in the case of a general study also including bulk peat geochemistry, there may be only a small quantity of peat available for mineralogical analyses. Finally the extraction method used is dependent on the type of mineral investigated because the reagents and temperature used could modify the minerals by oxidation (e.g. sulphides) or dehydration (e.g. clays). However, prior to mineralogical analyses, samples should not be milled. Many methods for extracting minerals grains from the bulk peat matrix are available from the literature, some of them designed for the extraction of specific fractions such as tephra glasses[43,44] or recent anthropogenic particles.

One method used in our laboratory and proposed by Steinman and Shotyk[45] is to ash the peat at 550 °C, remove the carbonates and other inorganic components formed during the ashing process using dilute HCl. These samples are then ready for optical microscopy and could also be analysed after preparation using Scanning Electron Microscope (SEM w/EDAX). Another approach is to digest the peat with 65% H_2O_2 in a Teflon beaker on a hot plate. Every ca. three days, the reagents are poured off and a new solution of 65% H_2O_2 is added until there is no visible trace of organic matter. However, this procedure is time-consuming and could last more than two weeks. It is possible to use an ultrasonic bath to mechanically extract the minerals before and after each H_2O_2 attack. Individual mineral grains which are large enough could be also directly analysed by microscopic techniques such as microbeam XRF.[46]

3.4. Age dating

Establishing high quality chronologies is a critical feature of paleoenvironmental studies, especially for the last few hundred years, which have witnessed so many changes. A reliable and detailed chronology is essential if peat bogs are to be compared with other high-resolution archives such as polar ice, laminated lake sediments, tree rings, bryophytes, including herbarium specimens. Multiple techniques can be used to develop peat chronologies including analyses of short-

lived radioisotopes (^{210}Pb, ^{137}Cs, ^{241}Am, ^{14}C bomb pulse), historical pollen, chronostratigraphic markers, tephra layers, and fly-ash particles.[47]

Radiocarbon age dating

It should be relatively straightforward to establish radiocarbon-based chronologies for most Holocene peats used for paleo-environmental reconstructions. However, there are a number of problems to be considered in radiocarbon dating peat. In the past, ^{14}C age dating was typically done using the decay counting method on bulk samples. This method had the disadvantage of wasting a large amount of material, because several grams of dry peat were needed. Moreover, radiocarbon age dating of bulk samples can be problematic as it may lead to ^{14}C age inversions in cases where older peat layers have been penetrated by younger plant roots.[48] Therefore macrofossils of *Sphagnum* moss specifically selected and cleaned are ideal for radiocarbon dating as mosses have no root systems and therefore cannot introduce younger carbon to lower layers. Careful sample selection and cleaning (removing roots of other plants), pre-treatment (washed water followed by an acid-base-acid treatment) circumvents other potential problems such as the mobility of carbon in the peat profiles. However some movements of carbon can occur, especially of dissolved organic carbon; the translocation of younger carbon to deeper horizons by vascular plant roots or the possible "reservoir" effect involving translocation of older carbon to contemporary vegetation also are real concerns.

Age dates of plant macrofossils younger than AD 1950 can be obtained using ^{14}C by directly comparing the absolute concentration of ^{14}C in the sample to the general-purpose curve derived from annually averaged atmospheric $^{14}CO_2$ values in the northernmost northern hemisphere: post-1950 ^{14}C concentrations in the atmosphere are elevated compared to natural levels due to atomic weapons testing. This approach which effectively matches the ^{14}C concentrations (percent modern carbon, or PMC) in successive plant macrofossils to the increase (since AD 1950) and subsequent decrease (since AD 1963) in ^{14}C concentrations is the so called "bomb pulse curve of ^{14}C" and has been successfully used to date peat accumulation in Denmark and in southern Greenland.[49] This comparatively new dating method has been found to provide high-resolution age dates, which are accurate to ± 2 years.

Radiometric age dating

^{210}Pb is widely used for dating environmental records in natural archives such as lake sediments, peat bogs and marine sediments spanning the last 130 years or so.[50] Assessing ^{210}Pb dates in conjunction with dates from longer time-scale dating methods such as ^{14}C can be beneficial in a number of respects. Age dating peat profiles by combining independent dating methods helps to provide a reliable long time-scale chronology. The main advantage of ^{210}Pb age dating is that it can be done in-house using low background gamma spectrometry and therefore eventually reduces the cost of age dating. In contrast, ^{14}C age dating of plant macrofossils can be done only at those labs with Acceleration Mass Spectrometry (AMS) facilities.

When building up an age dating strategy, an important question is what are we trying to date? The age dating strategy will be different if we try to provide dates for a few events such as the concentration peaks in a record or if we establish a chronology for an entire record. In the case of dating specific events, the optimum strategy would be to direct all the effort at these particular periods.[51] Therefore great attention is required in selecting material sent to the laboratory, to be sure that the most important events are dated. To establish a precise chronology for the entire peat profile, a regular interval of sample selection will guarantee the generation of an accurate age-depth model and therefore of a reliable peat chronology.

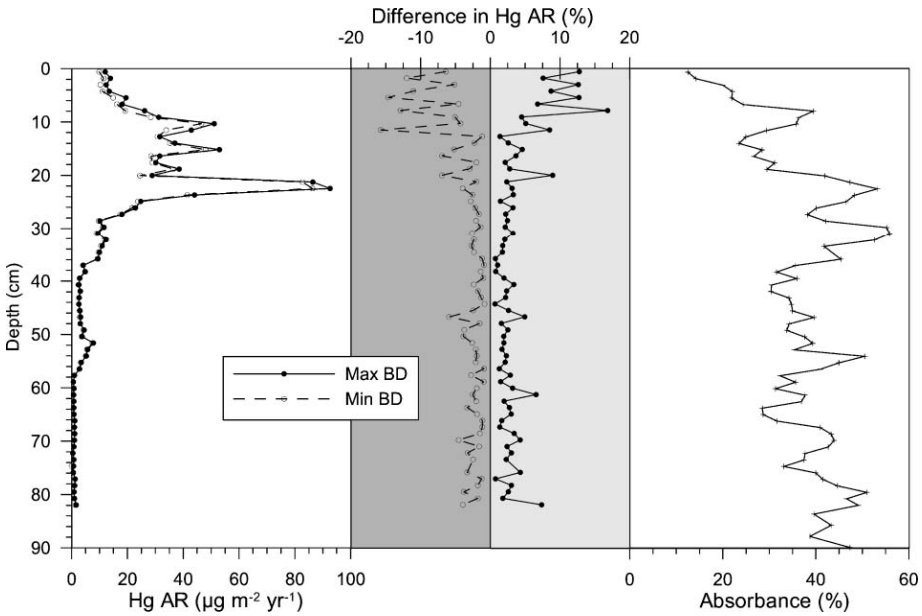

Figure 8 : Comparison of mercury accumulation rate profiles calculated using a) minimum bulk density value and b) maximum bulk density value for a peat core from southern Ontario, Canada. The corrected absorbance is an indicator of the degree of peat humification.

Modeling the age-depth relationship

Chronology reconstruction is based on a series of radiometric dates, sometimes supplemented by other markers (e.g. tephra layers…). As independent check, various models can be applied, all of which have underlying assumptions, even if they are not explicitly stated. The choice of model varies but is most often subjective, favouring linear model based on R^2 values, using central calibrated dates, and assuming continuous peat accumulation often without evaluating this assumption.

Without a large number of dates there is no convincing reason for preferring one regression to another or for using the same regression for all profiles.[52] We are forced to return to a subjective evaluation of curve fitting as well as our knowledge of peatland system. If we want to estimate maximum possible error then we should perhaps evaluate the age-depth function obtained from a range of models, which would give us an error range. Of course, this still excludes the error ranges on the calibrated ages used to generate the age-depth relationship. As far we are aware, there is no available method to deal with these errors, because the probability distribution of calibrated ages is non-normal.[53]

4. Conclusion

The protocol described here is time consuming and expensive. There is no need to apply it to poor quality cores. We recommend that for the study of the uppermost layers a peat bog, three Wardenaar cores should to be collected. The first one could be used to investigate the quality and the suitability of the peat deposit for paleoenvironmental purposes. This core could be visually inspected, described, and cut by hand in the field. Measurement of the pH and the calcium concentration in the porewater can be used to determine the trophic status of the peat profile, and the chlorine concentration to reveal the influence of marine aerosols. As first approximation of the chronology, Pb could be measured using XRF, which would clearly indicate the beginning of industrialisation. In Europe, this approach would also identify the Roman period, if this is present in the peat core. If the core is in good agreement with the selection criteria define during the first step of the study (ombrotrophic peat deposit, time period of interest), then the second core should be cut into 1 cm slices and the protocol proposed in this paper could be followed. The third core should be storage intact at -18 °C as an

"archive", which could be used in future studies.

Acknowledgement

Special thanks to Dr. A. Smirnov (1st Ti Wardenaar and Ti Belarus corer) and Mr H.-P. Bärtschi (Stainless steel Belarus corer) for assistance with field equipment. Financial support was provided by the Swiss National Science Foundation (grants 21-061688.00 and 21-55669.98 to W. S.), the International Arctic Research Center (IARC) and Cooperative Institute for Arctic Research (CIFAR), Fairbanks, Alaska (grant to W. S., H.F. Schöler and S.A. Norton), the Danish Cooperation for Environment in the Arctic (DANCEA) grant to M.E. G., W. S. and G. Asmund. This paper summarises twenty years of field studies by W.S., coring a great variety of peat bogs; I wish to thank my co-authors for all of the questions, comments, and suggestions, which have led to so many improvements with all aspects of this work. In addition, I am indebted to the Swiss NSF for many years of generous financial support.

References

1 A. B. MacKenzie, E. M. Logan, G. T. Cook and I. D. Pulford, *Sci. Total Environ.*, 1988, **222**, 157.
2 M. A. Vile, M. Novak, E. Brizova, R. K. Wieder and W. Schell, *Water, Air, Soil Pollut.*, 1995, **79**, 89.
3 J. G. Farmer, A. B. Mackenzie, C. L. Sugden, P. J. Edgar and L. J. Eades, *Water, Air, Soil Pollut.*, 1997, **100**, 253.
4 A. Martínez Cortizas, X. Pontevedra Pombal, E. García-Rodeja, J. C. Nóvoa Muñoz and W. Shotyk, *Science*, 1999, **284**, 939.
5 M. Novak, S. Emmanuel, M. A. Vile, Y. Erel, A. Veron, T. Paces, R. K. Wieder, M. Vanecek, M. Stepanova, E. Brizova and J. Hovorka, *Environ. Sci. Technol.*, 2003, **37**, 437.
6 F. Monna, C. Pettit, J.-P. Guillaumet, I. Jouffroy-Bapicot, C. Blanchot, J. Dominik, R. Losno, H. Richard, J. Lévêque and C. C. Chateau, *Environ. Sci. Technol.*, 2004, **38**, 665.
7 D. J. Charman, *Peatland and Environmental Change*, John Wiley and sons, Chichester, 2002.
8 W. Shotyk, D. Weiss, P. G. Appleby, A. K. Cheburkin, R. Frei, M. Gloor, J. D. Kramers and W. O. Van Der Knaap, *Science*, 1998, **281**, 1635.
9 W. Shotyk, D. Weiss, M. Heisterkamp, A. K. Cheburkin, P. G. Appleby and F. C. Adams, *Environ. Sci. Technol.*, 2002, **36**, 3893.
10 W. Shotyk and P. Steinmann, *Chem. Geol.*, 1994, **116**, 137.
11 A. K. Cheburkin and W. Shotyk, *Fresinus J. Anal. Chem.*, 1996, **354**, 688.
12 D. Weiss, W. Shotyk, J. D. Kramers and M. Gloor, *Atmos. Environ.*, 1999, **33**, 3751.
13 W. Shotyk, *Environmental Review*, 1996, **4**, 149.
14 N. Givelet, F. Roos-Barraclough, M. E. Goodsite, A. K. Cheburkin and W. Shotyk, *Environ. Sci. Technol.*, accepted for publication.
15 W. Shotyk, *Sci. Total Environ.*, 2002, **292**, 19.
16 F. Roos-Barraclough and W. Shotyk, *Environ. Sci. Technol.*, 2003, **37**, 235.
17 W. Shotyk, M. E. Goodsite, F. Roos-Barraclough, R. Frei, J. Heinemeier, G. Asmund, C. Lohse and T. S. Hansen, *Geochim. Cosmochim. Acta*, 2003, **67**, 3991.
18 M. Krachler, C. Mohl, H. Emons and W. Shotyk, *Environ. Sci. Technol.*, 2003, **37**, 2658.
19 M. Krachler and W. Shotyk, *J. Environ. Monit.*, 2004, this issue.
20 S. A. Norton, G. C. Evans and J. S. Kahl, *Water, Air, Soil Pollut.*, 1997, **100**, 271.
21 I. E. Belokopytov and V. V. Beresnevich, *Torf. Prom.*, 1955, **8**, 9.
22 T. Noernberg, M. E. Goodsite, W. Shotyk and N. Givelet, in preparation.
23 T. Noernberg, M. E. Goodsite and W. Shotyk, *Arctic*, accepted for publication.
24 M. E. Goodsite and W. Shotyk, *Long term deposition of atmospheric Hg, Cd, Pb and persistent organic pollutants (POPs) in peat cores from Arctic peatlands (Bathurst Island), Post expedition field and status report*, Institute of Environmental Geochemistry, Heidelberg, 2001.
25 C. J. Caseldine, A. Baker, D. J. Charman and D. Hendon, *Holocene*, 2000, **10**, 649.
26 W. Shotyk, D. Weiss, J. D. Kramers, R. Frei, A. K. Cheburkin, M. Gloor and S. Reese, *Geochim. Cosmochim. Acta*, 2001, **65**, 2337.
27 A. K. Cheburkin and W. Shotyk, *X-Ray Spectrometry*, 1999, **28**, 145.
28 A. K. Cheburkin and W. Shotyk, *X-ray Spectrometry*, 2004, **33**.
29 F. Roos-Barraclough, N. Givelet, A. Martinez-Cortizas, M. E. Goodsite, H. Biester and W. Shotyk, *Sci. Total Environ.*, 2002, **292**, 129.
30 M. Krachler, C. Mohl, H. Emons and W. Shotyk, *J. Anal. At. Spectrom.*, 2002, **17**, 844.
31 M. Krachler, C. Mohl, H. Emons and W. Shotyk, *Spectrochimica Acta Part B*, 2002, **57**, 1277.
32 M. Krachler, M. Burow and H. Emons, *Analyst*, 1999, **124**, 777.
33 M. Krachler, M. Burow and H. Emons, *Analyst*, 1999, **124**, 923.
34 M. Krachler, M. Burow and H. Emons, *J. Environ. Monit.*, 1999, **1**, 477.
35 M. Krachler, W. Shotyk and H. Emons, *Anal. Chim. Acta*, 2001, **432**, 303.
36 M. Krachler, H. Emons, C. Barbante, G. Cozzi, P. Cescon and W. Shotyk, *Anal. Chim. Acta*, 2002, **458**, 387.
37 B. Chen, M. Krachler and W. Shotyk, *J. Anal. At. Spectrom.*, 2003, **18**, 1256.

38 W. Shotyk, M. Krachler and B. Chen, *Global Biogeochem. Cycles*, 2004, **18**,
39 W. Shotyk and M. Krachler, *J. Environ. Monit.*, 2004, this issue.
40 M. Krachler, G. Le Roux, B. Kober and W. Shotyk, *J. Anal. At. Spectrom.*, 2004, **19**, 354.
41 C. Barbante, W. Shotyk, H. Biester, A. K. Cheburkin, H. Emons, J. G. Farmer, E. Hoffman, A. Martinez-Cortizas, J. Matschullat, S. A. Norton, J. Schweyer and E. Steinnes, Proceeding of the 11th Conference on Heavy Metals in the Environment, Ann Arbor, Michigan, USA, 2000.
42 C. Yafa, J. G. Farmer, M. C. Graham, J. R. Bacon, R. Bindler, I. Renberg, A. K. Cheburkin, A. Martinez-Cortizas, H. Emons, M. Krachler, W. Shotyk, X. D. Li, S. A. Norton, I. D. Pulford, J. Schweyer, E. Steinnes and D. Weiss, Proceeding of the 6th International Symposium on Environmental Geochemistry, Edinburgh, Scotland, 2003.
43 C. Persson, *Sveriges Geologiska undersökning*, 1971, **65**,
44 A. J. Dugmore, A. J. Newton and D. E. Sugden, *J. Quaternary Sci.*, 1992, **7**, 173.
45 P. Steinmann and W. Shotyk, *Chem. Geol.*, 1997, **138**, 25.
46 A. K. Cheburkin, R. Frei and W. Shotyk, *Chem. Geol.*, 1997, **135**, 75.
47 I. Renberg, R. Bindler and M.-L. Brännvall, *Holocene*, 2001, **11**, 511.
48 D. Weiss, W. Shotyk, J. Rieley, S. Page, M. Gloor, S. Reese and A. Martinez-Cortizas, *Geochimica and Cosmochimica Acta*, 2002, **66**, 2307.
49 M. E. Goodsite, W. Rom, J. Heinemeier, T. Lange, S. Ooi, P. G. Appleby, W. Shotyk, W. O. van der Knaap, C. Lohse and T. S. Hansen, *Radiocarbon*, 2001, **43**, 1.
50 P. G. Appleby, P. Nolan, F. Oldfield, N. Richardson and S. Higgitt, *Sci. Total Environ.*, 1988, **69**, 157.
51 D. Mauquoy, B. Van Geel, M. Blaauw and J. Van der Plicht, *Holocene*, 2002, **12**, 1.
52 R. J. Telford, E. Heegaard and H. J. B. Birks, *Quat. Sci. Rev.*, 2004, in press.
53 K. D. Bennet, *Holocene*, 1994, **4**, 337.

- Chapter 1.2 -

Accurate and precise Pb isotope ratio measurements in environmental samples by MC-ICP-MS

Dominik Weiss,[*a,b] Bernd Kober,[c] Alla Dolgopolova,[a,b] Kerry Gallagher,[a] Baruch Spiro,[b] Gaël Le Roux,[c] Thomas F. D. Mason,[a] Malin Kylander,[a] Barry J. Coles,[a,b]

[a]Department of Earth Science and Engineering, Imperial College London, Prince Consort Road, London SW7 2BP, England
[b]Department of Mineralogy, The Natural History Museum, Cromwell Road, London SW7 5BD, England
[c]Institute for Environmental Geochemistry, University of Heidelberg, Im Neuenheimer Feld 234, 69129 Heidelberg, Germany
[*]corresponding author: e-mail: d.weiss@imperial.ac.uk; Fax: +44 (0)20 7594 6464

International Journal of Mass Spectrometry 232, 205-215 (2004)

Abstract

Analytical protocols for accurate and precise Pb isotope ratio determinations in peat, lichen, vegetable, chimney dust and ore bearing granites using MC-ICP-MS and their application to environmental studies are presented. Acid dissolution of various matrix types was achieved using high temperature/high pressure microwave and hot plate digestion procedures. The digests were passed through a column packed with EiChrom Sr-resin employing only hydrochloric acid and one column passage. This simplified column chemistry allowed high sample throughput. Typically, internal precisions for approximately 30 ng Pb were below 100 ppm (±2σ) on all Pb ratios in all matrices. Thallium was employed to correct for mass discrimination effects and the achieved accuracy was below 80 ppm for all ratios. This involved an optimization procedure for the $^{205}Tl/^{203}Tl$ ratio using least square fits relative to the certified NIST-SRM 981 Pb values. The long-term reproducibility (±2σ) for the NIST-SRM 981 Pb standard over a 5-month period (35 measurements) was better than 350 ppm for all ratios. Selected ore bearing granites were measured with TIMS and MC-ICP-MS and showed good correlation (e.g., r=0.999 for $^{206}Pb/^{207}Pb$ ratios, slope = 0.996, n = 13). Mass bias and signal intensities of Tl spiked into natural (after matrix separation) and in synthetic samples did not differ significantly, indicating that any residual components of the complex peat and lichen matrix did not influence mass bias correction. Environmental samples with very different matrices were analyzed during two different studies: i.) lichens, vegetables and chimney dust around a Cu smelter in the Urals, and ii.) peat samples from an ombrotrophic bog in the Faroe Islands. The presented procedure for sample preparation, mass spectrometry and data processing tools resulted in accurate and precise Pb isotope data that allowed the reliable differentiation and identification of Pb sources with variations as small as 0.7% for $^{206}Pb/^{207}Pb$.

Keywords: accuracy, precision, Pb isotope ratios, MC-ICP-MS, source assessment, environmental samples, sample preparation

Introduction

The use of Pb isotopes has had a tremendous effect on our understanding of the geochemical cycling of Pb in the environment and the anthropogenic impact [1]. Lead isotopes in environmental samples, *i.e.,* soil, plant, sediment, peat, surface and subsurface waters, have mainly been measured using thermal ionisation mass spectrometry (TIMS) or quadrupole based inductive coupled plasma source mass spectrometry (ICP-QMS). The advantage of TIMS is that ratios including the least abundant ^{204}Pb isotope are measured with high reproducibility (down to 200 ppm) and it achieves good accuracy also in samples with low [Pb]. However, analytical procedures for TIMS are time consuming and involve intensive sample preparation steps, *e.g.,* two column passages are needed to achieve stable emission of Pb^+ ions from the filament analysing organic rich matrices such as lichen or peat. This severely restricts the sample throughput. Yet, many environmental problems require a large sample number to infer statistically significant conclusions. This is due to inherent temporal and spatial variability in the environmental context.

Consequently, most environmental investigations to date use ICP-QMS (e.g., Refs [2, 3]), which performs single measurements at the nominal mass value of each peak using either scanning or peak hopping modes. This results in poor peak shape and consequently in less precise measurements than using multi-collector sector instruments [4]. Typically, precisions of around 0.1-1.0% are achieved [5, 6], depending on the concentration and the ^{204}Pb isotope is seldom measured. However, isotopic ratios including the ^{204}Pb isotope are of crucial importance for source assessments.

Multi-collector inductively coupled plasma source mass spectrometry (MC-ICP-MS) combines the high ionization efficiency of the Ar-plasma with the precision attainable using multi-collector array. It is thus of great interest for the environmental geochemist as it allows the inclusion of the ^{204}Pb for routine measurements also in low [Pb] samples and a large sample throughput with less sample preparation and measurement time is possible. A number of papers have investigated Pb isotope ratio measurements with MC-ICP-MS using different mass spectrometer designs, *i.e.,* double [7-12] or single focussing [13-16] sector field MC-ICPMS. These papers showed that external precisions achieved are similar to TIMS and that mass fractionation, abundance sensitivity, baseline correction etc. affect data quality significantly.

With respect to instrumental mass fractionation, arguably a major source of error, the major draw back is that Pb has only one non-radiogenic isotope (^{204}Pb) and mass fractionation cannot be corrected internally. One way to correct for mass bias is to spike the sample with an element of similar mass and with two stable isotopes. In the case of Pb, Tl with isotopes 203 and 205 is the preferred choice [7, 12, 13]. However, it was shown that the ^{205}Tl/^{203}Tl normalizing ratio of the NIST-SRM 997 Tl (used as dopant) had to be adjusted to higher ratios than the certified value to generate normalized values within error for NIST-SRM 981 Pb determined using double and triple spikes [13]. The latter vary significantly themselves from laboratory to laboratory, *i.e.* for the ^{206}Pb/^{204}Pb ratios with values of 16.9405±0.0015 [17], 16.9409±0.0022 [18] and 16.9356±0.0023 [19]. White et al. [7] assessed the graphical technique previously developed for Cu and Zn isotope analysis [20], which plots measured ratios of the Tl dopant vs. the Pb isotope pair of interest in log-log space. This technique is not applicable on first generation *IsoProbe* instruments due to the small mass bias variations using dry plasma conditions, which consequently results in poor linear fits with high errors and inaccurate isotope ratios [13, 21].

To date, most investigations have been limited to synthetic and ‘simple’ silicate matrices and the Tl mass bias correction procedure has been object of intense discussions [8, 13, 15]. Consequently, more investigations on accurate and precise Pb isotope ratio measurements, especially with a focus on environmental samples, are needed. Recent applications of MC-ICP-MS to

environmental geochemistry included Pb isotope measurements in seawater matrices [9, 16].

The purpose of this contribution is to present a reliable and robust analytical protocol (including sample preparation and mass spectrometry) and data processing methodology for precise and accurate Pb isotope measurements in a wide range of environmental samples. To achieve this, we i.) re-assessed the Tl mass bias correction procedure using a simple optimization procedure, ii.) assessed its analytical merits and iii.) demonstrated its application in two environmental geochemical studies.

2. Experimental

2.1 MC-ICP-MS and TIMS instrumentation

A Micromass *IsoProbe* MC-ICP-MS based at the Imperial College London / Natural History Joint Analytical Facility (ICL/NHM JAF) was used during the study. The instrument is equipped with seven independently adjustable Faraday cups and a hexapole collision cell. A CETAC Aridus desolvating system (Omaha, NE, USA) with a T1-H microconcentric nebulizer was used for sample introduction. The optimized data acquisition parameters selected for Pb isotope ratio measurements are summarized in Table 1. For comparative purposes, Pb isotope analyses were also conducted at the Geochronology Laboratory of the University of Heidelberg using a Finnigan *MAT* 261 TIMS with multi-cup system for Pb isotopes and standard sample preparation techniques. Raw TIMS data were normalized to NIST-SRM 981 Pb international standard with reference values of Galer and Abouchami [17] and long-term reproducibility on the 95% confidence level was below 0.03% for ratios normalized to ^{204}Pb. Details of the TIMS procedure have been described in detail before [22].

2.2 Measurement procedures

All isotope measurements were performed by static multiple collection. The ion currents were measured using Faraday collectors at masses 200 (Hg), 203 (Tl), 204 (Pb and Hg), 205 (Tl), 206 (Pb), 207 (Pb) and 208 (Pb). The collector efficiencies were calibrated on a daily basis. Ion beam intensities of Pb and Tl were optimized adjusting accelerating voltage, lens system, torch settings and gas flows. Data collection was made using two blocks with 25 measurements each when analyzing samples and using one block with 20 measurements when analyzing the acid blank before the sample. Internal errors ($\pm 2\sigma$) for synthetic solutions of 50 ng ml^{-1} were below 50 ppm for all ratios. A 10-s integration and 5-s sample admission delay guaranteed stable signals before measurement started. The rinse out time between samples and acid blank was 6 minutes using 2% (v/v) HNO_3. A typical measurement procedure included five samples taken up in 2% (v/v) HNO_3 and spiked with NIST-SRM 977 Tl and one NIST-SRM 981 Pb standard spiked with NIST-SRM 977 Tl in 2% (v/v) HNO_3 to assess the reproducibility and to optimize the Tl ratio (see below).

Instrument settings	
Accelerating voltage	~6000 V
RF power	~1375 W
(reflected power)	<2W
Coolant Ar flow	~14 l min^{-1}
Auxiliary Ar flow	1.0-1.2 l min^{-1}
Nebulizer flow	0.6-0.8 l min^{-1}
Ar collision gas flow	1-2 ml min^{-1}
Abundance sensitivity	~25 ppm
Analyser pressure	~4.8 x 10^{-8} mbar under full gas load
Sensitivity for Pb	~300 V ppm^{-1}
Cones (Skimmer and Sample)	Ni
Sample introduction	
Spray chamber temperature	75 ˚C
Desolvator temperature	160 ˚C
Ar sweep gas flow	~2.8-3.5 ml min^{-1}
Sample flow rate	~40-60µl min^{-1}

Table 1: Typical instrument operating conditions of the *IsoProbe* MC-ICP-MS and the CETAC nebulizer

Analytical blanks for the total procedure, estimated from intensity data, were below 1 ng and can be accounted for by the Aristar grade acids used during sample preparation.

The blank was always below 1% of the total Pb and mixing calculation showed that contributions were insignificant at any time at the level encountered.

2.3 Data reduction and mass discrimination correction

To correct for Faraday cup offset, solvent blank and instrumental blank, averaged acid blank intensities were subtracted from individually measured raw isotope intensities and then the average was calculated. To account for the ^{204}Hg isobaric interference, the ^{200}Hg was measured on L2. This correction was very small and typically amounted to ≤0.1%. Previous work suggests that average abundance sensitivities are stable to approximately ±2ppm (±2σ) under same vacuum conditions [16]. Consequently, abundance sensitivity correction during this study was achieved by fixing the Pb/Tl ratio and concentration matching between samples and standards to within 10%.

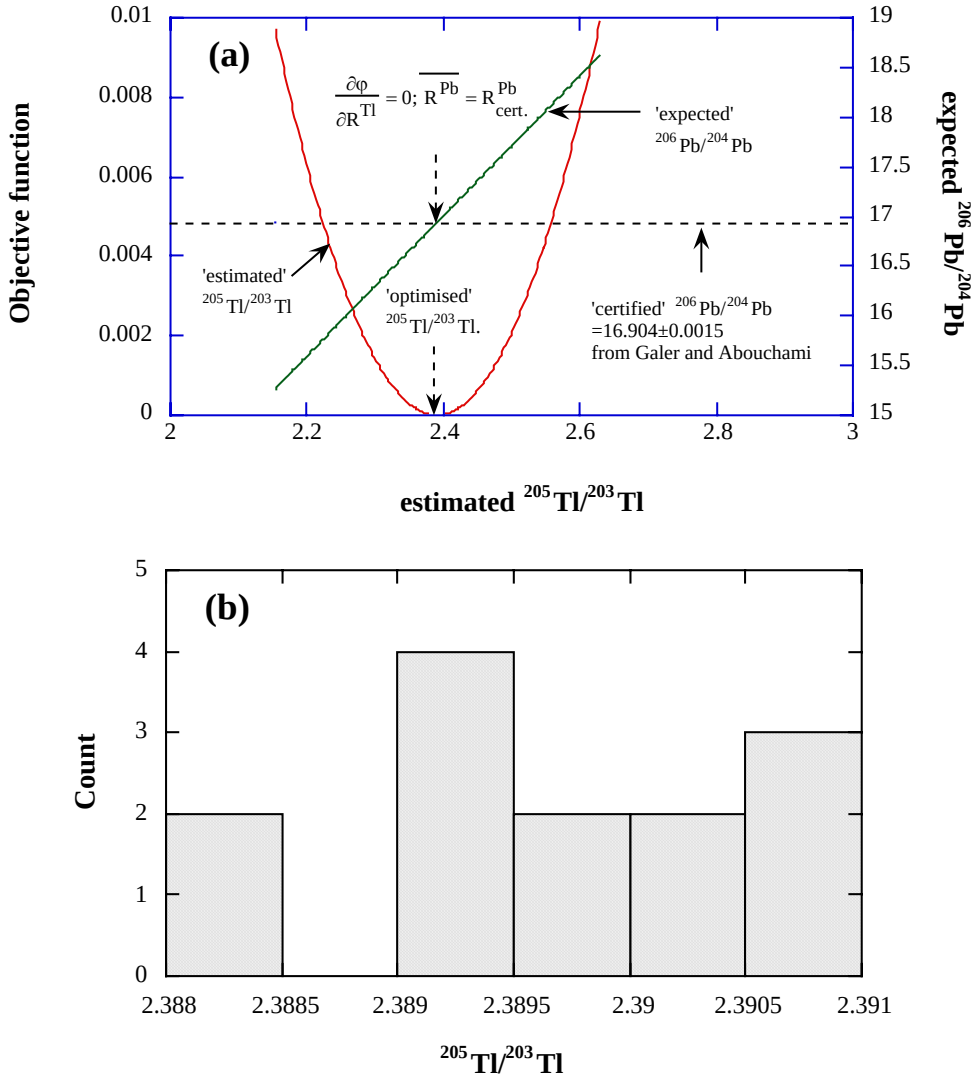

Figure 1: (a) Distribution of estimated ^{205}Tl/^{203}Tl (x-axes) as a function of the expected ^{206}Pb/^{204}Pb ratios ($\overline{R^{Pb}}$) and the objective function (φ). The optimized ^{205}Tl/^{203}Tl ratio of this measurement session (29.1.03) is given by 2.3905 and fulfills the conditions of $\partial\varphi / \partial R^{Tl} = 0$ and $\overline{R^{Pb}} = R^{Pb}_{cert.}$ (b) The distribution of optimized Tl ratios during 13 measurement sessions at the ICL/NHM JAF during one year (August 2002 to August 2003).

The run intensities corrected for background and isobaric interference were used to calculate the raw ratios, which then were corrected for instrumental mass bias using Tl as external dopant and the Tl mass fractionation factor f_{Tl}. The $^{205}Tl/^{203}Tl$ ratio used to calculate the mass fractionation factor f_{Tl} was optimized each measurement session from repeated NIST-SRM 981 Pb standard measurements dispersed between sample measurements (see below details of procedure). The exponential law proved to be the most accurate. The mass fractionation coefficient for Tl (f_{Tl}) was calculated as

$$f_{Tl} = \frac{\ln(R_{Tl} / r_{Tl})}{\ln(M_{205} / M_{203})} \quad \textbf{(1)}$$

where R_{Tl} is the 'true' Tl ratio, r_{Tl} the measured ratio and M represents the atomic masses of Tl (202.9723 and 204.9745, respectively). The Tl mass correction factor f_{Tl} was used to correct the calculated raw Pb isotope ratios (baseline, interference and abundance sensitivity corrected):

$$R_{Pb} = r_{Pb}\left(\frac{M_1}{M_2}\right)^{f_{Tl}} \quad \textbf{(2)}$$

where R_{Pb} is the 'true' Pb ratio, r_{Pb} is the measured ratio, $M_{1,2}$ are the atomic masses of isotope 1 and 2, respectively, and f_{Tl} is the mass fractionation co-efficient derived from Eq. (1).

2.4 Tl ratio optimization procedure

Instrumental mass fractionation was determined during a measurement session by repeated analyses of the NIST-SRM 981 Pb standard spiked with the NIST-SRM 997 Tl using the same Pb/Tl ratio and concentrations as the samples. The Tl ratio was optimised against the $^{206}Pb/^{204}Pb$ value of Galer and Abouchami [17]. The optimisation was achieved using a least squares method. The approach is based on the logarithmic law, which assumes that the 'true' Tl and Pb ratios are given by

$$R_i^{Tl} = r_i^{Tl}(c^{Tl})^f \quad \textbf{(3)}$$

and

$$R_i^{Pb} = r_i^{Pb}(c^{Pb})^f \quad \textbf{(4)}$$

where f is the mass bias fractionation factor given by $f = \ln(R_i^x / r_i^x)/\ln(c^x)$ (with x=Pb or Tl), R^{Tl} and R^{Pb} are the 'true' ratios, i is a given number of measured NIST-SRM 981 Pb standards, r^{Pb} and r^{Tl} are measured ratios of $^{205}Tl/^{203}Tl$ and $^{206}Pb/^{204}Pb$, respectively, $c^{Tl} = M_2/M_1 = 205/203 = 1.008852$, and $c^{Pb} = M_2/M_1 = 206/204 = 1.009804$.

Using repeated NIST-SRM 981 Pb measurements (between 6 to 12) during a measurement session, we defined $\overline{R^{Pb}}$ (the mean value) as:

$$\overline{R^{Pb}} = \frac{1}{N}\sum_{i=1}^{N} R_i^{Pb}, \text{ with } R_i^{Pb} = r_i^{Pb}(c^{Pb})^{\frac{\ln(R^{Tl}/r_i^{Tl})}{\ln(c^{Tl})}} \quad \textbf{(5)}$$

where N is the number of NIST-SRM 981 Pb measurements during the measurement session. $\overline{R^{Pb}}$ is a function of the 'true' Tl ratio (R^{Tl}), which we do not know reliably. Given $\overline{R^{Pb}}$ should be close to the certified value for Pb ($R^{Pb}_{cert.}$), we adjusted the unknown R^{Tl}, such that we minimized the prediction error for $\overline{R^{Pb}}$. Therefore, we choose an objective function $\varphi = \left(\frac{\overline{R^{Pb}}}{R^{Pb}_{cert.}} - 1\right)^2$, which has a minimum (of zero) when $\overline{R^{Pb}} = R^{Pb}_{cert.}$ The value of R^{Tl} was found by taking the denominator of φ with respect to R^{Tl} and setting this to zero ($\frac{\partial\varphi}{\partial R^{Tl}} = 0$). This leads to the final form:

$$R^{Tl} = \ln(c^{Tl}) \times \left(\frac{N\, R_i^{Pb}}{\sum_{i=1}^{N} r_i^{Pb}(c^{Pb})^{\ln(r_i^{Tl})/\ln(c^{Tl})}}\right)^{\ln(c^{Tl})/\ln(c^{Pb})} \quad \textbf{(6)}$$

2.5 Materials and reagents

Environmental samples included peat from an ombrotrophic bog in the Faroe Islands [23], lichens, vegetables, and chimney dust collected around a Cu smelter in Karabash, Southern Urals [24], and ore bearing and barren granites from the Orlovka-Spokoine mining district in Eastern

Transbaikalia [25]. The acids were of ultra-pure (Merck and sub-boiling acid) or Aristar (Merck) quality. Dilute solutions of acids for mass spectrometry were prepared with purified water obtained from quartz still or an 18 MΩ grade Millipore system (Bedford, MA). Lead, Tl and mixed Pb-Tl standard solutions were made up from previously prepared stock solutions of NIST-SRM 981 Pb (1240 µg ml^{-1} in 2% (v/v) HNO_3, from S. Bowring, MIT Cambridge) and NIST-SRM 997 Tl (732 µg ml^{-1} in 2M HNO_3, from M. Rehkaemper, ETH Zürich). All solutions and samples were prepared and handled in laminar flow hoods. Solutions were concentration matched to get a signal of ≥100 mV on ^{204}Pb and a Pb/Tl ratio of approximately 5:1.

2.6 Sample preparation of environmental samples

Peat samples were digested using a Milestone high pressure/high temperature microwave oven system [26]. Lichens and vegetables samples from the Karabash smelter were digested using a MARSX high pressure/high temperature microwave oven system [24, 27]. Both microwave digestion methods have been recently developed and showed quantitative recovery for Pb. The barren and Ta-Nb-W bearing granites from the Orlovka-Spokoine mining district and the chimney dust samples were dissolved using standard HNO_3/HF acid mixtures on a hot plate in closed Teflon beakers [25].

After digestion, all solutions were dried and the residues redissolved in 2mls of 2.4M HCl prior to the passage through the column. After conversion to the chloride form, Pb was separated using the Pb selective extraction chromatographic Sr resin from EiChrom [28] and following the distribution factor dependencies for Pb as reported elsewhere [29]. The method uses only hydrochloric acid and one column passage. It consists of a cleaning step with 6M HCl, a pre-conditioning and a loading step, both with 2.4M HCl and an elution step using 6M HCl (Table 2). The recovery of Pb from the column is quantitative from biological and silicate matrices.

Stage	Acid strength of HCl (M) and volume (ml) used
1. Cleaning step	**6M (6 x 1 ml)**
2. Conditioning step	**2.4M (2 x 0.5 ml)**
3. Sample loading step	**2.4M (1 x 1.5 ml)**
4. Matrix elution step	**2.4M (4 x 1 ml)**
5. Pb elution step	**6M (3 x 1 ml)**
6. Cleaning step	**6M (3 x 1 ml)**

Table 2: Ion Exchange Column chemistry procedure for separating Pb from sample matrix. The columns were made in house using Teflon tubing and packed with 600µl of EiChrom Sr resin resulting in a bed height of about 0.5 cm .

3. Results and Discussion

3.1 Assessing the Tl optimization procedure

Figure 1a shows the results of a Tl optimization calculation from one measurement session (16.8.2002) using twelve individual measurements of NIST-SRM 981 Pb standards doped with NIST-SRM 997 Tl. Plotted is the estimated $^{205}Tl/^{203}Tl$ ratio (R^{Tl}) vs. the objective function. Also shown are the corresponding estimated $\overline{R^{Pb}}$ and certified Pb ratios ($R^{Pb}_{cert.}$). Figure 1b shows a frequency distribution histogram of optimized Tl ratios determined during 13 individual measurement sessions in a time period of one year (August 2002 – August 2003). No systematic trend or bias is visible in the frequency distribution of the optimized Tl ratio. The $^{205}Tl/^{203}Tl$ ranged between 2.3885 and 2.3907 with a mean value of 2.3897±0.0015 (±2σ). The mean value is slightly higher that the originally 'certified' ratio of 2.38714±0.00101 [30] but has a similar error.

To achieve also accurate Pb isotope measurements in real samples using optimized Tl values derived from repeated NIST-SRM 981 Pb measurements, the mass bias of Tl in standard and samples has to be similar. Figure 2 shows the calculated mass bias factors f_{Tl} for spiked samples and NIST-SRM 981 Pb standards using the optimized $^{205}Tl/^{203}Tl$ during two measurement sessions: 16.8.02 (Figure 2a) when peat matrices were

measured and 13.12.02 (Figure 2b) when lichen matrices were measured. The average f_{Tl} in peat (-3.359±0.427; n=18) or lichen (-1.742±0.277; n=23) matrix does not differ significantly from the f_{Tl} in the NIST-SRM 981 Pb standards during the same measurement session (-3.456±0.359; n=8, and -1.769±0.222; n=11, respectively). The Tl mass bias is similar in samples and standards, suggesting that the ion exchange chemistry, high plasma temperature and/or the sample dilution prior to the measurements remove any possible interference. The significant different mass bias factors between two measurement sessions reflect the effect of an instrument upgrade which include a new interface.

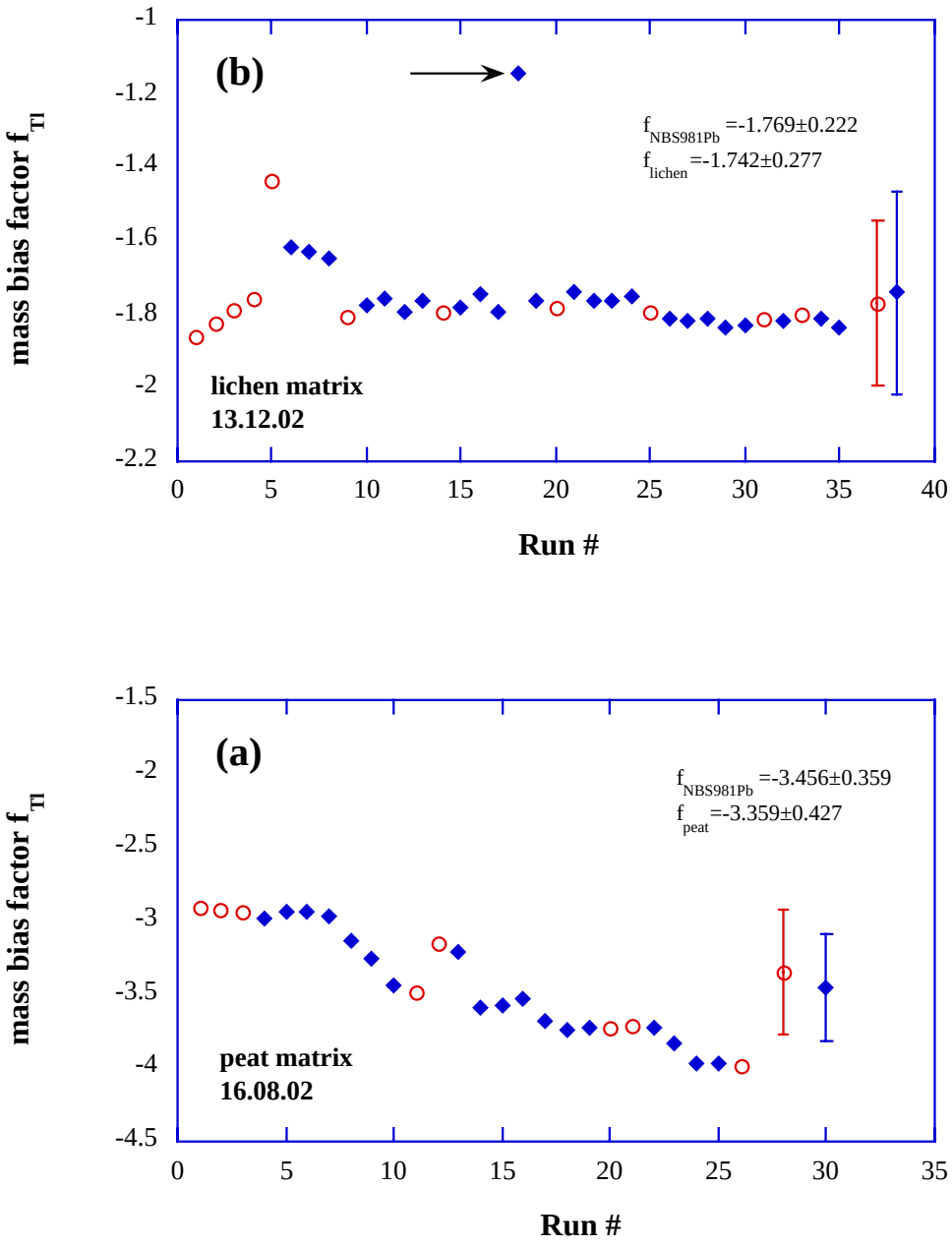

Figure 2: Changing mass bias factors (f_{Tl}) of the spiked Tl during two measurement sessions in samples and NIST SRM Pb 981: (a) measuring peat samples from the Faroe Islands, and (b) measuring lichens from the Karabash smelter. Open circles represent the NIST-SRM Pb 981 standard and the closed quadrangles represent the peat and lichen samples. The points with the error bars represent the mean value and the ±2σ standard deviation.

Authors	Mass Spectrometer	$^{208}Pb/^{206}Pb$	$^{207}Pb/^{206}Pb$	$^{206}Pb/^{204}Pb$	$^{207}Pb/^{204}Pb$	$^{208}Pb/^{204}Pb$
Todt et al. (1995)	TIMS	2.16701 (43)	0.914585 (132)	16.9356 (23)	15.4891 (30)	36.7006 (112)
Galer and Abouchami (1998)	TIMS	2.16771 (10)	0.914750 (35)	16.9405 (15)	15.4963 (16)	36.7219 (44)
Thirlwall (2000)	TIMS	2.16770 (21)	0.91469 (7)	16.9409 (22)	15.4956 (26)	36.7228 (80)
Hirata (1996)	MC-ICP-MS - *Plasma 54*	2.16636 (82)	0.914623 (37)	16.9311 (90)	15.4856	36.6800 (210)
Rehkaemper and Halliday (1995)	MC-ICP-MS - *Plasma 54*	2.16677 (14)	0.91469 (5)	16.9364 (55)	15.4912 (51)	36.7219 (44)
Belshaw et al. (1998)	MC-ICP-MS - Nu *Plasma*	2.1665 (2)	0.91463 (6)	16.932 (7)	15.487	36.683
White et al. (2000)	MC-ICP-MS - *Plasma 54*	2.1646 (8)	0.91404	16.9467 (76)	15.4899 (39)	36.6825 (78)
Rehkaemper and Metzger (2000)	MC-ICP-MS - *IsoProbe*	2.16691 (29)	0.91459 (13)	16.9366 (29)	15.4900 (17)	36.7000 (23)
Reuer et al. (2003)	MC-ICP-MS - *IsoProbe*	2.16639 (304)	0.91460 (18)			
This Study	MC-ICP-MS - *IsoProbe*	2.16767 (63)	0.914767 (120)	16.9413 (39)	15.4974 (51)	36.7239 (115)

Table 3: Comparison of selected published Pb isotopic composition of NIST-SRM 981 Pb measured by TIMS and MC-ICP-MS. The Tl ratios used in this study were adjusted to the Galer and Abouchami value. The TIMS data are based on double and triple spike measurements. Errors shown refer to the least significant digits and are all given as ±2σ.

3.2 Accuracy, precision and reproducibility

3.2.1 Accuracy

Table 3 shows the average Pb isotope ratio of the NIST-SRM 981 Pb standard from repeated measurements (n=35) during a five-month period using optimized $^{205}Tl/^{203}Tl$ ratios for mass bias correction (August to December 2002).

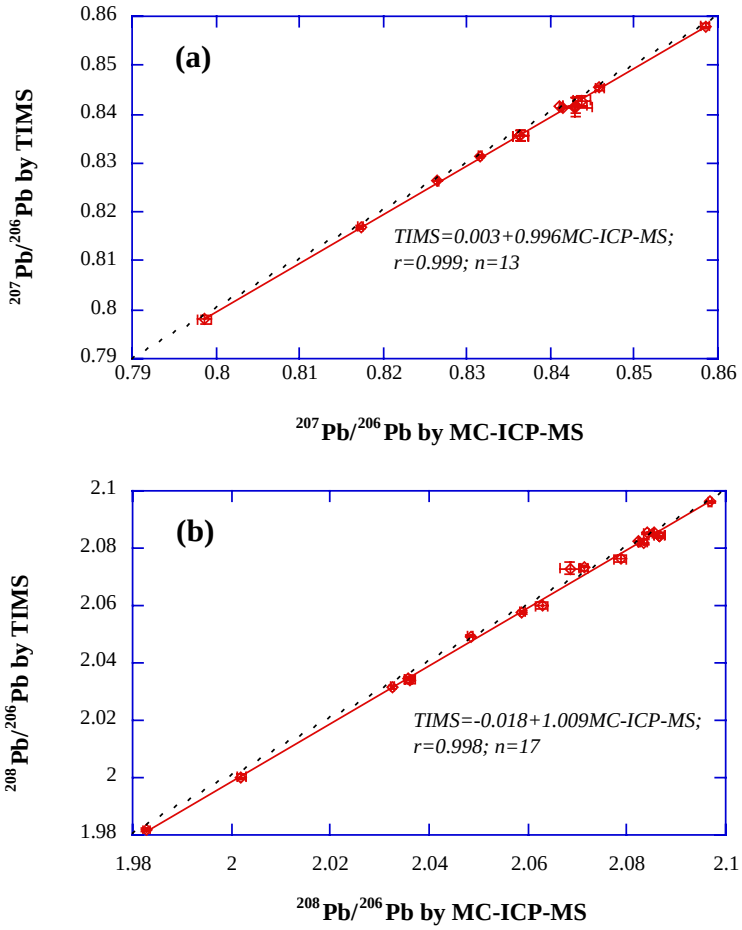

Figure 3: TIMS and MC-ICP-MS data from selected silicate samples (whole rock and mineral separates from Ta/W ore bearing granites). Shown is the best linear fit along with the theoretical (dashed) 1:1 line.

Sample number	Sample ID	Sample type	Pb (µg/g)	$^{206}Pb/^{204}Pb$	±2σ (%)	$^{207}Pb/^{204}Pb$	±2σ (%)	$^{208}Pb/^{204}Pb$	±2σ (%)	$^{207}Pb/^{206}Pb$	±2σ (%)	$^{208}Pb/^{206}Pb$	±2σ (%)
Cu smelter near Karabash													
1	I 15 3	Lichen	68.0	17.911	0.0051	15.550	0.0044	37.874	0.0109	0.86816	0.0038	2.11455	0.0051
2	I 17 3	Lichen	120.0	17.897	0.0151	15.535	0.0131	37.847	0.0327	0.86798	0.0038	2.11469	0.0056
5	I 19 3	Lichen	111.0	17.975	0.0032	15.607	0.0028	38.065	0.0070	0.86824	0.0030	2.11767	0.0164
6	I 34 12 (1)	Lichen	213.0	17.916	0.0025	15.571	0.0020	37.856	0.0050	0.86908	0.0032	2.11293	0.0164
7	I 35 12 (2)	Lichen	151.0	17.906	0.0074	15.549	0.0067	37.830	0.0163	0.86837	0.0051	2.11265	0.0041
8	I 37/C	Lichen	n.d.	17.929	0.0018	15.572	0.0013	37.908	0.0033	0.86852	0.0032	2.11427	0.0042
9	I 1 K1	Lichen	112.8	17.935	0.0036	15.557	0.0029	37.840	0.0073	0.86741	0.0030	2.10983	0.0069
10	I 2 K2	Lichen	64.0	17.801	0.0269	15.457	0.0232	37.635	0.0555	0.86831	0.0065	2.11424	0.0041
11	I 4 K3	Lichen	118.2	17.896	0.0040	15.545	0.0036	37.788	0.0087	0.86860	0.0030	2.11152	0.0040
12	II 5 (D-2)	Vegetable	n.d.	17.831	0.0126	15.506	0.0109	37.684	0.0270	0.86962	0.0036	2.11338	0.0085
13	II 40 3	Lichen	100.6	17.854	0.0144	15.518	0.0130	37.718	0.0322	0.86913	0.0052	2.11251	0.0039
14	II 41/4	Lichen	446.5	17.899	0.0026	15.553	0.0021	37.798	0.0055	0.86890	0.0032	2.11173	0.0059
15	II 42/5	Lichen	1199.9	17.824	0.0142	15.505	0.0127	37.708	0.0313	0.86988	0.0050	2.11558	0.0075
16	II 43/6	Lichen	482.7	17.830	0.0223	15.489	0.0195	37.616	0.0487	0.86871	0.0048	2.10966	0.0045
17	II 44 (2)	Lichen	278.3	17.710	0.0186	15.463	0.0161	37.517	0.0399	0.87313	0.0059	2.11839	0.0071
18	II C1 (D-9)	Chimney dust	n.d.	17.841	0.0014	15.596	0.0007	37.822	0.0019	0.87414	0.0036	2.11990	0.0089
19	II C2 (D-10)	Chimney dust	n.d.	17.844	0.0009	15.599	0.0006	37.833	0.0014	0.87419	0.0028	2.12016	0.0075
20	II C4	Chimney dust	n.d.	17.921	0.0022	15.618	0.0019	37.952	0.0047	0.87149	0.0031	2.11770	0.0044
21	III 46	Lichen	n.d.	17.875	0.0188	15.488	0.0164	37.683	0.0410	0.86646	0.0063	2.10814	0.0047
22	III 49 C/12	Vegetable	175.6	17.913	0.0015	15.574	0.0012	37.864	0.0029	0.86943	0.0036	2.11380	0.0035
23	III 14/1	Vegetable	n.d.	18.044	0.0007	15.727	0.0004	38.342	0.0010	0.87156	0.0021	2.12489	0.0043
24	III 14/2	Vegetable	n.d.	18.003	0.0015	15.599	0.0010	38.015	0.0027	0.86648	0.0035	2.11155	0.0085
25	III KA 26/5	Vegetable	n.d.	17.813	0.0066	15.533	0.0057	37.689	0.0144	0.87201	0.0045	2.11582	0.0045
26	III 26	Vegetable	n.d.	17.901	0.0078	15.527	0.0069	37.776	0.0173	0.86740	0.0034	2.11032	0.0029
27	III KA 4/2	Vegetable	n.d.	17.961	0.0017	15.570	0.0012	37.899	0.0030	0.86687	0.0034	2.11002	0.0045
Average					0.0079		0.0068		0.0169		0.0039		0.0063
Myramar peat core													
1	Myr Neo 01	Peat	6	17.738	0.0046	15.583	0.0048	37.606	0.0053	0.87853	0.0015	2.12014	0.0037
2	Myr Neo 02	Peat	14.8	17.688	0.0044	15.582	0.0046	37.577	0.0050	0.88092	0.0018	2.12441	0.0051
3	Myr Neo 03	Peat	45.3	17.657	0.0028	15.562	0.0026	37.503	0.0030	0.88133	0.0046	2.12393	0.0108
4	Myr Neo 04	Peat	65	17.774	0.0061	15.567	0.0054	37.651	0.0054	0.87587	0.0017	2.11838	0.0041
5	Myr Neo 05	Peat	109.1	18.043	0.0030	15.599	0.0029	38.004	0.0036	0.86454	0.0015	2.10633	0.0036
6	Myr Neo 07	Peat	107.1	18.307	0.0078	15.621	0.0086	38.326	0.0094	0.85331	0.0017	2.09358	0.0048
7	Myr Neo 09	Peat	95.9	18.383	0.0124	15.616	0.0161	38.348	0.0203	0.84948	0.0046	2.08601	0.0114
8	Myr Neo 15	Peat	28.1	18.404	0.0018	15.637	0.0020	38.443	0.0022	0.84962	0.0013	2.08879	0.0032
9	Myr Neo 17	Peat	26	18.396	0.0043	15.620	0.0056	38.381	0.0067	0.84911	0.0018	2.08640	0.0043
10	Myr Neo 19	Peat	6.2	18.470	0.0067	15.629	0.0059	38.505	0.0058	0.84618	0.0022	2.08479	0.0062
11	Myr Neo 32	Peat	6.4	18.428	0.0046	15.626	0.0048	38.452	0.0053	0.84796	0.0015	2.08666	0.0035
12	Myr Neo 42	Peat	5.4	18.557	0.0054	15.614	0.0054	38.600	0.0059	0.84137	0.0018	2.08003	0.0043
Average					0.0053		0.0057		0.0065		0.0022		0.0054

The errors shown represent 'with-in run' precisions, which are in general better than the long term reproducibility (see text for details).

Table 4:Complete Pb isotope data set measured during the two environmental geochemical studies (see text for details).

Also shown are TIMS and MC-ICP-MS data for the NIST-SRM 981 Pb standard from other laboratories. Average accuracy of 48, 70, 55, 41, and 77 ppm for the ratios $^{206}Pb/^{204}Pb$, $^{207}Pb/^{204}Pb$, $^{208}Pb/^{204}Pb$, $^{207}Pb/^{206}Pb$, and $^{208}Pb/^{206}Pb$, relative to the Galer and Abouchami value are achieved.

To get an estimate for the data accuracy for real samples, selected ore bearing and barren granites (whole rock) from the Orlovka-Spokoine mining district were measured with the *IsoProbe* MC-ICP-MS and with the *MAT* 261 TIMS. Figure 3 shows the $^{208}Pb/^{206}Pb$ and $^{207}Pb/^{206}Pb$ ratios measured in the same aliquot using the different instruments. Linear regressions ($[^{207}Pb/^{206}Pb]_{TIMS}=0.003+0.996[^{207}Pb/^{206}Pb]_{MC-ICPMS}$; r=0.999; n=13; $^{208}Pb/^{206}Pb]_{TIMS}=-0.018+1.009$ $[^{208}Pb/^{206}Pb]_{MC-ICPMS}$; r=0.998; n=17) and the theoretical 1:1 line are shown. A systematic offset between TIMS and MC-ICP-MS exists, which has been described also with the VG *Plasma54* [7]. The results agree on average within 0.08% for both $^{207}Pb/^{206}Pb$ and $^{208}Pb/^{206}Pb$ ratios. Similar agreements between MC-ICP-MS and TIMS data for real samples were described for ferromanganese crust [11], volcanic rocks [7], archeological samples [13] and peat samples [31].

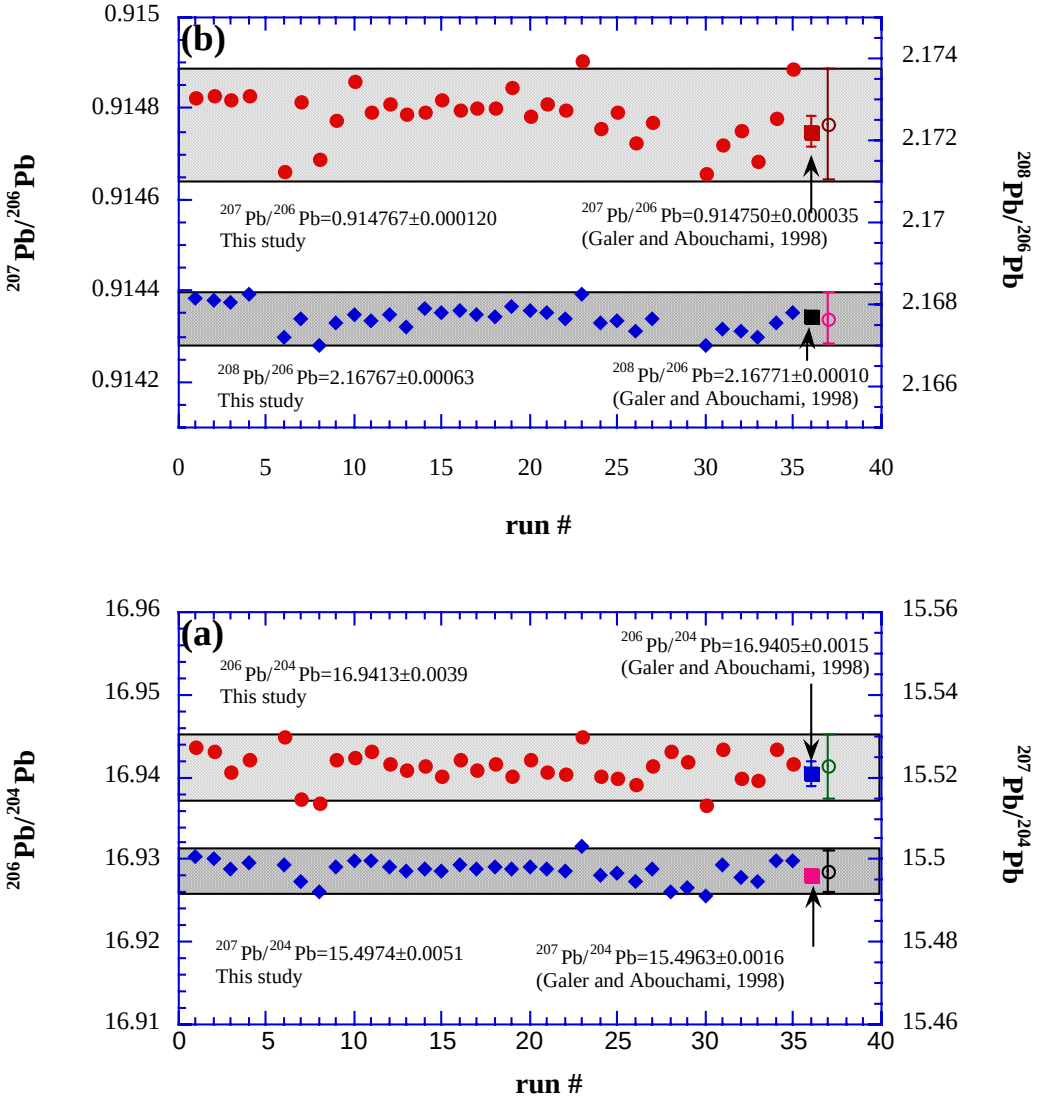

Figure 4: Typical long-term reproducibility achieved for the ratios (a) $^{208}Pb/^{206}Pb$ and $^{207}Pb/^{206}Pb$, and (b) $^{206}Pb/^{204}Pb$ and $^{207}Pb/^{204}Pb$ ratios on the Micromass *IsoProbe* MC-ICP-MS determined from repeated measurements of NIST-SRM 981 Pb standards spiked with NIST-SRM 997 Tl over the time period of five months (August to December 2002).

3.2.2 Precision and reproducibility

Table 4 shows the entire set of isotope ratios and internal precision expressed in ±2σ (%) measured during the two environmental studies in various different environmental matrices. The error of the internal isotope measurements is considerably better (on average below 100 ppm) than the errors estimated from the long-term reproducibility. The measured solutions were diluted to a concentration, which allowed a signal of ≥100 mV on ^{204}Pb. Typically, that was 50 ng ml^{-1}.

Figure 4 shows the long-term reproducibility of the *IsoProbe* MC-ICP-MS using repeated NIST-SRM 981 Pb measurements over a five-month period (August to December 2002). Errors (in ppm) are 227 for ^{206}Pb/^{204}Pb, 326 for ^{207}Pb/^{204}Pb, 314 for ^{208}Pb/^{204}Pb, 126 for ^{207}Pb/^{206}Pb and 292 for ^{208}Pb/^{206}Pb. The errors estimated using the long-term reproducibility are significantly higher than the ones estimated from a single measurement session (short-term reproducibility), which was in general below 200 ppm for the ^{208}Pb/^{204}Pb ratio and below 150 ppm for all the other ratios. The long-term reproducibility of the MC-ICP-MS is similar to the Heidelberg TIMS and agrees with other laboratories using MC-ICP-MS [7, 10-13, 32]. Reproducibility estimated from 'true' replicate measurements (different aliquots of same solution) showed similar errors to the ones determined by the repeated measurements of NIST-SRM 981 Pb [31].

3.3 Applications to environmental geochemical studies

Using these new analytical (ion exchange column, high temperature/high pressure microwave digestions) and modified data processing (^{205}Tl/^{203}Tl optimization, acid blank subtraction) procedures, we achieved high precision Pb isotope ratio measurements in peats, lichens, vegetables and chimney dust during two environmental geochemical projects conducted in London and Heidelberg. One study aimed to assess the local dispersal of Pb and other heavy elements from a Cu smelter using lichen as biomonitors [24], the second study aimed to characterize sources and pathways of Pb and Hg in the sub-Arctic region using a dated peat core in the Faroe Islands [23].

Figure 5 shows three isotope plots of ^{208}Pb, ^{207}Pb and ^{206}Pb measured during the two studies. The differences in the isotope ratios among the individual samples are significant on the ±2σ confidence level and the errors (derived from the long term reproducibility) plot within the symbols.

3.3.1 Lead sources from long-range atmospheric transport in the sub arctic

Figure 5a shows Pb isotope data measured in a peat bog profile collected in the Faroe Islands (representing *c.* 2,500 yrs of atmospheric Pb deposition) with variations of ^{206}Pb/^{207}Pb (1.13-1.19) and ^{208}Pb/^{206}Pb ratios (2.07-2.12), which are significantly larger (5 and 2%, respectively) than the estimated long-term reproducibility for these isotope pairs (0.013 and 0.029%, respectively). The large variations of isotope signatures in the peat samples are due to the different Pb sources (gasoline, coal, soil dust, waste incineration, represented as gray fields in Figure 6a and estimated from data taken from [33], which characterized the atmospheric Pb deposition in Europe during the last 2,500 years [1, 34]. The error bars plot well within the symbols and the individual samples are clearly discernible. The detail geochemical discussion is given elsewhere [23] but the conclusions taken agree well with other peat records in Europe covering the last 2,500 years of atmospheric Pb deposition [33, 35].

3.3.2 Lead sources around a Cu smelter

Figure 5b shows Pb isotope data measured in lichens, vegetables and chimney dust around the Cu smelter in Karabash, Southern Urals. The range of ^{206}Pb/^{207}Pb and of ^{208}Pb/^{206}Pb (1.14-1.15 and 2.11-2.12, respectively) is considerably smaller (0.9 and 0.7%, respectively) than in the peat study, but the variations are still an order of magnitude larger than the estimated errors of the individual data points using the long-term reproducibility. Most ratios of the lichens and vegetables plot on a mixing line between two end members - smelter dust (represented by the isotopic composition of the chimney dust) and natural background Pb (represented by

pre-anthropogenic aerosols [36]). However, a statistically significant scatter in the data is revealed and several samples are off the simple two component mixing line, which suggests that a third end member (most likely anthropogenic) with higher ^{208}Pb and higher ^{207}Pb concentrations remains unidentified. The data set shows that with the precision achieved, even on a local scale pollution with small variations, new end-members can be identified hinting to additional sources. Such detailed source assessment in a local pollution study has previously been achieved using TIMS [37] but not ICP-QMS [38].

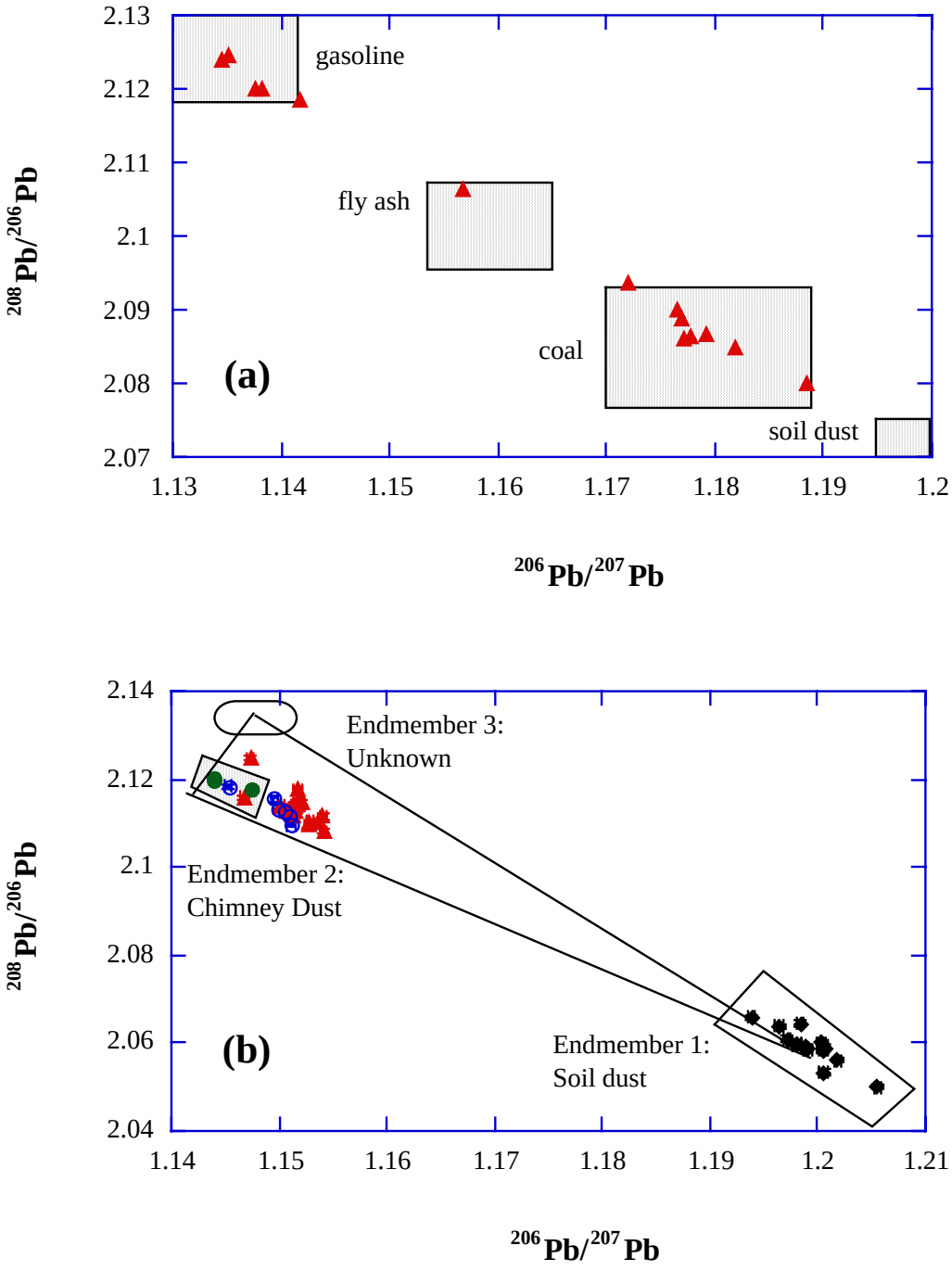

Figure 5: Three isotope plots including the isotopes ^{208}Pb, ^{207}Pb and ^{206}Pb of the two different environmental geochemical studies assessing Pb dispersal into the environment: (a) Pb isotope data from chimney dust, vegetable and lichens within the vicinity of a Zn smelter in the Urals (Purvis et al., in press) and (b) Pb isotope data from a peat core in the Faroe Islands (Shotyk et al., submitted).

4. Conclusions

A wide range of environmental samples was dissolved using microwave assisted acid digestion for biological samples or conventional hot plate acid digestion for silicates. After digestion, the solutions were passed through an ion exchange column packed with EiChrom Sr-resin applying a new simple monoacid elution procedure. The column chemistry yielded quantitative recoveries of Pb and allowed a high sample throughput.

Analysis of ^{204}Pb, ^{206}Pb, ^{207}Pb and ^{208}Pb in 50 ng ml^{-1} solutions on a *Isoprobe* MC-ICP-MS resulted typically in internal precisions of below 100 ppm (±2σ) on all Pb isotope ratios in all matrices. Mass bias correction using optimized ^{205}Tl/^{203}Tl ratios achieved accuracies below 80ppm for all ratios. The Tl optimization was achieved using repeated measurements of NIST-SRM 981 Pb spiked with NIST-SRM 977 Tl during a measurement session and fitting the ^{205}Tl/^{203}Tl ratio using a least square approximation. The optimized Tl ratio used for mass bias correction had to be adjusted for each measurement session up to 2.3907. The long-term reproducibility (expressed as ±2σ) determined over a five month period using repeated measurements of the NIST-SRM 981 Pb standard and optimized Tl values was below 350 ppm for all ratios. Ore bearing granites samples passed through the columns and measured with TIMS and MC-ICP-MS showed excellent correlation. The mass bias of Tl spiked into natural and synthetic samples during a measurement session did not differ significantly, indicating that the complex peat and lichen matrix did not affect the mass bias behavior of the Tl spike.

Acknowledgements

We thank Sara Russell, Eta Mullane, Caroline Smith, Teresa Jeffries and Derek Jones of the Natural History Museum, Mathieu Gounelle at the Université de Paris, Dietlinde Pingel and Nicole Rausch at the University of Heidelberg for the help in the laboratory and William Shotyk (University of Heidelberg) and William Purvis and Reimar Seltmann (The Natural History Museum) for the very stimulating collaborative research. Mike Warner and Helen Andy Fleet and Terry Williams (Natural History Museum) are thanked for support. Financial support from NERC, the Leverhulme Trust, Imperial College London and The Natural History Museum is gratefully acknowledged. This paper benefited greatly from the discussions with other isotope and environmental geochemists, especially Matthew Thirlwall, Mark Rehkaemper, Ed Boyle, Kevin Fox, Matt Reuer, and Jan Kramers. We also thank the anonymous reviewer and Prof Schwarz for editorial handling, D.W. dedicates this paper to Rosa, Jakob and Claudia.

References

1 M.K. Reuer and D.J. Weiss, Anthropogenic lead dynamics in the terrestrial and marine environment, Phil. Trans. R. Soc. Lond. A 360, 2889-2904, 2002.

2 J.G. Farmer, L.J. Eades, A.B. MacKenzie, A. Kirika and T.E. Bailey-Watts, Stable isotope record of lead pollution in Loch Lomond sediments since 1630 A.D, Environ. Sci. Technol. 30, 3080-3083, 1996.

3 D. Weiss, V. Chavagnac, E.A. Boyle, J.F. Wu and M. Herwegh, Determination of lead isotope ratios in seawater by quadrupole inductively coupled plasma mass spectrometry after $Mg(OH)_2$ co-precipitation, Spectrochim. Acta, B 55(4), 363-374, 2000.

4 F. Vanhaecke, L. Moens, R. Dams, I. Papadakis and P. Taylor, Application of high-resolution ICP-mass spectrometry for isotope ratio measurements, Anal. Chem. 69, 268-273, 1997.

5 I.S. Begley and B.L. Sharp, Characterization and correction of instrumental bias in inductively coupled plasma mass spectrometry for accurate measurements of lead isotope ratios, J. Anal. At. Spectrom. 12, 395-402, 1997.

6 C.R. Quétel, T. Bertrand, O.F.X. Donard and F.E. Grousset, Factorial optimization of data acquisition factors for lead isotope ratio determination by inductively coupled mass spectrometry, Spectrochim. Acta 52B, 177-187, 1997.

7 W.M. White, F. Albarède and P. Télouk, High-precision analysis of Pb isotope ratios by multi-collector ICP-MS, Chem. Geol. 167, 257-270, 2000.

8 J.D. Woodhead, A simple method for obtaining highly accurate Pb isotope data by MC-ICP-MS, J. Anal. At. Spectrom. 17, 1381-1385, 2002.

9 S. Ehrlich, Z. Karpas, L. Ben-Dor and L. Halicz, High precision lead isotope ratio measurements by multi collector ICP-MS in variable matrices, J. Anal. At. Spectrom. 16, 975-977, 2001.

10 M. Rehkaemper and A.M. Halliday, Accuracy and long-term reproducibility of lead isotopic measurements by MC-ICP-MS using an external

method for correction of mass discrimination, Intern. J. Mass. Spectrom. 58, 123-133, 1998.

11 N.S. Belshaw, P.A. Freedman, K.A. O'Nions, M. Frank and Y. Guo, A new variable dispersion double-focusing plasma mass spectrometer with performance illustrated for Pb isotopes, Intern. J. Mass Spectrom. 181, 51-58, 1998.

12 T. Hirata, Lead isotope analysis of NIST standard reference materials using multiple collector -inductively coupled plasma mass spectrometry coupled with external correction method for mass discrimination, Analyst 121, 1407-1411, 1996.

13 M. Rehkaemper and K. Mezger, Investigation of matrix effects for Pb isotope ratio measurements by multiple collector ICP-MS: verification and application of optimized analytical protocols, J. Anal. At. Spectrom. 15, 1451-1460, 2000.

14 M. Thirlwall, Inappropriate tail corrections can cause large inaccuracy in isotope ratio analysis by MC-ICP-MS, J. Anal. At. Spectrom. 16, 1121-1125, 2001.

15 M.F. Thirlwall, Multicollector ICP-MS analysis of Pb isotopes using a $^{207}Pb/^{204}Pb$ double spike demonstrates up to 400 ppm systematic errors in Tl-normalisation, Chem. Geol., 2002.

16 M.K. Reuer, E.A. Boyle and B.C. Grant, Lead isotope analysis of marine carbonates and seawater by multiple collector ICP-MS, Chem. Geol. 200, 137-153, 2003.

17 S.J.G. Galer and W. Abouchami, Practical application of lead spiking for correction of instrumental mass discrimination, Min. Mag. 62A, 491-492, 1998.

18 M.F. Thirlwall, Inter-laboratory and other errors in Pb isotope analyses investigated using a ^{207}Pb-^{204}Pb double spike, Chem. Geol. 163, 299-322, 2000.

19 W. Todt, R.A. Cliff, A. Hanser and A.W. Hofmann, Evaluation of a ^{202}Pb-^{205}Pb double spike for high precision lead isotope analysis, in: Earth Processes: Reading the Isotopic Code, S.R. Hart and A. Basu, eds. 95, pp. 429-437, American Geophysical Union, 1996.

20 C.N. Maréchal, P. Télouk and F. Albarède, Precise analysis of copper and zinc isotopic compositions by plasma-source mass spectrometry, Chem. Geol. 156, 251-273, 1999.

21 T.F.D. Mason, D.J. Weiss, M. Horstwood, R.R. Parrish, S.S. Russell, E. Mullane and B.J. Coles, High precision Cu and Zn isotope analysis by plasma source mass spectrometry: Part 2: Correcting for mass bias discrimination effects, J. Anal. At. Spectrom., 11-21, 2004.

22 B. Kober, M. Wessels, A. Bollhofer and A. Mangini, Pb isotopes in sediments of Lake Constance, Central Europe, constrain the heavy metal pathways and the pollution history of the catchment, the lake and the regional atmosphere, Geochim. Cosmochim. Acta 63(9), 1293-1303, 1999.

23 W. Shotyk, M.E. Goodsite, F. Roos-Barraclough, N. Givelet, G. LeRoux, D.J. Weiss, A.K. Cheburkin, K. Knudsen, J. Heinemeier, W.O. Van der Knaap, S.A. Norton and C. Lohse, Accumulation and predominant atmospheric sources of natural and anthropogenic Hg and Pb on the Faroe Islands since 5420 ^{14}C yr BP recorded by a peat core from a blanket bog, Geochim. Cosmochim. Acta, 69 (1), 1-17, 2005

24 O.W. Purvis, P.J. Chimonides, G.C. Jones, I.N. Mikhailova, B. Spiro, D. Weiss and B.J. Williamson, Lichen biomonitoring in one of the most polluted areas in the world, Proc. R. Soc. London B, in press.

25 A. Dolgopolova, R. Seltmann, B. Kober, D. Weiss, P. Dulski and C. Stanley, Geochemical characteristics and Pb isotope systematics of highly fractionated Li-F enriched amazonite granites and related host rocks of the Orlovka-Spokoine mining district, Eastern Tranbsbaikalia (Russia), Trans. Inst. Min. Metall.: Section B: Applied Earth Sciences, submitted.

26 M. Krachler, C. Mohl, H. Emons and W. Shotyk, Influence of the digestion procedure on the determination of rare earth elements in peat and plant samples by USN-ICP-MS, J. Anal. At. Spectrom. 17(8), 844-851, 2002.

27 A. Dolgopolova, D. Weiss, R. Seltmann and B. Coles, Improved high temperature/high pressure microwave digestion method for lichens, Intern. J. Environ. Anal. Chem., submitted.

28 E.P. Horwitz, M.L. Dietz, S. Rhoads, C. Felinto, N.H. Gale and J. Houghton, A lead selective extraction chromatographic resin and its application to the isolation of lead from geological samples, Anal. Chim. Acta 292, 263-273, 1994.

29 E.P. Horwitz, Extraction chromatography of actinides and selected fission products: principles and achievement of selectivity, in: Intern. Workshop on the application of extraction chromatography in radionucleide measurements, IRMM, Geel 9-10, Belgium, 1998.

30 L.P. Dunstan, J.W. Gramlich, I.L. Barnes and W.C. Purdy, Absolute isotopic abundance and the atomic weight of a reference sample of thallium, J. Res. Nat. Bur. Stand. 85, 1-10, 1980.

31 M. Kylander, D.J. Weiss, T. Jeffries and B. Coles, Sample preparation methods for Pb concentration and isotopic analysis in peat by laser ablation-multi collector-inductively coupled plasma mass spectrometry (LA-MC-ICP-MS), J. Anal. At. Spectrom., submitted.

32 K.D. Collerson, B.S. Kamber and R. Schoenberg, Applications of accurate, high-precision Pb isotope ratio measurement by multi collector ICP-MS, Chem. Geol. 188, 65-83, 2002.

33 D. Weiss, W. Shotyk, P.G. Appleby, J.D. Kramers and A.K. Cheburkin, Atmospheric Pb deposition since the Industrial revolution recorded by five Swiss peat profiles: Enrichment factors, fluxes, isotopic composition, and sources, Environ. Sci. Technol. 33(9), 1340-1352, 1999.

34 D. Weiss, W. Shotyk and O. Kempf, Archives of atmospheric lead pollution, Naturwissenschaften 86, 262-275, 1999.

35 A. Martinez-Cortizas, E. Garcia-Rodeja Gayoso and D. Weiss, Peat bog archives of atmospheric metal deposition, Sci. Total. Environ. 292(1-2), 1-5, 2002.

36 W. Shotyk, D. Weiss, J.D. Kramers, R. Frei, A.K. Cheburkin, M. Gloor and S. Reese, Geochemistry of the peat bog at Etang de la Gruere, Jura Mountains, Switzerland, and its record of Pb and lithogenic trace elements (Sc, Ti, Y, Zr, Hf, and REE) since 12,370 C-14 yr BP, Geochim. Cosmochim. Acta 65(14), 2337-2360, 2001.

37 C. Gobeil, W.K. Johnson, R.W. MacDonald and C.S. Wong, Sources and burden of lead in St. Lawrence Estuary sediments: Isotopic evidence, Environ. Sci. Technol. 28(1), 193-201, 1995.

38 J.M. Blais, Using isotopic tracers in lake sediments to assess atmospheric transport of lead in Eastern Canada, Water, Air, Soil Pollut. 92, 329-42, 1996.

COMPLEMENTARY INFORMATION

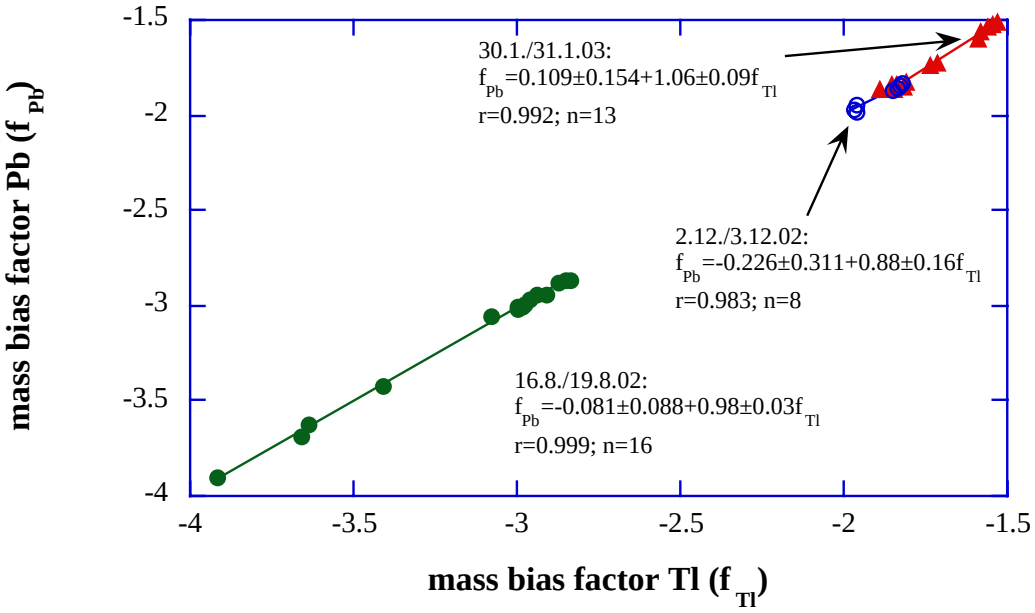

The mass bias factors of Pb and Tl (f_{Pb}, f_{Tl}) calculated using the Pb values published by Galer and Abouchami [17] and the optimized Tl ratio using our optimization procedure over a period of six months (Aug. '02 to Jan. '03). Shown are three measurement sessions (Aug. 2002, Dec. 2002 and Jan. 2003).

This figure shows mass bias factors for Pb (f_{Pb}) and Tl (f_{Tl}) plotted against each other using data collected over three different measurement periods (16.8/19.8.02, 2./3.12.02 and 30.1/31.1.2003). The mass bias factors were calculated with the exponential law using the 'true' ratios for Pb taken from Galer and Abouchami and the optimized ratio for Tl after running the optimization procedure. Given the boundary conditions for the Tl optimization procedure, all three measurement periods show the same mass bias factor for Pb and Tl on the 95% significance level, thus $f_{Tl}=f_{Pb}$, and all three data sets have an intercept at the origin within the error (calculated on the 95% significance level).

- Chapter 1.3 -

Optimising accuracy and precision of lead isotope measurement (^{206}Pb,^{207}Pb,^{208}Pb) in acid digests of peat with ICP-SMS using individual mass discrimination correction

Michael Krachler, Gaël Le Roux, Bernd Kober and William Shotyk

Institute of Environmental Geochemistry, University of Heidelberg, Heidelberg, Germany

Journal of Analytical Atomic Spectrometry (2004), 19, 354-361

Abstract

Using ICP-SMS, a robust analytical protocol for accurate and precise determination of the isotopic Pb composition (^{206}Pb, ^{207}Pb, ^{208}Pb) of acid digests of peat samples was developed. External precision better than 0.05% and 0.1% for Pb concentrations in the range of 1 μg l^{-1} and 0.1 μg l^{-1}, respectively, were achieved for both $^{207}Pb/^{206}Pb$ and $^{208}Pb/^{206}Pb$ ratios. These precisions have never before been achieved with ICP-SMS in a complex matrix containing such low concentrations of total Pb. Procedural Pb blank concentrations amounted to 0.003 μg l^{-1} and had no influence on the accuracy of the Pb isotope ratios. Corrections for mass discrimination were accomplished using the certified isotopic reference material SRM 981. However, mass discrimination was found to be non-systematic, and varied among the masses both with respect to magnitude and direction. To accommodate this phenomenon, an individual mass discrimination correction was applied to each ratio resulting in improved accuracy. Using this approach, the mass discrimination for both Pb isotope ratios was < 0.2%, compared to values on the order of ±0.35% if only a single Pb isotope ratio was used. The accuracy and precision of the ICP-SMS protocol was further evaluated using thermal ionisation mass spectrometry (TIMS) of selected samples and an in-house peat reference material. In general, the Pb isotope ratios determined using ICP-SMS deviated from the TIMS values by less than < 0.1%. Given the throughput of the ICP-SMS compared to the TIMS (which requires chemical separation of Pb), the approach described offers great promise for environmental studies to fingerprint the predominant sources of anthropogenic Pb. Two applications are presented here: a bog profile from the Black Forest (SW Germany) consisting of eight thousand years of peat accumulation, and a depth profile through a snowpack collected from the same site during the winter of 2003.

Keywords: *lead; isotope ratio; peat; snow; ICP-SMS*

Introduction

Ombrotrophic (rain-fed) peat bogs receive metals exclusively from the atmosphere[1] and are gaining popularity as archives of atmospheric trace element deposition.[2] While a growing range of trace metals has been investigated,[3-6] Pb has certainly attracted the most attention.[3,7,8] Precise measurements of Pb isotope ratios using thermal ionisation mass spectrometry (TIMS) of peat cores age dated using ^{210}Pb[8,9] and comparison with herbarium samples of *Sphagnum* moss[10] have shown that Pb is effectively immobile in peat profiles, and that bogs provide faithful records of the atmospheric deposition of this element.[7] Using the isotopic composition of Pb as a fingerprinting tool, age-dated peat profiles represent a potentially very powerful tool for the reconstruction of atmospheric fluxes and predominant sources of Pb and other trace metals.[11]

For any given sample, thermal ionisation mass spectrometry (TIMS) provides the most accurate and precise measurements of Pb isotope ratios. However, TIMS analyses are laborious and time-consuming because the analyte (Pb) has to be separated from the sample matrix prior to analysis. Quadrupole ICP-MS (Q-ICP-MS) has been used to measure the isotopic composition of Pb in acid digests of peat and lichens in several studies,[12,13] but accuracy and precision are poor compared to TIMS measurements; here, studies employing this technique are not discussed further. Multi-collector ICP-MS (MC-ICP-MS) may offer precision and accuracy comparable to TIMS, but this comparatively new method has not yet been applied to acid digests of peat.

Double focusing ICP-MS instruments with a magnetic sector (ICP-SMS) have become an increasingly attractive alternative to TIMS for the accurate and precise determination of isotope ratios.[14-23] The best precisions ever reported for the determination of ^{207}Pb/^{206}Pb and ^{208}Pb/^{206}Pb ratios by ICP-SMS in its standard sample introduction configuration made of glass range from 0.03 to 0.05%.[16,20,22,23] To achieve these precisions, however, total Pb concentrations in the analyte solutions had to be between 5 and 50 μg kg^{-1}. To date, because of the large dilution factors needed to overcome the effects of sample matrix and digestion reagents on instrument performance, in complex matrices only those samples with relatively high Pb concentrations could be analysed with acceptable precisions (e.g. 0.05%). Using an ultrasonic nebulizer (USN) with a membrane desolvation unit can help to overcome this limitation.[18] With the improved sensitivity of this instrumental set-up, ^{206}Pb/^{207}Pb and ^{206}Pb/^{208}Pb ratios with precisions of 0.07% and 0.02%, respectively, could be determined in a synthetic water reference material (diluted 100-fold) with a total Pb concentration of 0.182 μg l^{-1}.[18] This achievement, however, required a sample volume of more than 20 ml and this could be a critical issue in some environmental studies when only a limited amount of sample is available. A tandem spray chamber arrangement (combination of a cyclone spray chamber and a Scott-type spray chamber) provides an intensity enhancement by a factor of two to four times and a more stable signal compared to conventional or USN sample aspiration, but has not found widespread use so far.[19] At the 1 μg l^{-1} level, this sample introduction system provided precisions ranging from 0.03 to 0.09% for ^{207}Pb/^{206}Pb ratios in various diluted isotopic reference materials.[19]

Peat is a complex matrix containing very stable organic and inorganic (mineral) components which are resistant to decomposition even in the most aggressive digestions solutions. The present study was undertaken to further extend the application of Pb isotope ratio measurements by ICP-SMS and to improve the overall performance by addressing the following issues: i) extension of Pb isotope ratio measurements using an HF-resistant sample introduction system (PFA nebulizer, PFA spray chamber, sapphire injector) to allow analysis of digestion solutions containing HF and HBF_4; these are necessary to completely destroy the Pb-bearing mineral grains in peat which are derived from atmospheric soil dust particles;

ii) optimisation of data acquisition parameters for obtaining the best possible precision; iii) elucidation of precisions achievable at Pb concentrations < 1 μg l^{-1}; iv) comparison of the Pb isotope ratio determinations with data obtained for the same set of samples using TIMS and v) application of the optimised analytical protocols to the determination of Pb isotope ratios in acid digests of selected peat samples from a German bog. Finally, the protocol is also applied to fresh snow samples containing ultralow concentrations of total Pb collected from the same site.

1.EXPERIMENTAL

1.1 Instrumentation

All sample manipulations and preparations of standards were performed under laminar flow clean air benches (class 100) to minimize potential risk of contamination. Sample digestions were performed in a clean laboratory of class 10 000.

Two hundred mg of dried, powdered peat samples were dissolved in 3 ml HNO_3 and 0.1 ml HBF_4 in PTFE digestion vessels (20 ml) in a microwave heated autoclave (ultraCLAVE II, MLS GmbH, Leutkirch, Germany) as described in detail elsewhere.[24,25] Briefly, up to 40 samples were simultaneously heated to 240 °C within 75 min obtaining clear, homogeneous digestion solutions.

All ICP-MS measurements were carried out with an Element 2 ICP-SMS (Thermo Finnigan, Bremen, Germany) equipped with a guard electrode to eliminate secondary discharge in the plasma and to enhance overall sensitivity. The high resolution double focusing (reverse Nier-Johnson geometry) single collector ICP-MS instrument provides flat top peaks in the low resolution mode (m/Δm 300) which was used. A micro volume autosampler (ASX 100, Cetac Technologies, Omaha, NE, USA) and a HF resistant sample introduction kit consisting of a microflow PFA nebulizer, a PFA Scott-type double pass spray chamber and a sapphire injector tube were employed to transport the analytes into the plasma of the ICP-MS. The PFA spray chamber has an additional gas inlet which was flushed with about 0.1 l argon min^{-1} to increase sensitivity and stability of this sample introduction set-up. The dead time of the detector (13 ns) was determined following the manufacturer´s instructions. Peat samples were diluted with 0.1% (v/v) high-purity HNO_3 to reach a total Pb concentration of about 1 μg l^{-1} in the analyte solution; snow samples were directly analysed for both total lead concentration and Pb isotope ratios. Details on the ICP-MS operating conditions, the data acquisition and reduction parameters are summarised in Tables 1 and 2, respectively. Total Pb concentrations in solid peat samples were analysed by EMMA XRF.[26]

Forward power	1250 W
Coolant gas flow rate	16 l min^{-1}
Auxiliary gas flow rate	~ 0.8-1.0 l min^{-1}, optimised daily*
Sample gas flow rate	~ 0.8-1.0 l min^{-1}, optimised daily*
Spare gas flow rate	~ 0.1 l min^{-1}, optimised daily*
Sample cone	Ni, 1.1 mm aperture id
Skimmer cone	Ni, 0.8 mm aperture id
Resolution	300 (m/Δm)
Sample uptake rate (pumped)	~0.1 ml min^{-1}
Scan type	Fixed magnet with electric scan over small mass ranges
Ion sampling depth	Adjusted daily*
Ion lens settings	Adjusted when appropriate

Table 1: Operating conditions of the ICP-SFMS (*Optimised in order to obtain a stable ^{208}Pb signal (typically 700 000 cps for 1 μg l^{-1}) and the lowest possible oxide formation rate (see text for details).

Lead isotope ratio determinations using TIMS were carried out on a MAT 261 (Thermo Finnigan) following well established analytical procedures.[27,28]

1.2 Reagents and Standards

For the preparation of all solutions, high purity water (18.2 MΩ cm) from a MilliQ-Element system designed for ultra trace analysis (Millipore, Milford, MA, USA) was used. Nitric acid (65%, analytical-reagent grade, Merck, Darmstadt, Germany) was further purified by sub-boiling distillation (MLS GmbH). Other reagents for digestions were tetrafluoroboric acid solution (HBF_4, ~50%, purum, Fluka, Buchs, Switzerland) and hydrogen peroxide (30%, Baker analysed, J.T. Baker, Deventer, Holland).

Isotopes measured	^{206}Pb, ^{207}Pb, ^{208}Pb
Scan type	Magnet fixed at ^{206}Pb, electric scans over other masses (E-scan)
Mass scanning window	5%
Magnet settling time	1 ms (default minimum)
Dwell time per isotope	5 ms
Scan duration per scan	78 ms
Number of scans	1200
Total time per sample (5 replicates including uptake)	9 min 30 s
Sample uptake and equilibration time	100 s
Rinse time between sample and bracketing standard	1 min with 1% HNO_3
Detector dead time	13 ns

Table 2: Data acquisition parameters for Pb isotope ratio measurements

Lead calibration solutions were prepared daily by appropriate dilution of a 10 mg l^{-1} stock standard solution (Merck) with 0.14 mol l^{-1} high-purity nitric acid. To correct for instrumental drifts and plasma fluctuations, all solutions analysed for total Pb were spiked with an indium solution (Merck) to a final concentration of 1 μg l^{-1}.

For isotopic analysis, the National Institute of Standards and Technology (NIST) Standard Reference Material (SRM) 981 Common Lead Isotopic Standard was diluted to a Pb concentration of 250 μg g^{-1} with 1% (v/v) high-purity HNO_3. This standard solution was further diluted to about 1 μg Pb l^{-1} for daily analysis.

1.3 Collection of peat and snow samples

A 6 m long peat core was collected in the southern Black Forest (Germany) in June 2002 using a Ti Wardenaar and a Belarus corer using procedures similar to those described in detail elsewhere.[3] Immediately after collection the core was wrapped in polyethylene foil and transferred into boxes for transport into the laboratory. On arrival in the laboratory, the peat core was frozen, subsequently cut into 1 cm slices using a band saw and further processed for analysis.

A snow profile was dug in the 70 cm snow pack located on the ombrogenic part of the above mentioned peat bog in February 2003. Each 10 cm layer was collected with PET gloves in virgin plastic bags previously "rinsed" with snow from the same level. Snow bags were kept frozen in an insulated box until their transfer for filtration in the laboratory. Snowmelt was realized at room temperature overnight. Melt waters were filtered through 0.45 μm membranes (type HAWP, Millipore), collected in acid-cleaned polypropylene bottles and acidified with doubly distilled HNO_3 to reach a pH between 1 and 2.

1.4 Quality Control

The accuracy of the isotope ratio measurements by ICP-SMS were assessed by measuring the certified Pb isotope standard SRM 981. As an independent check of the obtained accuracy, selected peat samples were also analysed for Pb isotope ratios using TIMS. In both cases (SRM 981 and TIMS) Pb isotope ratios determined by ICP-SMS generally agreed to within < 0.1% of the "true" value.

Accuracy of the determination of total Pb in snow samples was ascertained by the determination of the Pb concentration in the riverine water reference material SLRS-2, National Research Council Canada, Ottawa, Canada (certified: 0.129 ± 0.011 μg l^{-1}; found 0.137 ± 0.011 μg l^{-1}, n = 9); for the peat samples, the certified plant material GBW 07602 Bush Branches and Leaves, Institute of Geophysical and Geochemical Exploration, Langfang, China, (certified: 7.1 ± 0.7 μg g^{-1}; found 7.2 ± 0.7 μg g^{-1}, n = 6).

2 RESULTS AND DISCUSSION

2.1 Data acquisition parameters

The data acquisition parameters for Pb isotope ratio measurements summarised in Table 2 were found to provide excellent performance of the ICP-MS instrument and were thus not further optimised. In fact, using 1200 scans per replicate with a dwell time of 5 ms per Pb isotope yielded comparable results to the best ever reported Pb isotope ratio measurements using a single collector ICP-MS instrument. Principal considerations for the appropriate selection of the number of scans, dwell time, mass integration window, etc. have been repeatedly reported in the recent literature.[15-18,20,23]

2.2 Data reduction, processing, and statistical analyses

The voluminous set of ICP-MS signals acquired during each sample run requires careful and thoughtful data reduction. As outlined by Gwiazda *et al.* in some detail, the procedures employed to reduce the data acquired by the ICP-MS signals may significantly influence the precision of the final results.[17] In the present study, the measurement sequence consisted of 5 x 1200 scans per sample. For data reduction, the 1200 scans per replicate were split into 6 x 200 scans which were used to calculate a mean Pb isotope ratio per replicate with a corresponding standard deviation; the *internal precision* (short term variability) is defined as the relative standard deviation (RSD) of this mean. Five replicates per sample were analysed without washing in between; this helped to keep measurement time to a minimum.

The results reported here are expressed as the mean of the means of all five replicates measured per sample, i.e. total of 6000 scans. The same holds true for the corresponding standard deviation and relative standard deviation; the RSD of this composite mean is defined as the *external precision* (long term variability). Before and after each sample the certified isotopic Pb standard solution was analysed twice to correct for mass discrimination drifts as outlined in detail below.

Applying the analytical scheme described above, four samples, including bracketing standards, can be analysed in about one hour by ICP-SMS and will provide the accuracy and precision described below.

2.3 Precision

Precise determination of the isotopic composition of a sample is a major prerequisite for a meaningful interpretation of the results. In addition to the limitations set purely by Poisson (counting) statistics, precision of isotope ratio measurements obtainable by a single collector ICP-MS instrument is influenced by effects such as plasma flickering, fluctuations in the sample aspiration due to the peristaltic pump, etc. Therefore, the relative standard deviations (RSD) of the isotope ratios for any given sample can only approach, but never achieve, that predicted by theoretical, idealized, considerations.

As mentioned above, the internal precision obtained from the isotope ratio measurement of a single sample (i.e. the RSD of 1200 scans) depends on the signal intensity. Figure 1 is a composite graphic illustrating the dependence of the internal precision of the $^{207}Pb/^{206}Pb$ ratio on the concentration of total Pb (as indicated by the number of ^{206}Pb counts per second) accumulated throughout this study. Internal precision amounted to approximately 0.2% at a level of 0.5 $\mu g\ l^{-1}$ total Pb in the analyte solution. In agreement with other researchers, the external precision, i.e. the RSD derived from five consecutive measurements of the same sample, was much better and approached 0.01% in some cases. However, on a routine basis, the protocol described here provided external precision of 0.05% for both $^{207}Pb/^{206}Pb$ and $^{208}Pb/^{206}Pb$ ratios at total lead concentrations of 1 $\mu g\ l^{-1}$.

Similarly low external precisions ($\leq 0.1\%$) for Pb isotope ratio measurements have been reported in other kinds of samples using ICP-SMS.[15,20] In these earlier studies, however, relatively high concentrations of total Pb (up to 50 $\mu g\ kg^{-1}$) were required in the digestion solutions to achieve this performance. For lower Pb concentrations, an ultrasonic

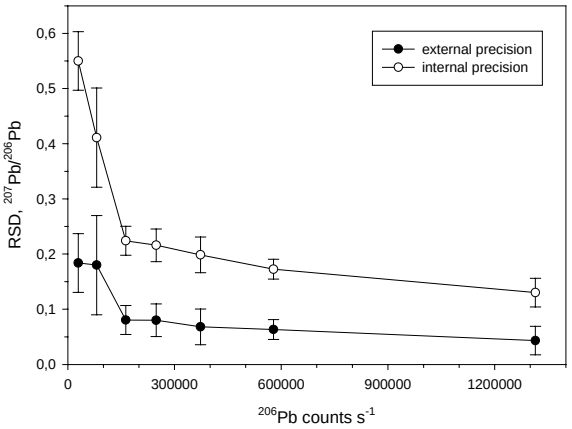

Figure 1: Dependence of internal and external precision (n = 5) on the count rate of the ICP-SMS.

nebulizer with a membrane desolvation unit requiring a sample volume of about 20 ml was necessary to obtain comparable precisions.[18] In contrast, during the present investigation, external precisions of 0.1% were achieved at concentrations of total Pb as low as 0.1 μg l^{-1}. In fact, in the present study no sample contained more than 1 μg l^{-1} Pb. Using an HF resistant low flow PFA sample introduction system, five replicate measurements of each sample consumed less than 1 ml per sample. In other words, the protocol described here provides Pb isotope ratios at precisions as good or better than ever obtained using ICP-SMS, but at far lower (10x or more) concentrations of total Pb, and in much smaller sample volumes. Higher Pb concentrations than 2 μg l^{-1} were not considered in order not to "contaminate" the ICP-MS.

Five replicate measurements of a sample under the selected experimental conditions proved to be sufficient to provide the reported RSD. An attempt to increase the number of replicates to up to 10 led to no further improvement of the precision of the Pb isotope ratio measurements. In summary, routine measurement of five replicate samples containing total Pb as little as 0.1 μg/L provides an external precision better than 0.1%.

Effect of sample dilution

Another important factor potentially influencing the precision of isotope ratio measurements was the dilution of the peat digests. When a minimum final dilution factor of 400 times of solid peat samples was applied, the obtained RSD was independent of the matrix. Below this value, RSD sometimes worsened depending on the matrix composition of the particular sample. Given the fact that the "cleanest" peat samples dating from pre-anthropogenic times (ca. six to nine thousand years old) typically contain 200 ng/g in the solid phase,[7] a dilution factor of 400 times ensures that all acid digests will contain at least 0.5 μg/L; this concentration of total Pb ensures that the external precision of the Pb isotope measurements of virtually all peat samples will exceed 0.1% (Fig. 1).

Instrument tuning

Tuning of the instrument (mainly torch position and gas flows) for best signal stability is another key point to obtain precise results. Experience has shown that it is not advisable to optimise instrumental parameters for maximum ^{115}In intensity and a smooth ^{115}In signal as is typically the case for elemental analyses, but rather to tune on Pb. Here, ^{208}Pb is preferred because it has the greatest natural abundance of all the Pb isotopes. At an initial stage of this study, the ICP-SMS was tuned on ^{115}In and the performance for Pb isotope ratio measurements was not acceptable. A closer look at this problem revealed that, although the ^{115}In signal was very stable, the time resolved signal for ^{208}Pb experienced considerable fluctuation. A perfectly stable signal obtained after optimisation of all gas flows using an In standard solution will not result in a stable Pb signal and vice versa. Therefore, the instrument was tuned for maximum stability and gain of the ^{208}Pb signal.

Formation of oxides

It should be also noted that the oxide formation rate after optimisation, established via monitoring the ratio of UO to U, ranged between 6-12%. This relatively high oxide formation rate is partly due to the use of the guard electrode increasing the oxide formation rate by about one order of

magnitude which can have a potentially serious drawback.[19] For example, polyatomic overlaps arising from Ar-based erbium and ytterbium interferences may negatively influence both precision and accuracy of all three Pb signals. The results of this study, however, revealed that this was not the case. Because of their comparatively low concentrations, other potential interferences originating from Os, Pt and Ir are very unlikely.In cases where oxide formation could be problematic, desolvating sample introduction systems, largely reducing the oxide formation rate, might be advantageous in that context.

2.4 Accuracy

Once the precision of the actual measurement has been optimised, the accuracy of the obtained isotope ratios largely depends on the determination of the detector dead time and the factor to be used for the mass discrimination correction. Both effects as well as adequate approaches to correctly quantify these two phenomena have been repeatedly discussed in the literature.[15,21]

Detector dead time

Compared to ICP-quadrupole mass analyzers (50-80 ns), the detector dead time for ICP-SMS is distinctly lower (20-50 ns).[15,16,18,20,22] For the Element 2, the detector dead time is even lower[21] and in the case of our instrument, it amounts to only 13 ns. The determination of the detector dead time is not critical for small isotope ratios such as the ratio between ^{206}Pb and ^{207}Pb which is more or less unity. However, if the ratio between the isotopes is 1:500, differences in dead time of only 1 ns may induce inaccuracies as large as 0.1%.[21]

Correction for mass discrimination

A distinctly larger influence on the accuracy of the results, however, can be attributed to the appropriate correction of the mass discrimination drift during a measurement sequence. "Mass discrimination", often referred to as "mass bias", is a measure of the deviation between the measured and true isotopic ratio. Two approaches are generally applied to correct for mass discrimination. *Internal mass discrimination* correction uses the drift of ^{203}Tl/^{205}Tl, for example, to correct the Pb isotope ratios.[14,18] This approach assumes, however, that the mass discrimination/mass unit is constant and therefore can be also applied to the correction of the determined Pb isotope ratios. A second problem with this approach is that Tl isotopes might fractionate differently during the measurement and thus might not perfectly match the behaviour of Pb; this could lead to a different mass discrimination for both elements. Additionally, spiking of Tl to all samples is necessary using this methodology. Moreover, time which could be spent on the acquisition of Pb counts is lost because the two Tl isotopes have to be monitored with great precision in every sample. Nevertheless, the mass discrimination is simultaneously determined together with corresponding Pb isotopes in each sample, which favors this approach.

External mass discrimination correction, using the certified isotopic lead standard reference material SRM 981, was applied throughout this study. Two replicates of SRM 981 were always measured before and after five replicate measurements of each sample. The Pb ratios of four replicates of SRM 981 (two before and two after each sample) were averaged and used to calculate the mass discrimination for the sample. The reason for always analysing two replicates of SRM 981 between real samples was to check for potential matrix effects of the sample which distinctly influenced the mass discrimination in the reference material. Generally, the two Pb isotope ratios of each of the two replicates of SRM 981 measured before and after a sample agreed within the standard deviation of their means. If a digest was insufficiently diluted thereby inducing serious matrix effects, a distinct drift of the mass discrimination determined before and after the sample was obvious. Such values were withdrawn and after appropriate dilution of the digest, the sample was measured once again yielding improved results. As mentioned before, a final dilution factor of

approximately 400 was generally required to obtain accurate and precise results as well as a stable and robust performance of the instrument. Under these conditions, the sensitivity of ICP-SMS remained unchanged for at least 14 hours. In contrast, previous studies[16] have reported drifts in sensitivity as great as 10% or more in as little as four hours; the experience obtained here suggests that these problems might have been caused by inadequate dilution of the sample. Other researchers did not comment on this important issue in detail[16,20,22] but they probably used even greater dilution factors than we have used here, as they analysed samples of galena, soil, or copper alloys, all of which have very high Pb concentrations.

Mass discrimination for $^{207}Pb/^{206}Pb$ and $^{208}Pb/^{206}Pb$

Common practice for correction of the mass discrimination is the calculation of a "mass discrimination/mass unit" using one Pb isotope ratio of a certified isotopic reference material. This mass discrimination/mass unit is considered constant (at least for some mass units) and is used to correct all measured isotope ratios. Reported values for this mass discrimination using ICP-SMS range from 0.2 to 0.75% per mass unit.[15,20,22] To further improve the accuracy of the Pb isotope ratio measurements, we investigated this assumption in more detail. We calculated the mass discrimination for both the ^{207}Pb/^{206}Pb and the ^{208}Pb/^{206}Pb ratio considering about 260 measurements of SRM 981 which have been measured between unknown samples. Figure 2A highlights the mass discrimination drift during several measurement sequences obtained on different days. As can be clearly seen from this Figure, the mass discrimination of the two Pb isotope ratios largely follow each other, assuming that, at least at first glance, the commonly applied mass discrimination correction is accurate. Sometimes, however, the mass discrimination of the two Pb isotope ratios largely differ from each other. To illustrate this effect, the ratio of both mass discriminations was plotted in Fig. 2B. Ideally, the ratio should be unity if both Pb isotope ratios were affected in the same manner. The data in Fig. 2B shows that

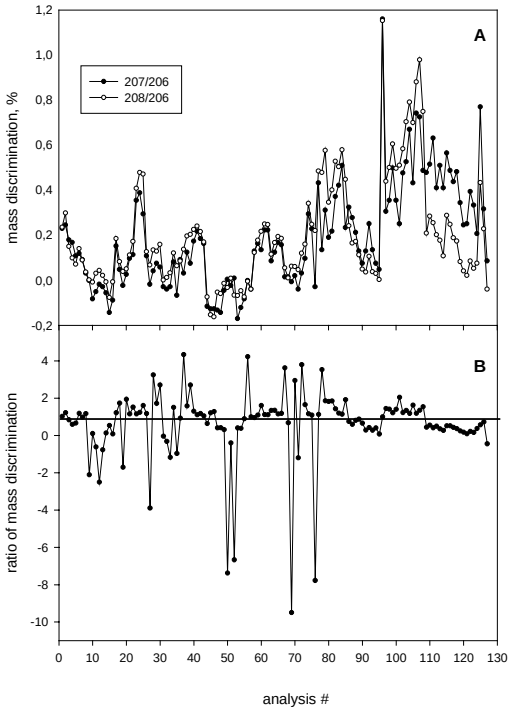

Figure 2: A. Changes in the mass discrimination of the ^{207}Pb/^{206}Pb and the ^{208}Pb/^{206}Pb ratio during several measurement sequences as determined on the certified isotopic reference material SRM 981.

B. Ratio of the mass discrimination of the ^{207}Pb/^{206}Pb and the ^{208}Pb/^{206}Pb ratio

this is certainly not always the case. As is evident from this plot, many values are centred around unity but large deviations ranging from about 4 to -10 are observed. It should be stressed that these deviations from the ideal case are not caused by instances of poor instrument performance which might occur at random. In fact, even larger differences in the mass discrimination for both pairs of Pb ratios yielded accurate results as confirmed by TIMS analysis of identical samples (see below). Considering the results from the analysis of SRM 981 starting from # 80 until the end of the sequence, it is evident that, even though the mass discrimination for the ^{207}Pb/^{206}Pb and the ^{208}Pb/^{206}Pb ratio largely differ from each other, the ratio of the mass discrimination of the two ratios is centred around unity and thus an accurate correction of the mass discrimination drift can be applied to the samples. If only a single Pb isotope ratio for the calculation of the mass discrimination would have been considered, the deviation from the true value could be as

large as ±0.35%. On an average, the mass discrimination for both Pb isotope ratios was < 0.2%, however, with standard deviations of 0.2%. As it is convenient to calculate the mass discrimination correction factor for each Pb isotope ratio, uncorrected Pb isotope ratios of samples were corrected by the individual mass discrimination of the same ratio in the SRM 981 standard reference material.

Already in 1998, Woolrad et al.[15] reported non-systematic mass discrimination that varied between the masses in both magnitude and mass direction. They concluded that a well characterised Pb isotope standard should be used to individually correct the mass discrimination for each Pb isotope ratio to obtain highest possible accuracy of the results. This finding is strongly supported by our detailed investigations graphically summarised in Fig. 2. Unfortunately, it is not clear from the data presented in several earlier publications, whether or not authors applied individual mass discrimination corrections for each Pb isotope ratio. It seems, however, that most of these authors only used a single mass discrimination correction factor to correct all measured Pb isotope ratios because most of them report a mass discrimination per mass unit.

Warm-up time

A second effect, namely the necessary warm-up of the magnet by running the analysis method for about 2 hours before beginning data collection, was not required with our ICP-SMS.[11,13] The best performance with the Element 2 was already obtained after igniting the plasma and warming up the electronics for about one hour. However, the number of pre-scans, which is normally set to 1 for concentration determinations, was set to 20 for isotope ratio measurements. Thus the magnet scans 20 times over the selected mass range before starting with the acquisition of data, thereby "conditioning" the magnet. This reduced warm-up time most probably is thanks to the new magnet and the fully thermostated analyser in the Element 2.

Regression models to calculate the mass discrimination factor

In agreement with other findings using the same ICP-SMS, a check of the three commonly applied models (linear, power law, exponential function) to calculate the mass discrimination correction factor revealed that all three models gave almost identical results.[21] It is important to note here that the limited precision obtainable by single collector ICP-SMS is the reason why all three correction models yield the same Pb isotope ratios. The distinctly higher precision of MC-ICP-MS and TIMS allows to describe physical effects in the mass spectrometer such as fractionation and thus clearly shows the dependence of the results on the applied model. All Pb isotope ratios reported in this study have been corrected using the power law function.

2.5 Comparison with results obtained using TIMS

To help evaluate the potential of the analytical procedure quantitatively, several peat samples analysed in this study by ICP-SMS have also been measured using TIMS after chemical separation of the analytes from the peat matrix by common column chemistry.[27,28] Additionally, the certified isotopic reference material SRM 981 has been analysed for quality control purposes. The results of this comparison are highlighted in Table 3. It is evident that external precisions (RSD) obtainable by TIMS are as much as one order of magnitude lower than those of ICP-SMS. However, the precision of the lead isotope ratio determinations by ICP-SMS is generally < 0.1%. Accuracy, established by comparison of the ICP-SMS data to the TIMS data, revealed that the deviation of the ICP-SMS results from the “true values” is generally < 0.1%.

It should be noted that in two cases (OGS 1878P and LDW 23) the difference between ICP-SMS and TIMS for $^{207}Pb/^{206}Pb$ ratios was > 0.1%, i.e. 0.16% and 0.14%, respectively (Table 3). The precision obtained by TIMS for the $^{207}Pb/^{206}Pb$ ratios in these two samples was worse than usual and comparable to that obtained by ICP-SMS. As the latter method gave RSD of 0.04% and 0.05%, respectively, TIMS data for these two Pb isotope ratios

Peat sample laboratory code		^{207}Pb/^{206}Pb mean	s	RSD (%)	^{208}Pb/^{206}Pb mean	s	RSD (%)
OGS 1878P	ICP-SMS	0.8701	0.0003	0.04	2.1042	0.0003	0.02
	TIMS	0.8687	0.00037	0.04	2.1046	0.00013	0.006
	Deviation from TIMS	*0.16%*			*-0.02%*		
LDW 3	ICP-SMS	0.8559	0.0006	0.07	2.0971	0.0013	0.06
	TIMS	0.8566	0.00002	0.003	2.0986	0.00006	0.002
	Deviation from TIMS	*-0.08%*			*-0.07%*		
LDW 6	ICP-SMS	0.8524	0.0007	0.08	2.0914	0.0017	0.08
	TIMS	0.8522	0.00003	0.003	2.0895	0.00005	0.003
	Deviation from TIMS	*0.02%*			*0.09%*		
LDW 23	ICP-SMS	0.8490	0.0004	0.05	2.0864	0.0010	0.05
	TIMS	0.8478	0.00018	0.021	2.0847	0.00036	0.017
	Deviation from TIMS	*0.14%*			*0.08%*		
SRM 981	ICP-SMS	0.9144	0.0008	0.09	2.1672	0.0012	0.05
	certificate	0.91464	0.00033	0.036	2.1681	0.00033	0.015
	Deviation from certificate	*0.03%*			*0.04%*		

Table 3: Comparison of ^{207}Pb/^{206}Pb and ^{208}Pb/^{206}Pb ratios determined in selected peat samples and the certified standard reference material SRM 981 by ICP-SMS and TIMS.

should be interpreted with some caution, as the quality of the data is poor compared to accuracy and precision of Pb isotope ratios obtained by geochronologists working with geological specimens.[27] In this context, however, it must be emphasised that the performance obtained using TIMS measurements employed "real world" samples of peat: this is a complex material containing a wide variety of both organic and inorganic components which are highly resistant to attack by oxidising, acidic digestion solutions. As a result, the comparative data given in Table 3 is not a reflection of the quality of Pb isotope data which can be obtained by TIMS generally, but does illustrate the complexity of the peat samples. The main reason for the limited precision may be due to organic matter which has survived the digestion of the peat samples, either interfering with the chemical separation of Pb on the ion exchange columns, or with the Re filament, giving unstable signals. Either way, the comparison with the TIMS data shows that ICP-SMS can provide excellent accuracy and precision for Pb isotope measurements in such difficult matrices as acid digests of peat.

2.6 Isotopic composition of Pb in a peat profile and snow profile

Peat profile. The Pb concentrations (obtained using the EMMA XRF[26]) as well as the ^{206}Pb/^{207}Pb ratio of selected samples (obtained using ICP-SMS) from the peat core collected in the Black Forest (SW Germany) are shown versus depth in Fig. 3. The preliminary data set of the ongoing research presented here serves to demonstrate the potential of the analytical protocol and is not yet a complete record of atmospheric lead deposition.

Ignoring the deepest samples which are "contaminated" by mineral matter from the sediment underlying the bog, the profile shows that peat samples dating from pre-anthropogenic times (4390 to 770 B.C.) contain less than 1 µg/g Pb and have ^{206}Pb/^{207}Pb ratios in the range 1.18 to 1.20 (Fig. 3). In contrast, there is a tremendous increase in Pb concentrations, and decrease in Pb isotope ratios, corresponding to the start of

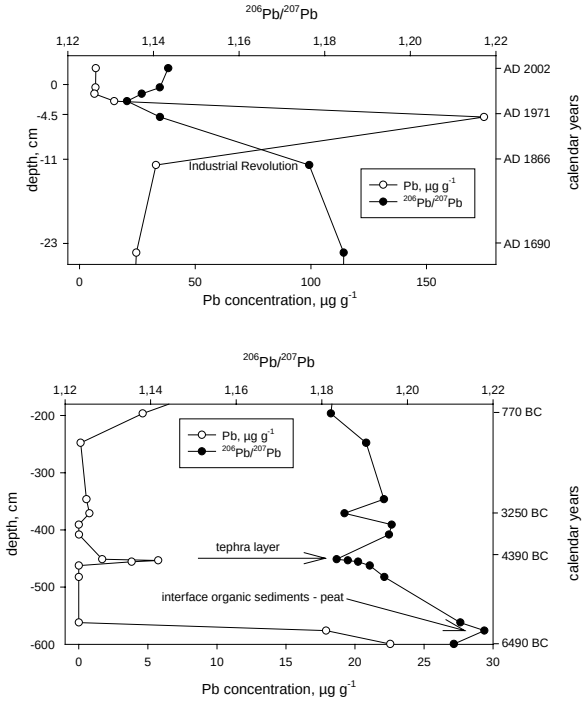

Figure 3: Lead concentration and isotopic Pb composition ($^{206}Pb/^{207}Pb$) profile of a peat core collected in the Black Forest (SW Germany) in June 2002. Error bars indicating one standard deviation of the mean of $^{206}Pb/^{207}Pb$ data are smaller than the diameter of the data points in the figure.

the Industrial Revolution in the second half of the 19th century, which is consistent with other records and due mainly to coal burning.[3,4,7,8] The lowest ratio of $^{206}Pb/^{207}Pb$ in the profile (< 1.14) indicates the maximum impact of leaded gasoline. The $^{206}Pb/^{207}Pb$ ratio of 1.143 established for the youngest peat sample (dating from 2002) is consistent with the corresponding ratio found in the snow samples (1.14 – 1.16) for the winter season 2002/2003 collected at the same site (see below). These most recent values are much less radiogenic than the samples dating from pre-anthropogenic times which shows unambiguously that there is *significant anthropogenic Pb contamination even today*, despite the ban on leaded gasoline in Europe. The tephra layer (volcanic eruption) found around 4390 BC in the peat profile is revealed by increased Pb concentrations and a distinct change in its isotopic composition, documenting a different predominant source of Pb. Clearly, the accuracy and precision of the Pb isotope ratio measurements obtained using ICP-SMS are not only sufficient for fingerprinting the predominant sources of Pb in modern, contaminated samples, but also for identifying much smaller, natural changes in atmospheric dust deposition, such as volcanic ash inputs. For most environmental applications, therefore, given the throughput of the ICP-SMS compared with the TIMS (which requires chemical separation of Pb), TIMS measurements are probably necessary only in those cases where the best possible accuracy and precision is needed.

It is important to note here that the Pb digestion blank was mainly caused by the purity of the digestion acids (HNO_3 and HBF_4), but was very low (0.003 µg l^{-1}) and stable. As the digestion solutions analysed for Pb isotope ratios in this study ranged between 0.5 and 1.5 µg Pb l^{-1}, no blank subtraction was performed prior to the determination of the Pb isotopic ratios. The agreement between ICP-SMS and TIMS data presented in Table 3 additionally justifies this approach.

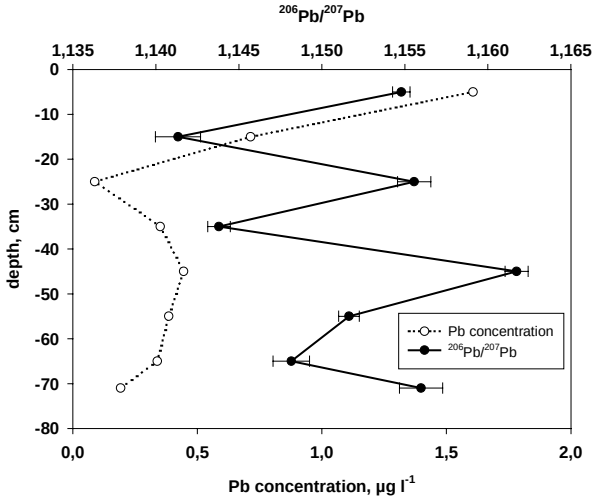

Figure 4: Lead concentration and isotopic Pb composition ($^{206}Pb/^{207}Pb$) profile of a snow core collected in the Black Forest (SW Germany) in February 2003.

Snow profile. The snow profile from the Black Forest (SW Germany) with a length of about 70 cm (10 cm increments) represents the snow fall of the winter period of 2002/2003. The snow was collected close to the site where the peat core was sampled in the year 2002. The $^{206}Pb/^{207}Pb$ ratio and the total Pb concentration (determined by ICP-SMS) are plotted against depth in Figure 4. The surface layer of the snow profile

contained the highest Pb concentration (1.6 μg l^{-1}), with no clear tendency for the other snow samples. The lowest Pb concentrations in snow amounted to 0.088 μg l^{-1}. These Pb concentrations are in good agreement with findings of Döring et al.[29] who reported Pb concentrations ranging from 0.02 to 5.5 μg kg^{-1} in snow samples from two high alpine sites. The ^{206}Pb/^{207}Pb ratio in the snow samples ranged from roughly 1.14 to 1.16 and is close to the values found for modern peat samples from the same site (see above). These ^{206}Pb/^{207}Pb ratios fit well into the range of 1.12 to 1.17 that was reported for 90 snow samples covering the years 1993-1996 from two alpine glaciers.[29] Other authors found ^{206}Pb/^{207}Pb ratios ranging from 1.161-1.128 in snow samples from 15 remote locations in the French Alps during the period 11/98-04/99.[30] Because of the high sensitivity of the employed ICP-SMS instrument, the ^{207}Pb/^{206}Pb and ^{208}Pb/^{206}Pb ratios could be analysed with an external precision of 0.12% and 0.24%, respectively, in the snow sample with the lowest Pb concentration (0.088 μg l^{-1}). External precision of Pb isotope ratios in the other snow samples was < 0.1%. The procedural blank (including filtering of the snow samples) was very low amounting to 0.003 μg l^{-1} and thus was not considered for the Pb isotope ratio determination.

Conclusions

This study clearly demonstrated that the accuracy of Pb isotope ratio determinations by ICP-SMS in acid digests of peat samples is comparable to TIMS analysis. Deviations of ICP-SMS results from the reference values obtained by TIMS are generally < 0.1%. Even though the precision obtained using TIMS is generally at least one order of magnitude superior to that of ICP-SMS (< 0.1% at sufficiently high count rates and dilution factor), many applications in earth and environmental sciences do not require such precision. In fact, the accuracy and precision of Pb isotope ratios obtained using ICP-SMS makes it a powerful tool for fingerprinting the predominant sources of anthropogenic Pb in environmental samples such as peat. Even natural, geological variations in atmospheric Pb deposition such as volcanic ash (tephra) are clearly seen using this approach. About 86% of the source discriminating power can be attributed to the ^{206}Pb, ^{207}Pb and ^{208}Pb isotopes.[31] Thus, highly precise and accurate analytical data rather than a lack of ^{204}Pb data (where TIMS is certainly superior to ICP-MS), is the most critical issue with respect to unequivocal identification of Pb sources in most cases.[31]

Considering the speed of ICP-MS (four samples h^{-1} including bracketing standards), the analytical approach presented here is an excellent alternative to the distinctly more laborious and time-consuming TIMS methodology.

Acknowledgement

Financial support from the German Research Council within the Graduiertenkolleg 273 of the Earth Sciences Faculty of the University of Heidelberg and the Forschungspool of the University of Heidelberg (Project: “Trace element analyses of geological archives: sediments, peat, and ice”) is gratefully acknowledged. Thanks to Dr. D. Aubert for careful collection and preparation of the snow samples. Special thanks from M.K. to Dr. Stephan Hahn of the University of Natural Resources and Applied Life Sciences, Institute of Chemistry, Vienna, Austria for a perspicuous introduction to Pb isotope ratio measurement using ICP-SMS.

References

1. W. Shotyk, *Earth Sci. Rev.*, 1988, **25**, 95.
2. W. Shotyk, A. K. Cheburkin, P. G. Appleby, A. Frankhauser and J. D. Kramers, *Earth Planet. Sci. Lett.*, 1996, **145**, E1.
3. W. Shotyk, D. Weiss, J. D. Kramers, R. Frei, A. K. Cheburkin, M. Gloor and S. Reese, *Geochim. Cosmochim. Acta*, 2001, **65**, 2337.
4. W. Shotyk, M. Krachler, A. Martinez-Cortizas, A. K. Cheburkin and H. Emons, *Earth Planet. Sci. Lett.*, 2002, **199**, 21.
5. M. Krachler, C. Mohl, H. Emons and W. Shotyk, *J. Environ. Monit.* 2003, **5**, 111.
6. M. Krachler, C. Mohl, H. Emons and W. Shotyk, *Environ. Sci. Technol.* 2003, **37**, 2658.
7. W. Shotyk, D. Weiss, P. G. Appleby, A. K. Cheburkin, R. Frei, M. Gloor, J. D. Kramers, S. Reese and W. O. van der Knapp, *Science*, 1998, **281**, 1635.

8. D. Weiss, W. Shotyk, P. G. Appelby, J. D. Kramers and A. K. Cheburkin, *Environ. Sci. Technol.* 1999, **33**, 1340.
9. W. Shotyk, D. Weiss, M. Heisterkamp, A. K. Cheburkin, P. G. Appleby and F. C. Adams, *Environ. Sci. Technol.* 2002, **36**, 3893.
10. D. Weiss, W. Shotyk, M. Gloor and J. D. Kramers, *Atmos. Environ.*, 1999, **33**, 3751.
11. W. Shotyk, M. E. Goodsite, F. Roos-Barraclough, R. Frei, J. Heinemeier, G. Asmund, C. Lohse and T. S. Hansen, *Geochim. Cosmochim. Acta*, 2003, **67**, 3991.
12. F. Monna, A. Aiuppa, D. Varrica and G. Dongarra, *Environ. Sci. Technol.* 1999, **33**, 2517.
13. J. G. Farmer, L. J. Eades, H. Atkins and D. F. Chamberlain, *Environ. Sci. Technol.* 2002, **36**, 152.
14. S. N. Chillrud, S. Hemming, E. L. Shuster, H. J. Simpson, R. F. Bopp, J. M. Ross, D. C. Pederson, D. A. Chaky, L.-R. Tolley and F. Estabrooks, *Chem. Geol.*, 2003, **199**, 53.
15. D. Woolard, R. Franks and D. R. Smith, *J. Anal. At. Spectrom.*, 1998, **13**, 1015.
16. A. T. Townsend, Z. Yu, P. McGoldrick J. A. and Hutton, *J. Anal. At. Spectrom.*, 1998, **13**, 809.
17. R. Gwiazda, D. Woolard and D. Smith, *J. Anal. At. Spectrom.*, 1998, **13**, 1233.
18. F. Poitrasson and S. H. Dundas, *J. Anal. At. Spectrom.*, 1999, **14**, 1573.
19. R. S. Olofson, I. Rodushkin M. D. and Axelsson, *J. Anal. At. Spectrom.*, 2000, **15**, 727.
20. T. Prohaska, M. Watkins, C. Latkoczy, W. W. Wenzel and G. Stingeder, *J. Anal. At. Spectrom.*, 2000, **15**, 365.
21. C. R. Quetel, T. Prohaska, M. Hamester, W. Kerl and P. D. P. Taylor, *J. Anal. At. Spectrom.*, 2000, **15**, 353.
22. G. De Wannemacker, F. Vanhaecke, L. Moens, A. van Mele and H. Thoen, *J. Anal. At. Spectrom.*, 2000, **15**, 323.
23. A. T. Townsend and I. Snape, *J. Anal. At. Spectrom.*, 2002, **17**, 922.
24. M. Krachler, C. Mohl, H. Emons and W. Shotyk, *Spectrochim. Acta B*, 2002, **57**, 1277.
25. M. Krachler, C. Mohl, H. Emons and W. Shotyk, *J. Anal. At. Spectrom.*, 2002, **17**, 844.
26. A. K. Cheburkin and W. Shotyk, *Fresenius J. Anal. Chem.*, 1996, **354**, 688.
27. B. Kober and H. J. Lippolt, *Contrib. Mineral. Petrol.*, 1985, **90**, 162.
28. E. P. Horwitz, M. L. Dietz, S. Rhoads, C. Felinto, N. H. Gale and J. Houghton, *Anal. Chim. Acta*, 1994, **292**, 263.
29. T. Döring, M. Schwikowski and H. W. Gäggeler, *Fresenius J. Anal. Chem.*, 1997, **359**, 382.
30. A. M. Veysseyre, A. F. Bollhöfer, K. J. R. Rosman, C. P. Ferrari and C. F. Boutron, *Environ. Sci. Technol.*, 2001, **35**, 4463.
31. D. F. Sangster, P. M. Outridge and W. J. Davis, *NRC-CNRC Environmental Reviews*, 2000, **8**

PART 2
INVESTIGATING ATMOSPHERIC Pb DEPOSITION USING PEAT BOGS

- Chapter 2.1 -

Biogeochemistry and Cycling of Lead

William Shotyk and Gaël Le Roux

Institute of Environmental Geochemistry, University of Heidelberg,
INF 236, D-69120 Heidelberg, Germany

Chap. 10 Of "Metal ions in Biological Science" (vol.43)
pp.239-279; Eds. Sigel, Sigel & Sigel

1. INTRODUCTION ***82***
2. CHEMISTRY OF LEAD AND BEHAVIOR IN THE ENVIRONMENT ***83***
2.1. Summary of Basic Chemical Properties
2.2. Abundance and Occurrence
2.3. Measuring Lead Concentrations
3. LEAD ISOTOPES AND THEIR MEASUREMENT ***86***
3.1. Stable Isotopes
3.2. Measurements of Stable Lead Isotopes
3.3. Intermediate Decay Products of U-Th Decay Series
4. ANCIENT AND MODERN USES OF LEAD ***87***
4.1. Ancient and Medieval Uses
4.2. Modern Uses
5. EMISSIONS OF LEAD TO THE ENVIRONMENT ***89***
5.1. Lead in Natural versus Anthropogenic Atmospheric Particles
5.2. Atmospheric Lead from Alkyllead Fuel Additives
6. INPUTS AND FATE OF ANTHROPOGENIC LEAD IN THE BIOSPHERE ***91***
6.1. Lead Concentrations in Soils
6.2. Cumulative Impact of Anthropogenic, Atmospheric Lead
6.3. The Fate of Anthropogenic Lead in Soils
6.4. Lead Concentrations in Solution
7. TEMPORAL TRENDS IN ATMOPSHERIC LEAD DEPOSITION ***93***
7.1. Lead in Sediments
7.2. Lead in Bryophytes
7.3. Lead in Tree Rings and Bark Pockets
7.4. Peat Bog Archives
7.5. Relative Importance of Gasoline Lead versus Other Sources of Industrial Lead
7.6. The Cumulative Input of Anthropogenic Lead
7.7. Lead in Polar Snow and Ice
7.8. Lead in Atmospheric Aerosols Today
8. ENVIRONMENTAL LEAD EXPOSURE AND HUMAN HEALTH ***99***
8.1. Blood Lead Levels and Their Significance
8.2. Mechanism of Lead Poisoning
8.3. Predominant Sources of Lead Exposure
8.4. Other Sources of Lead Exposure
9. SUMMARY AND CONCLUSIONS ***102***
Acknowledgement
References
Abbreviations

1. INTRODUCTION

The environmental geochemistry of Pb has probably stimulated more scientific interest than all other metallic elements combined. According to Jaworski [1], "the local, regional, and global biogeochemical cycles of lead have been affected by man to a greater degree than those of any other toxic element". Why? The main reasons are simple - lead is an extremely useful metal and is relatively simple to work with. Because it melts at a relatively low temperature (327^{o}C), however, it is easily emitted to the atmosphere during smelting and refining. And because it has been used since Antiquity, environmental contamination by Pb is probably as old as civilization itself.

Lead is malleable, ductile, dense, and resistant to corrosion. Thus, it has found a tremendous range of commercial and industrial applications in manufacturing and building since ancient times. In fact, the value of lead to mankind has been considered so great that it has even been termed a "precious metal" [2], an appellation which it much deserves. In addition, occurrences of lead ores are comparatively easy to find. Galena (PbS), the main Pb sulfide mineral, has a diagnostic color, lustre, and cleavage. Also, Pb is readily extracted from sulfide ores by oxidation and the technology for processing them was well known already in ancient times [3]. The low melting point of Pb makes it possible to process even with very primitive technology. The discovery of cupellation approximately five thousand years ago, when the ancients learned how to separate silver from lead ores, was a great stimulus for lead production worldwide [3]. Because of the widespread occurrence of its ores and the great value of both Pb and Ag, enormous quantities of lead have been produced ever since. As a consequence, anthropogenic emissions of Pb to the atmosphere, to soils, sediments, and waters, have been very extensive. In fact, there is probably no place on the surface of the Earth that is devoid of anthropogenic Pb [1].

Although Pb is one of the most useful of all the metals, it is also one of the most toxic [4]. Because it serves no biological role and occurs naturally at the surface of the Earth only in trace concentrations, there continues to be great interest in the environmental fate of anthropogenic Pb, and possible effects on human and ecosystem health [5]. Probably the single most compelling paper ever written about the Pb in the environment is the seminal work by Patterson [6] which still reads well today, forty years after it was published. As western philosophy is sometimes considered footnotes to Plato, modern studies of the environmental geochemistry of Pb may be viewed as footnotes to Patterson.

With respect to scientific study, one great advantage of Pb compared to other metals of environmental interest is the number of stable isotopes (^{204}Pb, ^{206}Pb, ^{207}Pb, ^{208}Pb) which can be used to help "fingerprint" the predominant sources of both natural and anthropogenic Pb, to identify predominant pathways, and to study the fate of this metal in the environment [7]. This opportunity is made possible by the wealth of information about the isotopic composition of Pb in rocks, minerals, and lead ores compiled over the past decades by economic geologists, geochronologists and isotope geologists [8-11]; many of the results most relevant to environmental studies have been summarized by Sangster et al. [12]. In addition, ^{210}Pb, an unstable daughter product of the decay of ^{238}U which is supplied naturally to the air via the decay of ^{222}Rn, is a valuable tracer of atmospheric scavenging, soil migration, adsorption, biological uptake and other processes affecting the behavior and fate of Pb in the environment [13].

Given the voluminous literature about the geochemistry of Pb in the environment (5000 papers in 1978 alone, according to Nriagu [14]), we have concentrated our efforts on new developments in the following areas:

1. **The isotopic composition of Pb** is a powerful tool, which allows natural sources of

anthropogenic Pb to be distinguished from anthropogenic ones. If quantitative measurements of Pb concentrations have allowed us to study the Pb problem in black and white, precise measurements of Pb isotope ratios allow us to see in color. Tremendous advances have been made regarding analytical developments for measuring Pb and Pb isotope ratios at ultra-trace concentrations, and some of these results are summarized here.

2. **Temporal trends in atmospheric Pb contamination**, including the fluxes and predominant sources of Pb using sediments, biomonitors, peat bogs, and polar ice. The historical trends in the predominant sources of atmospheric Pb are valuable indicators of recent changes in environmental policies such as the phasing out of leaded gasoline. In addition, long-term records of atmospheric Pb are essential to determine the natural background rates, for comparison with modern values, but also to help understand the geological processes which controlled these fluxes.

3. **Fate of anthropogenic Pb in the terrestrial biosphere**. By determining the isotopic composition of Pb in different soil horizons and measuring Pb in soil solutions, it is possible to begin to understand the ultimate fate of industrial Pb, which has contaminated the surface layers of soils worldwide.

Our summary has been stimulated by two recent findings. First, even though most attention during the past decades has been given to anthropogenic emissions of Pb from the use of gasoline Pb additives, this is just a part of the environmental Pb story, and some of the greatest episodes of environmental Pb contamination pre-date by a wide margin the introduction and use of gasoline Pb additives. Second, recent studies have identified deleterious health effects in children at blood Pb concentrations much lower than previously believed to be important. Taken together, these new findings suggest that concerns regarding the sources, transport, and fate of Pb in the environment are more important than ever. In fact, while great progress has been made in reducing atmospheric Pb emissions, the greatest part of this success has been due to the gradual replacement of gasoline Pb additives. Further reductions in atmospheric Pb emissions, and additional progress in limiting human exposure to Pb, is going to be more challenging as well as more expensive.

Readers interested in previous studies of Pb in the environment are referred to the books by Nriagu [15], Boggess and Wixson [16], the Committee on Lead in the Human Environment [17], and Harrison and Laxen [18]. The chemistry and geochemistry of lead in the aquatic environment has been outlined in Refs. [19], and lead in soils in Refs. [20].

2. CHEMISTRY OF LEAD AND BEHAVIOR IN THE ENVIRONMENT

2.1. Summary of Basic Chemical Properties

Lead (Z = 82, atomic weight 207.19) is dull grey, soft, and weak but dense (11.35 g cm^{-3}). With the electronic configuration [Xe] $4f^{14}5d^{10}6s^{2}6p^{2}$, Pb exhibits three formal oxidation states: (IV), (II), and (0). At Earth surface conditions, Pb(II) is by far the most common oxidation state (Fig. 1).

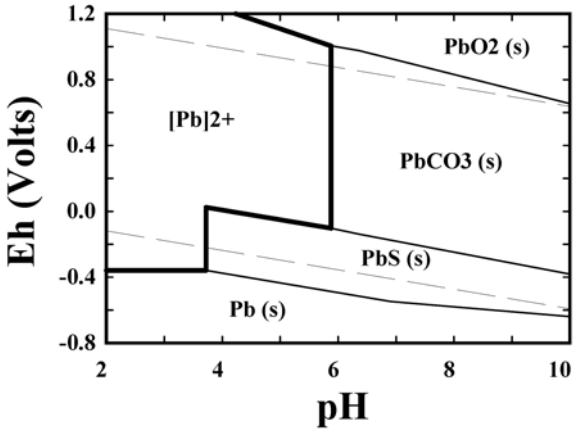

Figure 1: pH-Eh diagram for inorganic species of lead.

Lead readily loses two electrons, yielding Pb^{2+}, which hydrolyzes above pH 7. While Pb^{2+} is the dominant inorganic species throughout the pH and Eh range of most natural waters (Fig. 1), sulfate, carbonate,

chloride, and phosphate complexes of Pb can also be important, depending on the concentrations of these species and the pH of the solution [21]. Lead carbonate is an effective control on the solubility of Pb in oxic soils and sediments above pH values of approximately 6 (Fig. 1). In zones of active bacterial sulfate reduction such as anoxic sediments, the solubility of Pb is regulated by the formation of Pb sulfide. In neutral to alkaline soils, and in anoxic sediments, therefore, the mobility of Pb should be very limited. The behavior and fate of Pb in acidic soils, however, is more complicated: while solubility controls may be lacking, Pb^{2+} forms stable complexes with natural organic ligands, and is strongly adsorbed onto the surfaces of Mn and Fe hydroxides [22]. The solubilities of Pb phosphates are extremely low [22], and this can be a further control on Pb migration, especially in agricultural soils with added phosphorus.

2.2. Abundance and Occurrence

Typical Pb concentrations in rocks, soils, sediments, and fossil fuels (µg/g) are: basalt, 3; granite, 24; sandstone, 10; limestone, 6; shale, 23; soil, 35; coal; 10; sediment, 19. Manganese nodules may contain several hundred µg/g Pb. In the Earth's crust, the average Pb concentration is estimated to be 15 µg/g, with approximately 17 µg/g in the upper continental crust, and 13 µg/g in the lower continental crust [23]. Lead is one of the most abundant of the heavy trace elements, for three reasons [24]. First, the cosmic abundance of Pb is relatively high. Second, in addition to common Pb (^{204}Pb), which is non-radiogenic, Pb is derived from the radioactive decay of ^{238}U, ^{235}U, and ^{232}Th. In fact, roughly one-half of the ^{206}Pb, one-third of the ^{207}Pb, and one-fifth of the ^{208}Pb, is derived from the respective U and Th isotopes since the Earth differentiated into a separate crust and mantle approximately 4.5 billion years ago [25]. Third, Pb is enriched in crustal rocks, partly because the ionic radius of Pb^{2+} (132 pm) is so similar to that of K^+ (133 pm), allowing divalent Pb to substitute for K in potassium feldspars and micas. Lead can also substitute readily for Sr^{2+} and Ba^{2+}, which have similar ionic radii to divalent Pb, but Pb has even been found to substitute in other silicates for smaller cations such as Ca^{2+} and Na^+. While Goldschmidt [26] classified Pb as a chalcophile element because of its occurrence in galena (PbS), the lithophile character of Pb should not be overlooked. Micas and potassium feldspar, on average, contain 25 to 30 µg/g. The abundance of Pb in silicates has been summarized by Wedepohl [27].

About 240 minerals of Pb are known [27], but galena (PbS), cerussite ($PbCO_3$), and anglesite ($PbSO_4$), are the most important economically. Probably 90% of the world's primary Pb is recovered from mining and refining galena. Boulangerite ($5PbS•2Sb_2S_3$), Bournonite ($PbCuSbS_3$), and Jamesonite ($Pb_4FeSb_6S_{14}$) also are important Pb sulfides.

2.3. Measuring Lead Concentrations

Quantitative determination of Pb in environmental and biological samples is made possible using a variety of well-established techniques such as wave dispersive X-ray fluorescence spectrometry (XRF) for solid samples at higher Pb concentrations, atomic absorption spectroscopy (AAS), and inductively coupled plasma (ICP) atomic emission spectrometry (AES). Both XRF and ICP-AES have the advantage of being able to determine a wide range of trace elements simultaneously. The lower limit of detection (LOD) provided by energy dispersive XRF (ca. 2 µg/g for soils and sediments, and 0.5 µg/g for plant materials) allows this method to be used for many environmental samples of interest [28]; this approach is not only inexpensive and non-destructive, but it also avoids the time and expense of sample digestion. A high sensitivity XRF spectrometer was subsequently developed which can measure Pb down to 0.1 µg/g in biological materials [29]. Conventional methods such as graphite furnace atomic absorption spectroscopy are relatively inexpensive and can be used to measure Pb in acid digests and other aqueous samples down to a few µg/L. However, inductively coupled

plasma mass spectrometry with quadrupole mass analyzer (Q-ICP-MS) has become a workhorse in many laboratories, which need to measure Pb down to the ng/L range; a wide range of other trace elements can be measured simultaneously. Total reflection X-ray spectrometry can measure Pb in the ng/L range and is also a multi-element method, but the limits of detection are strongly dependent on the concentration of matrix elements [30]. Laser excited atomic fluorescence spectroscopy (LEAFS) is a novel method for measuring Pb in the ultra-trace concentration range [31, 32]. For extremely low concentrations (pg/L) of Pb in uncontaminated natural waters, including polar ice, double focusing (sector field) ICP-MS (ICP-SMS) is now the method of choice [33]. In fact, with this instrument, the main limitation is no longer detecting power, but rather eliminating all forms of possible sample contamination. As described by Boutron [34] and Nriagu et al. [35], many studies previous to the 1970's and 1980's have overestimated Pb concentrations, often by many orders of magnitude, due to inadequate contamination control. With respect to all dilute natural waters, but also with respect to many other samples pre-dating the development of metallurgy ("pre-anthropogenic samples"), there is a need for clean lab protocols to be employed at every stage of sample handling, preparation, and analyses [34, 35]. Using rigorous cleaning procedures and strict clean lab techniques, detection limits as low as 50 pg/L Pb have recently been achieved in samples of polar ice [33].

In cases, which require extreme accuracy and precision, isotope dilution mass spectrometry (ID-MS) may be used to measure Pb concentrations. This consists of an addition to the sample of a solution of well-known Pb concentration and isotopic composition ("spike") followed by determination of the isotopic composition of the spiked sample using mass spectrometry, Q-ICP-MS, ICP-SMS, multi-collector ICP-MS (MC-ICP-MS) or thermal ionization mass spectrometry (TIMS).

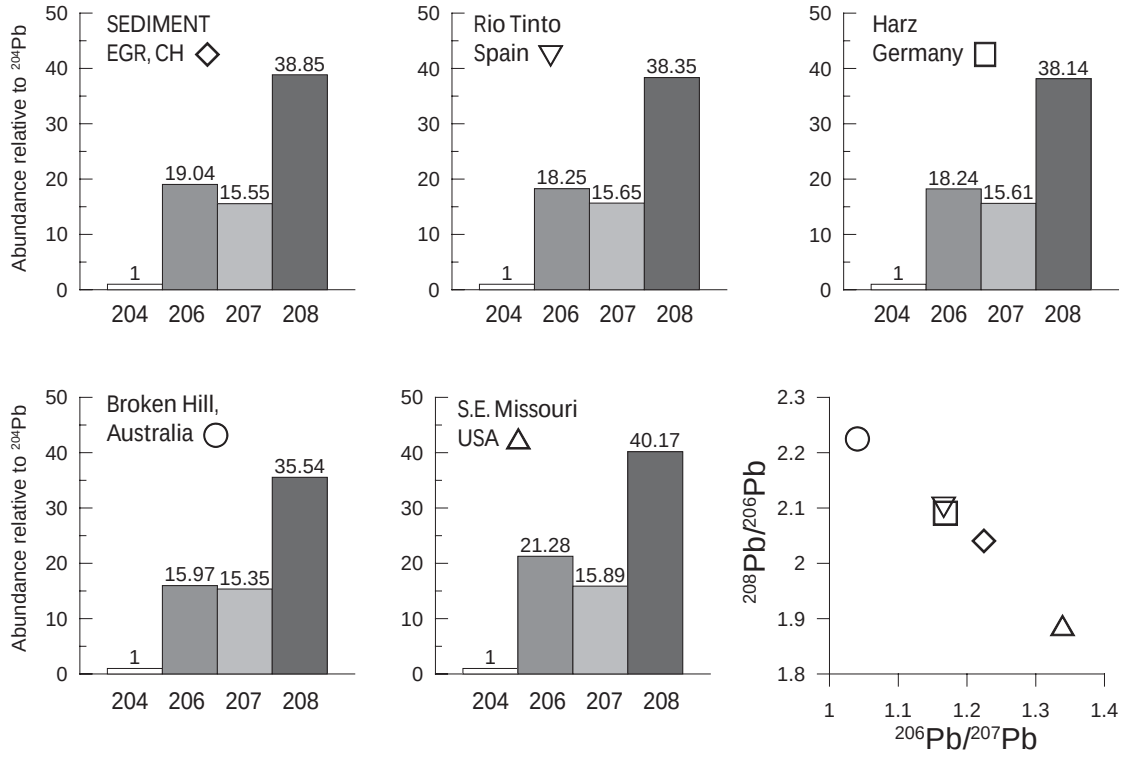

Figure 2: Isotopic composition of Pb in pre-anthropogenic aerosols (Étang de la Gruère(EGR), Switzerland (CH)), and in selected Pb ores [12].

To measure Pb concentrations in small particles such as aerosols, or to study the variation in Pb concentrations within solids such as mineral grains, there is a range in available techniques such as micro-beam XRF (including synchrotron methods), proton induced X-ray emission spectrometry (PIXE), secondary ionization mass spectrometry (SIMS), and laser ablation ICP-MS (LA-ICP-MS). These methods have been used for high spatial resolution even in 3-D, as well as for rapid analyses of biological or geological structures growing incrementally [36-40] or small, specific phases [41].

3. LEAD ISOTOPES AND THEIR MEASUREMENT

3.1. Stable Isotopes

Because of the range in geological age of Pb ores, and the U and Th concentrations of the rocks from which they are derived, the isotopic composition of Pb ores is variable, and each ore deposit can be described by its characteristic Pb isotope signature [11] (Fig. 2). For example, lead from the Broken Hill mine in Australia (the predominant source of industrial Pb used for gasoline Pb additives in Europe) has a $^{206}Pb/^{207}Pb = 1.04$, compared with crustal rocks which have a $^{206}Pb/^{207}Pb = 1.20$ [42]. Uncontaminated marine sediments [43, 44] as well as atmospheric soil dust dating from pre-anthropogenic times [45], both of which are derived from crustal rocks, also have a $^{206}Pb/^{207}Pb = 1.20$. Similarly, the Pb contained in coal and other fossil fuels, and in waste products, reflects the isotopic composition of the original Pb source [46, 47]. As a result, there has been widespread interest in determining the isotopic composition of Pb in environmental samples, with a view to identifying predominant atmospheric emission sources [12].

While this “fingerprinting” approach is growing in popularity [48], many lead ores and coal bodies have overlapping signatures, and interpretations of predominant source areas are not always unequivocal [49]. A further caveat involves emissions of atmospheric Pb from mixtures of Pb ores. For example, secondary Pb smelters today process scrap Pb from the most diverse sources. Even during the Medieval period, Pb ores from different mining regions were mixed to improve their metallurgical properties [50].

3.2. Measurements of Stable Lead Isotopes

Thermal ion mass spectrometry has traditionally been the method of choice to obtain precise Pb isotope determinations, with a typical RSD of 0.01 % (2σ) for the $^{206}Pb/^{207}Pb$ ratio. Moreover, TIMS allows precise measurement of all four Pb isotopes, especially with the double or triple spike techniques [51], allowing the radiogenic ones (^{206}Pb, ^{207}Pb, ^{208}Pb) to be normalized to ^{204}Pb which is non-radiogenic. Also, to distinguish among anthropogenic Pb sources, it can be very instructive to make a “three isotope plot” such as $^{207}Pb/^{204}Pb$ against $^{206}Pb/^{204}Pb$ and $^{208}Pb/^{204}Pb$ versus $^{207}Pb/^{204}Pb$, and this requires precise measurement of all four isotopes. It has been pointed out by Sangster et al. [12], however, that 86% of the discriminating power of Pb isotopes in environmental isotopes can be obtained without using ^{204}Pb, and that precise measurements of the three radiogenic stable Pb isotopes are more important. There is growing use of Q-ICP-MS measurements of the $^{206}Pb/^{207}Pb$ in environmental samples, but because of the poor precision (typical RSD of 0.3 to 0.7 % (2σ) for the $^{206}Pb/^{207}Pb$ ratio), it is not considered further here.

Recently it has been shown that Pb isotope ratios in environmental samples can be measured with acceptable accuracy and precision using ICP-SMS [52, 53]. This approach is rapid (no chemical separation of Pb is required) and reasonably accurate and precise. For example, Krachler et al. [54] have reported precisions of 0.1% for the $^{206}Pb/^{207}Pb$ and $^{208}Pb/^{206}Pb$ ratios at total Pb concentrations of only 0.1 µg/L in “real world” samples.

Equipped with an array of Faraday cups, the multiple collector-ICP-MS achieves comparable or better quality of measurements than TIMS without double spiking [55-57]. However, as for TIMS, a chemical separation

before measurement is required to obtain such precision. Micro-beam techniques such as the sensitive high resolution ion microprobe (SHRIMP) [36, 58] and LA-ICP-MS [55] are also useful for obtaining high resolution sampling of solid samples and simultaneous measurements of isotopic composition.

3.3. Intermediate Decay Products of U-Th Decay Series

Short-lived isotopes of Pb such as ^{210}Pb ($t_{1/2}$ = 22.26 yr), ^{212}Pb ($t_{1/2}$ = 10.6 h), ^{214}Pb ($t_{1/2}$ = 26.8 min) are useful tracers of transient signals for studying sediment fluxes in estuaries [59], deposition of atmospheric particles [60, 61], scavenging of trace metals by aquatic particles [62], and oceanic circulation [63]. Lead-210 in particular, has been extensively used as a geochronological tool for studying the accumulation rates of sediments, peat, and glacial ice during the past two centuries [64, 65].

4. ANCIENT AND MODERN USES OF LEAD

4.1. Ancient and Medieval Uses

Lead has been used since 6400 B.C. [66] and obtained as a by-product of silver mining for approximately five thousand years [3]. The Hanging Gardens of Babylon were floored with sheet lead. In classical times, Pb was used in all Mediterranean civilizations for construction, coinage, glass-making, water pipes, cosmetics and beverages [67]. Egypt had a Pb-based cosmetics industry as early as 2000 B.C. [68]. The most important Pb deposits in the Mediterranean region and in western Europe had already been prospected or/and mined in Roman times [69, 70]. As a result, environmental contamination by Pb has its origins in antiquity, a fact which is clearly revealed by peat bogs for example in England [71] and the harbor sediments from the Phoenician city of Sidon (Fig. 3) [74].

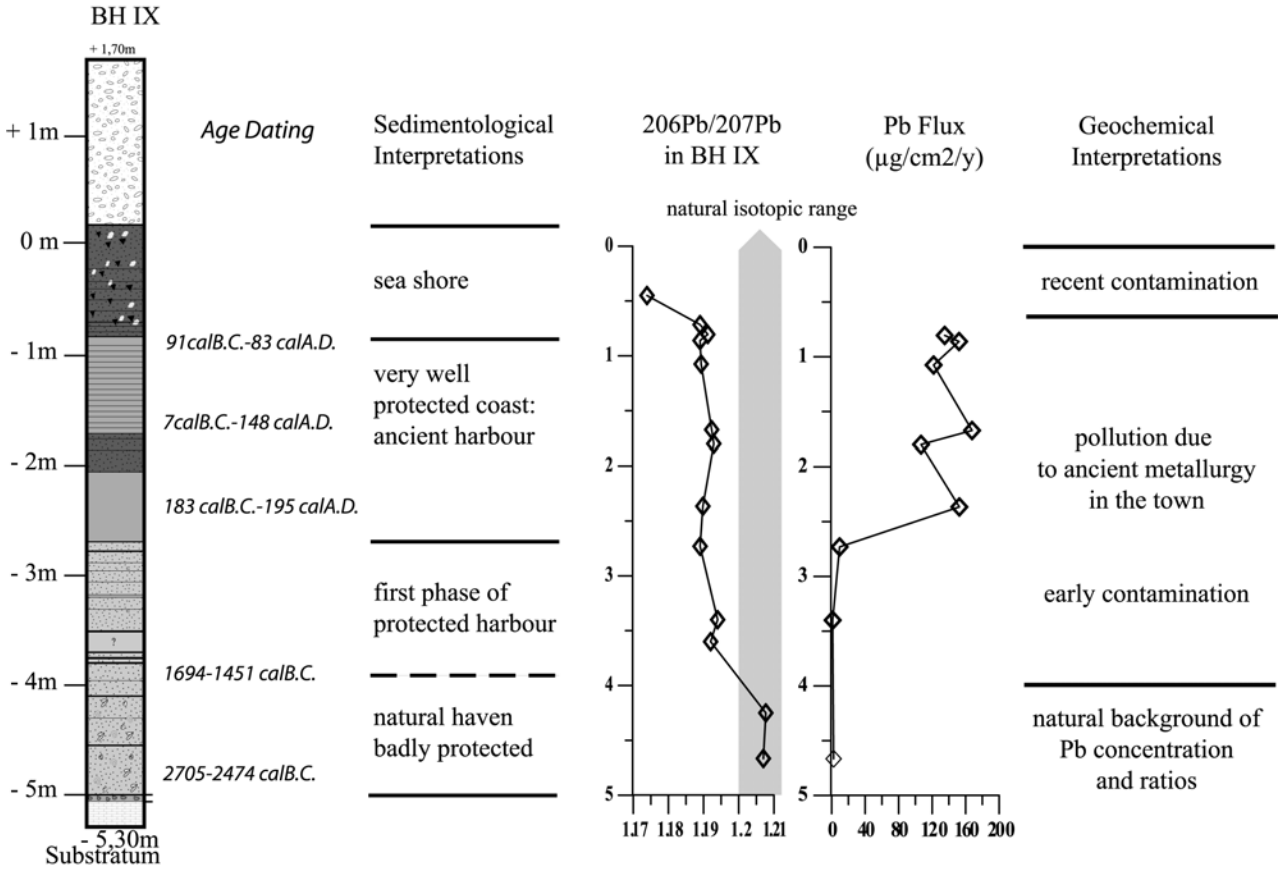

Figure 3: Pb contamination evidenced by Pb flux and Pb isotopes in sediments from the ancient harbour of the Phoenician city of Sidon [74].

Following the decline of the western Roman Empire, Pb production continued, but at a much reduced pace, as witnessed by sediments and peat bogs [72]. However, the atmospheric Pb flux did not reach background values: therefore, Pb continued to be mined and refined, especially in Asia [70]. Even at this time in Europe, Pb continued to be used for glass making and ceramic glazes [73]. Lead was needed for the cames of the stained glass windows of churches and cathedrals [50]; the abundance of these windows in Europe today is a testimony to the usefulness of metallic Pb as a construction material. Lead was also used to make colored glass during this period, as it had been used for the previous 2500 years.

The Medieval period in Europe experienced a renaissance in Pb production, with the development of "silver mines" across the German-speaking part of central Europe, as well as the Vosges mountains of France and the Silesia region of Poland. The Harz Mountains, the Ore mountains, and the Black Forest of Germany were particularly important mining areas. Already in the 13th century, the Harz Mountains alone produced 500 tonnes of Pb per year. In fact, peat bogs from mining regions of Germany show that the extent and intensity of recent Pb contamination from industrialization, fossil fuel burning, and leaded gasoline use, are dwarfed by Pb contamination from the Medieval Period [75].

4.2. Modern Uses

So many industrial and commercial uses have been found for Pb that it is difficult to list them all. The main uses of Pb which are most relevant to environmental contamination and human exposure are: lead-based indoor paints, lead water pipes, lead solder in cans for storing food, and leaded gasoline additives; these have either since been banned or are in the process of being banned. Action is also being taken with respect to lead glazes on pottery and ceramics, lead in ammunition and for weights in sport fishing, in certain plastics, and use of leaded crystal. In the EU, for example, Pb will be banned as a stabilizer in PVC by 2015. There are moves to replace Pb in ammunition used for hunting waterfowl; in Canada alone, several million waterfowl die annually from lead poisoning [76]. Replacements are being sought for sinkers used in sport fishing, and larger weights (used for sport fishing in deep waters) are being coated with plastic.

Since 1800, Pb use increased dramatically [77] with mining production reaching 2.8 million tonnes and total metal production of 6.7 million tonnes in 2003 [78]. With approximately 60% of the world's Pb obtained by recycling, it is the most re-used of all the metals [78]. Lead is mined worldwide, with the largest primary producers being Australia (19%), the U.S. (13%), China (12%), Peru (8%), and Canada (6%). Some new Pb is also produced in Mexico, Germany, and France. The two most important Pb mining areas are Broken Hill (Australia) and southeast Missouri (USA) with cumulative outputs last century each exceeding 30 million tonnes [12].

The main use for Pb today (74%) is lead-acid batteries, especially for cars. However, in the recent past, up to 300,000 tonnes of Pb per year was used for gasoline additives alone [14]. Lead additives in gasoline, beginning with tetraethyl lead in 1923 and supplemented with tetramethyl lead in Europe starting in 1960, were incompatible with catalytic converters, and are gradually being phased out: maximum allowable Pb concentrations were introduced first, during the early 1970's, allowing a gradual decline in gasoline Pb concentrations, followed by the introduction of unleaded fuels, and finally by outright bans on leaded gasoline in most developed countries, starting with the main "automotive" countries: the U.S., Germany, and Japan. Unleaded gasoline is expected to be used exclusively in all western and nearly all eastern European countries as of 2005, according to the Aarhus Treaty signed in 1998 [79]. Many nations in Asia, South America, Africa, and the Middle East have not yet banned the use of leaded gasoline [80, 81].

Lead is still used widely in building and construction (as sheet Pb for roofs, and for noise abatement and reducing vibrations,

and in lead-clad steel); for lead paints used to protect steel from corrosion (red lead) and for marking highways (lead chromate); in pipes for handling corrosive gases and liquids; as a sheathing material for power cables; for casting; in decorative leaded crystal (up to 36% lead oxide), optical glassware (opthalmic and scientific applications); for glazing heat-resistant ceramics; for radiation shielding; in ammunition; as a stabilizer in plastic; in petroleum refining; as a waterproofing material; in food packaging; insecticides; for making alloys such as antimonial lead, bronze, brass, and pewter; for solders, especially in consumer and industrial electronics; and for lead weights (from the smallest used for sport fishing, through those used to balance automobile wheels to the largest used in building keels for yachts; for counterweights in lift trucks and cranes). Hair dyes containing 0.5% Pb acetate are still available, even in OECD countries. In Canada, approximately one-half of the costume jewellery sold contains Pb.

The diverse uses and applications are outlined here because many Pb-bearing consumer products end up in residential waste streams, and burning municipal solid waste (MSW) is an additional source of Pb to the environment. For example, the glass screens on TV sets and personal computers each contain several hundred grams of Pb added to protect the viewer from radiation. The U.S. EPA estimates that 50,000 tonnes of Pb is added to the waste stream annually from consumer electronics alone.

5. EMISSIONS OF LEAD TO THE ENVIRONMENT

According to Pacyna and Pacyna [82], emissions of Pb to the global atmosphere have declined from 332,350 tonnes per year in 1983 to 119,259 tonnes per year in 1995. While this represents a tremendous reduction, the natural rates of atmospheric Pb emission estimated [83] are only 2,600 tonnes per year, with 1200 tonnes from volcanic emissions and 1400 tonnes from soil dust. For comparison, the natural rates of atmospheric Pb deposition estimated using a peat core from a Swiss bog is only 4400 tonnes per year [84]. As a consequence, the emissions of Pb to the global atmosphere today are still on the order of 45 times the natural value estimated by Patterson and Settle [83] and 27 times the value estimated by Shotyk et al. [84]. Even compared to the higher estimate of natural Pb (12,000 t/y) by Nriagu [85], the contemporary fluxes from anthropogenic sources are still an order of magnitude greater. These calculations apply to global scale emissions, so regional and local impacts must be even greater.

Source	Emission	Natural Emissions	Ratio Anthropogenic/ Natural
Vehicles	88739	2600	34.1
Non-ferrous metallurgy	14815	2600	5.7
Fossil fuel combustion, stationary sources	11690	2600	4.5
Iron and steel production	2926	2600	1.1
Waste incineration	821	2600	0.3
Cement production	268	2600	0.1
TOTAL	**119259**	**2600**	**45.8**

Table 1: Predominant anthropogenic sources of Pb to the global atmosphere (tonnes per year). Anthropogenic emissions for 1995 from [85], and natural emissions from [86].

The single most important anthropogenic source of Pb to the global atmosphere remains vehicle emissions; this source alone exceeds the natural fluxes [83] by a factor of approximately 30 times. Other important sources of atmospheric Pb are non-ferrous metallurgy and fossil fuel combustion from stationary sources (mainly coal-burning) (Table 1). Comparing the 1995 data with 1983 data shows strong declines in emissions from the production of primary and secondary Pb (6,216 t/y in 1995 versus 21,450 t/y in 1983), Cu (6271 t/y in 1995 versus 16,575 t/y in 1983), and Zn (2,123 versus 8,510t/y), as well as emissions from steel production (2,926 versus 7,633 t/y) and cement production (268 versus 7,129 t/y). In contrast, emissions from stationary fossil fuel

combustion actually increased over the same period, from 10,577 to 11,690 t/y [82].

5.1. Pb in Natural versus Anthropogenic Atmospheric Particles

While it is certainly useful to compare the magnitude of natural and anthropogenic fluxes of Pb to the atmosphere, and to quantify air Pb concentrations, there are a number of important differences in the nature of the Pb emitted. In pre-anthropogenic times, the majority of Pb in the air was supplied by atmospheric soil dust particles derived from rock weathering, and the Pb concentrations in these particles were more or less proportional to the abundance of Pb in crustal rocks [6, 45]. Most of these Pb-bearing particles would have been comparatively large: on the order of 50 µm if they had been supplied by local soils, and perhaps as small as 5 µm if they had been supplied by long-range transport of Sahara dust [86]. As the Pb in these particles is hosted mainly in silicate minerals such as potassium feldspar [27, 87] which has a very low solubility in aqueous solutions at atmospheric temperature and pressure, the bioavailability of this Pb is relatively low. Under natural conditions, therefore, atmospheric Pb was an insignificant source of Pb to humans [6]. In contrast, most of the anthropogenic Pb in the atmosphere is derived directly or indirectly from high temperature combustion processes such as leaded gasoline use, metallurgical processing, coal combustion, and refuse incineration. Lead emitted from these sources is released to the air in the form of sub-micron particles, with a median diameter of ca. 0.5 µm [88]: these particles, with an average atmospheric residence time of approximately one week, are not only amenable to long-range atmospheric transport (thousands of kilometers), but they are easily respirable. Moreover, the surfaces of these particles - where chemical reactions take place - are highly enriched in Pb, and this Pb has a relatively high solubility.

5.2. Atmospheric Lead from Alkyllead Fuel Additives

The chemistry of organolead compounds in the environment has been reviewed elsewhere [89-92], but a few salient aspects are summarized here. First, tetraalkyllead compounds are volatile: Henry's Law constant of 4.7×10^4 and 6.9×10^4 Pa m^3 mol^{-1} for tetramethyl and tetraethyllead, respectively, according to Wang et al. [93]. However, only a small fraction of the Pb leaving an automobile as exhaust is in this form, e.g., typically 0.1 to 10% [91]. In addition to the relatively low emission factor from leaded gasoline combustion, tetraalkyllead compounds are rapidly decomposed by homogeneous gas phase reactions such as photolysis, reaction with ozone, triplet atomic oxygen, or hydroxyl radical [94, 95] with half-lives of less than 10 hours in summer and 40 hours in winter. According to Harrison and Allen [90], the chemical cycle of alkyl lead compounds originating in gasoline lead additives can be summarized as:

$R_4Pb \rightarrow R_3Pb^+ \rightarrow R_2Pb^{2+} \rightarrow (RPb^{3+})^* \rightarrow Pb^{2+}$

where $()^*$ indicates an unstable species. Based on these observations, it is reasonable to expect, therefore, that organolead will represent a small percentage of total Pb in atmospheric samples, and that ionic alkyllead species will dominate the inventory of organolead compounds; this is also what is observed in direct air measurements [95]. Second, washout factors (concentration ratio in rainwater compared to air) for Pb(II) is typically a factor of ten greater than that for tetra-alkyllead compounds which predict a relative enrichment of alkyllead in an ageing air mass, as the alkyllead is less efficiently scavenged [90].

In the peat bog at Etang de la Gruère (EGR) at an elevation of 1005 m above sea level in Switzerland, not more than 0.02% of the total Pb in any one sample is in the form of alkyllead species [96]. In contrast, in snow and ice from Mont Blanc (4250 m above sea level), 0.1% of the total Pb is organic [92] and in Greenland snow and ice, 1% of the total

lead is in the form of organolead species [97, 98]. Compared to the peat bog at EGR, the total Pb concentrations in alpine snow and ice are typically 3 to 4 orders of magnitude lower, and in Greenland snow and ice 5 to 6 orders of magnitude lower. Thus, the relative importance of organolead in these archives increases with decreasing total Pb concentrations and decreasing proximity to the source; this most likely reflects the more efficient scavenging of ionic Pb species (greater washout), but other factors may be involved.

An elegant demonstration of the temporal changes in environmental fluxes of alkyllead concentrations is the study of trimethyl Pb in Châteauneuf-du-Pape wines: none was found in wine samples pre-dating the introduction of leaded gasoline, and peak concentrations were found in wine dating from 1978; since then, concentrations have declined markedly [99].

6. INPUTS AND FATE OF ANTHROPOGENIC LEAD IN THE BIOSPHERE

6.1. Lead Concentrations in Soils

Pioneering measurements of Pb concentrations in roadside plants from British Columbia, Canada [100] and Colorado, USA [101], provided some of the first indications of environmental Pb contamination, and isotopic studies by Chow [102] showed unambiguously that the anthropogenic Pb in surface soils originated from leaded gasoline. However, with respect to Pb in the soils of British Columbia, for example, it was difficult to unambiguously distinguish among natural enrichments Pb due to geological mineralizations, contamination by lead arsenate pesticides used in agriculture, and gasoline Pb residues [100].

One approach to quantify the extent of anthropogenic enrichment in soils is to use a conservative, lithogenic element such as Zr, to take into account the degree to which Pb might have become naturally enriched within a vertical profile due to chemical weathering [103]. However, if there is no place left on Earth devoid of anthropogenic Pb [1], then the natural background concentrations of Pb in surface soil layers can only be determined using archived samples pre-dating industrialization, provided that such samples exist, or by mathematical modeling. In southern Sweden, Pb concentrations in the mor layer of forest soils are on the order of 40 to 100 µg/g. However, using a combination of Pb concentrations, Pb isotope ratios, and an estimate of pre-anthropogenic rates of atmospheric Pb deposition using cores from ancient layers of peat bogs, Bindler et al. [104] have estimated that the natural concentration of Pb in the surface layers of these soils was 0.1 µg/g.

6.2. Cumulative Impact of Anthropogenic, Atmospheric Lead

In a mass balance study of Pb in soils from southern Germany, Dörr et al. [105] found that virtually all of the anthropogenic Pb could be found in the topmost 20 cm. Assuming that all of the gasoline Pb emitted in the former West Germany since 1950 (ca. 250×10^3 t) was evenly distributed over the land surface, they estimated a total deposition of anthropogenic Pb of approximately 1 g m^{-2}. Measurements of Pb inventories in individual soil profiles ranged from 1.4 g m^{-2} at a rural site to 10.8 g m^{-2} at an urban site. For comparison, the cumulative mass of atmospheric, anthropogenic Pb (CAAPb) was also calculated in Switzerland, using peat cores from 8 mires [106]. In Switzerland, CAAPb ranged from 1.0 to 10.0 g m^{-2}, in good agreement with the values from southern Germany [105], and with the highest values from the south side of the Alps with direct exposure to the highly industrial region of northern Italy. In Southern Sweden, Renberg et al. [107] estimated CAAPb at 2 to 3 g m^{-2}. This range is in good agreement with our values from Stoby Mose in Denmark (3 g m^{-2}). A summary of our unpublished data concerning CAAPb in other European bogs is given in Table 2.

Name and Location of Site	CAAPb ($g\ m^{-2}$)
Loch Laxford, NW Scotland	0.9
Flech's Loch, Island of Foula, Shetland	1.9
Myrarnar, Faroe Islands	1.9
Staaby Mose, Denmark	3.1
Nebuga, Ukraine	0.9
Babyn Moh, Ukraine	0.9
Bagno, Ukraine	4.6

Table 2: Cumulative mass of atmospheric, anthropogenic Pb (CAAPb) in different parts of Europe

The bog at Bagno in Ukraine is west of the Carparthian Mountains, and directly exposed to the industrial regions of the former Eastern Europe, compared to the other bogs (Nebuga and Babyn Moh) from the same country. For comparison with the values from bogs in Europe, we have studied three peat bog profiles in southern Ontario, Canada [108]. The Sifton Bog in the city of London, Ontario, recorded 2.4 $g\ m^{-2}$ CAAPb, the Luther Bog in a rural area 1.6 $g\ m^{-2}$, and the Spruce Bog in Algonquin Park, a comparatively remote site, 1.0 $g\ m^{-2}$.

All of these sites show a minimum of 1 $g\ m^{-2}$. Extrapolating to the land area of the northern hemisphere (ca. $100 \times 10^6\ km^2$) suggests that the total cumulative burden of atmospheric, anthropogenic Pb to the continents is approximately one million tonnes. However, given that the annual consumption of gasoline lead exceeded 300,000 tonnes per year during the late 1960's and early 1970's, this estimate seems too low.

6.3. The Fate of Anthropogenic Lead in Soils

Understanding the fate of anthropogenic Pb soils is vital to evaluating bioavailability, mobilization, and transport. In forest soils of the northeastern U.S., Miller and Friedland [109] suggested that Pb was being redistributed, but Wang et al. [110] concluded that Pb is efficiently retained. Dörr et al. [105] measured the distribution of ^{210}Pb, a naturally-occurring Pb isotope that is believed to be effectively independent of anthropogenic Pb emissions. Based on the distribution of this isotope, they concluded that Pb had penetrated no deeper than ca. 20 cm; they concluded, however, that the downward migration velocity of Pb was approximately 1 mm/yr. Using the abundance of stable Pb isotopes (primarily ^{206}Pb, ^{207}Pb, and ^{208}Pb), Steinmann and Stille [111] concluded that Pb mobilization in soils is very limited. Studying the isotopic composition of Pb at a Medieval Pb smelting site in England, Whitehead et al. [112] estimated a Pb migration rate of ca. 8 mm/y. Bacon et al. [113] reported changes in Pb isotope ratios in deeper soil layers of some Scottish soils, but these may have been due to geological changes or lateral flow.

To help evaluate the fate of metals in soils, it can be helpful to separate total Pb into the compartments by which it is predominantly bound: exchangeable, organically-complexed, adsorbed to Fe and Mn oxides, associated with sulfide minerals, and the residual fraction which is primarily the "natural" silicate fraction [114, 115]. This approach is especially useful when it is combined with the determination of the isotopic composition of Pb in these fractions. In soils from the Middle East, isotope analyses of the labile fractions were used [119] to show that there had been substantial penetration of anthropogenic Pb into deeper soil layers. However, in a comparable study of soils from central Europe, no such mobilization was found [116].

To summarize, the fate of any metal in soil is a response to a complex set of parameters including soil texture, mineralogy, pH and redox potential, hydraulic conductivity, abundance of organic matter and oxyhydroxides of Al, Fe, and Mn, in addition to climate, situation, and nature of the parent material [117-119]. As a result, it is not possible to make any general conclusions regarding the final fate of anthropogenic Pb in soils. In fact, the fate of Pb in soils will probably have to be evaluated on a soil-by-soil basis. However, the data shown in Fig. 1 clearly show that acidic soils will certainly have the greatest potential for Pb migration. The Pb isotope data from acidic soils in southern Sweden suggest that Pb is migrating and, along with Al and Fe, accumulating in

the B horizon of podzols [107].

6.4. Lead Concentrations in Solution

Because Pb has to be transferred from the solid phase to the aqueous phase before it can be taken up by plants and aquatic organisms, the concentration of Pb in natural waters can be a sensitive indicator of the potential for Pb to become biologically "available". To estimate how much of this Pb might be transferred to the aqueous phase, solutions collected from ten Swiss forest soils were measured for concentrations of total dissolved Pb (Peter Blaser, unpublished data) and found to range from < 1 to > 60 µg/L. Five of the profiles were acidic (pH 4 to 5) and these contained 20 to 60 µg/L Pb in the aqueous phase of the surface layers. These layers, however, are the most critical ecologically, as they represent the biologically active zone of acidic forest soils: this is also the zone which has been most impacted by anthropogenic Pb.

For comparison, with the Pb concentrations of the topmost layers, the solutions collected from the deeper soil horizons all had less than 1 µg/L and were below the LOD provided by ICP-Q-MS. Hirao and Patterson [120] reported 0.015 µg/L in stream runoff in the Sierra Nevada Mountains, but were only able to accomplish this because of the extreme cautions taken to avoid contaminating their samples with industrial lead, and because they used ID-MS to measure the Pb concentrations. The Sierra Nevada watershed is characterized by granitic rocks, and most of the Pb in uncontaminated streamwater is probably derived from the chemical weathering of biotite and potassium feldspar [121]. Therefore, their measured Pb concentration (15 parts per trillion) is probably not an unreasonable estimate of the natural Pb concentration in uncontaminated waters from crystalline terrains. Thus, any study of soil solution Pb has to be capable of reliably measuring Pb in this concentration range.

The problem of Pb determination at extremely low concentrations in seawater was discussed at length by Patterson et Settle [122], in polar snow and ice by Boutron [34], and in freshwaters by Nriagu [35]. Using clean lab procedures and double-focusing sector field ICP-MS, Krachler et al. [33] have shown that it is possible to now reliably measure Pb concentrations as low as 60 pg/L which is nearly three orders of magnitude less than the concentration of Pb in stream waters in [120]. Using this comparatively new approach, therefore, it is now feasible to begin detailed studies of anthropogenic Pb in soil solutions.

7. TEMPORAL TRENDS IN ATMOSPHERIC LEAD DEPOSITION

7.1. Lead in Sediments

Many studies have used lake sediments to document changes in the timing and intensity of Pb contamination, including cores collected in the U.S. [123, 124], the Canadian Arctic [125], Spain [126], Switzerland [127, 128], Scotland [129, 130], and the Middle East [131]. One of the main challenges has been to distinguish between atmospheric and non-atmospheric sources [132], but a mathematical approach to solving this problem using precision measurements of Pb isotope ratios in sediments of Lake Constance has recently been developed [133].

7.2. Lead in Bryophytes

Bryophytes such as mosses have no roots, but instead rely exclusively upon atmospheric inputs for nutrient elements. They also receive Pb from the air, and retain it efficiently, allowing moss analyses to be used as a monitoring tool for studying changes in atmospheric metal deposition. The isotopic composition of Pb in forest moss species such as *Hylocomium splendens* [134] and *Polytrichum formosum* [135] which have been collected annually during the past decades, allows a reconstruction of the predominant sources of anthropogenic Pb and their temporal variation. Lichens can be used for the same purposes [136], but because they grow on a rock substrate, more care might be needed to separate atmospheric from

lithogenic inputs. Herbarium samples for *Sphagnum* moss which had been collected from peat bogs in Switzerland since 1867 [137] and Scotland since 1830 [138] have documented temporal changes in the isotopic composition of atmospheric Pb over longer time periods. The absolute chronology which herbarium samples provide is a great advantage, compared to archives such as sediments or peat, which require radiometric age dating. Herbage samples from the Rothamsted experimental station in England have been collected annually since 1856, have also provided a valuable record of atmospheric Pb deposition [139].

7.3. Lead in Tree Rings and Barks Pockets

The use of tree rings as archives of atmospheric Pb contamination has been seriously questioned [140], although Aberg et al. [141] reported more success. Bark pockets which become trapped in a tree as two branches grow together, show much promise for reconstructing changes in the isotopic composition of Pb in atmospheric aerosols [142, 143].

7.4. Peat Bog Archives

Ombrotrophic bogs are excellent archives of atmospheric Pb deposition because they receive Pb only from the air, and because they efficiently retain this metal despite the low pH of the waters (pH 4), the abundance of natural, complex-forming organic acids and the seasonal variations in redox potential [45]. Bogs are probably the best continental archives of atmospheric Pb deposition and they are receiving increasing attention for this purpose [71, 74, 75, 108, 144-158]. With bogs commonly found in the temperate zone of both hemispheres, they offer the promise of high-resolution reconstructions of atmospheric Pb deposition worldwide.

A summary of atmospheric Pb deposition in Switzerland during the past 14,500 years is shown in Fig. 4 [159]. This graph shows that atmospheric Pb deposition in central Europe has been dominated by anthropogenic Pb continuously for three thousand years. Prior to this, Pb concentrations were proportional to those of Sc, which suggests that soil dust was the main factor regulating atmospheric Pb deposition. The background rate of atmospheric Pb deposition (10 $\mu g/m^2/y$) was only found in peat samples from 6,000 to 9,000 years old; peats from ca. 6,000 to 3,000 years old had elevated Pb concentrations because forest clearances and soil tillage for agriculture had already increased the dust flux. Peat samples from the early part of the Holocene (ca. 13,000 until 9,000 years ago) were more radiogenic which denotes a change in the predominant sources of atmospheric soil dust.

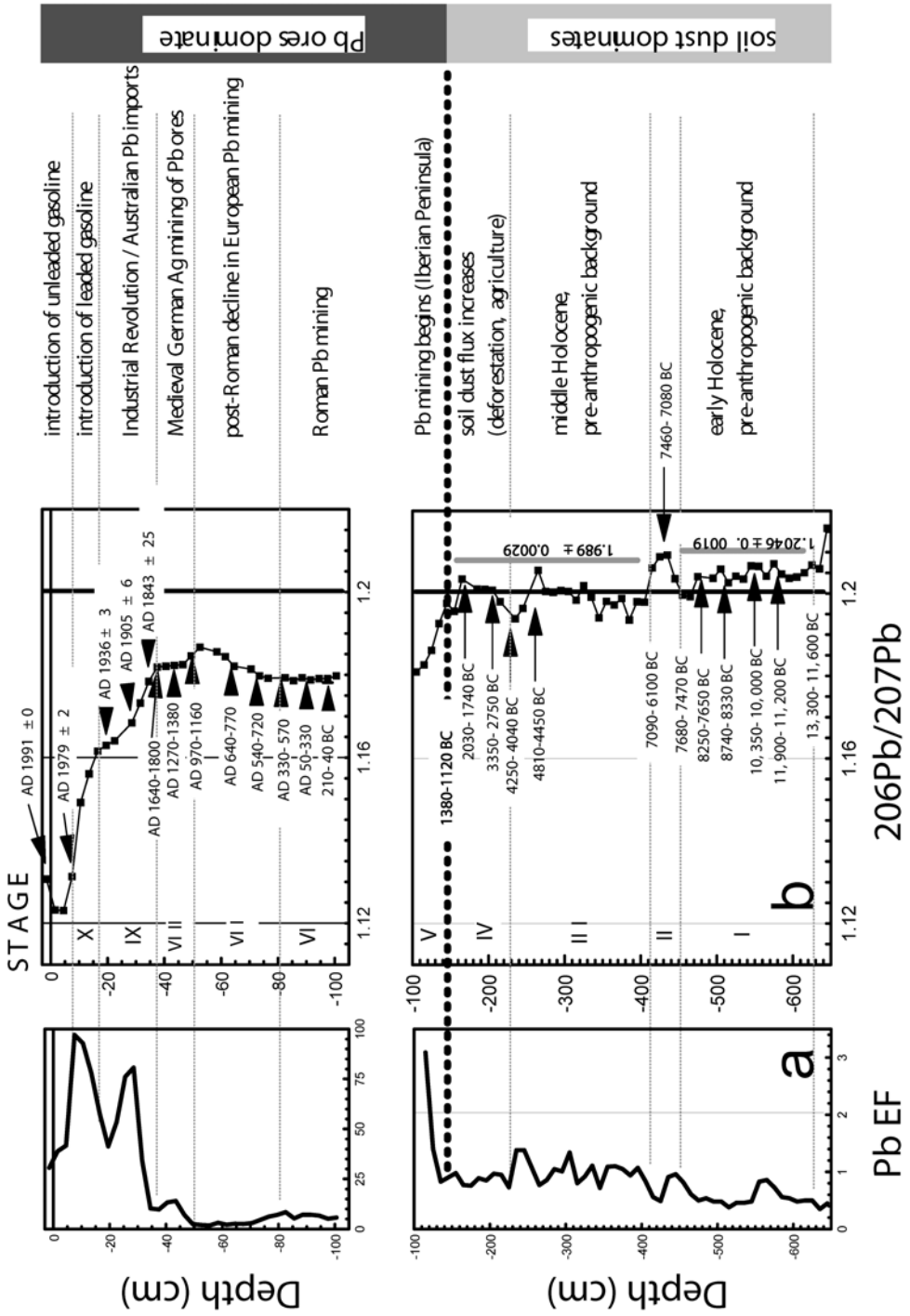

Figure 4: Pb profile in the Swiss peat bog of Étang de la Gruère [159]

(a) Pb enrichment factor calculated as the ratio of Pb/Sc in the peat normalized to background value. (b) Isotopic composition of Pb summarized as $^{206}Pb/^{207}Pb$.

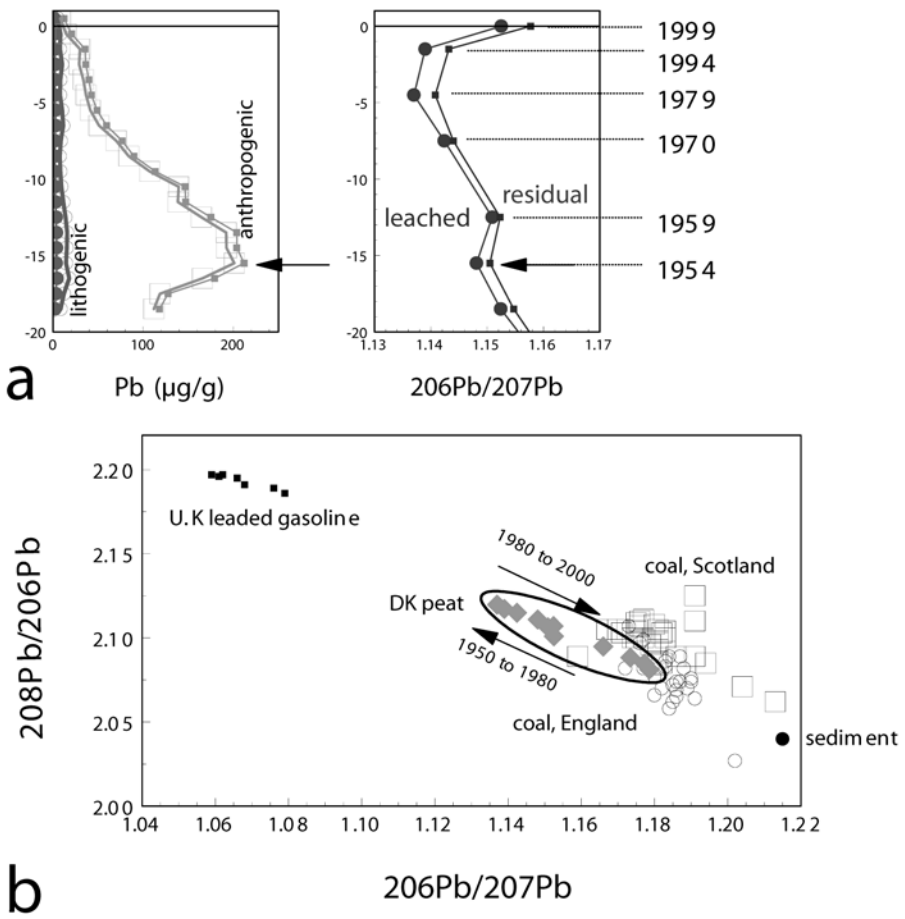

Figure 5: Pb profile in the Danish peat bog of Storelung Mose [48]. (a) Lithogenic Pb, anthropogenic Pb vs. depth (see ref. [48] for calculation details). (b) Diagram $^{206}Pb/^{207}Pb$ vs. $^{208}Pb/^{206}Pb$ for the leached fraction of the Danish peat samples, also shown U.K. coal [46], U.K. leaded gasoline in 1997 [160] and the isotopic composition of an oxfordian sediment [159].

7.5. Relative Importance of Gasoline Lead versus Other Sources of Industrial Lead

Using a peat core from Denmark which was cut into 1 cm slices and age dated using both ^{210}Pb and ^{14}C (atmospheric bomb pulse curve), Pb was separated into lithogenic and anthropogenic components using Ti as the reference element, and the isotopic composition of the Pb determined using TIMS [161]. The data show that the maximum concentration of anthropogenic Pb (1954) pre-dates the minimum in $^{206}Pb/^{207}Pb$ (1979) by more than two decades. In other words, the maximum impact of gasoline Pb (revealed by the isotopic composition) occurred approximately 25 years after the peak in Pb contamination (indicated by the EF).

Comparing the isotopic composition of the peat samples with gasoline leads [160] and British coals [46] (Fig. 5) suggests that coal burning was the predominant source of this Pb contamination. Clearly, even though gasoline Pb has certainly been an important source of anthropogenic Pb to the atmosphere during the past decades, other sources of industrial Pb were even more important.

7.6. The Cumulative Input of Anthropogenic Lead

To emphasize this point, the cumulative input of anthropogenic Pb to the peat bog at EGR is shown in Fig. 6. This graphic shows that 10% of the anthropogenic Pb was already in the

bog at the start of the medieval period and more than 20% before the start of the Industrial Revolution. Prior to the introduction of leaded gasoline, approximately 75% of the anthropogenic Pb inventory was already in the bog [106]. This graphic is helpful in many ways, as it indicates that reducing emissions of anthropogenic Pb by eliminating leaded gasoline is certainly not going to eliminate industrial emissions altogether. In fact, many other sources of atmospheric Pb are also important, and also have to been reduced.

7.7. Lead in Polar Snow and Ice

Ever since the pioneering paper by Murozumi [196] of Pb in Greenland snow and ice, these kinds of samples have provided much important information about temporal trends in atmospheric Pb deposition not only in Greenland [162-165] but also from the European Alps [166] and even Antarctica [167]. All of this work, however, was done using discrete samples, which had to be decontaminated individually: this not only introduces the risk of contamination, but is also expensive and time consuming. While these studies certainly documented the impact of gasoline additives and the subsequent declines in atmospheric Pb emissions, which followed the gradual phasing out of leaded gasoline, they provided very little information about Pb emissions from the early part of the 20th century.
A notable recent development has been the direct coupling of an ice melting head to an ICP-MS to allow continuous measurements of Pb on-line, offering unprecedented temporal resolution (Fig. 7). This new development is important, especially for ice which has accumulated during the industrial period, because it shows that the intensity and extent of Pb contamination prior to the introduction of leaded gasoline is comparable to that found afterward [168].

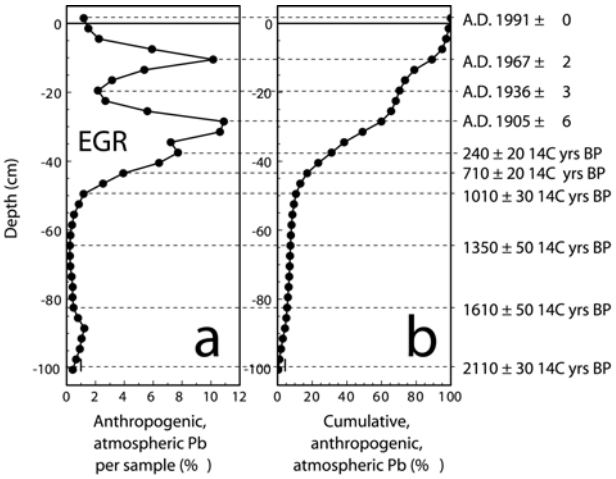

Figure 6: Pb profile in the Swiss peat bog of Étang de la Gruère since 151-117 BC (a) Proportion of anthropogenic atmospheric Pb for each sample compared to the complete profile. (b) Cumulative anthropogenic atmospheric Pb.

7.8. Lead in Atmospheric Aerosols Today

Many published studies of the isotopic composition of aerosols have been summarized by Bollhöfer and Rosman [169-172] who provide precise Pb isotope data for aerosols collected at 80 sites in the northern hemisphere. While there have been dramatic declines in air Pb concentrations in many developed countries, and changes in the isotopic composition of the Pb, significant atmospheric Pb contamination remains. Each of the papers cited here and describing the isotopic composition of Pb in atmospheric aerosols, as well as sediments, bryophytes, peat bogs, and polar snow and ice, shows that even the most recent samples are still contaminated by anthropogenic Pb. Aerosols today are typically enriched in Pb by 100 to 1000 times, relative to the abundance of Pb in crustal rocks [173]. As noted out by Bacon [174], a substantial portion of anthropogenic Pb now being deposited from the atmosphere has its origin other than in gasoline.

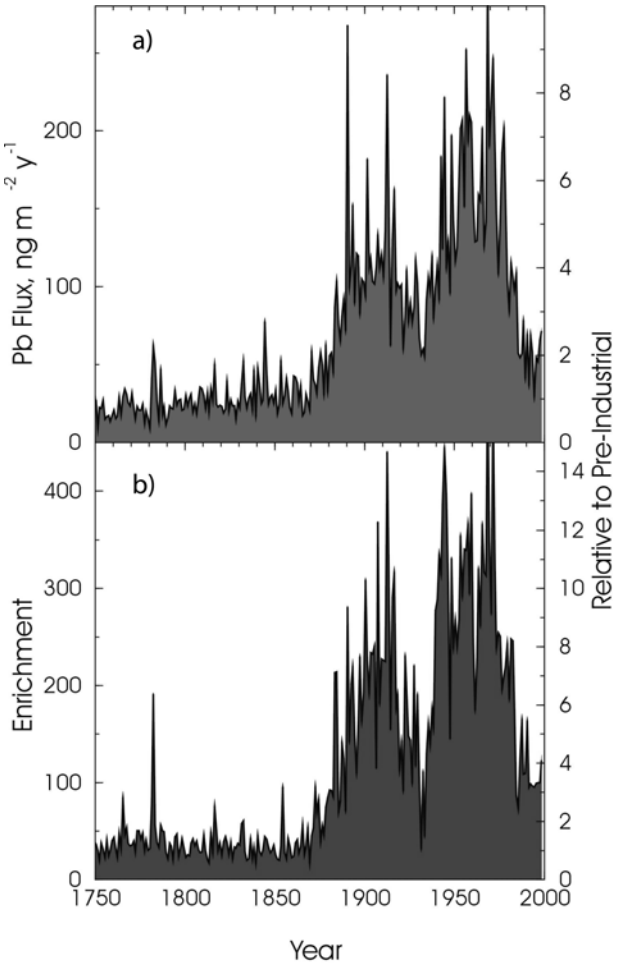

Figure 7: Annual average Pb flux (A) and crustal enrichment of Pb (B) in central Greenland

"J. R. McConnell, G. W. Lamorey, and M. A. Hutterli, *Geophy. Res. Lett., 29*, (2002), Copyright [2002] American Geophysical Union", reproduced by permission of American Geophysical Union.

As an example, we show the isotopic composition of Pb in snow samples collected in the Black Forest of southern Germany using clean lab techniques and measured using ICP-SMS by Krachler et al. [54]. Compared to the isotopic composition of atmospheric dust dating from pre-anthropogenic times, the snow samples are much less radiogenic (Fig.8.a) which clearly shows that industrial sources of Pb dominate the atmospheric Pb flux. For comparison, the isotopic composition of Pb from incinerators [160, 175] is also shown, and these overlap with the values from the snow collected in 2003.

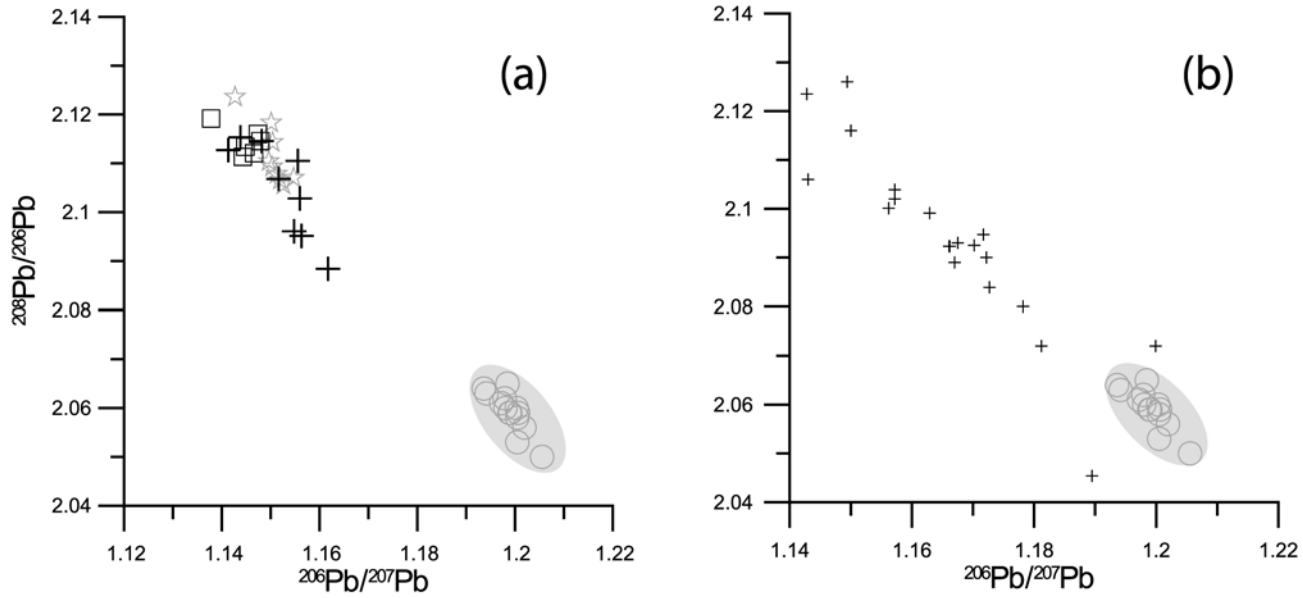

Figure 8: (a) Diagram $^{206}Pb/^{207}Pb$ vs. $^{208}Pb/^{206}Pb$ for snow samples from Black Forest (+), Germany, sampled during Winter 2002. For comparison are also shown the isotopic composition of natural dust (○) [45], isotopic composition of incinerators dust (☆) [160, 175], and aerosols composition from Southern Germany (□) [172]. (b) Diagram $^{206}Pb/^{207}Pb$ vs. $^{208}Pb/^{206}Pb$ for wine samples (+) [176], also shown "natural dust" (○) isotopic composition.

A second example (Fig.8.b) is provided by the isotopic composition of Pb in wines [176]. Again, compared to the natural isotope signature of Pb in atmospheric dust or soils, the values for the wines are much lower which shows unambiguously that the wines are contaminated with industrial Pb. The possible sources of this Pb are many: perhaps the soil solutions were contaminated because of past use of Pb arsenate as a pesticide; the grapes may have been contaminated by Pb-rich atmospheric aerosols; processing of the grapes, fermentation of the wines, and bottling of the final product are all possible sources of Pb contamination from contact with metal or glass surfaces.

8. ENVIRONMENTAL LEAD EXPOSURE AND HUMAN HEALTH

8.1. Blood Lead Levels and Their Significance

Lead is primarily absorbed via respiration and ingestion and carried throughout the body by the blood, which enables Pb to enter all tissues. For this reason, measurement of blood lead levels (BLL) is the most common method for establishing degree of exposure in humans, and is usually reported in units of µg/dL [177]. Environmental lead poisoning can affect both adults and children, but the greatest concern is for children as they experience symptoms at significantly lower BLL than do adults. Whereas many of the symptoms experienced by adults are reversed when exposure is ceased, children tend to develop permanent developmental and neurological problems when exposed chronically to Pb [178]. Unfortunately, once elevated BLL have been detected, it is too late to prevent the deleterious effects of Pb on the brain. Children are particularly sensitive because they absorb a greater proportion of ingested Pb from the gastrointestinal tract than do adults and retain more of that Pb. In addition, a greater proportion of systemically circulating lead gains access to the brain of children, especially those five years old or younger, than of adults. Finally, the developing nervous system is far more vulnerable to the toxic effects of Pb than the mature brain [177].

Low level lead exposure has serious deleterious and irreversible effects on brain function, such as lowered intelligence, and diminishes school performance, especially from exposures that occur in early life; hearing deficits and growth retardation have also been observed [179]. Prior to 1970, BLL greater than 60 µg/dL were considered critical for children. Today, subclinical lead toxicity is defined as a BLL of 10 µg/dL (100 parts per billion) or higher, and is estimated to affect one out of twenty children in the U.S. [179]. The recent findings published by Canfield et al. [180], however, show that BLL, even those below 10 µg/dL, are inversely associated with the IQ scores of children between the ages of three and five. Additional health effects in children with average BLL of 3 µg/dL, including decreased height and delayed puberty, has been reported [181]. To summarize, D. O. Carpenter, Director of the Institute of Health and Environment, State University of New York, was recently quoted as saying that “BLL as low as 1 µg/dL are associated with harmful effects on children’s learning and behavior. There may be no lower threshold for some of the diverse effects of lead in children” (Chem. Eng. News, April 7, 2003). Other recent developments in the area of childhood Pb neurotoxicity have been reviewed elsewhere [177].

To help put these concentration values into perspective, Patterson [6] estimated that the natural concentration of Pb in blood is 0.25 µg/dL. A more recent estimate, based on the Pb concentrations of human bones from pre-industrial times and the relationship between bone Pb and blood Pb concentrations, is 0.016 µg/dL [182]; these values are 40 and 600 times, respectively, lower than the blood Pb concentration (10 µg/dL) currently considered critical for children.

During the past two decades, average BLLs in the U.S. have declined by more than 90%. However, even today, approximately

890,000 pre-school children in the U.S. are estimated to have BLLs exceeding 10 µg/dL. In some cities in the northeastern region of the U.S., more than one-third of pre-school children have BLLs above 10 µg/dL [179]. To help put these values in perspective, in the Province of Ontario, Canada, in 1984, the average BLL in children was 12.0 ± 4.4 µg/dL [183]. For comparison with contemporary U.S. values, a recent study of 421 school children in Jamaica showed an average of 9.2 µg/dL in rural areas and 16.6 µg/dL in urban areas [184]; at the site of a former lead ore processing plant the average concentration was 35 µg/dL. In the Cape Province of South Africa, more than 90% of the children showed BLL above 10 µg/dL [185]. Today, lead poisoning is considered one of the most common pediatric health problems in the U.S. [178].

8.2. Mechanism of Lead Poisoning

Lead enters into brain cells, both neurons and glia, by channels that under normal conditions allow the passage of Ca^{2+}. Lead enters (and damages) mitochondria via the cellular mechanism that normally functions to bring calcium into this organelle [177]. The molecular mechanisms of Pb toxicity are incompletely understood, but it is known that Pb^{2+} can replace Zn^{2+} and Ca^{2+} at their binding sites in various proteins, thereby altering their structure and function [178]. The Zn enzyme δ-aminolevulinic acid dehydratase (ALAD) has received the most attention, as this is the only one known to be inhibited by lead. The mammalian form of ALAD contains a unique catalytic zinc-binding site with three cysteine residues. Lead, being a much larger and more polarizable cation than that of Zn forms much more stable complexes with these sulfur-bearing ligands and can easily replace Zn. With respect to Ca, Pb interferes with the ability of Ca to trigger exocytosis of neurotransmitters in neuronal cells, suggesting that Pb might generally target proteins involved in Ca-mediated signal transduction. Here, Pb promotes phospholipid binding at lower concentrations than does Ca, suggesting that Pb binds to the Ca site more tightly than does Ca itself [178].

8.3. Predominant Sources of Lead Exposure

During the last decades of the 20th century, thanks largely to the pioneering investigations of Patterson and co-workers at the California Institute of Technology, it was unambiguously established that aerosols in both rural and remote locations are contaminated by industrial Pb, mainly from the extensive use of gasoline lead additives [186]. These findings were obtained after years of careful study using soil, plant, and animal samples from the rural Sierra Nevada Mountains of California [120, 187-189], seawater from remote marine locations such as the mid-Atlantic [190], Bermuda [191], and the North Pacific [192]. Even snow and ice samples from glaciers in Greenland exhibit Pb concentrations which are up to 400 times higher than deeper, older ice layers dating from pre-anthropogenic times [193]. Between 1923 and 1986, seven million tonnes of gasoline lead additives were consumed in the U.S. alone. The complete history of leaded gasoline use since its introduction in 1923, has been reviewed elsewhere [14]. According to the United Nations, approximately 20% of the gasoline used worldwide today still contains lead additives.

Of particular interest here is the strong correlation in the temporal trend between BLLs and the concentration of lead in gasoline [194]. As leaded gasoline is replaced in developed countries by unleaded fuels, air Pb concentrations have been declining and BLLs along with it. Despite this, in the U.S., however, paint appears to be the single most important source of childhood lead poisoning. Children with BLLs above 55 µg/dL are more likely to have paint chips that are observable in abdominal radiographs, and most pre-school children with BLLs above 25 µg/dL are reported to have put paint chips in their mouths [195]. With respect to children with BLLs between 25 and 10 µg/dL, house dust contaminated with lead from deteriorating paint, and from lead-contaminated soil

tracked in from outdoors, is the major source of Pb exposure [195]. More than 95% of U.S. children who have elevated BLLs, fall within this range [179].

The lead problem of the inner cities in the U.S. has been studied in detail by Mielke [196] who has found that more than 50% of the children in some areas of New Orleans and Philadelphia have BLLs above the current guideline of 10 µg/dL. As pointed out [196], soils in urban areas have become so highly contaminated with industrial Pb that they are a "giant reservoir" of Pb-rich dust particles. In the inner city areas of New Orleans, the geographic distribution of BLLs in children strongly resemble the abundance of Pb in soils [196].

There have been several major sources of Pb contamination to urban soils. Leaded gasoline consumption is the most obvious one, with many major cities having soil Pb concentrations on the order of several thousand µg/g [197]. However, as these soils were probably already contaminated to some extent with Pb from other sources even before the introduction of leaded gasoline, with industrial emissions, disposal of consumer products (e.g., paint and plumbing), coal combustion and waste incineration all contributing to Pb contamination in urban areas [201]. Referring again to the seminal work by Patterson [6], the ablated and weathered residues from applying 3.4 million tonnes of leaded paint in the U.S. between 1925 and 1965 are sufficient to have increased the Pb concentrations in the top 5 cm of urban soils from the natural concentration of 15 mg/kg to 600 mg/kg. Even soils in rural areas may be contaminated with Pb, especially agricultural soils used for growing fruit, due to the past use of lead arsenate as a pesticide; at the peak of its use, several thousand tonnes was used in the U.S. alone [6].

8.4. Other Sources of Lead Exposure

Human exposure to environmental Pb occurs from air, soil, household dust, food, drinking water, and various consumer products. In an uncontaminated environment, human exposure has been estimated as follows: ingesting food, 20 µg Pb/day; drinking water, 0.5 µg Pb/day; breathing air, 0.01 µg Pb/day [6]. During the 1960's in the U.S., average body burdens were approximately 100 times greater than this.

In the U.S., Pb was used in residential paint from 1884 to 1978; it has been banned for household use since 1978, but is still used in specialty paints. Moreover, although the use of leaded paint was banned, there was no government mandate to have lead paints removed from interior surfaces where it already existed. As a result, there may be more than twenty million homes in the U.S. with "significant lead-based paint hazards" [177], and two million homes in the Province of Ontario, Canada, in the same category [76]. In addition, inappropriate methods of clean up such as sandblasting of painted surfaces, can exacerbate the problem [198]. In Canada, the Hazardous Substances Act has prohibited the use of lead-based paints in interior consumer paints, and paints for children's toys and furniture, since 1975 [76]. However, according to Health Canada (1999), interior paints are still allowed to contain up to 0.5% Pb. For comparison, exterior housepaints removed from houses in Toronto were found to contain up to 33% Pb.

Lead solder was used to seal canned foods in the U.S. until 1995. At its peak, several thousand tonnes of Pb per year was consumed for this application [6]. In Canada, use of lead-solder cans has decreased by 99%, but some canned foods imported into Canada may contain lead solder.

Leaded gasoline was banned in the U.S. in 1986, but lead additives are still used in racing fuels, as well as fuels for watercraft, light aircraft, and farm machinery [196]. In Canada, unleaded gasoline was introduced in 1975, and leaded gasoline was banned for use in motor vehicles in 1990. In Ontario, for example, ambient air Pb concentrations declined from 0.3 to 0.01 µg/m^3 between 1980 and 1990 [183]. For comparison with these air Pb concentrations, Patterson [6] calculated natural air Pb concentration of 0.0005 µg/m^3 which is a factor of twenty lower than the lower limit of detection for air

Pb employed by the OMEE.

Concerns remain about dietary Pb exposure from lead glazes on pottery and ceramics, and from leaded crystal. Lead exposure from surfaces used to contain food or drink (water pipes, lead solder, glazes on ceramics and pottery, and leaded crystal), is especially of concern when the foods or drinks they contain are acidic. In Canada, glazes currently may contain no more than 7 mg/kg Pb, but this value is being revised down to 2.5 or 0.5 mg/kg. Leaded crystal (containing up to 36% PbO) rapidly releases Pb to acidic solutions, with wine Pb concentrations increasing from 89 to 3518 µg/L after 4 months storage [199]. Even in the absence of leaded crystal glasses and decanters, the concentrations in wine are an ongoing concern. In a recent Danish study, 15 out of 50 wine bottles from EU countries tested exceeded the allowable limit for Pb in glass (250 mg/kg Pb). Rosman et al. [200] measured Pb in French wines from 1950 to 1980; the concentrations range from 78 to 227 µg/L and the Pb isotope data showed that all were contaminated by industrial Pb.

The maximum allowable concentration (MAC) of Pb in drinking water in Europe is currently 50 µg/L (which corresponds to the Pb concentration for water in contact with leaded pipes estimated by Patterson [6]), but this will be reduced to 10 µg/L by 2013. The MAC for Pb in drinking water in Canada today is 10 µg/L. The WHO recommended MAC had been 50 µg/L, but this was reduced in 1995 to 10 µg/L.

9. SUMMARY AND CONCLUSIONS

Lead has no biological function and is one of the most toxic metals. At the same time, it is one of the most useful, and perhaps no other metal has found such a wide range of industrial applications. It has been used extensively since Antiquity, which is when environmental Pb contamination began. With respect to contamination since industrialization, peat bogs and polar ice show that coal combustion and industrial emissions were as important during the first half of the 20th century as gasoline lead was during the second half.

Air Pb concentrations have generally declined since the introduction of pollution control technologies and the gradual elimination of leaded gasoline additives. However, all of the most recent published studies of the isotopic composition of Pb in aerosols and archival samples show that anthropogenic sources continue to dominate the atmospheric Pb flux by a considerable margin. The health effects of childhood Pb exposure is a growing concern, as deleterious effects are seen at BLL well below those currently believed to be safe, and safe levels are one or two orders of magnitude above the estimated natural values.

Mobilization of Pb-rich particles from highly contaminated soils in urban areas is an on-going health concern for many large cities. Even in areas far removed from industrial emission sources, Pb concentrations in the surface soil layers are far above their natural concentration range. In acidic forest soils, Pb concentrations are not only elevated in the biologically active zone, but also in their corresponding pore fluids. Accurate and precise measurements of the isotopic composition of Pb employing appropriate clean lab protocols, will continue to advance our understanding of the fate of Pb in the environment and its impact on human and ecosystem health.

ACKNOWLEDGEMENTS

Thanks from W.S. to Andriy Cheburkin for building the EMMA and OLIVIA XRF spectrometers, countless Pb measurements, many years of fruitful discussions, and on-going excitement with ^{210}Pb; Bernd Kober for his insight into Pb isotope systematics and for keeping Betsy alive, and Michael Krachler for bringing new meaning to “trace” analysis of Pb in environmental samples. Special thanks to B. Haas for patience and understanding, and the usual message.

REFERENCES

1. Jaworski, J.F., *Group report: Lead*, in *Lead, Mercury, Cadmium and Arsenic in the environment*, K.M. Meema, Editor. 1987, SCOPE, John Wiley and Sons: New York. p. 107-117.
2. Harn, O.C., *Lead, the precious metal*. 1924, London: Johnatan Cape. 323.
3. Nriagu, J., *Cupellation: The oldest quantitative chemical process.* Journal of Chemical Education, 1985. **62**(8): p. 668-674.
4. Lasdown, R. and W. Yule, *Lead toxicity. History and environmental impact*. 1986, Baltimore: John Hopkins University Press. 286.
5. Ewers, U. and H.W. Schlipkter, *Lead*, in *Metals and their compounds in the environment*, E. Merian, Editor. 1991, VCH: Weinheim. p. 971-1014.
6. Patterson, C.C. and M. Cambridge, *Contaminated and Natural Lead Environments of Man.* Arch Environ Health, 1965. **11**: p. 344-360.
7. Reuer, M.K. and D.J. Weiss, *Anthropogenic lead dynamics in the terrestrial and marine environment.* Philos Transact Ser A Math Phys Eng Sci, 2002. **360**(1801): p. 2889-904.
8. Russell, R.D. and R.M. Farquahr, *Lead isotopes in Geology*. 1960, London: Interscience. 243.
9. Doe, R.B., *Lead isotopes*. 1970, Heidelberg: Springer Verlag. 137.
10. Faure, G., *Principles of isotope geology 2nd ed°*. 1986, New York: John Wiley and Sons. 589.
11. Dickin, A.P., *Radiogenic isotope geology*. 1995, Cambridge: Cambridge University Press. 490.
12. Sangster, D.F., P.M. Outridge, and W.J. Davis, *Stable lead isotope characteristics of lead ore deposits of environmental significance.* Environmental Reviews, 2000. **8**: p. 115-147.
13. Robbins, J.A., *Geochemical and Geophysical Applications of Radioactive Lead*, in *The Biogeochemistry of Lead in the Environment*, J.O. Nriagu, Editor. 1978, Elsevier/North Holland Biomedical Press: New, York. p. 285-393.
14. Nriagu, J.O., *The rise and fall of leaded Gasoline.* Sci. Tot. Environ., 1990. **92**: p. 13-28.
15. Nriagu, J.O., ed. *Biogeochemistry of Lead in the Environment, Vol 1A. Ecological Cycles Vol 1B. Biological effects*. 1978, Amsterdam: Elsevier Biomedical Press.
16. Boggess, W.R. and B.G. Wixson, eds. *Lead in the Environment*. 1979, National Science Foundation: Washington D.C. 272.
17. Committee on Lead in the Human Environment, ed. *Lead in the Human Environment*. 1980, National Academy of Sciences: Washington D.C. 525.
18. Harrison, R.M. and D.P.H. Laxen, *Lead pollution, Causes and Control*. 1981, London and New York: Chapman and Hall. 168.
19. Förstner, U. and G.T.W. Wittmann, *Metal pollution in the Aquatic Environment 2nd ed°*. 1981, Berlin-Heidelberg-New York: Springer Verlag. 489.
20. Kabata-Pendias, A. and H.K. Pendias, *Trace Elements in Soil and Plants*. 1984, Boca Raton: CRC Press. 315.
21. Bodek, I., et al., eds. *Environmental Inorganic Chemistry. Properties, Processes and Estimations Methods*. 1988, Pergamon Press: New York-Oxford.
22. Lyndsay, W.L., *Chemical Equilibria in Soils*. 1979, New York: John Wiley and Sons. 449.
23. Wedepohl, K.H., *The composition of the continental crust.* Geochim. Cosmochim. Act, 1995. **59**: p. 1217-1232.
24. Wampler, J.M., *Lead :Element and Geochemistry*, in *Encyclopedia of Geochemistry and Environmental Sciences*, R.W. Fairbridge, Editor. 1972, Dowden, Hutchinson, and Ross: Stroudsburg, Pennsylvania. p. 642-645.
25. Long, L.E., *Lead :Interpretation of Stable Isotope Abundance*, in *Encyclopedia of Geochemistry and Environmental Sciences*, R.W. Fairbridge, Editor. 1972, Dowden, Hutchinson, and Ross: Stroudsburg, Pennsylvania. p. 646-648.
26. Goldschmidt, V.M., *Geochemistry*, ed. A. Muir. 1954, Oxford: Clarendon Press.
27. Wedepohl, K.H., *Lead, Chap.82*, in *Handbook of Geochemistry*, K.H. Wedepohl, Editor. 1969, Springer Verlag: Berlin. p. 82C1-82.
28. Cheburkin, A.K. and W. Shotyk, *An Energy-dispersive Miniprobe Multielement Analyser (EMMA) for direct analysis of Pb and other trace elements in peats.* Fresenius Journal of Analytical Chemistry, 1996. **354**: p. 688-691.
29. Cheburkin, A. and W. Shotyk, *A high sensitive XRF analyser (OLIVIA) using a multi-crystal pyrographite assembly (MPA) to reduce continuous background.* X-Ray spectrometry, 1999. **28**: p. 145-148.
30. Prange, A., K. Kramer, and U. Reus, *Determination of trace element impurities in ultrapure reagents by total reflection X-ray spectrometry.* Spectrochimica Acta Part B, 1991. **46**(10): p. 1385-1393.
31. Cheam, V., et al., *Direct Determination of lead in sea-waters by laser-excited atomic fluorescence spectrometry.* Journal of

Analytical Atomic Spectrometry, 1994. **9**: p. 315-320.
32. Cheam, V., et al., *Development of a laser-excited atomic fluorescence spectrometer and a method for the direct determination of lead in Great Lakes waters.* Analytica Chimica Acta, 1992. **269**: p. 129-136.
33. Krachler, M., et al., *Novel cleaning and calibration procedures for order of magnitude improvement in detection limits for trace elements in polar ice from Artic Canada using ICP-SMS.* Journal of Analytical Atomic Spectrometry, accepted for publication, 2004.
34. Boutron, C.F., *A clean laboratory for ultralow concentration heavy metal analysis.* Fresenius Journal of analytical chemistry, 1990. **337**: p. 482-491.
35. Nriagu, J.O., et al., *A protocol for minimizing contamination in the analysis of trace metals in Great Lakes waters.* Journal of Great Lakes Research, 1993. **19(1)**: p. 175-182.
36. Hoskin, P.W.O. and R.J. Wysoczanski, *In situ accurate and precise lead isotopic analysis of ultra-small analyte volumes (10-16 m3) of solid inorganic samples by high mass resolution secondary ion mass spectrometry.* Journal of Analytical Atomic Spectrometry, 1998. **13**: p. 597-601.
37. Lazareth, C.E., et al., *Sclerosponges as a new potential recorder of environmental changes: lead in Ceratoporella nicholsoni.* Geology, 2000. **28**(6): p. 515-518.
38. Narewski, U., et al., *Application of laser ablation inductively coupled mass spectrometry (LA-ICP-MS) for the determination of major, minor, and trace elements in bark samples.* Fresenius Journal of Analytical Chemistry, 2000. **366**: p. 167-170.
39. Reinhardt, H., et al., *Application of LA-ICP-MS in polar ice core studies.* Analytical Bioanalytical Chemistry, 2003. **375**: p. 1265-1275.
40. Watmough, S.A., T.C. Hutchinson, and R. Douglas Evans, *Application of laser inductively coupled plasma-mass spectrometry in dendrochemical analysis.* Environ. Sci. Technol., 1997. **31**: p. 114-118.
41. Rauch, S., et al., *Elemental Association and fingerprinting of traffic-related metals in road sediments.* Environ. Sci. Technol., 2000. **34**: p. 3119-3123.
42. Kramers, J.D. and I.D. Tolstikhin, *Two terrestrial lead isotope paradoxes, forward transport, core formation, and the history of the continental crust.* Chemical Geology, 1997. **139**: p. 75-110.
43. Hamelin, B., F. Grousset, and E.R. Sholkovitz, *Pb isotopes in superficial pelagic sediments from the North Atlantic.* Geochim. Cosmochim. Act, 1990. **54**: p. 37-47.
44. Sun, S.S., *Lead isotopic study of young volcanic rocks from mid-ocean ridges, ocean islands and islands arcs.* Phil.Trans.R.Soc.Lond., 1980. **A 297**: p. 409-445.
45. Shotyk, W., *Geochemistry of the peat bog at Etang de la Gruère, Jura Mountains, Switzerland, and its record of atmospheric Pb and lithogenic trace metals (Sc, Ti, Y, Zr, and REE) since 12,370 14C BP.* Geochim. Cosmochim. Act, 2001. **65**(14): p. 2337-2360.
46. Farmer, J.G., L.J. Eades, and M.C. Graham, *The lead content and isotopic composition of British Coals and their implications for past and present releases of lead to the UK Environment.* Environmental Geochemistry and Health, 1999. **21**: p. 257-272.
47. Bacon, J.R., *Isotopic characterisation of lead deposited 1989-2001 at two upland Scottish locations.* Journal of Environmental Monitoring, 2002. **4**: p. 291-299.
48. Hurst, R., T.E. Davies, and B.D. Chinn, *The Lead fingerprints of gasoline Contamination - Lead analysis of the lead additives in gasoline can improve estimates of the ages of leaks and spills.* Environ. Sci. Technol., 1996. **30**(7): p. 304A-307A.
49. Parkinson, G.S. and W.M. Catchpole, *The use of Isotopic Ratio as a Means of Detecting Sources of Lead Emissions.* J Inst. Petroleum, 1973. **59**: p. 59-65.
50. Wedepohl, K.H. and A. Baumann, *Isotope composition of Medieval lead glasses reflecting early silver production in Central Europe.* Mineralium Deposita, 1997. **32**: p. 292-295.
51. Thirlwall, M.F., *Inter-laboratory and other errors in Ph isotope analyses investigated using a Pb-207-Pb-204 double spike.* Chemical Geology, 2000. **163**(1-4): p. 299-322.
52. Woolard, D., r. Franks, and D.R. Smith, *Inductively coupled plasma magnetic sector mass spectrometry method for stable lead isotope tracer studies.* Journal of Analytical Atomic Spectrometry, 1998. **13**: p. 1015-1019.
53. Prohaska, T., et al., *Lead isotope ratio analysis by inductively coupled plasma sector field mass spectrometry (ICP-SMS) in soil digests of a depth profile.* Journal of Analytical Atomic Spectrometry, 2000. **15**: p. 365-369.
54. Krachler, M., et al., *Optimising accuracy and precision of lead isotope measurement (206Pb,207Pb,208Pb) in acid digests of peat with ICP-SMS using individual mass discrimination correction.* Journal of Analytical Atomic Spectrometry, 2004. **19**(3): p. 354-361.
55. Halliday, A.N., et al., *Applications of multiple collector-ICPMS to cosmochemistry, geochemistry, and paleoceanography.* Geochim. Cosmochim. Act, 1998. **62**(6): p.

919-940.
56. Rehkaemper, M. and K. Mezger, *Investigation of matrix effects for Pb isotope ratio measurements by multiple collector ICP-MS: verification and application of optimized protocols.* Journal of Analytical Atomic Spectrometry, 2000. **15**: p. 1451-1460.
57. Weiss, D., et al., *Accurate and precise Pb isotope ratio measurements in environmental samples by MC-ICP-MS.* International Journal of Mass Spectrometry, 2004. **232**: p. 205-215.
58. Stern, R.A., et al., *Reconstructing lead isotope exposure histories preserved in the growth layers of Walrus teeth using the SHRIMP II ion microprobe.* Environ. Sci. Technol., 1999. **33**: p. 1771-1775.
59. Swarzenski, P.W., et al., *The behaviour of U- and Th-series nuclides in the estuarine environment*, in *Uranium-Series geochemistry*, B. Bourdon, et al., Editors. 2003, Geochemical Society & Mineralogical Society of America: Washington D.C. p. 577-606.
60. Dibb, J.E., *Beryllium-7 and lead-210 in the atmosphere and surface snow over the Greenland ice sheet in the summer of 1989.* Journal of Geophysical Research, 1990. **95**(D13): p. 22,407-22,415.
61. Winkler, R. and G. Rosner, *Seasonal and long-term variation of 210Pb concentration in air, atmospheric deposition velocity in south Germany.* Sci. Tot. Environ., 2000(263): p. 57-68.
62. Radakovitch, O., R.D. Cherry, and S. Heussner, *210Po and 210Pb: tracers of particle transfer on the Rhône continental margin (NW Mediterranean).* Deep-Sea Research Part I, 1999. **46**: p. 1539-1563.
63. Henderson, G.M. and E. Maier-Reimer, *Advection and removal of 210Pb and stable Pb isotopes in the oceans: a general circulation model study.* Geochim. Cosmochim. Act, 2002. **66**(2): p. 257-272.
64. Appleby, P.G. and F. Oldfield, *The calculation of lead-210 dates assuming a constant rate of supply of unsupported 210Pb to the sediments.* Catena, 1978. **5**: p. 1-8.
65. Appleby, P.G. and F. Oldfield, *Application of lead-210 to sedimentation studies*, in *Uranium-series disequilibrium; application to Earth, marine, and environmental sciences*, R.S. Harmon, Editor. 1992, Clarendon Pr.: Oxford. p. 731-778.
66. Wertime, T.A., *The Beginnings of Metallurgy: A New Look.* Science, 1973. **182**(4115): p. 875-887.
67. Nriagu, J.O., *Lead and Lead Poisoning in Antiquity*. Environ. Sci. Technol., ed. J.W. Sons. 1983: New-York. 434.
68. Walter, P. and P. Martinetto, *Making make-up in Ancient Egypt.* Nature, 1999. **397**: p. 483-484.
69. Meier, S., *Blei in der Antike: Bergbau, Verhüttung, Fernhandel*, in *Philosophische Fakultät*. 1995, Zürich: Zürich.
70. Nriagu, J.O., *Tales Told in Lead.* Science, 1998. **281**: p. 16221623.
71. Le Roux, G., et al., *Identifying the sources and timing of ancient and medieval atmospheric metal pollution in England by a peat profile.* Journal of Environmental Monitoring in press, 2004.
72. Brännvall, M.-L., et al., *The Medieval Metal Industry was the cradle of modern large-scale atmospheric lead pollution in northern Europe.* Environ. Sci. Technol., 1999. **33**(24): p. 4391-4395.
73. Krysko, W.W., *Lead in history and art*. 1979, Stuttgart: Dr Riederer Verlag. 244.
74. Le Roux, G., et al.,*Geochemical evidences of early anthropogenic activity in harbour sediments from Sidon, Archaeology and History of Lebanon*., 2003. **18**: p. 58-61.
75. Kempter, H. and B. Frenzel, *The impact of early mining and smelting on the local troposheric aerosol detected in ombrotrophic peat bogs in the Harz, Germany*. Water, Air and Soil Pollution, 2000. **121**: p. 93-108.
76. Hazardous Contaminants Branch, *Rationale for the development of soil, drinking water, and air quality criteria for Lead*. 1993, Ministry of Environment and Energy, Ontario. 114.
77. Nriagu, J.O., *A history of global metal pollution.* Science, 1996. **272**: p. 223-224.
78. ILZSG, *Lead, review of trends in 2003*. 2004, International Lead and Zinc Study Group (Web page).
79. von Storch, H., et al., *Four decades of gasoline lead emissions and control policies in Europe: a retrospective assessment.* Sci Total Environ, 2003. **311**(1-3): p. 151-76.
80. Thomas, V., *The elimination of lead in gasoline.* Annu Rev. Energy Environ., 1995. **20**: p. 301-324.
81. Thomas, V. and A. Kwong, *Ethanol as a lead replacement: phasing out leaded gasoline in Africa.* Energy Policy, 2000. **29**: p. 1133-1143.
82. Pacyna, J.M. and E.G. Pacyna, *An assessment of global and regional emissions of trace metals to the atmosphere from anthropogenic sources worldwide*. Environmental Review, 2001. **9**: p. 269-298.
83. Patterson, C.C. and D.M. Settle, *Magnitude of the lead flux to the atmosphere from volcanoes.* Geochim. Cosmochim. Act, 1987. **51**: p. 675-681.
84. Shotyk, W., M. Krachler, and B. Chen, *Atimony in recent peat from Switzerland and Scotland: comparison with natural background values (5,320 to 8,020 14C BP),*

correlation with Pb, and implications for the global Sb cycle. Global Biogeochemical Cycles, 2004. **18**(1): GB1016.
85. Nriagu, J.O., *Global metal pollution.* Environment, 1990. **32**(7): p. 7-33.
86. Schütz, L., *Atmospheric mineral dust-properties and source markers*, in *Paleoclimatology and Paleometeorology: Modern and Past Patterns of Global Atmospheric Transport*, M. Sarnthein, Editor. 1989, Kluwer Academic Publishers: Dordrecht.
87. Heinrich, H., B. Schulz-Dobrick, and K.H. Wedepohl, *terrestrial geochemistry of Cd, Bi, Tl, Pb, Zn and Rb.* Geochim. Cosmochim. Act, 1980. **44**: p. 1519-1533.
88. Rahn, K.A., *The chemical composition of the atmospheric aerosol. Technical report.* 1976, Kingston, R.I., USA: Graduate school of oceanography, University of Rhode Island. 265.
89. Radojevic, M. and R.M. Harrison, *Concentrations and pathways of organolead compounds in the environment: a review.* Environ. Sci. Technol., 1987. **59**: p. 157-180.
90. Harrison, R.M. and A.G. Allen, *Environmental sources and sinks of alkyllead compounds.* Applied Organometallic Chemistry, 1989. **2**: p. 49-58.
91. Van Cleuvenbergen, R.J.A. and F.C. Adams, *Organolead compounds*, in *Handbook of Environmental Geochemistry*, B.G. Wixson, Editor. 1990, Springer: Weinheim. p. 97-153.
92. Heisterkamp, M., et al., *Present century record of organolead pollution in high altitude alpine snow.* Environ. Sci. Technol., 2000. **21**: p. 260-266.
93. Wang, Y., A.B. Turnbull, and R.M. Harrison, *Concentrations, phase partitioning and deposition of specific alkyl-lead compounds in the atmosphere.* Applied Organometallic Chemistry, 1997. **11**: p. 889-901.
94. Harrison, R.M. and D.P.H. Laxen, *Sink processes of tetra-alkylead in the atmosphere.* Environ. Sci. Technol., 1978. **12**: p. 1384-1392.
95. Wang, Y. and A.G. Allen, *Determination of octanol-water partition coefficients, water solubility and vapour pressure of alkyl-lead compounds.* Applied Organometallic Chemistry, 1996. **10**: p. 773-778.
96. Shotyk, W., et al., *A new peat bog record of atmospheric lead pollution in Switzerland: Pb concentrations, enrichment factors, isotopic composition, and organolead species.* Environ Sci Technol, 2002. **36**(18): p. 3893-900.
97. Lobinski, R., et al., *Northern hemisphere organic lead emissions in fresh Greenland snow.* Environ. Sci. Technol., 1994. **28**: p. 1459-1466.
98. Lobinski, R., et al., *Present century snow record of organolead pollution in Greenland.* Environ. Sci. Technol., 1994. **28**: p. 1467-1471.
99. Lobinski, R., et al., *Organolead in wine.* Nature, 1994. **370**: p. 24.
100. Warren, H.V. and R.E. Delavault, *Observations on the Biogeochemistry of Lead in Canada.* Transactions of the Royal Society of Canada, 1960. **LIV**(III): p. 11-20.
101. Cannon, H.L. and L.C. Bowles, *Contamination of vegetation by tetraethyl lead.* Science, 1962. **137**: p. 765-766.
102. Chow, T.J., *Lead accumulation in roadside soil and grass.* Nature, 1970. **225**(229): p. 295-6.
103. Blaser, P., et al., *Critical examination of trace element enrichments and depletions in soils: As, Cr, Cu, Ni, Pb, and Zn in Swiss forest soils.* Sci Total Environ, 2000. **249**(1-3): p. 257-80.
104. Bindler, R., et al., *Natural lead concentrations in pristine boreal forest soils and past pollution trends: A reference for critical load models.* Environ. Sci. Technol., 1999. **33**(19): p. 3362-3367.
105. Dörr, H., et al., *Gasoline Lead in West German Soils.* Naturwissenschaften, 1990. **77**: p. 428-430.
106. Shotyk, W., et al., *A new approach for quantifying cumulative, anthropogenic, atmospheric lead deposition using peat cores from bogs: Pb in eight Swiss peat bog profiles.* Sci Total Environ, 2000. **249**(1-3): p. 281-95.
107. Renberg, I., et al., *Atmospheric Lead Pollution History during Four Millennia (2000BC to 2000AD) in Sweden.* Ambio, 2000. **29**(3): p. 150-156.
108. Givelet, N., et al., *A 6,000-years record of atmospheric mercury accumulation in the high Arctic from peat deposits on Bathurst Island, Nunavut, Canada.* Journal De Physique IV, 2003. **107**: p. 545-548.
109. Miller, E.K. and A.J. Friedland, *Lead migration in forest soils; response to changing atmospheric inputs.* Environ. Sci. Technol., 1994. **28**(4): p. 662-669.
110. Wang, E.X, Bormann F.H., Gaboury B. *Evidence of complete retention of atmospheric lead in the soils of northern hardwood forested ecosystems*, Environ. Sci. Technol., 1995, **29**: p. 735-739
111. Steinmann, M. and P. Stille, *Rare earth element behaviour and Pb, Sr, Nd isotope systematics in a heavy metal contaminated soil.* Applied Geochemistry, 1997. **12**: p. 607-623.
112. Whitehead, K., et al., *Determination of the extent of anthropogenic Pb migration through fractured sandstone using Pb isotope tracing.* Applied Geochemistry, 1997. **12**: p. 75-81.
113. Bacon, J.R., M.L. Berrow, and C.A. Shand, *Isotopic composition as an indicator of origin*

of lead accumulations in surface soils. Intern. J. Environ. Anal. Chem., 1992. **46**: p. 71-76.
114. Jersak, J., R. Amundson, and G. Brimhall, *Trace Metal Geochemistry in Spodosols of the Northeastern United States.* J Environ Qual, 1997. **26**: p. 511-521.
115. Lin, Z., et al., *The source and fate of Pb in contaminated soils in the urban area of Falun in central Sweden.* Sci. Tot. Environ., 1998. **209**: p. 47-58.
116. Emmanuel, S. and Y. Erel, *Implications from concentrations and isotopic data for Pb partitioning processes in soil.* Geochim. Cosmochim. Act, 2002. **66**(14): p. 2517-2527.
117. Jenny, H., *Factors of soil formation*. 1941, New York: McGraw-Hill.
118. Bear, F.E., *Chemistry of the soil, 2nd ed°*. 1964, New York: Reinhold. 515.
119. Sposito, G., *The chemistry of soils*. 1989, New York: Oxforf University Press. 277.
120. Hirao, Y. and C.C. Patterson, *Lead aerosol pollution in the High Sierra overrides natural mechanism which exclude lead from a food chain.* Science, 1974. **184**(140): p. 989-92.
121. Garrels, R.M. and F.T. MacKenzie, *Origin of the chemical compositions of some springs and lakes*, in *Equilibrium concepts in natural water systems*, R.F. Gould, Editor. 1967, Amer.Chem.Soc. p. 222-242.
122. Patterson, C.C. and D.M. Settle, *The reduction of orders of magnitude errors in lead analyses of biological materials and natural waters by evaluating and controlling the extent and sources of industrial lead contamination introduced during sample collecting, handling, and analysis.* National Bureau of Standards Special Publication, 1974. **422**: p. 321-351.
123. Graney, J.R., et al., *Isotopic record of lead pollution in lake sediments from northeastern United States.* Geochim Cosmochim Acta, 1995. **59**(9): p. 1715-1728.
124. Callender, E. and P.C. Van Metre, *Reservoir Sediment Cores Show U.S. Lead Declines.* Environ. Sci. Technol., 1997. **31**(9): p. 424a-428a.
125. Outridge, P.M., M.H. Hermansson, and W.L. Lockhart, *Regional variations in atmospheric deposition and sources of anthropogenic lead in lake sediments across the Canadian Arctic.* Geochim Cosmochim Acta, 2002. **66**(20): p. 3521-3531.
126. Camarero, L., et al., *Historical variations in lead fluxes in the Pyrenees (northeast Spain) from a dated lake sediment core.* Water Air and Soil Pollution, 1998. **105**(1-2): p. 439-449.
127. Moor, H.C., T. Schaller, and M. Sturm, *Recent Changes in Stable Lead Isotope Ratios in Sediments of Lake Zug, Switzerland.* Environ. Sci. Technol., 1996. **30**(10): p. 2928-2933.
128. VonGunten, H.R., M. Sturm, and R.N. Moser, *200-year record of metals in lake sediments and natural background concentrations.* Environ. Sci. Technol., 1997. **31**(8): p. 2193-2197.
129. Farmer, J.G., et al., *Stable Lead Isotope Record of Lead Pollution in Loch Lomond Sediments since 1630 A.D.* Environ. Sci. Technol., 1996. **30**(10): p. 3080-3083.
130. Eades, L.J., et al., *Stable lead isotopic characterisation of the historical record of environmental lead contamination in dated freshwater lake sediment cores from northern and central Scotland.* Sci. Tot. Environ., 2002. **292**(1-2): p. 55-67.
131. Erel, Y., et al., *Lead concentrations and isotopic ratios in the sediments of the Sea of Galilee.* Environ Sci Technol, 2001. **35**(2): p. 292-9.
132. Norton, S.A., et al., eds. *Sources , Deposition, and Canopy Interactions*. Acid Precipitation, ed. S.E. Lindberg, A.L. Page, and S.A. Norton. Vol. 3. 1990, Springer Verlag: Berlin.
133. Kober, B., et al., *Pb isotopes in sediments of Lake Constance, Central Europe constrain the heavy metal pathways and the pollution history of the catchment, the lake and the regional atmosphere.* Geochim. Cosmochim. Act, 1999. **63**(9): p. 1293-1303.
134. Rosman, K.J.R., C. Ly, and E. Steinnes, *Spatial and temporal variation in isotopic composition of atmospheric lead in Norvegian moss,* Environ. Sci. Technol., 1998. **32**: p. 2542-2546.
135. Kunert, M., et al., *Lead isotope systematics in Polytrichum formosum: Am Example from Filed Study with mosses.* Environ. Sci. Technol., 1999. **33**: p. 3502-3505.
136. Monna, F., et al., *Pb isotopes composition in lichens and aerosols from Eastern Sicily: Insights into the Regional impact of Volcanoes on the Environment.* Environ. Sci. Technol., 1999. **33**(15): p. 2517-2523.
137. Weiss, D., et al., *Sphagnum mosses as archives of recent and past atmospheric lead deposition in Switzerland.* Atmospheric Environment, 1999. **33**(23): p. 3751-3763.
138. Farmer, J.G., et al., *Historical Trends in the lead composition of archival Sphagnum Mosses from Scotland (1838-2000).* Environ. Sci. Technol., 2002. **36**: p. 152-157.
139. Bacon, J.R., et al., *Isotopic Character of Lead Deposited from Atmosphere at a Grassland Site in the UK Since 1860.* Environ. Sci. Technol., 1996. **30**(8): p. 2511-2518.
140. Hagenmeyer, J. and H. Schäfer, *Are there seasonal variations of trace element concentrations (Cd, Pb, Zn) in wood of Fagus trees in Germany.* Vegetatio, 1992. **101**: p. 55-63.

141. Aberg, G., et al., *The origin of atmospheric lead in Oslo, Norway, studied with the use of isotopic ratios.* Atmospheric Environment, 1999. **33**(20): p. 3335-3344.
142. Bellis, D.J., C.W. McLeod, and K. Satake, *Pb and 206Pb/207Pb isotopic analysis of a tree bark pocket near Sheffield, UK recording historical change in airborne pollution during the 20th century.* Sci Total Environ, 2002. **289**(1-3): p. 169-76.
143. Bellis, D.J., et al., *Evaluation of the historical records of lead pollution in the annual growth rings and bark pockets of a 250-vear-old Quercus Crispula in nikko, Japan.* Sci. Tot. Environ., 2002. **295**: p. 91-100.
144. Vile, M.A., et al., *Historical rates of atmospheric Pb deposition using 210Pb dated peat cores: corroboration, computation, and interpretation.* Water, Air and Soil Pollution, 1995. **79**: p. 89-106.
145. Vile, M.A., R.K. Wieder, and M. Novak, *Mobility of Pb in sphagnum-derived peat.* Biogeochemistry, 1999. **45**: p. 35-52.
146. Vile, M.A., R.K. Wieder, and M. Novak, *200 years of Pb deposition throughout the Czech Republic: patterns and sources.* Environ. Sci. Technol., 2000. **34**(1): p. 12-20.
147. Brännvall, M.L., et al., *Stable isotope and concentrations records of atmospheric lead pollution in peat and lake sediments in Sweden.* Water Air and Soil Pollution, 1997. **100**: p. 243-252.
148. Farmer, J.G., et al., *A comparison of the historical lead pollution records in peat and freshwater lake sediments from Central Scotland.* Water, Air and Soil Pollution, 1997(100): p. 253-270.
149. Kempter, H., M. Görres, and B. Frenzel, *Ti and Pb concentrations in rainwater-fed bogs in Europe as indicators of past anthropogenic activities.* Water, Air, and Soil Pollution, 1997. **100**: p. 367-377.
150. Martinez Cortizas, A., et al., *Atmospheric Pb deposition in Spain during the last 4600 years recorded by two ombrotrophic peat bogs and implications for the use of peat as archive.* Sci Total Environ, 2002. **292**(1-2): p. 33-44.
151. MacKenzie, A.B., J.G. Farmer, and C.L. Sugden, *Isotopic evidence of the relative retention and mobility of lead and radiocaesium in Scottish ombrotrophic peats.* Sci. Tot. Env., 1997. **203**(2): p. 115-127.
152. MacKenzie, A.B., et al., *A historical record of atmospheric depositional fluxes of contaminants in west-central Scotland derived from an ombrotrophic peat core.* Sci. Tot. Environ., 1998. **222**: p. 157-166.
153. Norton, S.A., G.C. Evans, and J.S. Kahl, *Comparison of Hg and Pb fluxes to hummocks and hollows of ombrotrophic Big Heath Bog and to Nearby Sargent Mt., Maine, USA.* Water Air and Soil Pollution, 1997. **100**: p. 271-286.
154. Weiss, D., et al., *Atmospheric Pb deposition since The industrial Revolution Recorded by Five Swiss Peat Profiles: Enrichment Factors, Fluxes, Isotopic Composition, And Sources.* Environ. Sci. Technol., 1999(33): p. 1340-1352.
155. Weiss, D., et al., *Comparative study of the temporal evolution of atmospheric lead deposition in Scotland and eastern Canada using blanket peat bogs.* Sci. Tot. Environ., 2002. **292**(1-2): p. 7-18.
156. Bell, K. and I.M. Kettles, *Lead-isotope ratio measurements on hummock an hollow peat from Detour Lake area, Ontario.* Geological Survey of Canada, 2003.
157. Nieminen, T.M., L. Ukonmaanaho, and W. Shotyk, *Enrichment of Cu, Ni, Zn, Pb and As in an ombrotrophic peat bog near a Cu-Ni smelter in southwest Finland.* Science of the Total Environment, 2002. **292**(1-2): p. 81-89.
158. Klaminder, J., I. Renberg, and R. Bindler, *Isotopic trend and background fluxes of atmospheric lead in northern Europe: analyses of three ombrotrophc bogs from south Sweden.* Global Biogeochemical Cycles, 2003. **17**(1).
159. Shotyk, W., et al., *History of atmospheric lead deposition since 12,370 14C yr BP from a peat bog, Jura mountains, Switzerland.* Science, 1998. **281**: p. 1635-1640.
160. Monna, F., et al., *Ph isotopic composition of airborne particulate material from France and the southern United Kingdom: Implications for Pb pollution sources in urban areas.* Environ. Sci. Technol., 1997. **31**(8): p. 2277-2286.
161. Shotyk, W., et al., *Anthropogenic contributions to atmospheric Hg, Pb and As accumulation recorded by peat cores from southern Greenland and Denmark dated using the 14C "bomb pulse curve".* Geochim. Cosmochim. Act, 2003. **67**(21): p. 3991-4011.
162. Boutron, C., et al., *Decrease in anthropogenic lead, cadmium and zinc in Greenland snows since the late 1960s.* Nature, 1991. **353**: p. 153-156.
163. Hong, S., et al., *Greenland Ice Evidence of Hemispheric Lead Pollution Two Millenia Ago by Greek and Roman Civilizations.* Science, 1994. **265**: p. 1841-1843.
164. Rosman, J. and W. Chisholm, *Determination of lead isotopes in Arctic and Antarctic Snow and ice.* Analysis Magazine, 1994. **22**(7): p. M51-M53.
165. Rosman, K.J.R., et al., *Lead from Carthaginian and Roman Spanish mines isotopically identified in Greenland ice dated from 600 BC to 300 AD.* Environ. Sci. Technol., 1997. **31**(12): p. 3413-3416.
166. Rosman, K.J.R., et al., *A two century record of lead isotopes in high altitude Alpine snow*

and ice. Earth and Planetary Science Letters, 2000. **176**(3-4): p. 413-424.
167. Vallelonga, P., et al., *The lead pollution history of Law Dome, Antarctica, from isotopic measurements on ice cores: 1500 AD to 1989 AD.* Earth and Planetary Science Letters, 2002. **204**(1-2): p. 291-306.
168. McConnell, J.R., G. Lamorey, W., and M.A. Hutterli, *A 250-year high-resolution record of Pb flux and crustal enrichment in central Greenland.* Geophysical Research Letters, 2002. **29**(23).
169. Bollhöfer, A. and K.J.R. Rosman, *The temporal stability in lead isotopic signatures at selected sites in the Southern and Northern Hemispheres.* Geochim. Cosmochim. Act, 2002. **66**(8): p. 1375-1386.
170. Bollhöfer, A. and K.J.R. Rosman, *Lead Isotopic Ratios in European Atmospheric Aerosols.* Physic and Chemistry of the Earth (A), 2001. **26**(10): p. 835-838.
171. Bollhöfer, A., W. Chisholm, and K.J.R. Rosman, *Sampling aerosols for lead isotopes on a global scale.* Analytica Chimica Acta, 1999. **390**(1-3): p. 227-235.
172. Bollhöfer, A. and K.J. Rosman, *Isotopic source signatures for atmospheric lead: The northern hemisphere.* Geochim Cosmochim Acta, 2001. **65**(11): p. 1727-1740.
173. Flament, P., et al., *European isotopic signatures for lead in atmospheric aerosols: a source apportionment based upon 206Pb/207Pb ratios.* Sci Total Environ, 2002. **296**(1-3): p. 35-57.
174. Bacon, J.R., *Isotopic characterisation of lead deposited 1989-2001 at two upland Scottish locations.* J Environ Monit, 2002. **4**(2): p. 291-9.
175. Hansmann, W. and V. Koppel, *Lead-isotopes as tracers of pollutants in soils.* Chemical Geology, 2000. **171**(1-2): p. 123-144.
176. Barbaste, M., et al., *Evaluation of the accuracy of the determination of lead isotope ratios in wine by ICP MS using quadrupole, multicollector magnetic sector and time-of-flight analysers.* Talenta, 2001. **54**: p. 307-317.
177. Lidsky, T.I. and J.S. Schneider, *Lead and public health: review of recent findings, re-evaluation of clinical risks.* Journal of Environmental Monitoring, 2004. **4**: p. 36N.
178. Godwin, H.A., *The biological chemistry of lead.* Current Opinion in Chemical Biology, 2001(5): p. 223-227.
179. Lanphear, B.P., *The paradox of lead poisoning prevention.* Science, 1998. **281**(5383): p. 1617-8.
180. Canfield, R.L., et al., *Intellectual impairment in children with blood lead concentrations below 10 micro-g per deciliter.* N Engl J Med, 2003. **348**(16): p. 1517-26.
181. Selevan, S.G., et al., *Blood lead concentration and delayed puberty in girls.* The New England Journal of Medicine, 2003. **348**: p. 1527-1536.
182. Flegal, A.R. and D.R. Smith, *Current needs for increased accuracy and precision in measurements of low levels of lead in blood.* Environ Res, 1992. **58**(2): p. 125-33.
183. Energy, *Scientific criteria document for multimedia environmental standards development- Lead*. 1994, Ontario: Queen´s printer for Ontario.
184. Lalor, G.C., et al., *Blood lead levels in Jamaican school children.* Sci. Tot. Environ., 2001. **269**: p. 171-181.
185. Nriagu, J., et al., *Atmospheric lead pollution in KwaZulu/Natal, South Africa.* Sci Total Environ, 1996. **191**(1-2): p. 69-76.
186. Patterson, C.C., *An alternative perspective - lead pollution in the human environment: origin, extent, and significance*, in *Lead in the human environment*, Committee on Lead in the Environment, Editor. 1980, National Academy of sciences: Washington D.C. p. 525.
187. Elias, R., et al., *Improved techniques for studies of mass balances and fractionations among families of metals within terrestrial ecosystems.* Geochim Cosmochim Acta, 1976. **40**: p. 523-587.
188. Shirahata, H., et al., *Chronological variations in concentrations in isotopic compositions of anthropogenic atmospheric lead in sediments of a remote subalpine pond.* Geochim Cosmochim Acta, 1980. **44**: p. 149-162.
189. Elias, R.W., Y. Hirao, and C.C. Patterson, *The circumvention of the natural biopurfication of calcium along nutrient pathways by atmospheric inputs of industrial lead.* Geochim Cosmochim Acta, 1982. **46**: p. 2561-2580.
190. Tatsumoto, M. and C.C. Patterson, *Concentrations of common lead in some atlantic and mediterranean waters and snow.* Nature, 1963. **199**: p. 350-352.
191. Chow, J.C. and C.C. Patterson, *Concentration profiles of Barium and lead in Atlantic waters off Bermuda.* Earth and Planetary Science Letters, 1966. **1**: p. 397-400.
192. Schaule, B.K. and C.C. Patterson, *Lead concentrations in the northeast Pacific: evidence for global anthropogenic perturbations.* Earth and Planetary Science Letters, 1981. **54**: p. 97-116.
193. Murozumi, M., J.C. Chow, and C.C. Patterson, *Chemical concentrations of pollutant lead aerosols, terrestrial dusts and sea salts in Greenland and Antarctic snow strata*. Geochim Cosmochim Acta, 1969. **33**: p. 1247-1297.
194. Thomas, V., et al., *Effects of Reducing Lead in*

Gasoline:An Analysis of the International Experience. Environ. Sci. Technol., 1999. **22**: p. 3942-3948.
195. Lanphear, B.P., et al., *The contribution of lead-contaminated house dust and residential soil to children's blood lead levels. A pooled analysis of 12 epidemiologic studies.* Environ Res, 1998. **79**(1): p. 51-68.
196. Mielke, H.W., *Lead in the inner cities.* American Scientist, 1999. **87**(1): p. 67-73.
197. Wong, M.H., *A review on lead contamination of Hong Kong´s Environment*, in *Lead, Mercury, Cadmium and Arsenic in the Environment*, K.M. Meema, Editor. 1987, SCOPE, John Wiley and Sons: New York.
198. Mielke, H.W., et al., *Multiple metal contamination from house paints: consequences of power sanding and paint scraping in New Orleans.* Environ Health Perspect, 2001. **109**(9): p. 973-8.
199. Graziano, J.H. and C. Blum, *Lead crystal : an important potential source of lead exposure.* Chemical Speciation Bioavailibility, 1991. **3**: p. 81-85.
200. Rosman, K.J., et al., *Lead concentrations and isotopic signatures in vintages of French wine between 1950 and 1991*. Environ Res, 1998. **78**(2): p. 161-7.

ABBREVIATIONS

Eh: standard potential
XRF: X-ray fluorescence spectrometry
AAS: atomic absorption spectrometry
ICP-AES: inductively-coupled plasma-atomic emission spectrometry
LOD: detection limit
LEAFS: laser-excited atomic fluorescence spectroscopy
ICP-SMS: inductively coupled plasma-sector field mass spectrometry
ID-MS: isotope dilution mass spectrometry
MC-ICP-MS: multi-collector inductively coupled plasma mass spectrometry
TIMS: thermal ionization mass spectrometry
PIXE: proton induced X-ray emission spectrometry
SIMS: secondary ionization mass spectrometry
LA-ICP-MS: laser ablation inductively coupled plasma mass spectrometry
RSD: relative standard deviation
Q-ICP-MS : inductively-coupled plasma-atomic emission spectrometry with quadrupole mass analyzer
SHRIMP: sensitive high resolution ion microprobe
EU: European Union
PVC: polyvinyl chloride
OECD: Organization for Economic Cooperation and Development
MSW : municipal solid waste
EPA : Environmental Protection Agency
EGR : Etang de la Gruère, Switzerland
CAAPb: cumulative mass of atmospheric anthropogenic lead
BC/AD: Before Christ/ Annum Domini (After Christ): in the text and the figures means always calendar years.
EF: enrichment factor
BLL: blood lead level
ALAD: δ-aminolevulinic acid dehydratase
OMEE: Ontario Ministry of Energy and Environment
MAC: maximum allowable concentration
WHO:World Health Organization

- Chapter 2.2 -

Recent atmospheric Pb deposition at a rural site in Southern Germany assessed using a peat core and snowpack, and comparison with other archives

Gaël Le Roux[1*], Dominique Aubert[1,#], Peter Stille[2], Michael Krachler[1], Bernd Kober[1], Andriy Cheburkin[1], Georges Bonani[3], William Shotyk[1]
[1] Institute of Environmental Geochemistry, University of Heidelberg,
[2] Centre de Géochimie de la Surface, University of Strasbourg, France
[3] Institute of Particle Physics, ETH Zürich, Switzerland
[#] Present adress : LMTG, University of Toulouse, France

Submitted to Atmospheric Environment, in Review

Abstract:

In an ombrotrophic peat bog from Black Forest, Southern Germany, the rate of atmospheric Pb accumulation was quantified using peat core dated by ^{210}Pb. The most recent Pb accumulation rate (2.5 mg m^{-2} y^{-1}) is similar to that obtained from a snowpack on the bog surface, which was sampled during the winter 2002 (1 to 4 mg m^{-2} y^{-1}). These values are 50 to 200 times greater than the "natural" average background rate of atmospheric Pb accumulation (20 µg m^{-2} y^{-1}) obtained using peat samples from the same bog dating from 3300 to 1300 years cal. B.C. The isotopic composition of Pb was measured in both the modern and ancient peat samples as well as in the snow samples, and clearly shows that recent inputs are dominated by anthropogenic Pb. The chronology and isotopic composition of atmospheric Pb accumulation recorded by the peat from the Black Forest is similar to from ombrotrophic bogs can yield accurate records the chronologies reported earlier using peat cores from various peat bogs and point to a common Pb source to the region for the past 200 years. Taken together, the results show that peat cores of atmospheric Pb deposition, provided that the cores are carefully collected, handled, prepared, and analysed using appropriate methods.

Keywords: Pb flux; Peat bogs; Lead isotopes; Pollution; Snow cover

Introduction

Lead (Pb) is one of the most extensively investigated heavy metals. Indeed Pb, which is very toxic and non-essential, has been widely dispersed in the environment since the beginning of metallurgy (Nriagu, 1996). There are numerous studies about Pb contamination in various Earth's surface reservoirs. One major dispersion pathway for Pb is atmospheric transport because Pb is dispersed by the aerosols emitted from industrial activities, combustion of coal and leaded gasoline (Nriagu, 1979; Shotyk and Le Roux, in press). There were different periods of enhanced use of Pb but scientists and also researchers in the humanities have paid more attention to two of them: the use of Pb during the Roman Period (Edmondson, 1989; Gilfillan, 1965; Nriagu, 1983; Rosman et al., 1997) and the recent use of leaded gasoline (Hamilton et al., 1925; Nriagu, 1998; Patterson, 1965).

One powerful aspect of Pb studies is that Pb sources can be traced using their isotopic compositions. Lead has four stable isotopes (^{204}Pb, ^{206}Pb, ^{207}Pb, ^{208}Pb), the last three being respectively end-products of the decay chains of ^{238}U, ^{235}U and ^{232}Th (Dickin, 1995). The isotopic composition of lead ores depends on the age and geological history of the deposit and the initial concentrations of U-Th-Pb in the host rocks.

Trying to determine and quantify the changing rates and sources of atmospheric deposition of Pb is one of the major goals of environmental Pb research. Various techniques can be used to monitor Pb contamination: for example direct measurements of aerosols and wet/dry deposition or bio-monitoring. Past atmospheric Pb deposition (i.e. "pre-anthropogenic" and pre-industrial) can be assessed using environmental archives such as ice, firn and snow cores (Hong et al., 1994; Krachler et al., 2004b; McConnell et al., 2002; Schwikowski et al., 2004), lake sediments (Brännvall et al., 1999; Eades et al., 2002; Kober et al., 1999) and peat bogs (Klaminder et al., 2003; Murozumi et al., 1996; Shotyk et al., 1998) as well as herbarium samples of bryophytes and other plants (Bacon, 2002; Bacon et al., 1996; Farmer et al., 2002; Weiss et al., 1999b). Ombrotrophic peat bogs are useful archives of past Pb deposition because (1) they are widely distributed, (2) they receive only atmospheric inputs (i.e. they are rain-fed) and (3) they can be precisely dated using ^{14}C (bomb-pulse and "traditional") or ^{210}Pb methods.

However, despite numerous studies and reasonable agreement between modelled deposition rates (Goodsite et al., 2001; Von Storch et al., 2002), the comparison between atmospheric Pb deposition rates and the Pb accumulation rates by peat bogs has been called into question. For example, a recent study by Bindler et al. (2004) of peat bogs in Sweden suggested that individual cores collected in peat hummocks yield different cumulative Pb inventories during the last 110 years. Possible explanations include the difference in snow cover due to the shape and the micro-topography of the bog surface and differences in canopy interception. Novak et al. (2003a) in a study of sulfur deposition in peat bogs dated by ^{210}Pb also point out that "a single depth profile per peat bog may seriously under-represent the typical history of peat accretion" and therefore the record of atmospheric deposition. In contrast, Givelet et al. (2004) suggested that the principal limitation using peat cores as archives is not caused by the heterogeneity of the bogs themselves but rather the inadequate care in collecting, handling and preparing the peat core.

In this study, we compared the accumulation rate of Pb in a peat profile with that of the snow cover directly overlying the bog in the Black Forest, Southern Germany using state of the art techniques. The main aim of this study is to compare the accumulation rate and isotopic composition of atmospheric Pb in the snowpack, a single season record, with that of the peat core, a longer term record. Additionally, we compare the single peat record from the Black Forest with previously published data for three peat cores from Étang de la Gruère, a peat bog 100 km away in

Northern Switzerland. To compare the accumulation rate quantitatively, Pb fluxes were calculated using the Pb concentrations and peat accumulation rates derived using ^{210}Pb.

Finally we examine the recent anthropogenic impact on the atmospheric Pb deposition record in this rural site and compare it with the natural rate of Pb deposition during the past 8,000 years at the same site.

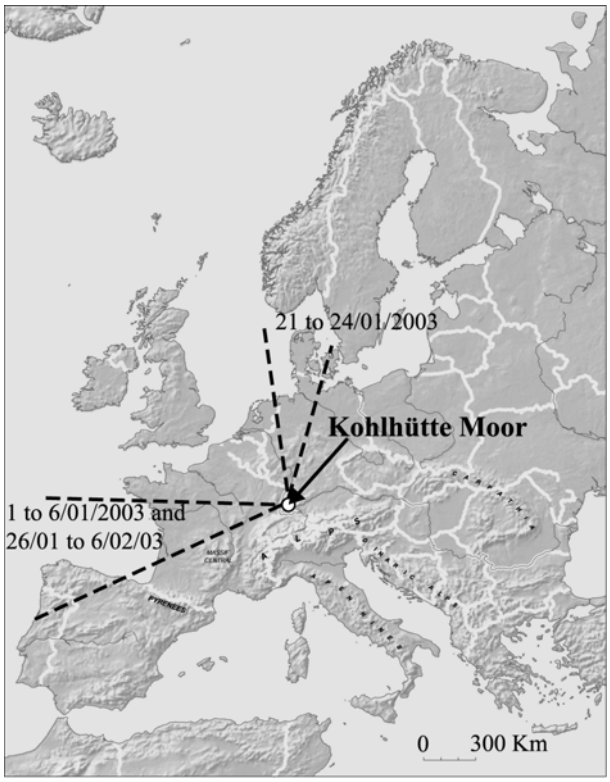

Figure 1: Location of Kohlhütte Moor and air mass sectors for the three main periods of snow deposition in 2003 based on HISPLYT back trajectory calculations

Experimental

Material

The "Kohlhütte Moor" is one of many *Sphagnum*-dominated peat bogs located in the Southern Black Forest, S.W. Germany **(Figure 1)**. It is a visibly domed bog, which has accumulated more than 5m peat during the last 8000 years. This accumulation occurred on a basement consisting of glacial clays. This peat bog is ombrotrophic as demonstrated (1) by the low pH values of the porewaters (~ 4 for the first meter, ~ 4.5 for the following meters), (2) the major element chemistry of bulk peat and (3) the chemical composition of the porewaters relative to rainwater. For example from the Sr concentration profile **(Figure 2)**, two distinct depositional environments can be distinguished: the deeper part (330 cm to 600 cm) with high concentrations reflecting inputs of Sr from mineral weathering, aquatic and atmospheric deposition and the upper part (-330 cm, surface) with low Sr concentrations supplied only by atmospheric inputs.

A complete peat profile was sampled following the procedure described by Givelet et al. (2004). The top meter was collected at the transition between an hummock and an hollow with a Ti Wardnaar Corer and the following five meters with a stainless steel Belarussian Corer. A detailed description of the site and the field work are given in the Field Report (Le Roux et al., 2002). The cores were cut precisely every cm (Givelet et al., 2004). The edges of each slice were trimmed away to avoid possible contamination. Sub-samples were dried at 105°C and pulverized in a Ti mill (Retsch GmbH and Co., Haan, Germany). Density and pore water content were calculated as described elsewhere (Givelet et al., 2004).

The peat bog is typically covered each winter by one to two meters of snow. On the 19th of February 2003, we sampled a 70 cm snow pack at a distance of ca. four meters from the peat-coring site. A detailed description of the site and the field work are given in a second Field Report (Le Roux and Aubert, 2003). The snow was collected in increments of 10 cm, including the mixed layer between moss and snow. The surface snow of a larger area was also sampled. In addition, a snow sample was also collected near the road outside the pine forest surrounding the bog. The sampling of snow was done using strict clean lab procedures to avoid possible contamination (Boutron, 1990; Nriagu et al., 1993). The hole was hand-dug while wearing polyethylene gloves and snow samples were collected in acid-washed bags, which were first rinsed twice with snow from the same layer. Snow samples were transported frozen until they could be processed at the Centre de Géochimie de la Surface (CNRS, Strasbourg).

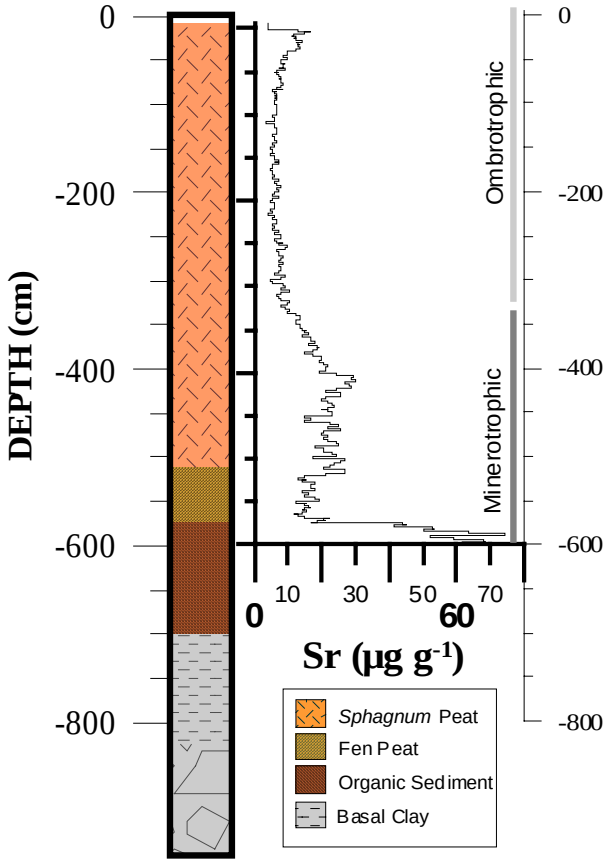

Figure 2: Peat stratigraphy, Sr concentration profile and the identification of ombrotrophic and minerotrophic zones

After melting at room temperature in clean room conditions (class 100) the samples were filtered with HAWP filters (0.45 µm) previously rinsed with high purity water (Millipore, Milford®, MA, USA) (Simonetti et al., 2000). Aliquots were acidified with HNO_3 (1 ml of suprapur HNO_3 for 250 ml of liquid) to avoid possible precipitation and adsorption of metals to the container walls. Snow particles collected on the filters were also removed using an ultrasonic bath to estimate dry (particulate) deposition.

Age dating

Peat profile

Radionuclides (^{210}Pb, ^{241}Am, ^{214}Pb, ^{137}Cs) were measured using low background gamma spectrometry (GCW4028, HPGE, Canberra) in Heidelberg. The maximum depth at which unsupported ^{210}Pb could be detected is 18 cm. The age-depth relationship was calculated using the CRS model (Appleby and Oldfield, 1978) **(Figure 3 b).** This model is in good agreement with the peak of ^{241}Am corresponding to the period of atmospheric nuclear weapons tests from 1945-1980, peaking at 1963. Uncertainties in the ^{210}Pb CRS Model and in the peat accumulation rate were calculated following Appleby (Appleby, 2001).

For deeper samples, twenty-three ^{14}C AMS dates were performed at the ETH Zürich allowing the calculation of a robust age-depth model **(Figure 3 a).** Age-depth models based on ^{14}C and ^{210}Pb are in good agreement when they overlap **(Figure 3 b).** Here, we used the ^{210}Pb age-depth model to study recent Pb pollution and use the deeper samples dated using ^{14}C to assess natural Pb accumulation rates.

Snow Samples

The snowpack was divided into seven samples of 10 cm each. Unfortunately, the snow did not accumulate continuously and phases of compression and even melting occurred during that winter especially for the bottom samples (Le Roux and Aubert, 2003). Therefore it is difficult to attribute precisely individual samples to specific snow events. However three phases of snow deposition could be distinguished from the snow accumulation inventory at the Feldberg weather station 15 km away: 1-6/01/2003; 26/01-6/02/2003 and 21-24/02/2003.

Back Trajectories

Three-days back trajectories were calculated using the HYSPLIT model (Draxler and Rolph, 2003) for the three phases of snow deposition **(Figure 1)**. They are in good agreement with wind directions measured at the Feldberg weather station (15 km North of the site). Two dominant directions could be distinguished: for the first and last episodes of snow deposition, a Western influence (i.e. France and the Atlantic) and for the intermediate snow episode a Northern influence (North-West Germany, Holland, the North Sea).

Analytical Measurements

XRF

Strontium, Ti and Pb were measured directly on peat powders using home-made X-ray fluorescence analysers in Heidelberg (Cheburkin and Shotyk, 1996; Shotyk et al., 2002a). Detection limits were 0.8 µg g^{-1}; 1.5 µg g^{-1}; 0.6 µg g^{-1} respectively for Sr, Ti, Pb.

The XRF method did not provide sufficiently low detection limits for Pb in the deeper and older samples. Precision of the XRF analysers is discussed elsewhere (Cheburkin and Shotyk, 1996; Givelet et al., 2003), but for Pb was approximately 30% at 1 µg g^{-1}, 10% at 10 µg g^{-1} and 6% at 60 µg g^{-1}.

ICP-OES

Strontium, Ca, Na, Mg, K were measured in snow samples in Heidelberg by inductively coupled plasma optical emission spectrometry (ICP-OES, Vista MPX, Varian, Darmstadt, Germany). The validity of the measurements was verified by repeated measurements of certified river water standard reference materials SRM 1640 (NIST, USA) and SLRS 2 (NRC, Canada) as well as internal standards. The procedural blanks were under the limit of detection of the instrument. Sodium was also measured by electro-thermal absorption atomic spectrometry (ET-AAS, Hitachi Z-8200, Ibaraki, Japan) in Strasbourg yielding good agreement between both techniques.

ICP-SF-MS and ICP-QMS measurements of snow samples

Concentrations of Pb, Ba in snow were determined by inductively coupled plasma-sector-field-mass spectrometry (ICP-SF-MS, Element 2, Thermo Electron, Bremen, Germany) in Heidelberg and by ICP-QMS (ICP-QMS, PQ 2+, VG) in Strasbourg. Measurements between the two instruments were in good agreement (for Pb, r^2=0.997, n=10 ; for Ba, r^2=0.94, n=10). Procedural

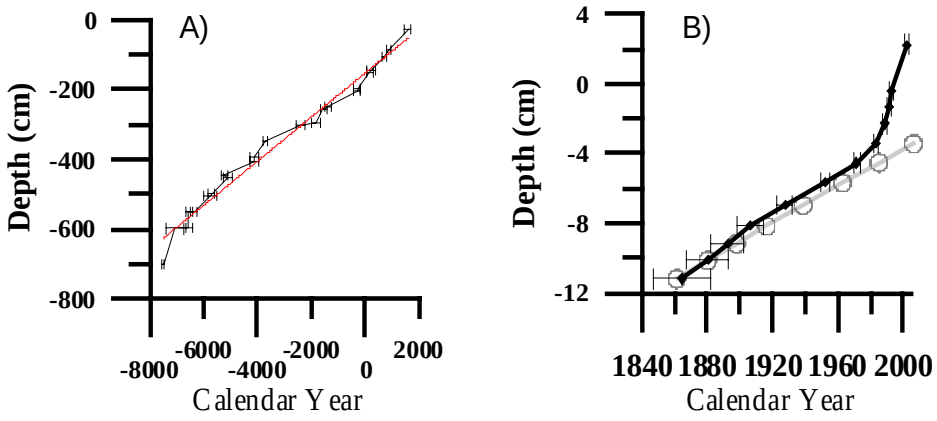

Figure 3:Age depth models
A) ^{14}C age depth model; B) ^{210}Pb CRS model and comparison with the upper end of the model based on ^{14}C dates (grey circles)

blanks always accounted for less than 10% of the concentrations of both elements and these values only for the smallest measured concentrations. *Analytical* blanks were negligible and suggest that our washing procedures for the filters were the causes of contamination.

In addition, Sr also measured in Heidelberg using ICP-SMS was in good agreement (r^2=0.992, n=10) with measurements by ICP-OES in Heidelberg.

ICPQ--MS for peat digests

Two hundred mg of each sample was first digested in an HNO_3-HBF_4 mixture in a microwave autoclave (ultraCLAVE II, MLS, Leutkirch, Germany) at elevated pressure (Krachler et al., 2002). Digested samples were brought to Strasbourg and measured using ICP-OES and ICP-QMS for major and trace elements. Only Pb concentrations are discussed here and the reader could refer to Le Roux (2005) for details on other elements. Lead concentrations measured by Q-IPC-MS were in excellent agreement with measurements using XRF (r^2=0.991, n=25). Lead concentrations measured by Q-ICP-MS are useful for some deeper pre-anthropogenic samples, which have Pb concentrations under the lower limit of detection of the XRF. Pb concentrations in Plant Reference Standards (Peach Leaves NIST 1547, Rye Grass BCR-CRM 281, Bush Branches and Leaves GBW

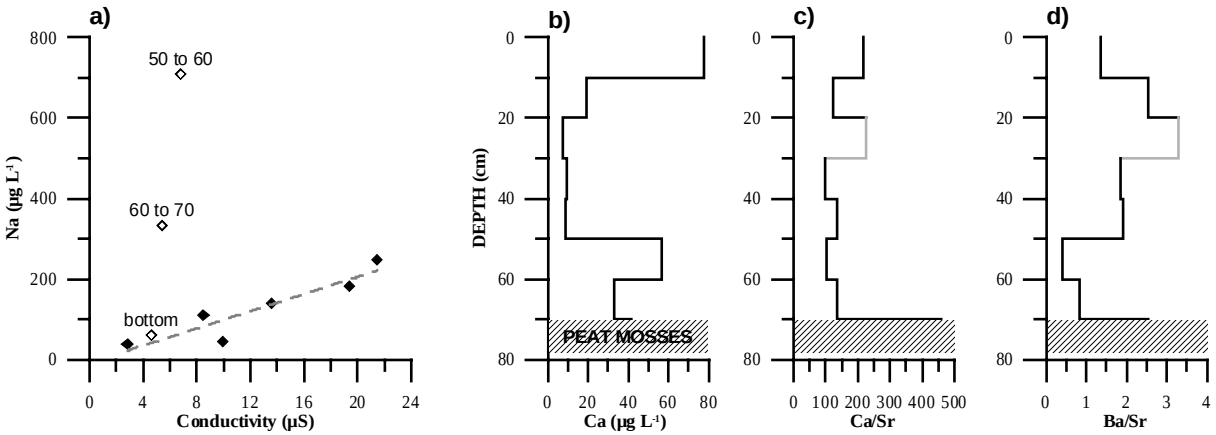

Figure 4: Chemistry of the snow pack
a) Na (µg L^{-1}) vs. conductivity (µS)
b) Ca (µg L^{-1})
c) Ca/Sr d) Ba/Sr

07602, Lichen IAEA 336) were also in agreement with certified values (less than 10 % difference).
In addition, the elemental concentrations in the particles, obtained from the two snow samples (surface and road), were also measured by Q-ICP-MS after HNO_3 digestion.

Pb isotopes in snow and peat samples by ICP-SF-MS
$^{206}Pb/^{207}Pb$ and $^{208}Pb/^{206}Pb$ ratios in peat and snow were also measured using ICP-SF-MS as described elsewhere (Krachler et al., 2004a).

Results

Wet Deposition

Major elements
As represented by Na, the concentrations of elements generally follow the electrical conductivity **(Figure 4 a)**, in other words, the ionic strength. However some elements such as Na and Sr show high concentrations at the base of the snowpack (50-60 cm, 60-70 cm) where icy layers are located **(Figure 4 a).** Thus, there is clearly a compositional difference between the bottom 20 cm of compacted snow and the rest of the snow snowpack, which consisted of fresh uncompacted snow.
The Ca concentration profile **(Fig. 4 b)** shows elevated concentration at both the bottom and the top of the snow pack. The elevated concentration at the top reflects the hiatus in snow fall for the two weeks prior to collection. During this period, the snow continued to receive atmospheric particles in absence of fresh snow. These particles could have also dissolved during snow melt in the laboratory and partially explain the higher concentrations in the surface snow sample. The elevated Ca concentration at the bottom of the snow pack probably reflects "contamination" of the snow by living plants. The Ca/Sr ratio of the snow pack is elevated at the base indicating that Ca is more affected than Sr, but it corresponds with the Ca/Sr ratio of the surface water at the surface of the bog (ca. 400:1). Leaching of elements from particles due to rising acidity can also be invoked to explain increasing acidity in some snow layers (Barbaris and Betterton, 1996) (not shown).
Lead concentration and isotopic composition
Lead concentrations **(Figure 5 a)** generally follow the concentrations of other elements. Whereas the top layer reveals elevated concentrations of both Ca and Pb, in contrast to Ca, there is no influence of the surface peat layer on the Pb concentration at the bottom **(Figure 5 a).** Whereas the snowpack appears to have liberated some Ca from the plant surface, this is neither true for Sr **(Figure 4)** or Pb **(Figure 5)**.
The Pb enrichment factor was calculated using Ba **(Figure 5 c)**:
$Pb\ EF_{Ba} = (Pb/Ba)_{sample} / (Pb/Ba)_{cc}$,

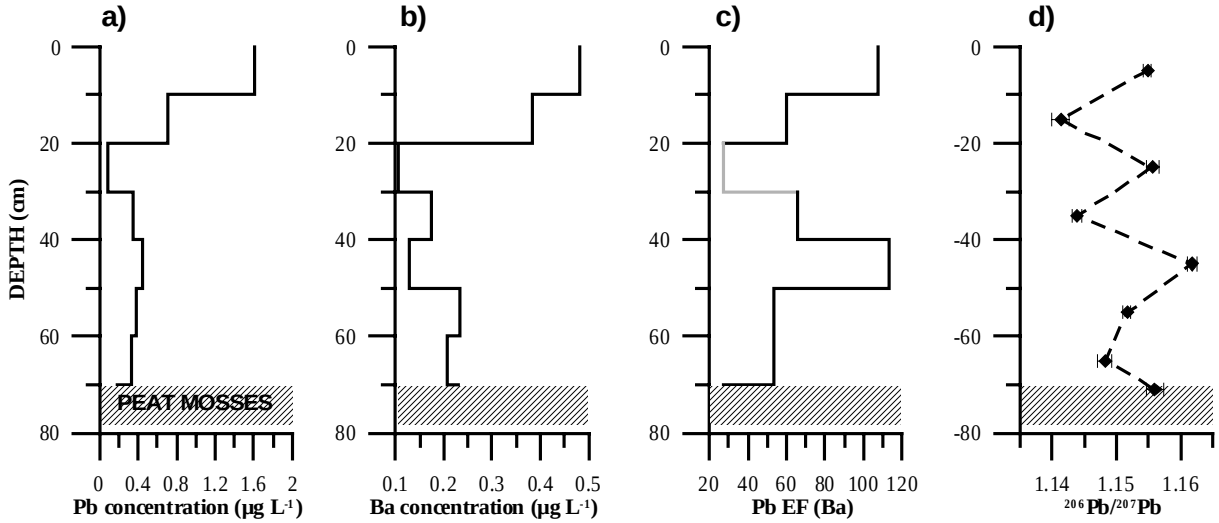

Figure 5: Pb and Ba chemistry in the snow: Pb and Ba concentrations, Pb Enrichment Factor in the snow and $^{206}Pb/^{207}Pb$

where $(Pb/Ba)_{cc}$ is the ratio (17/550 = 0.03) of these two elements in the Upper Continental Crust (McLennan, 2001). Uncontaminated sediments under the peat have a Pb EF_{Ba} (substrate) of 1.14 ± 0.15 (n = 7). Therefore, calculation of the EF using the Pb/Ba ratio of crustal rocks and local sediments will provide similar results.

Barium has been used as a reference element in many studies of Pb contamination in snow and ice (Planchon et al., 2003; Vallelonga et al., 2002a; Vallelonga et al., 2002b; Veysseyre et al., 2001) as a proxy of soil dust deposition for the reasons given by Patterson and Settle (1987). The calculated values are in the same order of the enrichment factors found in fresh snow samples collected in the Alps in 1998-99 (Veysseyre et al., 2001) **(Figure 5 c).**

The Pb isotopic composition is neither correlated with the Pb concentration nor other elements. The $^{206}Pb/^{207}Pb$ ratio varies between 1.14 and 1.16 (**Figure 5 d**).

Particulate Deposition

Particulate deposition was estimated using the solid particles collected on the filters. Scanning Electron Microscope analyse showed that the majority part of these particles are quartz and aluminosilicates. Biogenic particles (pollen and vegetation) are also present. Anthropogenic compounds such as framboidal particles were also found but in small quantities, even in the sample collected near the road.

Using the filtered water volume, the contribution of Pb contained in the particles to the volume of snow originally collected can be calculated. Particles account for approximately 2% of Pb deposited at the bog surface compared to up 33% in the snow sample collected near the road **[Table 1]**. Particulate deposition was estimated only for the surface snow and the road samples. Because the snow samples were collected on the 19th of February 2003 and the last snowfall was the 6th February 2003, these surface samples were exposed to the air for 13 days, which may explain why they yielded a higher particle load.

In addition to particles emitted by vehicles near the road, differences in particulate deposition between the bog and the roadside might also be explained by particle capture by the tall pine trees growing around the perimeter of the bog (i.e. canopy interception).

Pb in the peat profile

Pb concentrations in the peat profile are comparable to other peat profiles investigated in Europe (Farmer et al., 1997; Klaminder et al., 2003; Le Roux et al., 2004; Martinez-Cortizas et al., 2002; Novak et al., 2003b; Shotyk et al., 1998) with a large increase in the topmost samples (**Figure 6**).

SNOW SAMPLE	ELEMENT	Particulate DEPOSITION (µg/g)	Particulate DEPOSITION (ng/L)	WET DEPOSITION (ng/L)	Part./TOT(%)	Part.; EF(Ba)	Part.; EF(Ti)	WET, EF(Ba)
ROAD	Ti	2550	5440	n.d.	-	**1,0**	1,0	-
	Ba	340	720	870	45	1,0	**1,0**	1
	Pb	300	640	1260	34	**28,8**	**28,4**	**47**
SURFACE	Ti	446	700			**0,8**	1,0	
	Ba	74	116	480	19	1,0	**1,2**	1
	Pb	27	42	1600	3	**11,7**	**14,5**	**108**

Table 1: Comparison between particulate and wet deposition in snow

The two peaks resulting from intensive local mining during the Roman Period and the Middle Ages (**Figure 6**) correspond to well-known periods of Pb dispersion (Le Roux et al., 2004; Nriagu, 1996; Renberg et al., 2001). Background Pb concentrations are low in the ombrotrophic part (0.40 ± 0.07 µg g^{-1}, n = 20 corresponding to the period 3300 B.C- 1300 B.C), and lower than in Étang de la Gruère, a Swiss peat bog, for the same period of time (0.66 ± 0.19 µg g^{-1}, n = 8). These smaller concentrations are mainly due to the faster peat growth rates in the German bog (6 m of peat accumulation in 9000 years) compared to the Swiss bog (6 m of peat accumulation in 12000 years).

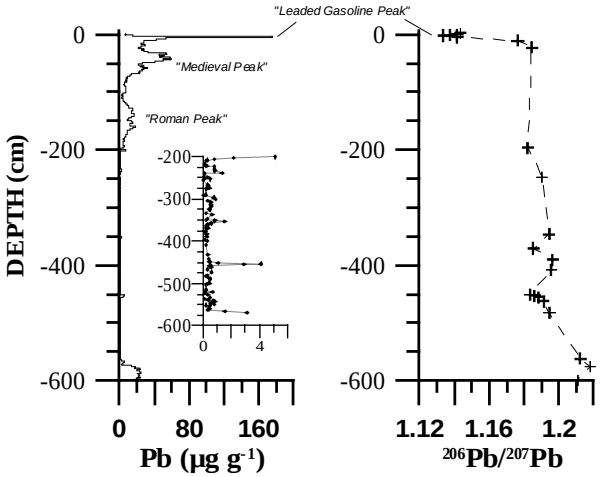

Figure 6: Pb and 206Pb/207Pb profiles in the Kohlhütte Moor peat core (for the 206Pb/207Pb ratio, the symbols are larger than the error (2s)).

The Pb isotope ratios also follow trends similar to other bogs in Central Europe (Novak et al., 2003b; Shotyk, 2001; Weiss et al., 1999a) with less radiogenic values at the surface. The background Pb isotopic signature is for the $^{206}Pb/^{207}Pb$ ratio ~1.18-1.19; n = 10, 5500 B.C. – 1300 B.C.). The bottom three samples, which are sediments (>50 % ash) show a different isotopic ratio ($^{206}Pb/^{207}Pb$ = 1.21). The large difference in Pb isotope ratio for the peats and the sediments, therefore, indicate that all of the Sphagnum peat samples above 500 cm have received Pb exclusively from the air.

Discussion

Background Accumulation rate of Pb in the Black Forest and comparison to other sites in Europe

Based on the age-depth model and the density measurements, the accumulation rate (AR) of pre-anthropogenic Pb averages 20 ± 1 µg m^{-2} y^{-1} in the ombrotrophic part of the pre-anthropogenic peat (until 3300 B.C). In the minerotrophic peat, the Pb accumulation rate is similar. These Pb AR are similar to other observations obtained using peat cores in Central and Northern Europe **[Table 2]**. The Pb AR for the Black Forest, which is more variable than in Sweden and Switzerland could be explained by the greater temporal resolution. Indeed in this study, each sample represents 20 years of peat accumulation whereas, for example, in the study in Switzerland, one sample represents ~ 150 years.

Recent Accumulation rate of Pb in the Black Forest and comparison with Swiss peat cores

Cumulative inventory of ^{210}Pb and Pb for the period 1850-2000

Cumulative Pb and ^{210}Pb were calculated for the period ~1850-2000 **[Table 3]**. This period corresponds mainly to the industrial period and can be dated using ^{210}Pb. We use this approach to compare the Black Forest peat bog with data from three previously studied peat cores collected in Étang de la Gruère

Study	Country	pre-anthropogenic AR µg/m2/y	Period	Note
this study	Southern Germany	20 ± 1 (range : 1-40, n = 20)	3300-1300 cal. BC	geochemically ombrotrophic
this study	Southern Germany	30 ± 14 (1-90, n = 51)	5800-1300 cal. BC	botanically ombrotrophic*
Shotyk et al. (1998)	Northern Switzerland	14 ± 3 (9-18, n = 6)	3500-1400 cal. BC	geochemically ombrotrophic
Shotyk et al. (1998)	Northern Switzerland	10 ± 2 (5-14, n = 18)	7000-4100 cal. BC	botanically ombrotrophic
Klaminder et al.(2003)	Southern Sweden	1-10	4000-1500 cal. BC	botanically ombrotrophic

Table 2: pre-anthropogenic AR of Pb in the present study compared to previous studies, "botanically ombrotrophic": Sphagnum peat; "geochemically ombrotrophic": strict non-influence of substrate on the samples as demonstrate by mobile elements like Ca or Sr

(Switzerland) in 1991 and 1993: EGR 2F and 2K (Appleby et al., 1997; Shotyk, 2001; Weiss et al., 1999a) and EGR 2G (Shotyk et al., 2002b). In contrast to EGR 2F and 2K (cut three cm slices by hand), EGR G was frozen and precisely cut into 1 cm slices (Givelet et al., 2004). It is also the first time that a complete and comparative interpretation on atmospheric Pb and ^{210}Pb deposition is presented for these three cores together.

CORE and year of collection	Pb cumulative inventory until no unsupported ^{210}Pb (g m^{-2})	^{210}Pb cumulative inventory (Bq m^{-2})
Black Forest (cut every cm) (2002)	1.2	7800
EGR 2G (cut every cm) (1993)	1.28	3300
EGR 2K (cut every 3 cm) (1993)	1.34	3100
EGR 2F (cut every 3 cm) (1991) (Appleby et al., 1997)	1.3	4400

Table 3: Cumulative inventories of Pb and 210Pb in the Black Forest peat core and the Étang de la Gruère cores

The cumulative Pb inventories recorded by the four cores are similar (1,2-1,3 g m^{-2}) even though the Black Forest core was collected 10 years after the Swiss cores (which represent peat accumulation pre-dating 1992). In comparison, the cumulative ^{210}Pb inventory is higher in the Black Forest (7800 Bq m^{-2}) than in Étang de la Gruère (EGR) (2800-4400 Bq m^{-2}). This is probably due to the geology of the Black Forest (crystalline rocks) compared to the calcareous Jura Mountains where EGR is situated. Between the three cores of EGR, there are variations in the ^{210}Pb cumulative inventory, but not in that of total Pb. One possible explanation is that the atmospheric pathways for ^{210}Pb and Pb are different (e.g. a larger ratio dry/wet deposition for ^{210}Pb). Difference in particle deposition could be due to differences in interception, which reflect variations in micro-topography capture effects [Bindler, 2004]. However these processes appear to affect only ^{210}Pb: this would be in good agreement with the fact that wet Pb deposition is predominant in the peat bog **[Table 1]**. Indeed, the snow analyses presented here show that recent Pb supplied to the bog is mainly in the form of wet deposition. The Pb inventories for the three EGR cores are very similar suggesting that wet deposition is relatively uniform across the bog surface. In contrast ^{210}Pb, which is mainly absorbed onto soil-derived dust particles (Robbins, 1978), shows much more variation within the surface of EGR.

Another explanation for the differences might be the way the cores were collected and prepared (Givelet et al., 2004). For example, the measurement of the density depends on careful sample preparation. Density is a key parameter to model the ^{210}Pb ages and for calculating the peat AR. Peat density might be affected by the heterogeneity of the samples, which, in turn, might reflect botanical differences.

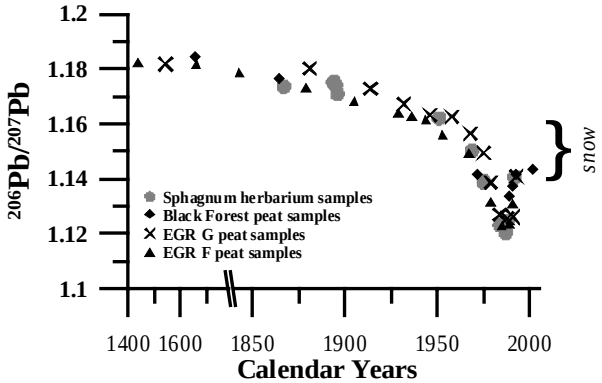

Figure 7: ^{206}Pb/^{207}Pb vs. calendar years for herbarium samples (Weiss et al., 1999b) and peat cores

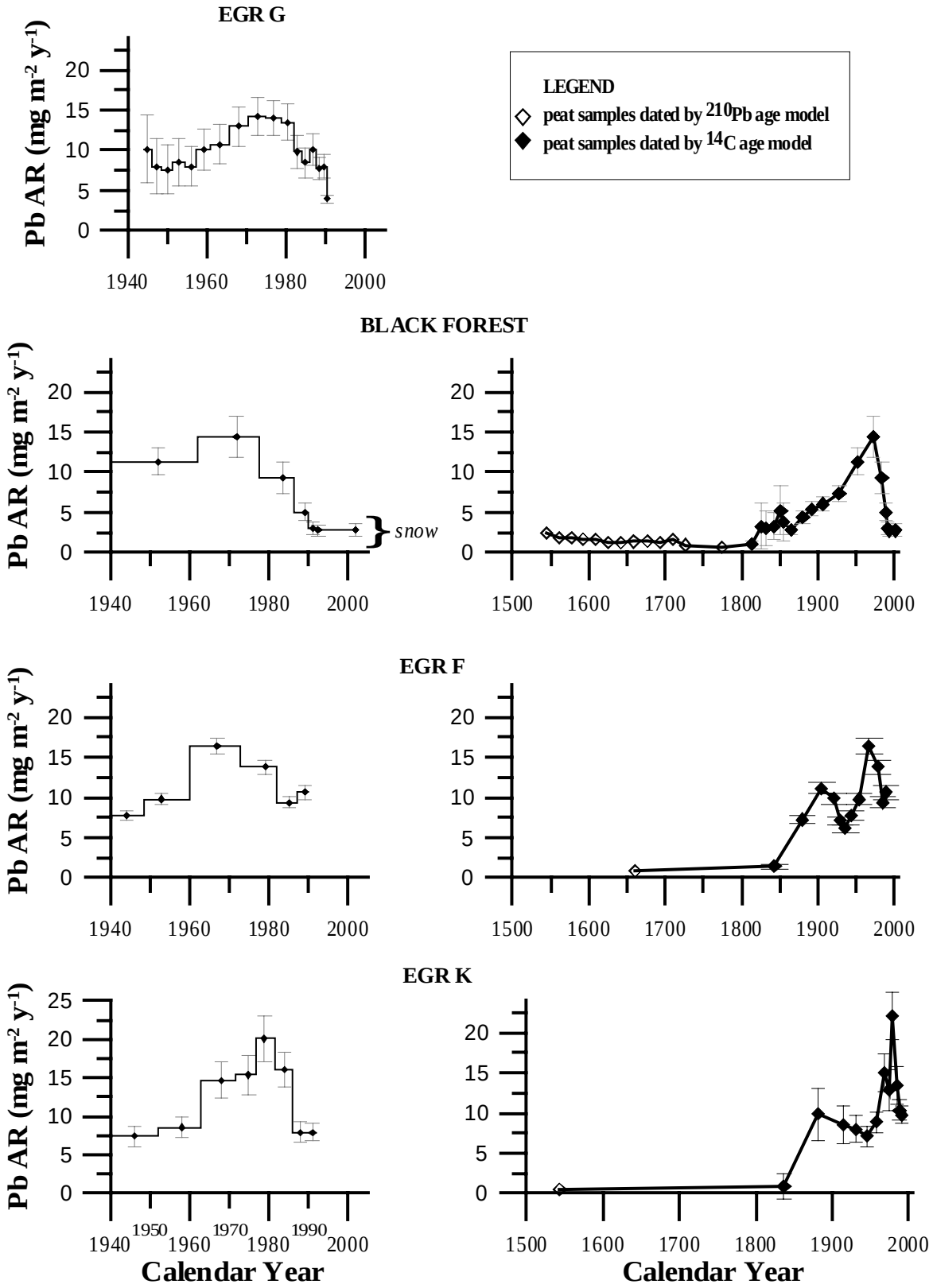

Figure 8: Pb Accumulation rate in the Kohlhütte Moor compared with peat cores from EGR on two different time scales.

For the samples dated by ^{210}Pb (◆), Pb AR was calculated using the sedimentation rate given by the CRS model (Appleby and Oldfield, 1978), errors on Pb AR were then calculated by error propagation using the errors on the sedimentation rate (Appleby, 2001) and the analytical error of the concentration measurement. Also are plotted data for samples dated by the ^{14}C (◇) assuming a linear peat accumulation rate.

Pb isotopes

The approach used by Weiss et al. (1999b) is used to compare our isotope measurements in the bog with measurements in herbarium *Sphagnum* samples collected during the last 200 y in the Black Forest and in Switzerland **(Figure 7).** As already demonstrated by Weiss et al, the isotope measurements in the Swiss peat cores are in very good agreement with the herbarium samples. Here we find that the peat core from the Black Forest provides the isotopic composition of atmospheric Pb, which is also similar to the herbarium record. The similarities in the Pb isotopic composition of Pb in peat from EGR, the Black Forest and in the herbarium moss samples suggest that the age-depth models are valid and that Pb is immobile in the peat profiles. Moreover these data are evidence for common regional pollutant sources of Pb during the last 200 years in NW Switzerland and SW Germany.

Pb accumulation rates

The Pb accumulation rates of the different profiles are in good agreement **(Figure 8).** They show peaks between 1970 and 1980 with a maximum Pb AR between 15 and 20 mg m^{-2}. During the past 10 years, however, the Pb AR appears to have stabilized at approximately 2.5 mg m^{-2} y^{-1}.

Explanations for the small differences in the chronology of Pb accumulation are diverse: local variations within the bog (Bindler et al., 2004), regional variations in Pb deposition (Le Roux et al., 2004; Weiss et al., 1999a), differences in sampling techniques and core quality (Givelet et al., 2004) and errors in the age-depth modelling.

Recent Accumulation of Pb and comparison with Pb in snow deposition

Despite some variations in isotopic composition, the snow deposited in 2003 has an isotopic composition ($^{206}Pb/^{207}Pb$: 1.141 to 1.161; weighted average: 1.151) similar to the bog ($^{206}Pb/^{207}Pb$: 1.141 to 1.143; 1992 to 2002). The average isotopic signature represents a mixture of different atmospheric pollutants such as smelter or municipal incinerators. The most radiogenic snow sample ($^{206}Pb/^{207}Pb$: 1.161) has a different origin since its presumed period of deposition coincides with an air mass coming not from the West but rather from the North **(Figure 1).**

It is possible to estimate the Pb flux based on the snow Pb concentration, and the yearly average precipitation (~ 1800 mm/y). This approach has some limitations because the Pb concentration in precipitation could vary seasonally. However the calculation yields a Pb flux of 1 to 4 mg m^{-2} y^{-1}, which is comparable with the Pb AR in the most recent peat samples of Black Forest peat profile (2.5 mg m^{-2} y^{-1}). The similarities in the Pb fluxes confirm that the peat profile is faithfully recording the Pb atmospheric flux.

These fluxes of Pb obtained both using recent snow and peat are at least 100 times greater than the natural flux. While the decision to ban Pb from gasoline certainly has been helpful (as revealed by the declining Pb fluxes since 1970-1980), other sources of anthropogenic Pb must be dominating the atmospheric emissions.

Conclusions

A peat bog in Southern Germany provides a record of the atmospheric flux and Pb isotopic signature since at least 5800 cal. B.C. The temporal trends and isotopic signatures are similar to those preserved in Swiss peat cores and point to a common Pb source to the region for the past 200 years. Moreover the data show that peat bogs constitute powerful tools to study atmospheric deposition over the ages. Direct comparison between a short-term archive (snowpack) and the peat profile also show good agreement both for the Pb flux and isotopic composition. Most of the Pb deposited during the winter on the bog surface is in the form of wet deposition.

Regardless of the Pb concentration and AR, Pb isotopes compared to the natural background show that anthropogenic Pb is still dominating the Pb input. Despite a decrease in Pb flux due to ban on leaded

gasoline in Europe, the Pb flux recorded in recent peat and snow is at least 100 larger than natural pre-anthropogenic flux in these rural sites. Lead deposition near a road is a factor of ten greater, which suggests modern Pb fluxes in urban areas deserve further investigation.

Acknowledgements:

We would like to thank C. Scholz for the measurements of snow samples with the ICP-OES in Heidelberg, S. Person from the Regierungpräsidium Freiburg for coring permission, T. Noernberg (Ostende), A. Martinez-Cortizas (Santiago de Compostella), H.J. Küster (Hannover), N. Rausch and N. Givelet (Heidelberg) for help during the different field trips and L. Pourcelot (Cadarache) for the internal peat radionuclides standard. This work was funded by the Deutsche Forschung Gemeinschaft through the GRK 273 (www.geofluids.de).

Bibliography

Appleby P. G., 2001 Chronostratigraphic techniques in recent sediments. In: W. M. Last and J. P. Smol (Eds.), Tracking Environmental Change Using Lake Sediments: Basin Analysis, coring, and chronological techniques, Vol. 1 Kluwer Academics, pp. 171-203.

Appleby P. G. and Oldfield F., 1978. The calculation of lead-210 dates assuming a constant rate of supply of unsupported 210Pb to the sediments. Catena 5, 1-8.

Appleby P. G., Shotyk W., and Fankauser A., 1997. Lead-210 Age Dating of Three Peat Cores in the Jura Mountains, Switzerland. Water Air Soil Pollution 100 (3/4), 223-231.

Bacon J. R., 2002. Isotopic characterisation of lead deposited 1989-2001 at two upland Scottish locations. Journal of Environmental Monitoring 4, 291-299.

Bacon J. R., Jones K. C., McGrath S. P., and Johnston A. E., 1996. Isotopic character of lead deposited from the atmosphere at a grassland site in the United Kingdom since 1860. Environmental Science and Technology 30, 2511-2518.

Barbaris B. and Betterton E. A., 1996. Initial snow chemistry survey of the Mogollon Rim in Arizona. Atmospheric Environment 30 (17), 3903-3103.

Bindler R., Klarqvist M., Klaminder J., and Förster J., 2004. Does within-bog spatial variability of mercury and lead constrain reconstructions of absolute deposition rates from single peat records? The example of Store Moss, Sweden. Global Biogeochemical Cycles 18 (GB3020).

Boutron C. F., 1990. A clean laboratory for ultralow concentration heavy metal analysis. Fresenius Journal of Analytical Chemistry (337), 482-491.

Brännvall M.-L., Bindler R., Renberg I., Emteryd O., Bartnicki J., and Billström K., 1999. The Medieval Metal Industry was the cradle of modern large-scale atmospheric lead pollution in northern Europe. Environmental Science and Technology 33 (24), 4391-4395.

Cheburkin A. K. and Shotyk W., 1996. An Energy-dispersive Miniprobe Multielement Analyser (EMMA) for direct analysis of Pb and other trace elements in peats. Fresenius Journal of Analytical Chemistry 354, 688-691.

Dickin A. P., 1995. Radiogenic isotope geology. Cambridge University Press.

Draxler R. R. and Rolph G. D., 2003, HYSPLIT (HYbrid Single-Particle Lagrangian Integrated Trajectory) Model access via NOAA READY Website (http://www.arl.noaa.gov/ready/hysplit4.html) . NOAA Air Resources Laboratory.

Eades L. J., Farmer J. G., MacKenzie A. B., Kirika A., and Bailey-Watts A. E., 2002. Stable lead isotopic characterisation of the historical record of environmental lead contamination in dated freshwater lake sediment cores from northern and central Scotland. The Science of the Total Environment 292 (1-2), 55-67.

Edmondson J. C., 1989. Mining in the later Roman empire and beyond: continuity or disruption. Journal of Roman Studies 79, 84-102.

Farmer J. G., Lorna J. E., Atkins H., and Chamberlain D. F., 2002. Historical Trends in the lead composition of archival Sphagnum Mosses from Scotland (1838-2000). Environmental Science and Technology 36, 152-157.

Farmer J. G., MacKenzie A. B., Sugden C. L., Edgar P. J., and Eades L. J., 1997. A comparison of the historical lead pollution records in peat and freshwater lake sediments from Central Scotland. Water, Air and Soil Pollution (100), 253-270.

Gilfillan S. C., 1965. Lead poisoning and the fall of Rome. Journal of occupational Medecine 7 (2), 53-60.

Givelet N., Le Roux G., Cheburkin A. K., Chen B., Frank J., Goodsite M. E., Kempter H., Krachler M., Noernberg T., Rausch N., Rheinberger S., Roos-Barraclough F., Sapkota A., Scholz C., and Shotyk W., 2004. Suggested protocol for collecting, handling and preparing peat cores and peat samples for physical, chemical, mineralogical and isotopic analyses. Journal of Environmental Monitoring 6, 481-492.

Givelet N., Roos-Barraclough F., and Shotyk W., 2003. Predominant anthropogenic sources and rates

of atmospheric mercury accumulation in southern Ontario recorded by peat cores from three bogs: comparison with natural "background" values (past 8,000 years). Journal of Environmental Monitoring 5 (6), 935-949.

Goodsite M. E., Rom W., Heinemeier J., Lange T., Ooi S., Appleby P. G., Shotyk W., Van der Knapp W. O., Lohse C., and Hansen T. S., 2001. High-resolution AMS 14C dating of post-bomb peat archives of atmospheric pollutants. Radiocarbon 43 (3), 453-473.

Hamilton A., Reznikoff A., and Burnham G. M., 1925. Tetra-ethyl Lead. Journal of the American Medical Association 84 (20), 1481-1487.

Hong S., Candelone J.-P., Patterson C. C., and Boutron C. F., 1994. Greenland Ice Evidence of Hemispheric Lead Pollution Two Millenia ago by Greek and Roman Civilizations. Science 265, 1841-1843.

Klaminder J., Renberg I., and Bindler R., 2003. Isotopic trend and background fluxes of atmospheric lead in northern Europe: analyses of three ombrotrophic bogs from south Sweden. Global Biogeochemical Cycles 17 (1).

Kober B., Wessels M., Bollhöfer A., and Mangini A., 1999. Pb isotopes in sediments of Lake Constance, Central Europe constrain the heavy metal pathways and the pollution history of the catchment, the lake and the regional atmosphere. Geochimica et Cosmochimica Acta 63 (9), 1293-1303.

Krachler M., Le Roux G., Kober B., and Shotyk W., 2004a. Optimising accuracy and precision of lead isotope measurement (206Pb,207Pb,208Pb) in acid digests of peat with ICP-SMS using individual mass discrimination correction. Journal of Analytical Atomic Spectrometry 19 (3), 354-361.

Krachler M., Mohl C., Emons H., and Shotyk W., 2002. Analytical procedures for the determination of selected trace elements in peat and plant samples by inductively coupled plasma spectrometry. Spectrochimica Acta Part B 57.

Krachler M., Zheng J., Fisher D., and Shotyk W., 2004b. Direct determination of lead isotopes (206Pb, 207Pb, 208Pb) in artic Ice Samples at Picogram per Gram Levels Using Inductively Coupled Plasma-Sector Field Ms coupled with a High-Efficiency Sample Introduction System. Analytical Chemistry 76, 5510-5517.

Le Roux G., 2005. Fate of natural and anthropogenic particles in peat bogs. PhD thesis, Ruprecht Karl Universität (available on the library web).

Le Roux G. and Aubert D., 2003, Post expedition field and Status report (http://cf.geocities.com/gwanach/fieldreportWINTER.pdf), pp. 11. Institute of Environmental Geochemistry.

Le Roux G., Shotyk W., and Kober B., 2002, Post expedition field and Status report (http://cf.geocities.com/gwanach/fieldreport.pdf), pp. 15. Institute of Environmental Geochemistry.

Le Roux G., Weiss D., Grattan J. P., Givelet N., Krachler M., Cheburkin A. K., Rausch N., Kober B., and Shotyk W., 2004. Identifying the sources and timing of ancient and medieval atmospheric lead pollution in England using a peat profile from Lindow bog, Manchester. Journal of Environmental Monitoring 6, 502-510.

Martinez-Cortizas A., Garcia-Rodeja E., Pontevedra Pombal X., Novoa Munoz J. C., Weiss D., and Cheburkin A., 2002. Atmospheric Pb deposition in Spain during the last 4600 years recorded by two ombrotrophic peat bogs and implications for the use of peat as archive. The Science of the Total Environment 292 (1-2), 33-44.

McConnell J., R., Lamorey G., W., Lambert S., W., and Taylor K., C., 2002. Continuous Ice-Core Chemical Analyses Using Inductively Coupled Plasma Mass Spectrometry. Environmental Science and Technology 36 (1), 7-11.

McLennan S. M., 2001. Relationships between the trace element composition of sedimentary rocks and upper continental crust. Geochemistry, Geophysics, Geosystems 2.

Murozumi M., Nakamura S., and Patterson C. C., 1996 Industrial Lead Contamination. In: A. Basu and S. Hart (Eds.), Earth Processes; Reading the Isotopic Code, Vol. 95 American Geophysical Union,

Novak M., Adamova M., and Milicic J., 2003a. Sulfur metabolism in polluted Sphagnum peat bogs: a combined 34S-35S-210Pb study. Water, Air and Soil Pollution 3, 181-200.

Novak M., Emmanuel S., Vile M. A., Erel Y., Véron A., Paces T., Wieder R. K., Vanecek M., Stepanova M., Brizova E., and Hovorka J., 2003b. Origin of Lead in eight central European Peat bogs determined from Isotope Ratios, Strengths, and operation times of regional pollution sources. Environmental Science and Technology 37 (3), 437-445.

Nriagu J., 1998. Clair Patterson and Robert Kehoe´s Paradigm of "Show me the Data" on environmental lead poisoning. Environmental Research section A 78, 71-78.

Nriagu J. O., 1979. Global inventory of natural and anthropogenic emissions of trace metals to the atmosphere. Nature 279, 409-411.

Nriagu J. O., 1983. Lead and Lead Poisoning in Antiquity. New-York.

Nriagu J. O., 1996. A history of global metal pollution. Science 272, 223-224.

Nriagu J. O., Lawson G., Wong H. K. T., and Azcue J. M., 1993. A Protocol for Minimizing Contamination in the Analysis of Trace Metals in Great Lakes Waters. Journal of Great Lakes Research 19 (1), 175-182.

Patterson C. C., 1965. Contaminated and Natural Lead Environments of Man. Arch Environ Health 11, 344-360.

Patterson C. C. and Settle D. M., 1987. Review of data on eolian fluxes of industrial and natural lead to lands and seas in remote regions on a global scale. Marine Chemistry 22, 137-162.

Planchon F., Van de Velde K., Rosman K. J. R., Wolff E. W., Ferrari C. P., and Boutron C. F., 2003. One hundred fifty-year record of lead isotopes in Antarctic snow from Coats Land. Geochimica et Cosmochimica Acta 67 (4), 693-708.

Renberg I., Bindler R., and Brännvall M.-L., 2001. Using the historical atmospheric lead-deposition record as a chronological marker in sediments deposits in Europe. The Holocene 11 (07), 511-516.

Robbins J. A., 1978 Geochemical and Geophysical Applications of Radioactive Lead. In: J. O. Nriagu (Eds.), The Biogeochemistry of Lead in the EnvironmentElsevier/North Holland Biomedical Press, pp. 285-393.

Rosman K. J. R., Chisholm W., Hong S., Candelone J.-P., and Boutron C. F., 1997. Lead from Carthaginian and Roman Spanish Mines Isotopically Identified in Greenland Ice Dated from 600 B.C. to 300 A.D. Environmental Science and Technology 31 (12), 3413-3416.

Schwikowski M., Barbante C., Doering T., Gaggeler H. W., Boutron C. F., Schotterer U., Tobler L., Van de Velde K., Ferrari C. P., Cozzi G., Rosman K., and Cescon P., 2004. Post 17th Century changes of European Lead emissions recorded in high-alpine snow and ice. Environmental Science and Technology.

Shotyk W., 2001. Geochemistry of the peat bog at Etang de la Gruère, Jura Mountains, Switzerland, and its record of atmospheric Pb and lithogenic trace metals (Sc, Ti, Y, Zr, and REE) since 12,370 14C BP. Geochimica et Cosmochimica Acta 65 (14), 2337-2360.

Shotyk W., Krachler M., Martinez-Cortizas A., Cheburkin A. K., and Emons H., 2002a. A peat bog record of natural, pre-anthropogenic enrichments of trace elements in atmospheric aerosols since 12370 14C yr, and their variation with Holocene climate change. Earth and Planetary Science Letters 199, 21-37.

Shotyk W. and Le Roux G., in press Biogeochemistry and Cycling of Lead. In: A. Sigel, H. Sigel, and R. K. O. Sigel (Eds.), Biogeochemical Cycles of the elements, Vol. 43 M.Dekker,

Shotyk W., Weiss D., Appleby P. G., Cheburkin A. K., Frei R., Gloor M., Kramers J. D., Reese S., and Van Der Knaap W. O., 1998. History of atmospheric Lead Deposition since 12,730 14C yr BP from a Peat Bog, Jura Mountains, Switzerland. Science 281, 1635-1640.

Shotyk W., Weiss D., Heisterkamp M., Cheburkin A. K., and Adams F. C., 2002b. A new peat bog record of atmospheric lead pollution in Switzerland: Pb concentrations, enrichment factors, isotopic composition, and organolead species. Environmental Science & Technology 36 (18), 3893-3900.

Simonetti A., Gariépy C., and Carignan J., 2000. Pb and Sr isotopic compositions of snowpack from Québec, Canada: Inferences on the sources and deposition budgets of atmospheric heay metals. Geochimica et Cosmochimica Acta 64 (1), 5-20.

Vallelonga P., Van de Velde K., Candelone J. P., Ly C., Rosman K. J. R., Boutron C. F., Morgan V. I., and Mackey D. J., 2002a. Recent advances in measurements of Pb isotopes in polar ice and snow at sub-picogram per gram concentrations using thermal ionisation mass spectrometry. Analytica Chimica Acta 453, 1-12.

Vallelonga P., Van de Velde K., Candelone J. P., Morgan V. I., Boutron C. F., and Rosman K. J. R., 2002b. The lead pollution history of Law Dome, Antarctica, from isotopic measurements on ice cores: 1500 AD to 1989. Earth and Planetary Science Letters 6347, 1-16.

Veysseyre A. M., Bollhöfer A., Rosman K. J. R., Ferrari C. P., and Boutron C. F., 2001. Tracing the Origin of Pollution in French Alpine Snow and Aerosols using Lead isotopic ratios. Environmental Science and Technology 35, 4463-4469.

Von Storch H., Hagner C., Costa-Cabral M., Feser F., Pacyna J. M., Pacyna E. G., and Kolb S., 2002. Reassessing Past European Gasoline Policies. EOS, Transactions, American Geophysical Union 83 (36), 393+ 399.

Weiss D., Shotyk W., Appleby P. G., Kramers J. D., and Cheburkin A. K., 1999a. Atmospheric Pb deposition since the industrial Revolution Recorded by Five Swiss Peat Profiles: Enrichment Factors, Fluxes, Isotopic Composition, And Sources. Environmental Science and Technology (33), 1340-1352.

Weiss D., Shotyk W., Kramers J. D., and Gloor M., 1999b. Sphagnum mosses as archives of recent and past atmospheric lead deposition in Switzerland. Atmospheric Environment 33, 3751-3763.

- Chapter 2.3 -

Identifying the sources and timing of ancient and medieval atmospheric lead pollution in England using a peat profile from Lindow Bog, Manchester

Gaël Le Roux[1*], Weiss Dominik[2,3], Grattan John[4], Givelet Nicolas[1], Krachler Michael[1], Cheburkin Andriy[1], Rausch Nicole[1], Kober Bernd[1] and Shotyk William[1]

[1] Institute of Environmental Geochemistry, University of Heidelberg,
Im Neuenheimer Feld 236
69120 Germany
gleroux@ugc.uni-heidelberg.de
tel: 49(0)6221546063
fax:49(0)6221545228
[2] Department of Earth Science and Engineering, Imperial College London, U.K.,
[3] Department of Mineralogy, Natural History Museum, London, U.K.
[4] The Institute of Geography and Earth Sciences. The University of Wales Aberystwyth, U.K.
* To whom correspondence should be addressed

Journal of Environmental Monitoring 6, 502-510 (2004)

Abstract

A peat core from Lindow Bog near Manchester, England, was precisely cut into 2 cm slices to provide a high-resolution reconstruction of atmospheric Pb deposition. Radiocarbon and ^{210}Pb age dates show that the peat core represents the period ca. 2000 B.C. to AD 1800. Eleven radiocarbon age dates of bulk peat samples reveal a linear age-depth relationship with an average temporal resolution of 17 yrs per cm, or 34 yrs per sample. Using the Pb/Ti ratio to calculate the rates of anthropogenic, atmospheric Pb deposition, the profile reveals Pb contamination first appearing in peat samples dating from ca. 900 B.C. which clearly pre-date Roman mining activities. Using TIMS, MC-ICP-MS, and SF-ICP-MS to measure the isotopic composition of Pb, the ^{208}Pb/^{206}Pb and ^{206}Pb/^{207}Pb data indicate that English ores were the predominant sources during the pre-Roman, Roman, and medieval periods. The study shows that detailed studies of peat profiles from ombrotrophic bogs, using appropriate preparatory and analytical methods, can provide new insight into the timing, intensity, and predominant sources of atmospheric Pb contamination, even in samples dating from ancient times.

Introduction

Evidence of Pb contamination caused by ancient and medieval Pb mining and metallurgy has been found in environmental archives such as polar ice,[1] lake sediments[2,3] and peat bogs.[4-6] Indeed, characterization of Pb pre-industrial contamination is critical to help assess the quantitative importance of modern anthropogenic impacts.[7] Furthermore, archives can provide new insight into the identification of ancient metallurgical activities such as mining, ore processing and smelting even when archaeological evidence is scarce and written sources are absent. Archives such as bogs and lakes also allow palaeobotanical studies of associated impacts caused by mining and metallurgy such as deforestation and other land use changes.[7]

Changes in *atmospheric* Pb deposition recorded in environmental archives show some similarities.[8] Greenland ice core[1,9] and continental European archives such as peat bogs in Switzerland,[5] Spain[10] as well lake sediments in Sweden[11] show synchronous changes in Pb atmospheric deposition around 0 A.D. and 1000-1200 A.D. correlating with both intense Roman and medieval mining. Renberg *et al.*[8] suggested that Pb enrichments corresponding to these time periods could be used as chronostratigraphic markers, to identify these time periods in sediments from northern Europe. They added, however, that more detailed studies are needed to determine how general these Pb enrichments are and to what extent there are geographical differences in the chronology of their occurrence. With reference to published studies of Pb accumulation in peat bogs and lake sediments, however, in most cases the spatial resolution provided is inadequate, the number of age dates used to constrain the changes in accumulation rate insufficient, or both. As a result, possible differences in the chronology of Pb accumulation between study sites usually cannot be discerned.

Lead has four stable isotopes (^{204}Pb, ^{206}Pb ^{207}Pb, ^{208}Pb) with the last three being radiogenic decay products of the U-Th decay series.[12] The isotopic composition of lead ores depends on the age and geological history of the deposit and the initial concentrations of U-Th-Pb in the host rocks. As a result, Pb isotope ratios ("signatures") are powerful tools to distinguish between natural atmospheric Pb (supplied primarily by soil dust) and Pb from anthropogenic sources (originating from Pb ores). For example, in areas far removed from ancient Pb mining regions such as Greenland[1] or Switzerland,[5] isotopic, archaeological and historical data suggested that most of the detected Roman lead pollution originated from Spain, especially the Rio Tinto District.

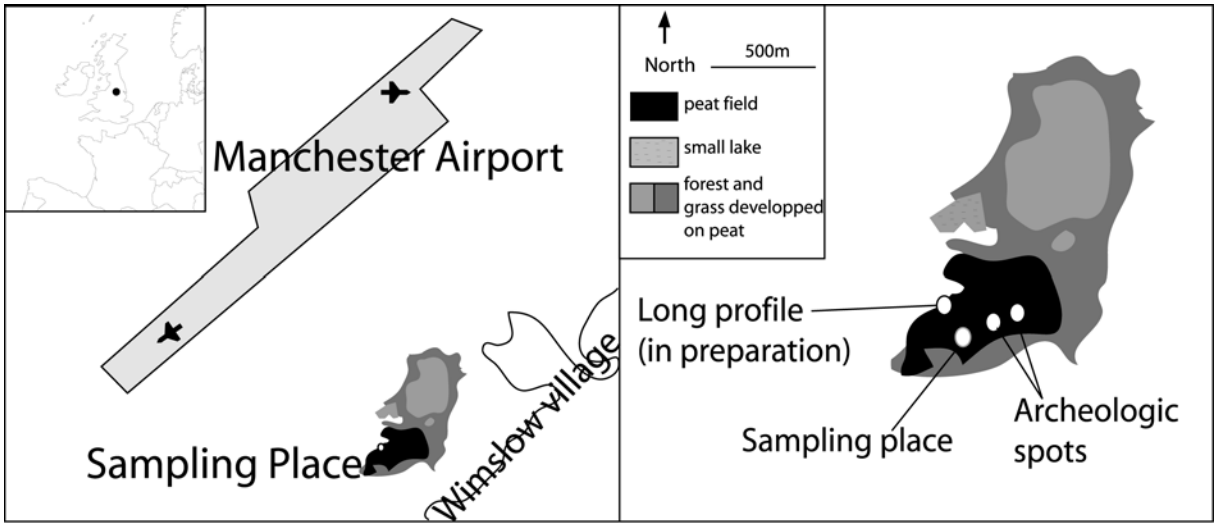

Figure 1: Location and map of Lindow bog.

Unlike ice cores, which are archives exclusively of Pb supplied by long-range atmospheric transport, peat bogs are significantly affected by local and regional metal inputs. With their broad geographic distribution and their long accumulation history, peat bogs are ideal archives for quantifying regional differences in Pb deposition histories. Moreover, *ombrotrophic* peat bogs only record *atmospheric* Pb deposition because the inorganic constituents are supplied only by the air.[13] It is crucial to emphasize these points because the Pb accumulation record in any given peat bog depends on the strength of the pollution source (i.e. duration and intensity of the emission), the distance between the bog and the source, and the *deposition pathway* of the pollutant. These considerations are particularly important for understanding archaeological problems and to help facilitate inter-comparisons between different archives and sites.

In Great Britain, which has a metallurgical history extending back to at least the third Millennium B.C, peat bogs have already been use to identify ancient metal pollution assigned to local or regional sources.[14-18] However these earlier investigations pre-date the widespread use of such analytical tools as Pb isotope fingerprinting,[19] the development of precise multi-elemental analysis[20] and the availability of radiometric dating tools employing ^{14}C and ^{210}Pb.[21] For instance, the pioneering study of Lee and Tallis[14] focused only upon total Pb concentrations. As a consequence, the Pb concentrations could not be corrected for variations due to changes in the abundance of soil dust particles, peat accumulation rates, or both. The chronology of the changes in Pb concentrations was poorly constrained, with only one peat profile employing any radiocarbon age dates: the age dates in a second profile were estimated using pollen markers, and a third core was not dated at all. As a result, the timing of the onset of Pb contamination in these cores is difficult to identify, and no Pb accumulation rates are given. Also, the "natural background" Pb concentrations in the peat profiles were poorly constrained, so the impact of anthropogenic contributions could not be quantified. Finally, there were no measurements of Pb isotope ratios, which would have enabled the origin of the Pb to be determined. The paper by Lee and Tallis, however, clearly illustrated the great potential, which peat bogs represent as archives of atmospheric Pb contamination.

With respect to the chronology of environmental Pb contamination in Britain, much work is still needed. Even in more recent studies[17,18] located near a Bronze Age copper mine in the remote uplands of Wales, only one or two age dates was provided for the entire peat profile, and this is insufficient to model the age-depth relationship and precisely date the Roman peak. On the other hand, there have been detailed studies in the U.K. of Pb deposition using lake sediments[22,23] and herbarium collections.[24,25] However, these only go back to 1630 A.D. for the lake sediments and 1838 A.D. for a herbarium collection *Sphagnum*.[25] As a result, they do not provide any information about environmental Pb contamination, which apparently was so extensive during Ancient and Medieval times.

In the present study, using state-of-the-art analytical and dating methods, we investigate a peat profile representing 4000 years of peat accumulation from Lindow Moss, an ombrotrophic peat bog situated near Manchester, Cheshire, a region with a rich mining and industrial history. The objectives of the study are to i) distinguish between natural and anthropogenic Pb, using Ti as a conservative, lithogenic reference element to quantify the Pb associated with soil dust particles, ii) using ^{14}C age dates, to model the peat accumulation rate, and to use this to calculate the rates of atmospheric deposition of both natural and anthropogenic Pb, and iii) using the isotopic composition of Pb, to identify the predominant sources of anthropogenic Pb to the peat profile. The overall objective of the study is to understand the timing, intensity, and predominant sources of pre-industrial atmospheric Pb contamination at this site, for comparison with other regions of Europe.

Experimental

Material

The peat samples were collected at Lindow Moss, which represents the remnants of a raised bog located south of Manchester, Cheshire, England (Fig.1). In the past, Lindow Moss (Z=71 m, N:53°19´17,2´´, W: 002°16´18,4´´) was a very extensive post-glacial peat bog (600 ha)[26] dominated by *Sphagnum* species, sedges, and cotton grass (*Eriophorum Angustifolium*)[27] which had developed above a fossilized pine woodland.[28] There are extensive palaeocological and archaeological studies of this bog because of discoveries of bog bodies dating from the Iron Age or the Roman Period.[26,27] Because of recent industrial peat removal, the surface layers had probably been lost due to removal or oxidation. The bog was sampled by excavating a peat column from a face which had already been cut by machine, but only after cleaning the face by excavating a further ca. 20 cm into the cut by hand. Nine large blocks of peat were removed sequentially, varying in length between 20 and 30 cm. These were shipped to Berne where they were immediately frozen.

In the laboratory, the frozen peat blocks were sectioned into 2 cm slices using a stainless steel band saw. The outside edges of each slide (1 cm) were cut away by Ti knife to avoid possible contamination of the innermost layers. The residual peat was dried at 105°C for 2 days and pulverized in a centrifugal Ti mill (Retsch GmbH and Co., Haan, Germany). Bulk density was measured on the replicates following the protocol by Givelet et al.[29]

Age dating

Bulk samples of peat powder were age dated using ^{14}C by decay counting at the Institute of Environmental Physics, Heidelberg and calibrated using the BCal[30] online software (http://bcal.shef.ac.uk). Age-depth models and estimated errors were calculated using PSIMPOLL[31] using the weighted average of the calibrated radiocarbon dates' probability distribution given by BCal.

Lead-210 was measured directly in the topmost samples using low background gamma spectroscopy (GCW4028, HPGE, Canberra) in the topmost samples. Only the surface sample and the one following it contained unsupported ^{210}Pb. This result shows that the peat was not growing at the time of sample collection, and that the accumulation record is incomplete, with as much as two centuries of peat accumulation missing.

XRF measurements

Strontium, Ti and Pb were measured directly on peat powders using home-made X-ray fluorescence analysers.[32,33] Detection limits were 0.8 μg g^{-1}; 1.5 μg g^{-1}; 0.6 μg g^{-1} respectively for Sr, Ti, Pb. The XRF method did not provide sufficiently low detection limits for Pb in the deeper and older samples. Precision of the XRF analysers is discussed elsewhere,[29,32] but for Pb was approximately 30% at 1μg g^{-1}, 10% at 10 μg g^{-1} and 6% at 60 μg g^{-1}.

ET-AAS

High purity water (Millipore, Milford, MA, USA), subboiled HNO_3 and HCl (from 65% acid, analytical-reagent grade, Merck, Darmstadt, Germany), HBF_4 (~50%, purum, Fluka, Buchs, Switzerland) and H_2O_2 (30%, Baker analysed, J.T. Baker, Deventer, Holland) were employed for all samples and preparation of standards.

Two hundred mg of each sample was first digested in an HNO_3-HBF_4 mixture in a microwave autoclave (ultraCLAVE II, MLS, Leutkirch, Germany) at elevated pressure.[20]

Digested samples from 60cm to the bottom of the profile were measured for Pb using electrothermal atomic absorption spectrometry (ET-AAS) (AAS5 EA, Analytik Jena, Germany). Because no certified reference material for peat is available, we used a plant certified reference material (Rye Grass, CRM281). Our measured values agreed to within 10% of the certified values (Pb=2.38 ± 0.11 μg g^{-1}). Reproducibility was tested measuring different aliquots of the same samples on different days ($n_{samples}$=3; $n_{aliquots}$=3) and these varied by less than 10%.

Lead isotope measurements

The isotopic composition of Pb was measured in selected samples using the digestion procedure described above, but employing three different methods of measurement: thermal ionization mass spectrometry (TIMS), multi-collector inductively coupled plasma mass spectrometry (MC-ICP-MS), and sector field inductively coupled plasma mass spectrometry (SF-ICP-MS). The samples were selected on the basis of Pb concentration variations. For example, samples were taken from the beginning, maximum, and end of any peaks in Pb concentrations, as well as from depths of the bog possibly containing "background" values. A detailed description of the methodologies are provided in separate publications.[34,35]

Briefly, for TIMS and MC-ICPMS, after the same digestion procedure as for ET-AAS measurements, selected samples were evaporated in Teflon® beakers. Dried samples were redissolved in 2.4N HCl. In a laminar flow class 100 clean air cabinet in Heidelberg, Pb was separated using 300-400µl of EiChrom Sr-resin (EiChrom Europe, Rennes, France) and HCl elution. For TIMS, the obtained samples were deposited on a single rhenium filament with a H_3PO_4 (Merck, Germany)-silicagel (Serva, Germany) mixture before measurement on a MAT Finnigan 261[36] (Thermo Finnigan, Bremen, Germany). Mass Fractionation was corrected using repeated measurements of NIST SRM 981 and was 1.1 ± 0.2 ‰ per amu (n=13).

With respect to the MC-ICP-MS, Pb isotope ratios were determined using a *MicroMass Isoprobe* instrument (Micromass, England) at the Imperial College/Natural History Museum Joint Analytical Facility (JAF), London. Mass fractionation was corrected using NBS 997 Tl as an internal standard.[34] The Pb/Tl ratio was kept constant. Daily repeated measurements of spike NIST 981 Pb solutions permit the optimisation of the $^{205}Tl/^{203}Tl$ ratio used for mass discrimination correction.

For TIMS and MC-ICP-MS, procedural blanks were insignificant compared to the total amount of Pb in the samples and no blank correction was necessary. Precision of measurements was below or at 0.05% at the 2σ level for $^{206}Pb/^{207}Pb$ and $^{208}Pb/^{206}Pb$ ratios for the both methods.[34]

Some digested samples were directly measured for Pb isotope ratios using SF-ICP-MS (Element 2, Thermo Finnigan, Bremen, Germany) after appropriate dilution.[35] Correction for mass discrimination was accomplished by bracketing samples with SRM 981 certified reference material. The SF-ICP-MS measurements were not as precise as those obtained using TIMS and MC-ICP-MS, but precision was still better than 0.1% for $^{206}Pb/^{207}Pb$ and $^{208}Pb/^{206}Pb$ ratios at the 2σ level.[35]

Results

Age dating

The ^{14}C age-depth relationship is linear meaning that the peat accumulation rate was effectively constant (Fig. 2). Therefore, the elemental fluxes in this peat profile are proportional to the volumetric concentration. The average rate of peat growth during the last 4000 years was 0.054 cm y^{-1}, which means that 1 cm on average represents 18.5 years, and that each slice represents 37 years.

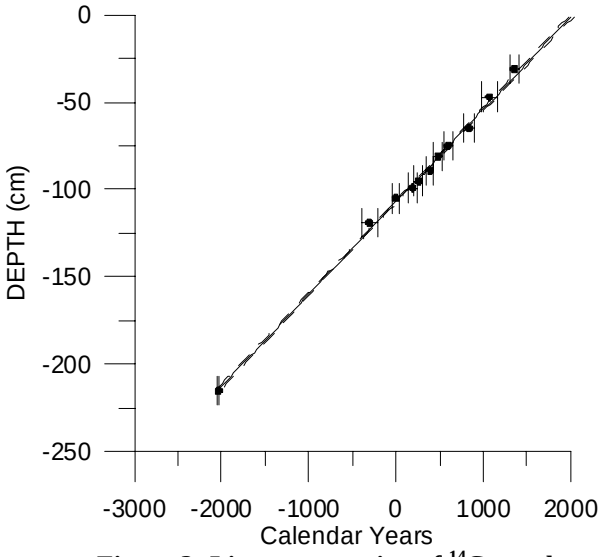

Figure 2: Linear regression of ^{14}C age dates versus depth in the peat profile with 95% confidence intervals estimated by PSIMPOLL[31]

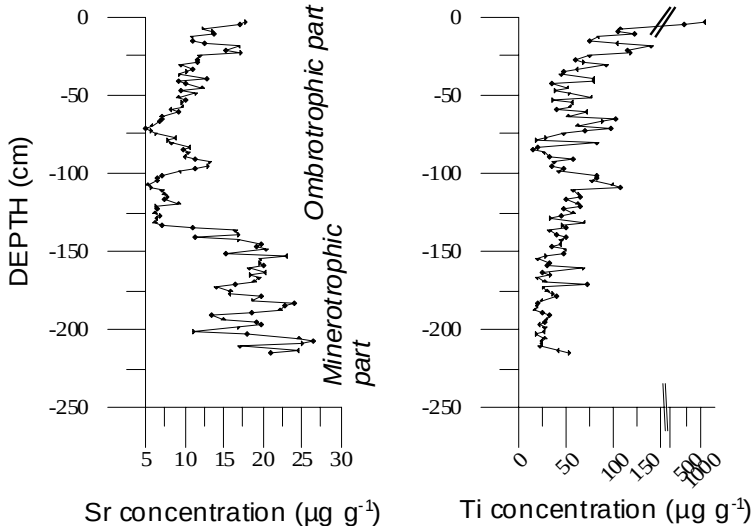

Figure 3: Sr and Ti concentrations (µg g^{-1}) in the peat profile

^{210}Pb was only detected in the top two samples. This is in good agreement with field observations showing a severe disturbance at the surface of the bog. The ^{210}Pb data is consistent with the date given by the ^{14}C age-depth model for the third sample (1895 ± 30 A.D) (Fig. 2). As a result, the top two samples of the core, which was collected, are all that remains of the past ca. one hundred and fifty years of peat accumulation. Furthermore, the distribution of ^{210}Pb data indicates that the disturbance to the bog by peat cutting is restricted to the past two centuries, which were removed. The age-depth plot (Fig. 2) supports this interpretation, and shows that the core studied represents nearly four thousand years of continuous and un-interrupted peat accumulation.

Dominant sources of metals to the peat profile
From the Sr concentration profile (Fig. 3), two distinct depositional environments can be distinguished: the deeper part (130 cm to 220 cm) with high concentrations reflecting inputs of Sr from mineral weathering and the upper part (-130 cm, surface) with low Sr concentrations supplied only by atmospheric inputs. This is in good agreement with previous botanical studies,[26] which show two main botanical phases of peat development: fen peat in the bottom half part and bog peat in the top half.[27]

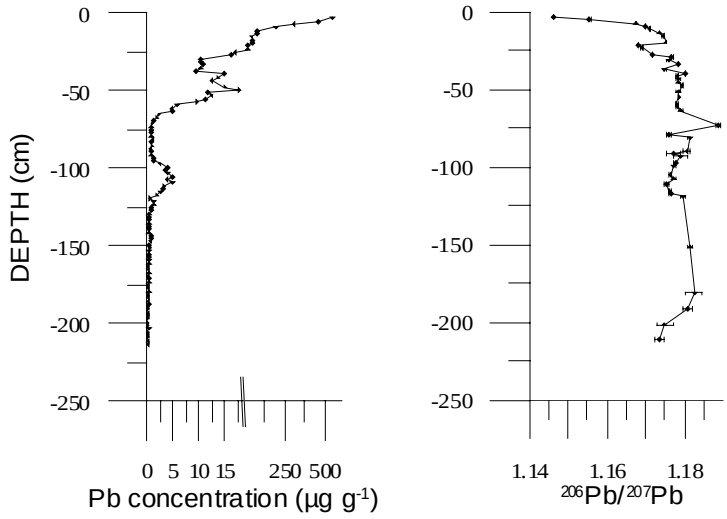

Figure 4: Pb concentrations (µg g^{-1}) and ^{206}Pb/^{207}Pb vs. depth in the Lindow peat profile

Titanium shows a pronounced increase at the top of the profile. Given the constant rate of peat accumulation, the Ti concentration must reflect differences in atmospheric deposition of soil dust. Because the bog receives mineral matter only from the atmosphere, Ti is a sensitive indicator of changing dust fluxes. The sharp increase in Ti concentration at the top should not be interpreted as changing rates of dust accumulation and anthropogenic particles because the peat bog at the sampling place is no longer growing. This peat profile demonstrates the care needed to interpret element concentration profiles and highlights the importance of excellent age dating. The Lindow profile described here has only recorded atmospheric deposition prior to approximately 1800-1850 A.D.

Lead shows the greatest concentrations in the topmost layers and decreasing concentrations with depth. Lead concentrations are elevated by two orders of magnitude from 30 cm to the surface (Fig. 4), relative to deeper, older layers. In the deeper samples, there are two broad peaks centred at 103 cm (Pb= 4.8 µg g^{-1}) and 47 cm (Pb = 19.5 µg g^{-1}). The bottom samples have lower Pb concentrations (Pb = 0.1-0.3 µg g^{-1}). In contrast to Sr, which is elevated in the peats below 125 cm, the lowest Pb concentrations in the entire peat profile are found in these samples. While chemical weathering has certainly added Sr to the deeper layers of the peat profile, this process has not measurably contributed to the Pb inventory. Lead in this peat profile, therefore, was supplied exclusively by atmospheric inputs since ca. 2000 B.C.

Isotopic composition of Pb

The Pb isotope data is summarised as the $^{206}Pb/^{207}Pb$ ratio (Fig. 4). Ascending from the bottom of the core, the two deepest measured samples (211 and 201 cm) are less radiogenic ($^{206}Pb/^{207}Pb$ = 1.174 - 1.175) than the four overlying samples measured between 191 cm and 119 cm ($^{206}Pb/^{207}Pb$=1.182 ± 0.002). Between 117 cm and 89 cm, there is a marked shift toward less radiogenic signatures ($^{206}Pb/^{207}Pb$ ~ 1.175) compared to the deeper layers. Between 89 cm and 65 cm, the isotopic composition is more variable ($^{206}Pb/^{207}Pb$ = 1.176 - 1.189) but between 65 cm and 30 cm, the Pb isotope composition is less variable ($^{206}Pb/^{207}Pb$=1.175-1.180).

Between 30 cm and 21 cm, there is another shift to less radiogenic values (from 1.177 to 1.168 for $^{206}Pb/^{207}Pb$): no comparable values were found in the deeper samples. Between 21 cm and 19 cm, there is a change toward more radiogenic signatures (Fig. 4). However above 19 cm and up to the surface, there is again a shift to less radiogenic values ($^{206}Pb/^{207}Pb$=1.146); this latter set of values is similar to the isotopic composition of atmospheric aerosols in England today. These samples, therefore, and are clearly influenced by leaded gasoline and industrial emissions.[37]

Discussion

Quality of Age dating and age-depth modelling

The challenges associated in absolute age dating with Quaternary sediments is a well-known problem.[31,38,39] Quality of organic samples and the model employed to quantify the age-depth relationship are two of the major issues, which need to be resolved in order to be able to correlate past events in different sites.[40]

Dating bulk sediments can introduce problems such as contamination by the presence of younger vascular plants remains However in Lindow Bog, the peat is homogeneous and is mainly composed of *Sphagnum* macrofossils, which make the risk of contamination smaller[40] as this plant has no roots.

Modelling the age-depth relationship in sediments is a complex problem and apart from expensive ^{14}C wiggle-match dating, there is no simple answer to the question.[38] However to obtain the best possible chronology, we followed the approach of Bennett,[31,39] which at least allows us to obtain error estimates and to compare different models. The simplest and more realistic model (two terms polynomial fitting) was

used to obtain the depth-age relationship. Following Bennett,[39,41] other models were also tested but those yielded similar results *(Electronic Supporting Information*), especially between ca. 80 and 100 cm where there is a cluster of five ^{14}C age dates, this method being encouraged around points of interest.[38]

Distinguishing between natural and anthropogenic lead sources

Using Ti as a conservative lithogenic element in peat and which has no anthropogenic source, we can calculate the natural soil dust contribution for Pb (Pb_{nat}):

$$[Pb]_{nat} = [Ti]_{peat} \times (Pb/Ti)_{crust} \quad \textbf{(1)}$$

where $(Pb/Ti)_{crust}$ is the ratio in the Upper Continental Crust.[42] Instead of normalizing to upper crust values, a more relevant calculation would be to normalise to local background values from the deeper samples of the Lindow Bog. However, in the Lindow peat profile studied here (4000 years old), even the oldest peat layers may have been contaminated by copper metallurgy, which began around 2750 B.C. in England.[43] As a consequence, even in the deepest layers obtained here, it is not possible to determine with any degree of certainty whether the samples are contaminated with Pb or not.

Using Equation 1, excess Pb (Pb_{ex}) is calculated as:

$$[Pb]_{ex} = [Pb]_{peat} - [Pb]_{nat} \quad \textbf{(2)}$$

As mentioned in the paragraph concerning age dating, it is now possible to calculate the Pb flux in excess from Equation 2:

$$F_{Pbex} = [Pb]_{ex} \times BD \times GR \times 10 \quad \textbf{(3)}$$

where F_{Pbex} is the Pb flux (mg m^{-2} y^{-1}), which is in excess of the natural flux, $[Pb]_{peat}$ the Pb concentration (µg g^{-1}), BD the bulk density of the peat (g cm^{-3}) and GR the peat growth rate (cm y^{-1}). The results of these calculations are shown in Figure 5a. as a function of time obtained using the age-depth model.

Another approach is to use Pb isotope signatures as fingerprints[5,44] of anthropogenic Pb. Because the isotopic composition of Pb ores is often considerably different and less radiogenic compared to natural dust, Pb isotopes can help to identify the source of predominant Pb. This approach is particularly valuable when the isotopic composition of pollutants and natural dust are very different, as was the case between natural dust in Switzerland ($^{206}Pb/^{207}Pb$~1.19-1.21) and leaded gasoline ($^{206}Pb/^{207}Pb$~1.08-1.14)[19] or between Pb ores mined in ancient times ($^{206}Pb/^{207}Pb$~1.15-1.19) and natural local dust in Sweden ($^{206}Pb/^{207}Pb$~1.4-1.5).[11] In England, however, as mentioned before, there is no long environmental record pre-dating the beginning of metallurgy in England. Therefore, there is no indication of the Pb isotopic composition of natural dust in England. The only study of Pb from prehistoric times is the recent report by Budd *et al*.[45] of human tooth enamel where $^{206}Pb/^{207}Pb$ ranged from 1.176 to 1.207. Unfortunately, this range of values overlaps with those of Pb ores in Great Britain ($^{206}Pb/^{207}Pb$~1.16-1.19) and extends to soil dust values. Therefore, in England, Pb isotopes alone cannot distinguish between Pb_{ex} and Pb_{nat} in samples from ancient and medieval periods.

History of lead deposition in England from 2000 B.C. to 1800 A.D. (fig. 5)

Pre-roman period. From 2000B.C. to 900B.C. (fig. 5 b), Pb_{ex} flux is nearly constant (0.007± 0.004 mg m^{-2} yr^{-1}) and represents approximately 50% of the lead deposited in the peat bog (Pb_{nat} flux = 0.007± 0.003 mg m^{-2} yr^{-1}). This calculated Pb_{nat} flux is comparable to the lowest values measured in the Holocene for peat bogs in Switzerland[46] and in Sweden[47] (0.001-0.010 mg m^{-2} yr^{-1}). This finding largely validates our assumption that Ti represents natural dust inputs and that the Pb/Ti ratio in natural dust deposited to the bog is close to the crustal Pb/Ti ratio. However the significance of the Pb_{ex} flux between 2000B.C. and 900B.C. remains unclear. Two hypotheses could be proposed: either the Pb_{ex} flux reflects a natural enrichment of Pb in soil dust particles, relative to crustal rocks, or small but significant Pb contamination related either to local early copper metallurgy or to long range transport contamination from the Mediterranean World.

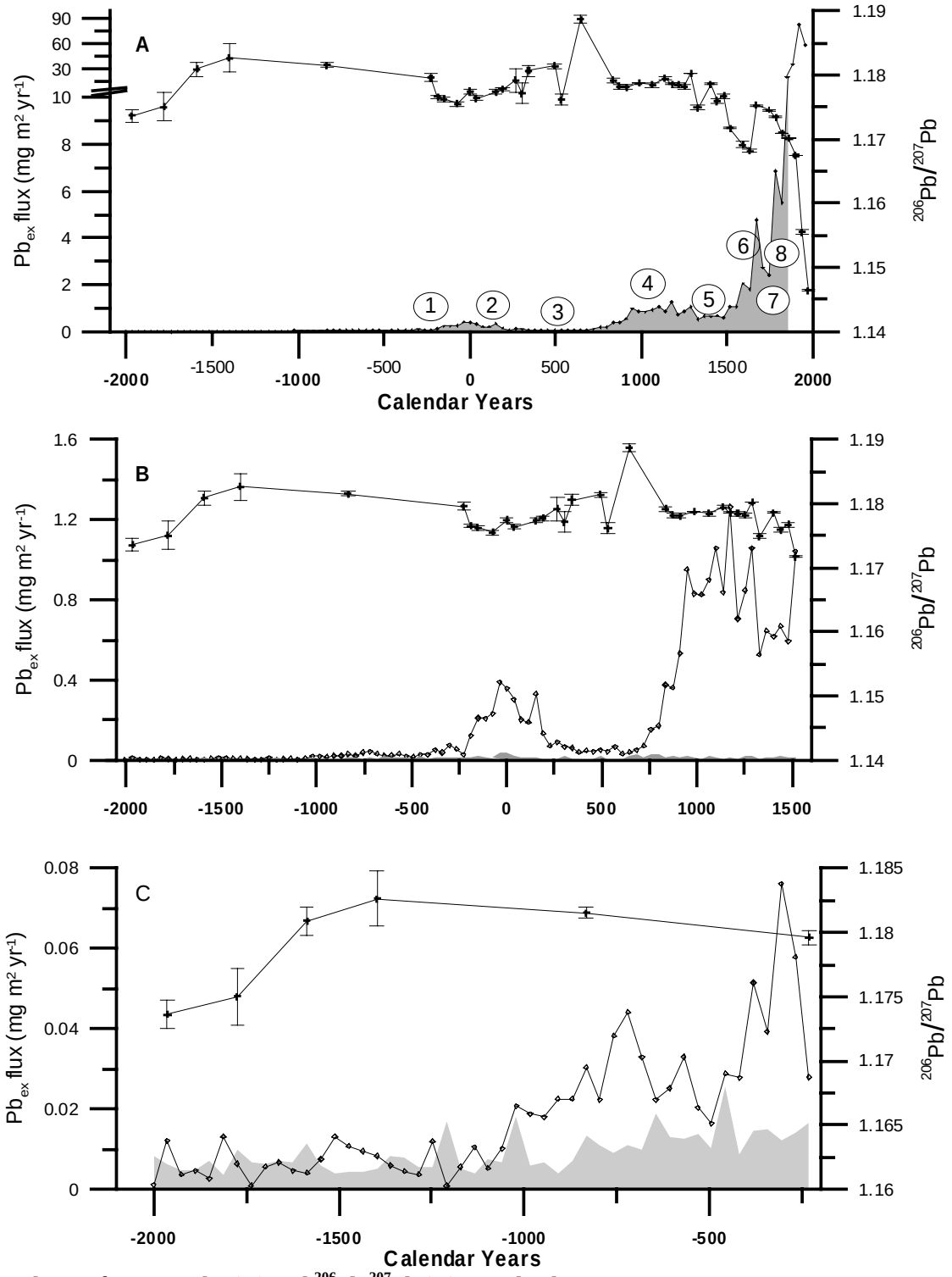

Figure 5 Fluxes of "excess Pb" (◇) and $^{206}Pb/^{207}Pb$ (✚) vs. calendar year
(A): from 2000 B.C. to 1800 A.D.: (1) Iron Age; (2) Roman Occupation (43 A.D-410 A.D.); (3) Dark Ages; (4): Norman-Medieval Period; (5) Hundred Years War, Plague Epidemic (1349 A.D.); (6) Germans workers brought to re-organize the mines (16th century); (7) Plague Epidemic (1645 A.D)? (8) Industrial Revolution
(B): from 2000 B.C. to 700 A.D.: The Pb_{nat} flux is shown in light grey (C): from 2000 B.C. to 400 B.C.: Zoom Focus on the pre-Roman period to emphasize the early increase in Pb deposition around 1000 B.C; the Pb_{nat} flux is also represented in light grey.

Indeed, Lindow Moss is situated only a few km away from Bronze Age mines such as Alderley Edge (Cheshire) and not far from Great Ormes Head (N.E. Wales). There is also a variation in the Pb isotopes data circa 1600 B.C. but it is not correlated with any variations of Pb_{ex} flux. The explanation for this isotopic variation is not known and points

out the need to study longer records and for further research to enable us to distinguish long-range transport from southern Europe and the Mediterranean region, from local pollution or natural enrichment of Pb in the natural dust in England.

After 900B.C, Pb_{ex} flux increased progressively and unambiguously (Fig. 5 c). This change correlated with the beginning in leaded bronze production around 1000B.C.[43] and trade of lead objects with Continental Europe.[48] This date could be interpreted as the turning point where the Pb flux from anthropogenic sources became clearly significant (Fig. 5 c). Until 200B.C, it remained approximately four times higher (0.026 ± 0.011 µg m^2 y^{-1}) than the previous period. Pollen data from Lindow Moss and other bogs from the North-West of England suggest also an environmental change in the early/mid-Iron Age characterised by woodland clearance and cereal cultivation.[49]

200 B.C. to 200 A.D. There is a dramatic increase in Pb_{ex} flux from 200 B.C. to 200 A.D. (Pb_{ex} flux = 0.22 ± 0.1mg m^2 y^{-1}). This is a double peak, one around 0 A.D. and another around 140 A.D (Fig. 5 b.). This is again in good agreement with other studies in Europe and Greenland which show a peak due to Roman lead mining around 0 B.C.[8] However, the first invasion of Britain by Roman Legions is dated from 50 B.C. and Roman Occupation from 43 A.D. Therefore the results presented here show clearly that the increase in atmospheric Pb flux beginning around 200 B.C, represents an increase in Pb emissions which pre-dates by two centuries the Roman Occupation. This finding suggests the existence of a pre-Roman lead extraction industry in the British Isles and is consistent with the statement of Nriagu[48] that: "the exploitation of the British lead deposits shortly after the Romans arrived further suggests the prior existence of a well-established local mining industry". It seems also that the invasion of England by the Romans was correlated with a short but significant decrease of Pb_{ex} flux. The second peak around 140 A.D. is correlated with the zenith of Roman influence in England (e.g. the construction of Hadrian's Wall in 122 A.D. and the Antoine's Wall in 138 A.D). The "Roman" period is also correlated with pollen evidence of major woodland clearance which began in the Iron Age and peaked at a level dated from 130-410 A.D.[49] The uncertainty in the age dating of the woodland clearance, however, does not allow a detailed examination of the correlation between it and the peaks of Pb deposition.

One way to determine the predominant source of anthropogenic lead is to plot the Pb isotope ratios from the peat samples as well as those of local ores (Fig. 6a). Normally, the Pb isotopes plotted on such a diagram are corrected for the natural Pb contribution. However, the natural background Pb isotope values are not yet established. Consequently, it is not possible to calculate the isotopic composition of the anthropogenic lead deposited onto the bog. However, because there is between 10 and 30 times more anthropogenic Pb than natural Pb in the samples dating from the Roman Period, the influence of natural Pb even in those samples is negligible. The isotope ratios dating from 200B.C. to 200A.D. cluster around 1.176 for $^{206}Pb/^{207}Pb$ and 2.087 for $^{208}Pb/^{206}Pb$ (fig. 6a) whereas pre-200 B.C. samples have a larger range of values ($^{206}Pb/^{207}Pb$: 1.178-1.182; $^{208}Pb/^{206}Pb$: 2.08-2.10). The clustering of values suggests a fairly homogenous source.[45] While it might to be desirable for archaeological reasons to be able to distinguish between specific Pb mines, this is not possible because all English lead ores have similar isotopic signatures. Despite this limitation, the data does show clearly that Roman and pre-Roman Pb contamination was caused by mining and refining of English ores, and not Spanish ores.

"Dark Ages". After 200 A.D, the Pb_{ex} flux decreases to pre-Roman values and the isotopic ratios increase until the 7th century. The end of the Roman Occupation in England dates from 410A.D.[50] However the decline of metallurgical activities as recorded in the peat began earlier. The more radiogenic and variable isotope composition (Fig. 6b) during this period could be attributed to a broader range of minor Pb sources. Pollen data suggest a recovery of local woodland after

"the Roman Period" indicating smaller population density.[49,51]

Medieval Period. During the Medieval Period, the Pb_{ex} flux increased to a maximum of 1.24 mg m^{-2} y^{-1}around 1150 A.D. and remained quite stable until 1500 A.D. The maximum Pb_{ex} flux during this period occurred (~1150 A.D) is in good agreement with a previous study[11]. A small decrease after 1200 A.D. is also found in Swedish sediments[11] and probably linked to an economic decline marked in England by the "Black Death" and the "Hundred Years War" between France and England (cf. Fig.5 a). During the Medieval Period, the samples have quite similar signatures, which again match well with English ores (Fig. 6b).

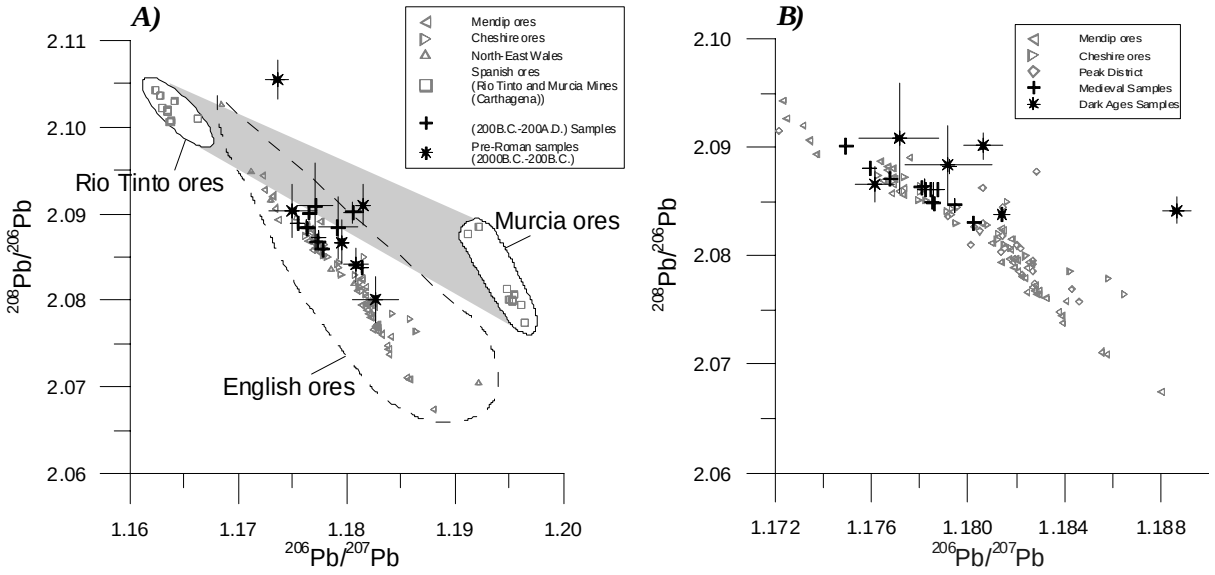

Figure 6: (A): diagram $^{206}Pb/^{207}Pb$ vs. $^{208}Pb/^{206}Pb$ for peat samples before 200B.C. and samples during the 200B.C.-200A.D. period. Also plotted are "local" Cheshire mines, NE Wales mines, which are downwind from Lindow, and the Mendip mines[55], which are supposed to be the most exploited during Roman Occupation in England. Also shown Spanish mines: Rio Tinto district and Murcia (Carthagena) Mines[56]; the light grey field is the possible composition of lead if it was derived from a mixture of Rio Tinto and Murcia ores; (B): diagram $^{206}Pb/^{207}Pb$ vs. $^{208}Pb/^{206}Pb$ for samples between 200A.D. and 700 A.D. ("Dark Ages" samples) and for samples between 700A.D. and 1500 A.D. ("Medieval" samples). Also plotted Mendip Mines and "local" Peak District and Cheshire Mines[55]. Note that all of the English Pb ores have similar isotopic compositions[55] (i.e. that they plot within the same field in $^{206}Pb/^{207}Pb$ and $^{208}Pb/^{206}Pb$ space). Furthermore the use of ^{204}Pb as an additional "fingerprint" does not bring any further information. In both diagram, errors of measurement on the ores are not shown but they are around 0,05% for $^{206}Pb/^{207}Pb$ and 0,1% for $^{208}Pb/^{206}Pb$ at the 2σ level[55].

Modern Period. From 1500 A.D to 1670, the flux of Pb_{ex}, increases. During the reign of Elizabeth I, Germans workers were brought to England to reorganise the Pb mines,[43] including those in the Peak district,[52] which is 30 km east of Manchester. Technological improvements were introduced such as new furnaces for smelting. Consequently, metallurgical activities were increased and lead pollution along with it. These changes could be explained by an increase in metallurgical activities but also simply by urban and industrial development around the bog. Around this time, the Pb isotope signature became less radiogenic declining from 1.176 to 1.168 for $^{206}Pb/^{207}Pb$, and suggests that there were additional new sources of atmospheric Pb.

Around 1670, there is a brief period with a fall in metal fluxes and increasingly radiogenic Pb isotope values ($^{206}Pb/^{207}Pb$~1.175): this suggests a decline in Pb metallurgy, which could perhaps be linked to the Plague Epidemic from 1665 A.D. (Fig. 6). After 1700, the Pb_{ex} flux increased drastically and this is correlated with the

beginning of the Industrial Revolution in England. At this time, the lead isotope composition again becomes less radiogenic which certainly reflects the introduction of foreign ores. In the sample dating from c.a. 1800, the lead isotope composition ($^{206}Pb/^{207}Pb$= ~1.17) is in good agreement with the oldest herbarium samples from south England and Scotland.[24,25]

Comparison between pre and post-industrial atmospheric Pb deposition

Unfortunately, the top part of the peat profile (A.D. 1850-present) is missing. As a result, the Lindow Bog can no longer provide information about recent changes in Pb deposition. However a trend toward less radiogenic values can be noticed in the top samples (ca. A.D. 1800- A.D. 1850), which were surely influenced by modern industrial Pb. This part of the peat profile is highly enriched in Pb (up to 500 ppm) reflecting intense urban pollution especially from coal burning and industrial emissions in Manchester. Fortunately, there are accumulation rate data available for peat studies from the Southern Pennines close to Lindow Bog.[53,54] Lead fluxes measured in those peat bogs in 1979 (~ 3 µg cm^{-2} yr^{-1}) were comparable to or smaller than the Pb flux measured during the 18th century in Lindow Bog. In fact, the Pb flux reached its maximum around A.D. 1930 due to a peak in coal combustion.[53] Comparison between cumulative Pb deposited between 1860 A.D. and 1979 A.D. in peat profiles from Ringinglow Bog[54] (~700 µg m^{-2}) and cumulative Pb deposited between 1500 A.D. and 1800 A.D. in Lindow Bog (~1000 µg m^{-2}) shows that they are in the same order of magnitude. However "Medieval Pb" and "Roman Pb" are not negligible and account for 30 and 6% respectively of total Pb accumulated between 2000 B.C. and 1800 A.D.

Conclusions and perspectives

This study presents the first record of atmospheric Pb and Pb isotope deposition in England over a period of 4000 years and provides detailed information on ancient and medieval metallurgy in England. The first evidence of detectable Pb contamination dates from c.a. 900 B.C. A dramatic increase in Pb pollution occurred 300 years before the Roman Occupation. Lead contamination also continued during the Roman Occupation. Lead isotope analyses indicate that this contamination was derived from British ore sources. Lead contamination decreased significantly before the end of Roman Occupation. The peat bog also recorded a large increase in Pb deposition during the Medieval period, which is in good agreement with similar studies in Continental Europe. The absolute chronology provides new information about important features in lead pollution history such as technological developments, variations in population and economic changes. As in previous studies, this research demonstrates the usefulness of environmental archives to complement historical and archaeological studies. Moreover this research illustrates the potential inherent in geochemical studies of ombrotrophic peat bogs, especially if state of the art analytical and dating methods are employed.

In this study, the pre-anthropogenic background and the industrial period could not be investigated since the bottom of the collected monolith was not enough old and the surface peat layers were missing. Further studies on deeper peat profiles in England are still needed to characterise the fluxes and isotopic composition of pre-anthropogenic Pb.

Acknowledgements

We thank Thierry Marbach, Dietlinde Pingel and Stefan Rheinberger for help in trace element and isotope analyses. Critically reading and several useful remarks by two anonymous reviewers are acknowledged.

References

1 K. J. R. Rosman, W. Chisholm, S. Hong, J.-P. Candelone, and C. F. Boutron, *Enviro. Sci. Technol.*, 1997, **31**, 3413.

2 I. Renberg, M. W. Persson, and O. Emtery, *Nature*, 1994, **368**, 324.

3 M. B. Abbott and a. P. Wolfe, *Science*, 2003, **301**, 1893.
4 H. Kempter, M. Görres, and F. B., *Water, Air, and Soil Pollution*, 1997, **100**, 367.
5 W. Shotyk, D. Weiss, P. G. Appleby, A. K. Cheburkin, R. Frei, M. Gloor, J. D. Kramers, S. Reese, and W. O. Van Der Knaap, *Science*, 1998, **281**, 1635.
6 A. Martinez-Cortizas, X. Pontevedra-Pombal, E. Garcia-Rodeja, J. C. Novoa-Munoz, and W. Shotyk, *Science*, 1999, **284**, 939.
7 F. Monna, C. Petit, J. P. Guillaumet, I. Jouffroy-Bapicot, C. Blanchot, J. Dominik, R. Losno, H. Richard, J. Lévêque, and C. C. Chateau, *Enviro. Sci. Technol.*, 2004, **38**, 665.
8 I. Renberg, R. Bindler, and M.-L. Bränvall, *The Holocene*, 2001, **11**, 511.
9 S. Hong, J.-P. Candelone, C. C. Patterson, and C. F. Boutron, *Science*, 1994, **265**, 1841.
10 A. M. Cortizas, P. P. X., J. C. Novoa Munoz, and E. Garcia-Rodeja, *Water Air Soil Pollution*, 1997, **100**, 387.
11 M.-L. Bränvall, R. Bindler, I. Renberg, O. Emteryd, J. Bartnicki, and K. Billström, *Enviro. Sci. Technol.*, 1999, **33**, 4391.
12 A. P. Dickin, 'Radiogenic isotope geology', Cambridge, Cambridge University Press, 1995.
13 W. Shotyk, *Earth Science Reviews*, 1988, 95.
14 J. A. Lee and J. H. Tallis, *Nature*, 1973, **245**, 216.
15 M. H. Martin, P. J. Coughtrey, and P. Ward, *Proceedings of the Bristol naturalist´s Society*, 1979, 91.
16 S. West, D. J. Charman, G. J.P., and C. A.K., *Water, Air, and Soil Pollution*, 1997, 343.
17 T. M. Mighall, J. P. Grattan, S. Timberlake, J. A. Lees, and S. Forsyth, *Geochem, Explor, Enviro, Anal*, 2002, **2**, 175.
18 T. M. Mighall, P. W. Abrahams, J. P. Grattan, D. Hayes, S. Timberlake, and S. Forsyth, *Sci. Total. Environ.*, 2002, **292**, 69.
19 D. Weiss, W. Shotyk, P. G. Appleby, J. D. Kramers, and A. K. Cheburkin, *Enviro. Sci. Technol.*, 1999, 1340.
20 M. Krachler, C. Mohl, H. Emons, and W. Shotyk, *Spectrochim. Acta, Part B*, 2002, **57**.
21 N. Givelet, G. Le Roux, A. K. Cheburkin, J. Frank, M. E. Goodsite, H. Kempter, M. Krachler, T. Noernberg, N. Rausch, F. Roos-Barraclough, A. Sapkota, C. Scholz, and W. Shotyk, *J. Enviro. Monit.*, **This issue**.
22 J. G. Farmer, E. L. J., A. B. Mackenzie, A. Kirika, and T. E. Bailey-Watts, *Enviro. Sci. Technol.*, 1996, **30**, 3080.
23 L. J. Eades, J. G. Farmer, A. B. MacKenzie, A. Kirika, and A. E. Bailey-Watts, *Sci. Total. Environ.*, 2002, **292**, 55.
24 J. R. Bacon, K. C. Jones, S. P. McGrath, and A. E. Johnston, *Enviro. Sci. Technol.*, 1996, **30**, 2511.
25 J. G. Farmer, J. E. Lorna, H. Atkins, and D. F. Chamberlain, *Enviro. Sci. Technol.*, 2002, **36**, 152.
26 R. C. Turner and R. G. Scaife, 'Bog bodies, new discoveries and perspectives', London, British Museum, 1995.
27 I. M. Stead, J. B. Bourke, and D. Brothwell, 'Lindow Man, the body in the bog', London, British Museum, 1986.
28 J. G. A. Lageard, P. A. Thomas, and F. M. Chambers, *Palaeogeography, Palaeoclimatology, Palaeoecology*, 2000, **164**, 87.
29 N. Givelet, F. Roos-Barraclough, and W. Shotyk, *J. Enviro. Monit.*, 2003, **5**, 935.
30 C. E. Buck, J. A. Christen, and G. N. James: http://bcal.shef.ac.uk
31 K. D. Bennett, *The Holocene*, 1994, **4**, 337.
32 A. K. Cheburkin and W. Shotyk, *Fresenius´ J. Anal. Chem.*, 1996, **354**, 688.
33 W. Shotyk, M. Krachler, A. Martinez-Cortizas, A. K. Cheburkin, and H. Emons, *Earth Planet. Sci. Lett.*, 2002, **199**, 21.
34 D. Weiss, B. Kober, A. Dolgopolova, K. Gallagher, B. Spiro, G. Le Roux, T. F. D. Mason, M. Kylander, and B. J. Coles, *International Journal of Mass Spectrometry*, 2004, **232**, 205.
35 M. Krachler, G. Le Roux, B. Kober, and W. Shotyk, *J. Anal. At. Spectrom.*, 2004, **19**, 354.
36 B. Kober, M. Wessels, A. Bollhöfer, and A. Mangini, *Geochim. Cosmochim. Acta*, 1999, **63**, 1293.
37 F. Monna, J. Lancelot, I. W. Croudace, A. B. Cundy, and J. T. Lewis, *Enviro. Sci. Technol.*, 1997, **31**, 2277.
38 R. J. Telford, E. Heegaard, and H. J. B. Birks, *Quaternary Science Reviews*, 2004, **23**, 1.
39 K. D. Bennett, *Journal of Quaternary Science*, 2002, **17**, 97.
40 D. Charman, Holivar Workshop: Holocene dating, chronologies, and age modelling, Zeist, The Netherlands, 2003.
41 K. D. Bennett and J. L. Fuller, *The Holocene*, 2002, **12**, 421.
42 S. M. McLennan, *G^3*, 2001, **2**.
43 R. F. Tylecote, 'The prehistory of metallurgy in British Isles', London, The Institute of Metals, 1986.
44 K. J. R. Rosman, W. Chisholm, C. F. Boutron, J. P. Candelone, and S. Hong, *Geochim. Cosmochim. Acta*, 1994, **58**, 3265.
45 P. Budd, J. Montgomery, J. Evans, and M. Trickett, *Sci. Total. Environ.*, 2004, **318**, 45.
46 W. Shotyk, *Geochim. Cosmochim. Acta*, 2001, **65**, 2337.
47 J. Klaminder, I. Renberg, and R. Bindler, *Global Biogeochemical Cycles*, 2003, **17**.
48 J. O. Nriagu, 'Lead and Lead Poisoning in Antiquity', ed. J. W. Sons, New-York, 1983.
49 P. Dark, *Britannia*, 1999, **30**, 247.

50 N. Faulkner, 'The decline and fall of Roman Britain', Stroud, Tempus, 2000.
51 H. J. B. Birks, *The Journal of Ecology*, 1965, **53**, 299.
52 T. D. Ford and J. H. Rieuwerts, 'Lead mining in the Peak district', Bakewell, Peak District Mines Historical Society, 1968.
53 E. A. Livett, J. A. Lee, and J. H. Tallis, *Journal of Ecology*, 1979, **67**, 865.
54 E. A. Livett, *Advances in Ecological Research*, 1988, **18**, 65.
55 B. M. Rohl, *Archaeometry*, 1996, **38**, 165.
56 Z. A. Stos-Gale, N. H. Gale, J. Houghton, and R. Speakman, *Archaeometry*, 1995, **37**, 407.

Depth (cm)	Lab-number	Sample name	conv. ^{14}C Age BP	δ^{13}C	cal. Age 1σ	calibr. Age 2σ	Age Modelling with a linear depth-age relationship (Calendar years)	error estimation (2s) by PSIMPOLL (years)	210Pb detectable?
-1		LDW0 (Surface)					2008	29	
-3		LDW1					1970	28	yes
-5		LDW2					1932	28	yes
-7		LDW3					1895	28	no
-31	Hd-22750	LDW 15	612±26	-26.5	cal AD 1305-1400	cal AD1300-1410	1440	23	
-47	Hd-22876	LDW 23	996±46	-26.5	cal AD 990-1160	cal AD 980-1160	1137	19	
-65	Hd-22877	LDW 32	1196±41	-25.4	cal AD 720-850	cal AD710-890	796	16	
-75	Hd-22696	LDW 37	1468±37	-26.8	cal AD 580-640	cal AD555-655	607	15	
-81	Hd-22710	LDW 40	1588±24	-26.5	cal AD 486-532	cal AD 445-540	493	14	
-89	Hd-22697	LDW 44	1659±41	-26.0	cal AD 335-390	cal AD260 - 420	341	14	
-95	Hd-22704	LDW 47	1771±37	-26.8	cal AD 219-260	cal AD170 - 190	228	13	
-99	Hd-22661	LDW 49	1829±23	-24.7	cal AD 128-170	cal AD80-200	152	13	
-105	Hd-22654	LDW 52	1997±38	-24.8	cal BC 20- cal AD 55	cal BC40-cal AD70	38	13	
-119	Hd-22655	LDW 59	2264±47	-25.2	cal BC320-200	cal BC390-200	-227	13	
-215	B-7425	LDW 107	3670±34	-27,1	cal BC 2140-1970	cal BC 2150-1940	-2045	30	

ESI TABLE 1: Age dating data and age modelling results for the 2-terms polynomial (linear) fitting

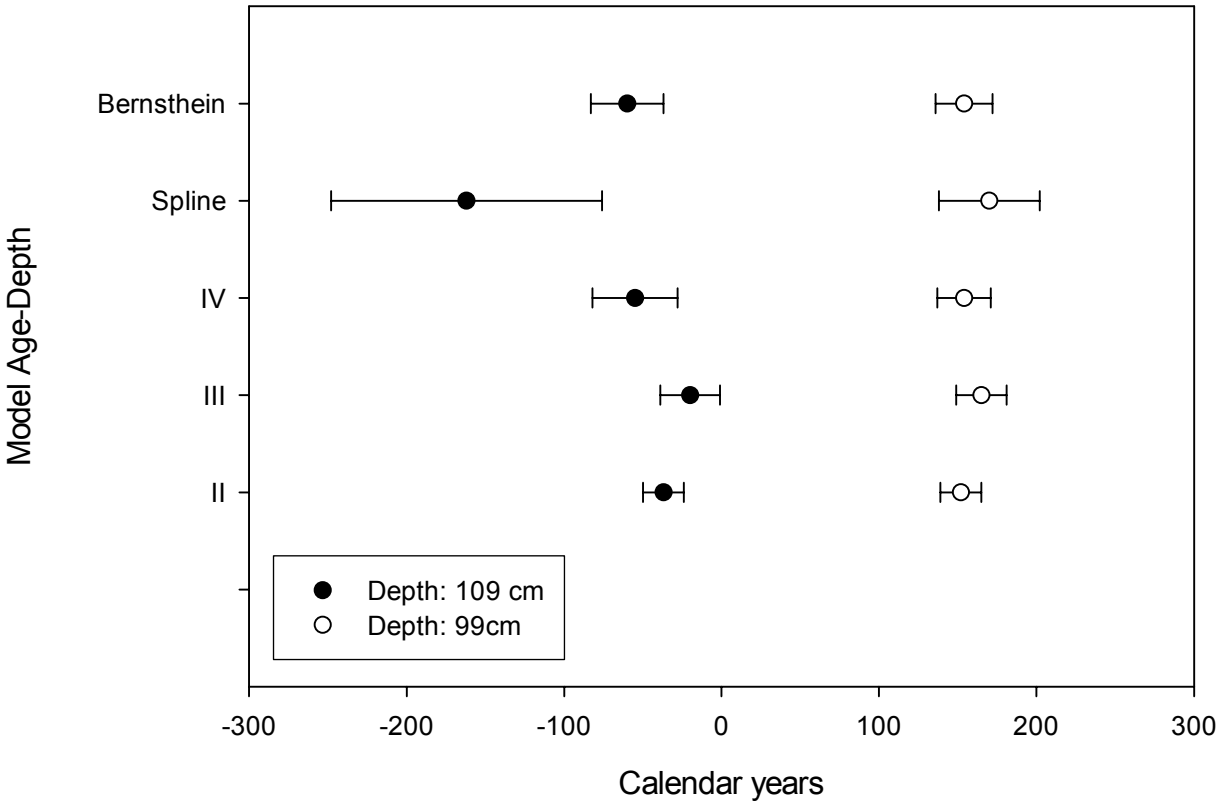

ESI figure 1: comparison between the different age-depth models calculated by PSIMPOLL using the ^{14}C age dating calibrated by BCAL, II (used in the article), III and IV are the number of terms in polynomial fitting, spline and Bernsthein curves are other ways to model the age-depth relationship.[1]

1 K. D. Bennett, *Journal of Quaternary Science*, 2002, **17**, 97.

ESI TABLE 2: Pb isotopes data in the Lindow peat samples

SAMPLE	*208/206 corr*	*SD (2s)*	*207/206 corr*	*SD (2s)*	*206/207corr*	Pb concentration µg/g
TIMS measurements						
LDW1	2,116	0,0001	0,872	0,0000	1,146	548,2
LDW2	2,110	0,0007	0,865	0,0003	1,156	460,5
LDW3	2,099	0,0001	0,857	0,0000	1,167	305,2
LDW4	2,096	0,0002	0,855	0,0001	1,170	190,3
LDW5	2,095	0,0001	0,854	0,0000	1,171	77,6
LDW6	2,090	0,0001	0,852	0,0000	1,173	75,1
LDW7	2,090	0,0001	0,851	0,0001	1,175	41,9
LDW9	2,088	0,0001	0,851	0,0000	1,175	45,6
LDW10	2,104	0,0010	0,856	0,0002	1,168	47,2
LDW11	2,100	0,0009	0,855	0,0005	1,169	21,2
LDW13	2,095	0,0002	0,853	0,0001	1,172	22,0
LDW16	2,085	0,0003	0,848	0,0001	1,179	16,5
LDW19	2,083	0,0001	0,847	0,0000	1,180	15,0
LDW22	2,086	0,0002	0,848	0,0001	1,179	19,5
LDW23	2,085	0,0004	0,848	0,0002	1,179	15,2
LDW27	2,086	0,0000	0,848	0,0000	1,179	11,3
LDW39	2,087	0,0016	0,850	0,0008	1,176	0,83
LDW55	2,089	0,0007	0,854	0,0009	1,171	3,3
LDW55	2,096	0,0014	0,854	0,0005	1,171	3,3
MC-ICPMS measurements						
LDW14	2,087		0,850		1,177	10,5
LDW15	2,088		0,850		1,176	10,5
LDW18	2,090		0,851		1,175	9,5
LDW20	2,086		0,849		1,178	13,7
LDW21	2,086		0,849		1,178	12,5
LDW25	2,085		0,849		1,179	11,7
LDW29	2,086		0,849		1,178	5,9
LDW30	2,086		0,849		1,178	4,7
LDW40	2,084		0,846		1,181	1,1
LDW48	2,086		0,849		1,178	2,5
LDW49	2,087		0,849		1,177	4,1
LDW52	2,088		0,850		1,176	4,8
LDW53	2,087		0,849		1,177	3,9
LDW55	2,089		0,851		1,175	3,3
LDW57	2,088		0,850		1,176	2,6
LDW58	2,090		0,850		1,177	2,0
Reproducibility (ppm)		263		222		
SF-ICPMS measurements						
LDW3	2,097	0,0013	0,856	0,0006	1,168	305,2
LDW6	2,091	0,0017	0,852	0,0007	1,173	75,1
LDW23	2,086	0,0010	0,849	0,0004	1,178	15,2
LDW31	2,088	0,0014	0,848	0,0007	1,179	4,8
LDW36	2,084	0,0012	0,841	0,0006	1,189	0,69
LDW44	2,090	0,0012	0,847	0,0008	1,181	0,84
LDW45	2,091	0,0050	0,850	0,0017	1,177	0,89
LDW46	2,088	0,0036	0,848	0,0018	1,179	1,4
LDW55	2,091	0,0033	0,851	0,0004	1,175	3,3
LDW59	2,087	0,0025	0,848	0,0006	1,180	0,61
LDW75	2,091	0,0024	0,846	0,0004	1,182	0,56
LDW90	2,080	0,0027	0,846	0,0022	1,183	0,23
LDW95	2,084	0,0019	0,847	0,0011	1,181	0,16
LDW100	2,090	0,0031	0,851	0,0022	1,175	0,16
LDW105	2,105	0,0022	0,852	0,0011	1,174	0,24

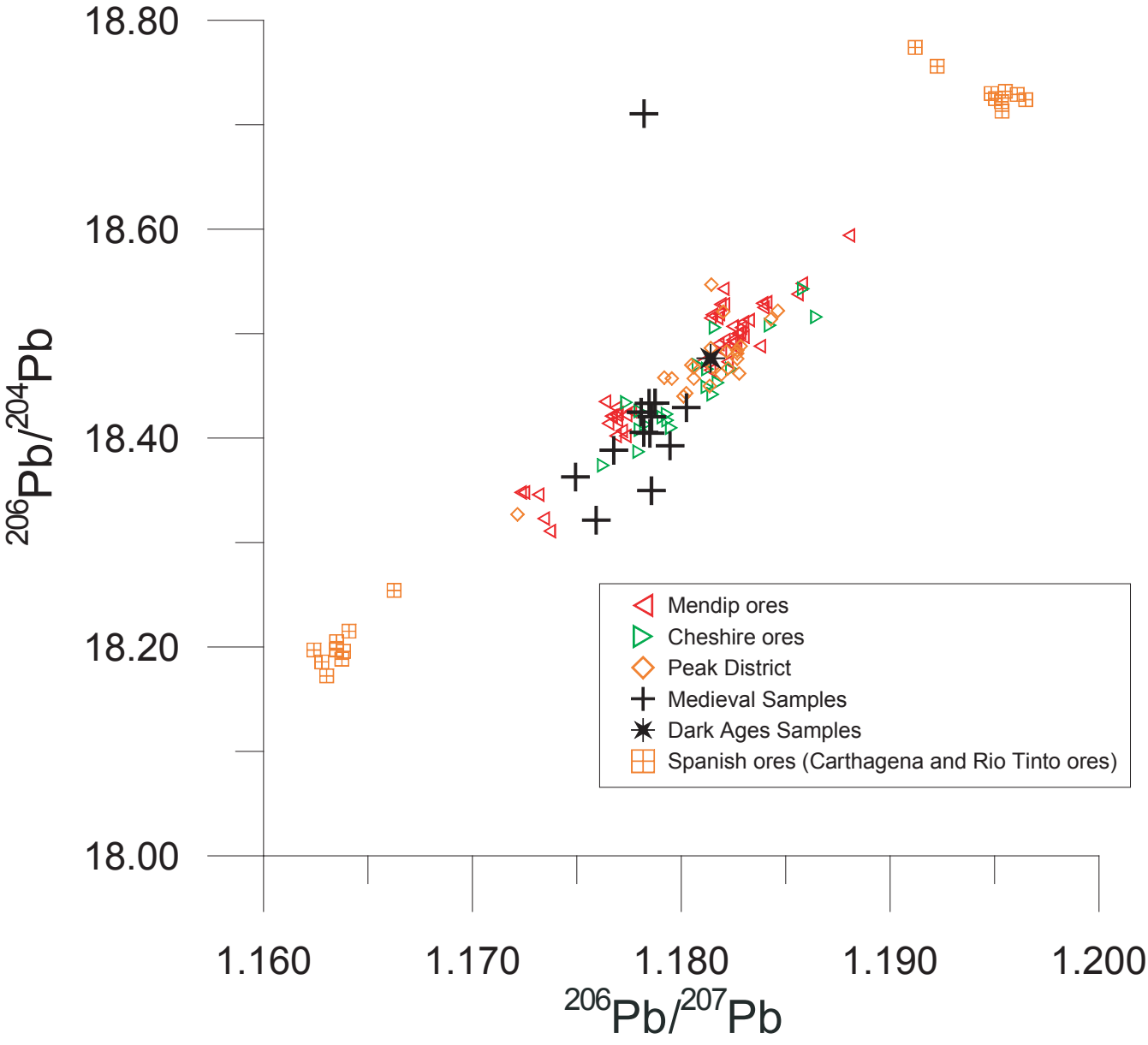

ESI figure 2: 206Pb/207Pb vs. 206Pb/204Pb diagram for samples dated from the Medieval Period. This diagramm illustrates that 204Pb does not help to further distinguish the sources of Pb ores to the bog.

PART 3
FATE OF MINERALS in PEAT BOGS

- Chapter 3.1 -

Alteration of inorganic matter in peat bogs

Gaël Le Roux[1], William Shotyk[2]

[1]: Laboratory of Geochronology
Institute of Environmental Geochemistry
University of Heidelberg
Im Neuenheimer Feld 234
D-69120 Heidelberg
Germany
e.mail: gleroux@ugc.uni-heidelberg.de

[2]: Institute of Environmental Geochemistry,
University of Heidelberg
Im Neuenheimer Feld 236
D-69120 Heidelberg
Germany
e.mail:shotyk@ugc.uni-heidelberg.de

Accepted with minor revisions, Uncorrected Proof
Chapter B.a.11 Of "Peatlands: basin evolution and depository of records on global environmental change and climatic changes"

editors: P. Martini, A. Martinez Cortizas, W. Chesworth

Summary

Inorganic material entering a peat bog, principally quartz, clays, feldspars and calcite, enters a reactive material, anoxic, acid and dominated by organic matter. Whereas theoretical and laboratory studies say us that many minerals such as aluminosilicates are unstable in this type of acid environment, reactivity and dissolution are slower than expected. This is surely due to the complexity of the organic matter encountered in peat in comparison with small organic acids used in experiments.
Despite discrepancy between laboratory and natural results, pH played a crucial role in the dissolution of minerals in peat. Actual ombrotrophic peat bogs are always acid at their surface, however deeper the conditions could be neutral modifying the dissolution reactions. Any attempts to reconstruct dust deposition should take this in account and present pH data for the surface (one way to prove the ombrotrophic status of the bog) and in the deeper parts to understand possible differentiation between surface and processes at depth.
Modern geochemical tools like microanalysis instruments and isotopic analysis should be employed to better understand weathering of minerals in peat bogs.

Introduction

Because of their unique geochemical properties, weathering associated with wetlands has been the subject of scientific investigations since at least the 18th Century (Bischoff, 1854; Blanck and Keese, 1928; Blanck and Rieser, 1925; Endell, 1911; Humphreys and Julien, 1911; Hunt, 1875; Shotyk, 1992). Since these pioneering works where reductive conditions, abundance of organic acids and low pH have been cited to explained intense weathering on different classes of minerals, few studies have been made using modern geochemical tools to study the rates and mechanisms of weathering by peatlands.

There is a real need to bridge this gap because peatlands may play a globally significant role in the weathering cycle (Shotyk, 1992):

- Wetlands cover more than 5% of the Earth's total land area and their role in large scale weathering of the upper continental crust is poorly understood.
- The unique geochemical properties of peatlands, namely an anaerobic water column, abundance of natural organic matter and low-pH, makes them an ideal milieu to study the action of organic acids on weathering of minerals. Moreover the possibility of age dating the peat column where weathering takes place permits the kinetics of mineral dissolution to be quantified. Study of weathering at a larger scale is of importance to understand soil and sediment formation as well as the chemical composition of surface waters. In addition, wetlands play an important role in the global climate system by removing atmospheric CO_2 and releasing CH_4.
- Wetlands are known to function as source regions for metals, which are more soluble under anoxic conditions (e.g. Fe, Mn), but the details of reductive dissolution remain obscure. On the other hand, for elements with reduced solubility under anoxic conditions (e.g. Cu, U, Hg, As) and for elements, which form sulphide minerals (e.g. Ni, Cu, Zn, As, Cd, Sb, Hg, Pb), wetlands are effective geochemical traps, removing these elements from surface waters. Because modern peatlands serve as analogues for coal formation (Cross and Phillips, 1990; Martini and Glooschenko, 1985), they could help to provide us with a better understanding of mineral matter and trace elements in coal.
- Finally, reactions and processes in the peat column also influence the ability of peat bogs to preserve records of atmospheric dust, volcanic emissions and anthropogenic deposition.

Our approach in this paper is to focus on weathering reactions and processes in raised, ombrotrophic peat bogs. Our goals are to first briefly describe the physical and chemical characteristics of peat bogs, then explain the predominant sources of mineral matter. The most common minerals occurring in bogs are identified and the main mechanisms of weathering discussed.

Characterisation of weathering milieu

In this part, our aim is to illustrate the main characteristics of the peat bog, which could have an influence on the fate of the mineral matter in the bog.

Botanical composition

The first modern scientific studies of ombrotrophic peat bogs were undertaken in Europe, especially Germany, Switzerland, Sweden, Denmark, and Scotland (Shotyk, 1988). As a consequence, our knowledge of the botanical composition of ombrotrophic bogs is largely biased toward European mires where peat formation is dominated by *Sphagnum* mosses. However, except for the arid and semi-arid regions, ombrotrophic bogs are found nearly worldwide (Von Bülow, 1929). For example, even in the tropics there are extensive formations of raised, ombrotrophic peat, which consist mainly of partly decomposed remains of deciduous

trees. In the Falkland Islands, raised bogs are dominated by *Poa flabellata*, a tussock-forming grass (Lewis Smith and Clymo, 1984). In New Zealand, large, deep ombrotrophic peat bogs are dominated by *Sporodanthus* (Shearer, 1997). Extensive blanket bogs are found on the "sub-Antarctic" islands such as Campbell Island, 600 km south of New Zealand (McGlone et al., 1997). Even in the High Arctic, in the Carey Islands of Greenland, there are peat hummocks formed by *Aplodon wormskioldii*, a moss whose growth is promoted by the constant supply of seabird excrement.
As far as we know, there are only studies on retention of minerals and elements by *Sphagnum* mosses (Malmer, 1988; Punning and Alliksaar, 1997) and very little about retention of elements by the other vascular plants forming bogs in the Southern Hemisphere.

Climate
The climatic regimes of ombrotrophic peatlands are extreme, ranging from warm and wet in the tropics, through cool and humid in the temperate maritime regions of the northern hemisphere, to below freezing in the High Arctic of Canada. These extremes of temperature and humidity play an inordinate role in governing the botanical composition of the peat, the microorganisms, which are found there, and the rates of all chemical reactions.

Ionic content of bog water
Peat bogs are only fed by rainwater. Therefore concentrations of dissolved solids in the surface waters are very low, with concentrations varying from 10 to 100 mg/l (Bennett et al., 1991; Gorham et al., 1984; Göttlich, 1990). Consequently, the electrical conductivity is on the order 10 to 30 µS/cm (Göttlich, 1990; Malmer, 1986).

pH
A low pH (3.7-4.2) is characteristic of ombrotrophic bog (Shotyk, 1989). Because of the low alkalinity of rainwater, the abundance of dissolved organic acids controls the pH by carboxylate buffering (Shotyk, 1989).

Depending on the type of rock under the bog and its historical development, pH generally increases with depth (Fig. 1).

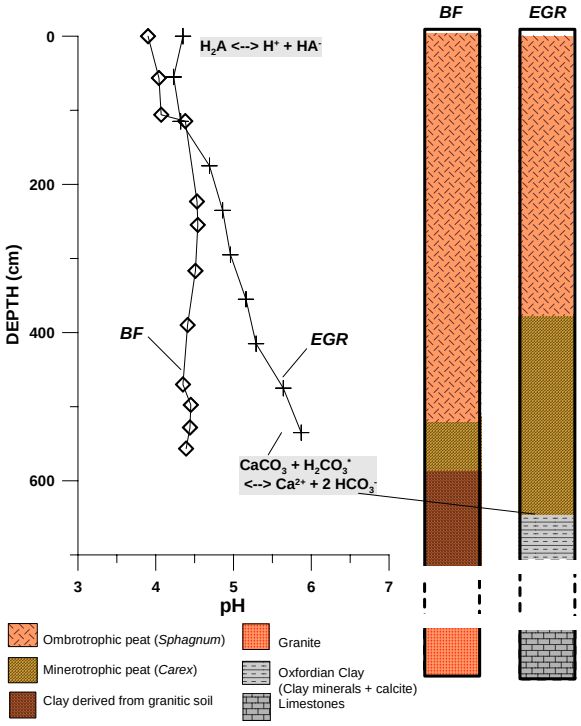

Figure 1:pH profiles and stratigraphy of peat bogs on different geological substrates: Étang de la Gruère in Switzerland (EGR) and Kolhütte Moor in Germany (BF) the former developed upon calcareous clay and the latter on clays derived from a granite. Notice that the difference in geology and geochemistry had a profound influence on the botanical composition of the peat.

Eh
Whereas pools of water at the bog surface may be oxygen-saturated, the major part of water is below the surface and anoxic (Göttlich, 1990; Shotyk, 1989; Shotyk, 1992). The range of Eh values in measured bog water is given in Figure 4.

Geological Substrate
The geological substrates, which function as templates of peat formation, are diverse (Fig. 1). Peatlands are generally found on impermeable layers such as clay or fine-grained glacial tills which impede the drainage of surface water. The distribution of peatlands in the Jura Mountains of Switzerland and France illustrates the degree to which peat formation depends on the

availability of water-saturated substrates: in this highly fractured, well drained, karstic terrain, peat formation is found exclusively on pockets of Oxfordian clays which became exposed at the Earth's surface following extensive folding of the bedrock and erosion of the overlying limestones. While peat might be most commonly found on impermeable substrates, peat also forms on highly permeable substrates such as coarse sands, in areas of groundwater discharge (Anderson, 1797).

Distribution and supply of inorganic compounds in bog profile

The abundance of inorganic material in peat is usually quantified by the ash content, which is the dry weight of material left after combusting the peat overnight at 450°C (ASTM). The ash content in ombrotrophic peats is typically on the order of 1 to 3 % by weight. Lower ash contents have been reported in the tropical ombrotrophic peat bogs of Kalimantan, Indonesia; here, many samples contain as little as 0.5% ash (Weiss et al., 2002) but it is not yet clear whether this reflects lower rates of atmospheric deposition of mineral matter, higher rates of peat accumulation, accelerated rates of mineral weathering, or elevated inputs of mineral phases which are more susceptible to chemical weathering. Greater concentrations of mineral matter have been reported at discrete depths in many ombrotrophic bogs, reflecting either changes in peat accumulation rate (Steinmann and Shotyk, 1997b), variations in the rate of deposition of atmospheric soil dust (Shotyk, 2001), or episodic inputs of volcanic ash particles (Dugmore and Newton, 1992; Wastegard et al., 2003).

Elevated concentrations of mineral matter are also found in the surface layers of all ombrotrophic bogs, as well as in the deepest peat layers, giving rise to "C shaped" concentration profiles. At the bog surface, the elevated concentrations of mineral matter are often thought to be due to biological uptake and recycling of essential elements (especially K, Mg, Ca, but also P, S and perhaps Si) by the living plant layer. *Sphagnum* mosses for example are enriched in K, N and P in their upper part (Malmer, 1988). However, various human activities have contributed to elevated fluxes of soil dust, namely deforestation, the increasing intensity of modern agricultural practices (Gorham and Tilton, 1978), as well as construction. Concentrations of refractory trace metals with very low solubilities and no known biological functions (e.g. Sc, Ti, Zr) are also more abundant in the surface layers of ombrotrophic peat bogs, suggesting that human impacts on the dust fluxes are leaving their mark in the bog archives (Gorham and Tilton, 1978; Shotyk, 2001).

Preparation of peat samples for mineral identification

In ombrotrophic peat, the ash content is less than 5%; therefore it is really difficult to observe minerals in situ.

The challenges posed for mineral identification by the paucity of mineral particles in peat has been succinctly described by Raymond et al.(1983):

"Another problem of major consequence in studying mineral matter in peat is that some inorganic fractions may be so scarce that they will not be observable either in thin section or in the X-ray diffraction patter of a low- or high temperature ash…. However, the peat contains some non-biogenic mineral particles of both siliceous and non-siliceous compositions that can be separated from the organic peat material for SEM analysis by ashing and acid bath techniques. Though the specific relationships between minerals and botanical constituents are lost using this technique, very minor mineralogical constituents that would otherwise be ignored are observable."

Another technique discussed by Raymond et al (1983) is impregnating the peat using a resin to slice it sufficiently thin to allow the optical microscope to be used. This technique was used successfully for swamp peat containing abundant mineral matter, but for low ash peat may challenges remain.

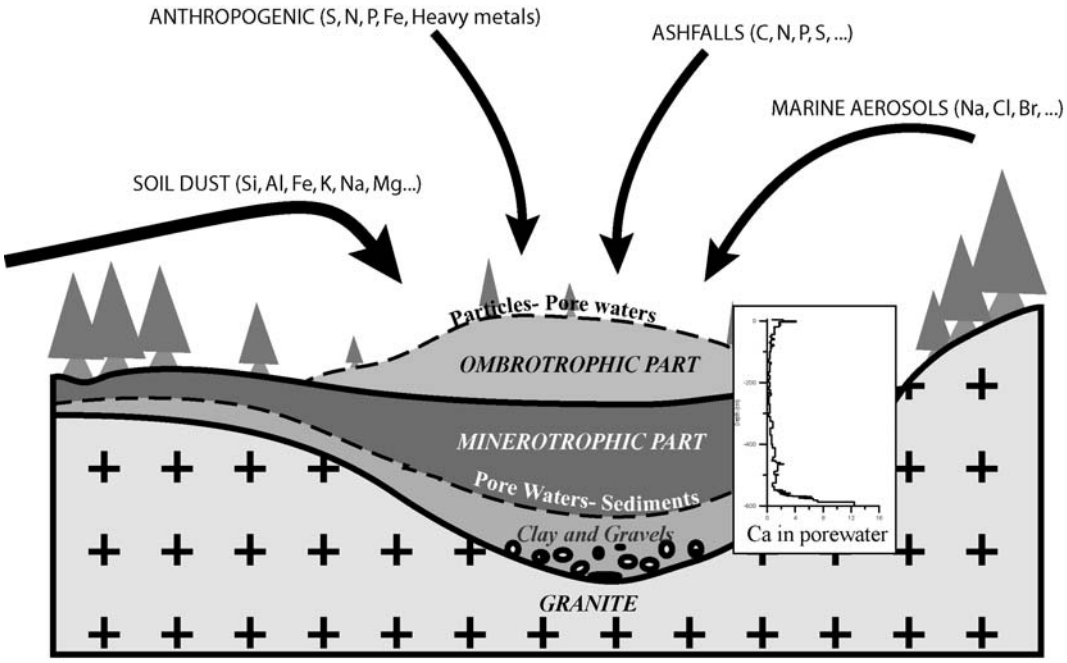

Figure 2: Supply of inorganic material to ombrotrophic bog and shape of Ca distribution in pore water of the Kohlhütte Moor, Southern Germany illustrating the two main reaction fronts: atmosphere-peat surface and peat-substrate

An alternative approach is to concentrate minerals (Givelet et al., 2004). However one problem, which remains, is the risk of change to the mineralogical composition due to processing. The most commonly used technique is a combination of ashing and washing with diluted HCl (Raymond et al., 1983; Steinmann and Shotyk, 1997b). Another possibility is to use oxidising agents such as H_2O_2 to destroy the organic matter (Givelet et al., 2004). Again the possible importance of mineralogical artefacts cannot be ignored.
It should be noticed that similar problems are encountered for mineral observation in coal (Ward, 2002).

Inorganic constituents supplied by atmospheric deposition:

Mineral matter in atmospheric precipitation has different origins (Mattson and Koutler-Andersson, 1954) (table 1 and Fig. 2):
Pedogenic resulting from soil erosion,
Oceanogenic from salt sprays,
Pyrogenic from smoke and ash supplied by fires,
Plutogenic particles from volcanic emanations,
Cosmogenic from meteorites and cosmic dust,
Anthropogenic from industrial, vehicle etc… emissions.

Aerosol	Natural (N) or Anthropogenic (A)	Annual flux 10^{12}g y^{-1}
Sea Spray (Oceanogenic)	N	1000-10000
Dust (Pedogenic)	N, A	60-750
Forest Fires (Pyrogenic)	N, A	35-1500
Volcanic Emissions (Plutogenic)	N	6.5-150
Meteors (Cosmogenic)	N	1
Anthropogenic combustion	A	50
Condensation	N, A	1500

Table 1 : Estimated ranges of yearly input fluxes of particles that make up atmospheric aerosols modified from Van Loon and Duffy (2000) and Nriagu (1979; 1989) and references therein

Soil erosion is the major source of atmospheric particles to most bogs. Particles from local soils but also from more remote areas are deposited constantly in the bog. Large storms could increase considerably the mineral content of the peat by either local (Shotyk, 1997) or long-range (Shotyk et al., 1998) transport of particles. The major part of

the dust particles have a radius between 0.1 and 100 µm (Schütz, 1989). Distances from the source of dust and wind speed are the dominant factors affecting the average particle size. The grater are the transport distance and the lower the wind speed, the smaller is the average radius of the particle (Schütz, 1989).
The elemental composition of soil dust reflects the soil it is derived (Schütz, 1989). However there is some elemental and moreover mineral fractionation during erosion and wind transport (Schütz, 1989).
Because peat bogs are situated in zones of humid climate, where the soil is stabilized by a cover of native vegetation, wind erosion of the soil is reduced to a minimum (Mattson and Koutler-Andersson, 1954). Therefore a large contribution of dust in the bog could be expected from more remote place like deserts. We could speculate that this phenomenon is also larger in mountainous peat bogs. Sahara dust for example is mainly composed of quartz, clays, carbonates and feldspars and is a main source of mineral dust to European peat bogs. As an example, Bücher and Lucas (1984) studied the mineralogy of dust coming from Sahara and deposited in the Pyrenees. They found that the main part of the dust has a radius between 2 to 30 µm and that the main minerals are quartz (50%), clays (25%) mainly kaolinite, carbonates (15%) and feldspars (<5%).

Sea salt particles due to chemical conditions are not retained in peat bogs. Shotyk (1997) showed that less than 10% of Na, Mg, Ca and Sr supplied principally by sea salt inputs in oceanic peat bogs are preserved.

Fires concentrate inorganic compounds of the soil and vegetation cover around the bog and also increase soil erosion. Higher ash content due to fires is indicated by with the presence of pieces of charcoal in the peat (Hölzer and Hölzer, 1998).

Some volcanic eruptions produce large amounts of minerals and glasses dispersed more or less far away from the crater. Layers of this type of material are called tephra layers and when found in bogs are useful to establish a regional or larger time stratigraphy (tephrostratigraphy) and can function absolute age markers. The material deposited varies according to the type of volcanoes, the time of eruption and the distance to the bog (Hodder et al., 1991). Silicate minerals emitted by volcanic eruptions are mainly feldspars, glasses and ferromagnesian silicates.

Cosmogenic material is rarely found in bogs but some traces of meteorite impacts have been found in peat bogs of Russia (Kolemikov and Shestakov, 1979) and Estonia (Veski et al., 2001).

Material from anthropogenic sources is abundant in the surface peat layers. Vegetation of peat bogs, e.g. in the vicinity of smelter, may be affected when the contamination is severe (Glooschenko, 1986). Different particles of anthropogenic origin containing metals and sulphur are deposited due to fossil fuel burning, especially coal, and emissions from heavy industries (Glooschenko et al., 1986; Novak et al., 2003) (Fig. 3)
.

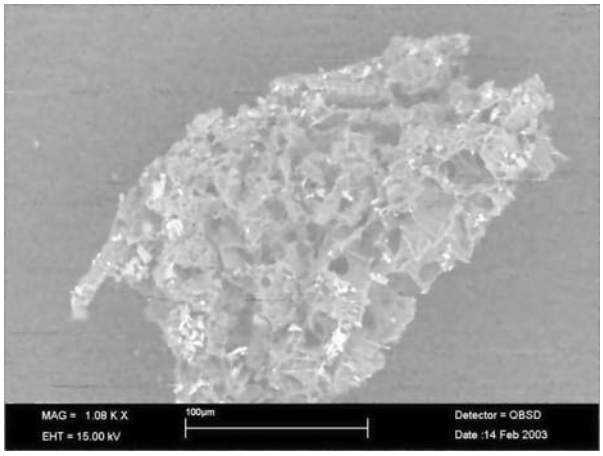

Figure 3: Anthropogenic compound found in a heavily polluted peat bog near Manchester in England from fossil fuel burning (fly ash). The compound is mainly composed by Ca, Fe and S.

Anthropogenic components such as spherical carbonaceous particles are very resistant to acids and are trapped by the *Sphagnum* mosses at the surface of their leaves (Punning and Alliksaar, 1997). In their experiment, they

showed that during a 341 day experiment, deposited fly-ash particles (80%<5µm diameter) were mostly trapped within the first 3 cm. The mechanism of the trapping appeared to be a sorption mechanism on the surface of the plants or localisation of the particles within the pores of hyalocysts. The effective entrapment of atmospheric particles suggested that peat cores could be used as archive of atmospheric deposition.
Magnetite spherules derived from coal burning could also be present especially in bogs from urban areas in England (Williams, 1992).
Other exotic anthropogenic compounds found in peat coming are derived from smelting, fuel combustion and other human activities.

Plants, invertebrates and micro-organisms living on, in and around the bog can produce biogenic silicates in the form of phytoliths or diatoms (Andrejko et al., 1983). In the ombrotrophic part of a tropical peat deposit, Wüst (2002) found that the main part (up to >75%) of ash content is made by biogenic inorganic material.

Mechanisms and rates of weathering

Reductive dissolution
Reductive dissolution is one of the most important weathering processes in anaerobic terrains for three reasons. First, Fe is the second most abundant metal in the Earth's upper crust (3.5%) (McLennan, 2001) after Al (8%). Second the solubility of Fe is strongly dependant on its redox state. Third, Fe in orthosilicates and inosilicates commonly form relatively weak links between silicon tetrahedral (e.g. olivine) and single chains of tetrahedral (e.g. pyroxenes). Breaking down these minerals, therefore, is achieved simply by attacking the relatively weak Fe-O bonds. In Table 2 is an example of a pioneering study by Endell (Endell, 1911) which shows the differences in the chemical composition of a weathered basalt underneath a peat bog (anoxic conditions) versus the basalt outside the peatland.

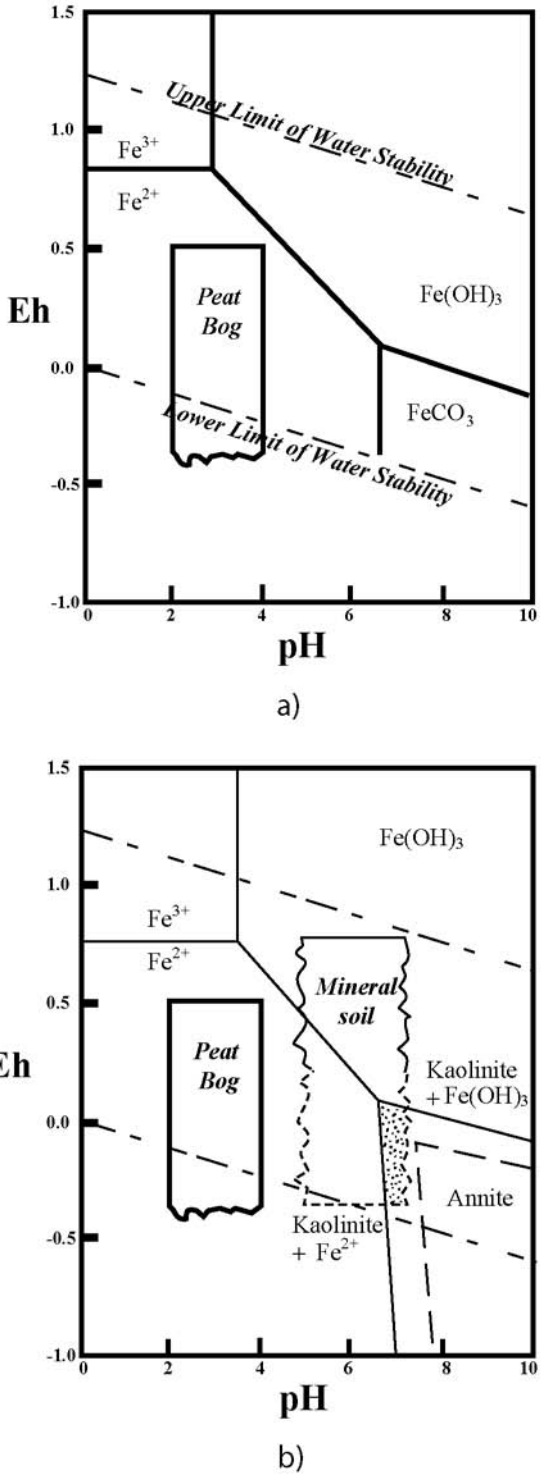

Figure 4: Eh-pH diagram for iron in peat bog environment. Iron activity is $a_{Fe3+}=10^{-6}$ mol L^{-1} in both diagram. Diagram (B) is adapted from Hodder (1991) and represents Fe mica (annite) assuming that in the dissolution all the Al is used to formed kaolinite ($a_{K+}=10^{-6}$ mol L^{-1}, $a_{H4SiO4}= 10^{-2.7}$ mol L^{-1}).

In an oxidizing soil environment (Chesworth and Macias-Vasquez, 1985), the mobility of Fe released by weathering is severely restricted by the insolubility of the hydroxide

$Fe(OH)_3$, which has a K_{sp} of approximately $10^{-38.7}$. In contrast, the solubility of $Fe(OH)_2$ is $10^{-14.5}$, which means that in an anaerobic and acid environment, the dissolved Fe concentration is higher and the mobility of Fe released by weathering is much less restricted (Fig. 4).

Oxide (%)	Weathered basalt near but outside the peatland	Weathered basalt Underneath 125cm of peat
SiO_2	45.21	59.98
Al_2O_3	7.82	11.50
TiO_2	1.69	1.92
FeO	8.08	1.86
Fe_2O_3	3.41	2.42
CaO	12.31	2.80
MgO	8.43	0.75
K_2O	2.94	1.48
Na_2O	6.64	1.18
SO_2	0.56	0.21
P_2O_5	0.52	trace
LOI	1.82	16.53
TOTAL	99.43	100.63

Table 2 : Chemical composition of weathered basalt under and near a peat bog (Endell, 1911)

For example, considering the concentration of [Fe] encountered in the bottom of EGR of 100µM and the P_{CO2} –0.9, the necessary pH to precipitate Fe CO_3 (siderite is) ~ 6.2 (Fig.4 a) Figure 4 b (Hodder et al., 1991) shows that most of the ferromagnesian minerals (here annite as an analogue of mica) are far from the stability field in a peat environment. Hodder et al. also suggest that anoxic conditions present in the bog prevent the formation of Fe-hydroxide which would have protect against further weathering (Hodder et al., 1991).

Anthropogenic magnetite is also subject to reductive dissolution, which might be further enhanced by dissolved sulphide (Williams, 1992). Indeed above the water table, ferromagnetic spherules are not weathered whereas at a depth of 20 cm in anoxic conditions, they show a strong alteration and absence of oxide coating.

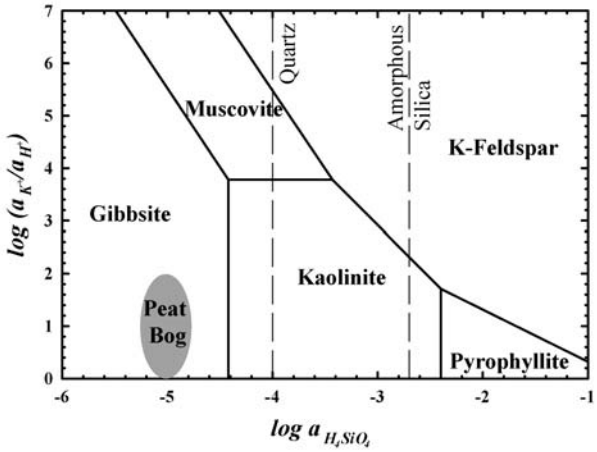

Figure 5: K-Feldspar stability diagram (log a_{H4SiO4} vs. log (a_{K+}/a_{H+})) with ellipse showing normal concentrations in pores water of peat bog. The diagram indicates that all mineral phases shown, as well as amorphous silicate, except for gibbsite, are thermodynamically unstable in peat.

Proton-promoted dissolution

The low pH of bog water promotes also the dissolution of minerals except for quartz whose solubility is independent of pH below pH 9. Feldspars are thermodynamically unstable in peat bogs, because of the low pH and paucity of dissolved major element cations. Figure 5 shows for example the instability of K-feldspar weathered by the incongruent reaction:

$2KAlSi_3O_8 + 2H^+ + 9H_2O \leftrightarrow Al_2Si_2O_5(OH)_4 + 2K^+ + 4H_4SiO_4^0$.

Experimentally, at pH<6, the dissolution rate R of K-feldspars and Albite is pH-dependant ($R \propto [H^+]^{\sim 0.5}$) (Blum, 1994).

As shown in the Figure 5, kaolinite is also not thermodynamically stable in peat waters. Feldspars, kaolinite and other clay minerals therefore, should all be subjected to proton-promoted dissolution reactions (Cama et al., 2002).

The end product of the weathering of K-feldspar is gibbsite. Gibbsite weathering is also enhanced by increase of acidity:

$Al(OH)_3 + 3H^+ \leftrightarrow Al^{3+} + 3\ H_2O$,

the solubility of this reaction in pure water at 25°C and pH 4 being $10^{-4.26}$ mol L^{-1} corresponding to a pore water concentration of ~ 1500µg L^{-1} Al. Typical values of aluminium in bog waters are around 50 and 250 µg L^{-1}: peat waters are therefore under-saturated with respect to gibbsite.

Organic acids--promoted dissolution

The role of organic acids in mineral weathering processes has been reviewed elsewhere (Bennett and Casey, 1994; Drever and Vance, 1994). The reductive dissolution of Fe-bearing minerals is well known because of the elevated concentrations of Fe in anoxic peatland waters (Endell, 1911; Humphreys and Julien, 1911; Hunt, 1875; Johnson, 1866; Niklas, 1912; Ramann, 1895). Except for the obvious effects on Fe-containing minerals, however, the effects of organic ligands on the rates and mechanisms of aluminosilicate weathering are imperfectly understood.

In peatland waters there is a wide range of organic ligands capable of sequestering Al. These ligands range in chemical complexity from simple, small molecular weight organic acids such as oxalic acid (molecular weight: 90) to large molecular weight, polymeric, polyelectrolytic "humic" acids (MW 10,000 or more). These ligands could affect weathering several ways:

- they lower the pH as they dissociate: $H_2A \leftrightarrow 2\ H^+ + A^-$;
- they form complexes with metals, especially Al, which not only affects the solubility of the metal, but also decreases the concentration of free metal ions, which further promotes mineral dissolution: $Me^{n+} + n\ L^- \leftrightarrow$ Me-L;
- they form surface complexes, which may accelerate the detachment of ions from the crystal, depending on the molecule size of the ligand.

Bennett et al. (1991) investigate weathering of quartz and aluminosilicates in a peat bog from Minnesota . They proposed the following model based on the pore water chemistry and mineralogical investigations:

- in the first meter characterized by a low pH (4.6), only aluminosilicates are weathered by dissolution promoted by the formation of Al-organic-acid-complex,
- in deeper samples, where pH is neutral and Al-complexation less favourable, Si-organic-acid complex promoted dissolution dominates (Bennet et al., 1988) and both aluminosilicates and quartz are weathered due to ligand exchange-promoted pathways at the silicon containing groups.

One of their main arguments is the difference between the aspect of minerals at the surface of the bog and in deeper layers. Minerals in deeper layers show indeed chemical weathering features whereas at the surface minerals show only features of wind erosion. Unfortunately their evidence is restricted to only five samples within a 3m peat profile and variations in mineralogy could be due to other causes like variations of mineral source. For example, the chemically weathered quartz samples were located in the minerotrophic layer where input is not exclusively atmospheric. However their approach reintroduced the idea of peatlands as strong agent of weathering in and underneath them (Blanck and Keese, 1928; Blanck and Rieser, 1925; Endell, 1911; Humphreys and Julien, 1911) and it serves a case study to be followed by future investigations.

Moreover weathering of quartz and amorphous of silica in peat bogs is of importance to understand tephra stability. Silicic grains from Holocene tephra found in North-European peat bogs show geochemical stability for at least the last 4000 years (Dugmore et al., 1992). Unfortunately in that study, no data on pH was given. Siever (1962) studied amorphous silica dissolution using pore waters at pH ~5 for 2 years. He showed that dissolution is lower in peat waters than in distilled waters. To confirm dissolution of silica enhanced by organic acids at neutral pH and not at acid pH, one possible way will be to study in parallel a tephra layer in a fen (pH 7) and in a bog (pH 4).

Finally, the dissolution of clay minerals, which constitute a main part of the mineral dust deposited in the peat, is also enhanced experimentally by the presence of *simple* organic acids (Ganor and Lasaga, 1994; Hamer et al., 2003; Huang and Keller, 1971).

Rates of weathering

Based on a mineralogical composition hypothesized by optical observations and

calculated by major elements compositions of insoluble ash of peat, Steinmann and Shotyk argued that Fe-hydroxides dissolution was very slow, slower than predictive models. They claimed that a possible "coating" by organic molecules could have protected the Fe-bearing particles from weathering. A possible alternative is that they include only simple minerals in their calculations and no other Fe-bearing minerals than Fe_2O_3. Hodder (Hodder et al., 1991) showed in a peat bog from New Zealand a complete dissolution of biotite and a strong depletion of other ferromagnesians from a tephra layer within 770 years. He found also consistencies between differences in rates of dissolution of amphibole and pyroxenes in peat bogs compared with kinetic studies, but no absolute comparison between experimental rates of dissolution and observed rates were given.

Rates of dissolution of feldspars was estimated to be at least 100-1000 times slower in a Swiss bog than in experimental studies at pH 4 in HCl (Steinmann and Shotyk, 1997b). Different hypotheses were proposed such as the lower temperature in bog compared to the experiments, or the development of an amorphous Si layer around the mineral layer controlling the rate of dissolution. In addition, Al and other conservative elements such as Sc, Ti and Zr are preserved in the peat column (Shotyk, 2001; Shotyk et al., 2002) surely in a inorganic solid phase (Bennett et al., 1991), which is consistent with their conservative behaviour during chemical weathering.

Whereas there is no doubt of the presence of weathered aluminosilicates in peat bog (Fig. 6), it is not yet known whether there are enhanced rates of dissolution of aluminosilicates because of the abundance of organic acids in bog waters or if these minerals could have been weathered before their entry into the bog. In addition, the high molecular weight humic substances, by becoming strongly adsorbed, may act more like an inhibitor of dissolution rather than a catalyst (Stumm et al., 1987). This phenomenon was studied by Eggenberger (1999) who found that the dissolution rate of plagioclase feldspar (bytownite) in aqueous extracts of leaf litter (LLE) at pH 4.0 was not significantly different compared to the rate in HCl at the same pH; while the LLE extract did contain higher Al concentrations, the rate-controlling step in the dissolution of plagioclase feldspar in acidic solutions is the destruction of the siliceous leached layer at the weathered mineral surface (Shotyk and Metson, 1994). The decomposition of this layer, apparently is not affected by organic ligands in the low pH environment characteristic of peat bogs.

An interesting study by Curran et al. (2002) investigates the burial of archaeological stones in a bog environment during 2000 years. This tocks of 2 types: quartz porphyry and porphyritic andesite, placed there by humans are present buried and not buried in the bog environment. A comparison showed a transformation of biotite and secondary chlorite to fine-grained micaceous products and clay minerals, alteration of sericitised potassium feldspars to clay minerals, decomposition of plagioclase feldspars to iron oxihydroxides and removal of alteration products in solution. However because of peat cutting, pre-weakening of stones before burial and episodes of freeze-thaws episodes, it is difficult to understand exactly the mechanisms and rates of these changes.

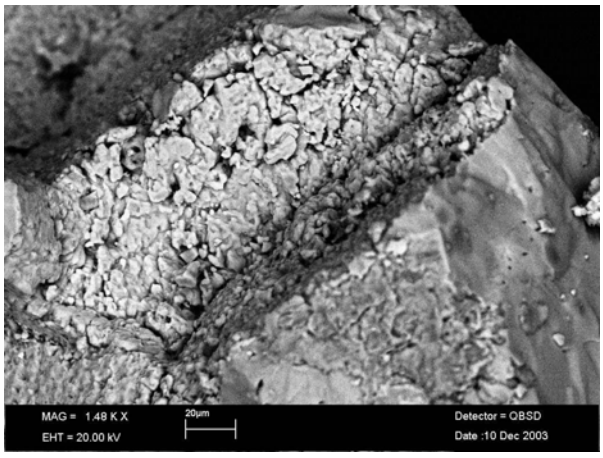

Quartz

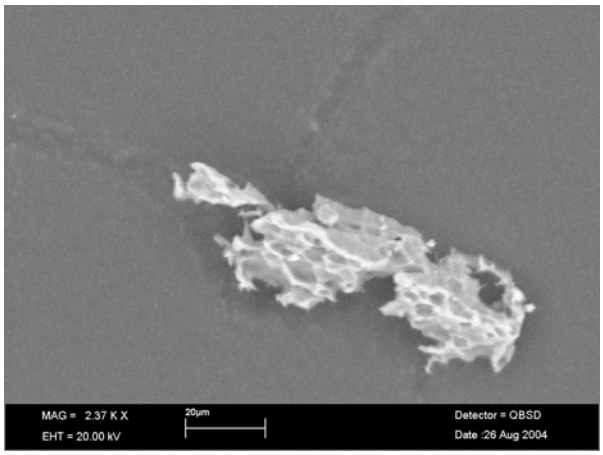

Plagioclase

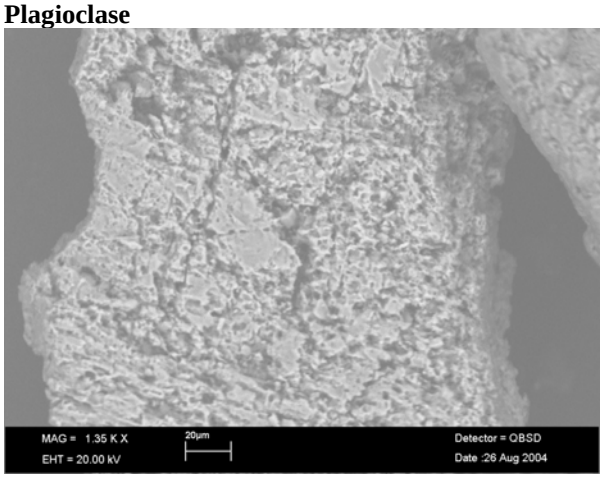

K-feldspath

Figure 6: Altered surface of Quartz macro-grain found in Kolhütte Moor peat bog at 450 cm deep. In the same layer are also found macro-grains of K-feldspar characteristic of the granite around and smaller plagioclase

Special case: carbonates dissolution

At low pH, the dissolution rate of carbonate is proportional to the activity of H^+ (Plummer et al., 1978). Rate of dissolution for carbonates at pH 4-5 is experimentally around 10^{-8}-10^{-9} mol cm^{-2} sec^{-1}.

In the Black Forest peat bog (Fig. 1), analyses of snow samples reveal that the largest calcite minerals entering the bog are 40µm wide (G. Le Roux, unpublished data). Assuming the mineral has a form a cube, the time needed for the minerals to be completely dissolved will be 30 min-5 hours. Rapid dissolution of calcite is consistent with XRD and Optical and Scanning Electron Microscope examinations, which failed to reveal carbonate minerals in the peat. Calcite was found , however, in Sphagnum mosses of the living plant layer, possibly because they had not yet been submerged in the acidic bog waters.

At the peat-substrate interface, the peat bog could also be subjected to intense weathering of carbonates if they are present in the rock (Steinmann and Shotyk, 1997a). However the mechanism of dissolution could be different if the substrate is a basic rock. In this case, the pH is higher (~6-7) and the lower dissolution rate is also dependant on the activity of HCO_3^-, which, in turn, depends on the P_{CO2} (Chou et al., 1989; Plummer et al., 1978) (Fig, 1).

Perspectives

Micro-organisms

Bennett et al. (1994; 1991) suggested that microorganisms are enhancing dissolution rate of silicates in organic milieu such as peat bogs. Indeed microorganisms may create pronounced chemical gradients near colonies and also produce organic acids.

Unfortunately, little is known about the microbiology of peatlands and the chemical processes, which these organisms might regulate.

Weathering rate and mass balance

By studying bogs with varying pH profiles and peat accumulation rates in areas of given atmospheric deposition, it should be possible to perform chemical and mineralogical mass balances over time, to identify and quantify bulk changes. Experimental studies of specific mineral phases in acid bog waters using micro-analytical techniques such as synchrotron XRF and XRD, PIXE, LA-ICP-MS, TOF-ICP-MS and electron microprobe are badly needed.

Pb and Sr isotopes tracers of dust sources and mineral weathering

Lead and Sr isotopes can be used to trace sources of atmospheric dust as well as to identify weathering reactions (Emmanuel and Erel, 2002; Erel et al., 1994; Harlavan and Erel, 2002; Klaminder et al., 2003; Shotyk et al., 1998). For example, Pb isotopic signature is depending on the mineral, where it is hosted. Composition of water leaching the rock will depend therefore on the minerals

weathered. Because Pb is immobile in peat bog, surely because of high affinity with organic matter, we can speculate a different signature between the mineral and the organic matters in the peat. The isotopic composition of the organic matter would reflect the state of weathering of the minerals possibly increasing with age and depth of the peat. Unfortunately the surface layer of all peat deposits studied to date have been found to be contaminated by anthropogenic Pb, thereby masking natural inputs. Moreover in ombrotrophic part of peat not affected by anthropogenic contamination, Pb concentrations are very low and making difficult to achieve necessary precision to reconstruct dust sources and weathering intensity

References:

Anderson J. (1797) *A practical treatise on draining bogs and swampy grounds, ilustrated by figures; with cursory remarks upon the originality of Mr. Elkington´s mode of draining*. Paternoster-Row.

Andrejko M. J., Cohen A. D., and Raymond R. J. (1983) Origin of mineral matter in peat. In *Mineral matter in peat, its occurrence, form and distribution* (ed. R. J. Raymond and M. J. Andrejko), pp. 3-24. Los Alamos National Laboratory.

Bennet P. C., Melcer M. E., Siegel D. I., and Hasset J. P. (1988) The dissolution of quartz in dilute aqueous solutions of organic acids at 25°C. *Geochimica et Cosmochimica Acta* **52**, 1521-1530.

Bennett P. C. and Casey W. (1994) Chemistry and mechanisms of low-temperature dissolution of silicates by organic acids. In *Organic acids in geological processes* (ed. E. D. Pittman and M. D. Lewan), pp. 162-200. Springer-Verlag.

Bennett P. C., Siegel D. I., and Glaser P. H. (1991) Fate of silicate minerals in a peat bog. *Geology* **19**, 328-331.

Bischoff G. (1854) *Elements of chemical and physical geology*. Cavendish Society.

Blanck E. and Keese H. (1928) Über sogenannte Kaolinitisierung eines Granits unter Rohhumusbedeckung im Schwarzwald. *Chemie der Erde* **4**, 33-41.

Blanck E. and Rieser A. (1925) Über die chemische Veränderung des Granits unter Moorbedeckung. *Chemie der Erde* **2**, 15-48.

Blum A. (1994) Feldspars in weathering. In *Feldspars and their reactions*, Vol. 421 (ed. I. Parsons), pp. 595-630. Kluwer Academic Publishers.

Bücher A. and Lucas C. (1984) Sédimentation éolienne intercontinentale, poussières sahariennes et géologie. *Bulletin du Centre de recherche, exploration et production Elf-Aquitaine* **8**, 151-165.

Cama J., Metz V., and Ganor J. (2002) The effect of pH and temperature on kaolinite dissolution rate under acidic conditions. *Geochimica et Cosmochimica Acta* **66**(22), 3913-3927.

Chesworth W. and Macias-Vasquez F. (1985) pe, pH, and podzolization. *American journal of Science* **285**(2), 128-146.

Chou L., Garrels R. M., and Wollast R. (1989) Comparative study of the kinetics and mechanisms of dissolution of carbonates minerals. *Chemical Geology* **78**, 269-282.

Cross A. T. and Phillips T. L. (1990) Coal-forming plants through time in North America. *International Journal of Coal Geology* **16**, 1-46.

Curran J., Smith B., and Warke P. (2002) Weathering of igneous rocks during shallow burial in an upland peat environment: observations from the Bronze Age Copney Stone Circle Complex, Northern Ireland. *Catena* **49**, 139-155.

Drever J. I. and Vance G. F. (1994) Role of soil organic acids in mineral weathering processes. In *Organic acids in geological processes* (ed. E. D. Pittman and M. D. Lewan), pp. 138-161.

Dugmore A. J. and Newton A. J. (1992) Thin Tephra layers in peat revealed by X-Radiography. *Journal of Archeological Science* **1992**, 163-170.

Dugmore A. J., Newton A. J., Sugden D. E., and Larsen G. (1992) Geochemical stability of fine-grained silicic Holocene tephra in Iceland and Scotland. *Journal of Quaternary Science* **7**(2), 173-183.

Eggenberger U. (1999) PhD Thesis, Bern.

Emmanuel S. and Erel Y. (2002) Implications from concentrations and isotopic data for Pb partitioning processes in soils. *Geochimica et Cosmochimica Acta* **66**(14), 2517-2527.

Endell K. (1911) Über die chemische und mineralogische Veränderung basicher Eruptivgesteine bei der Zersetzung unter Mooren. *Neues Jahrbuch für Mineralogie, Geologie, und Paläontologie* **31**, 1-54.

Erel Y., Harlavan Y., and Blum J. D. (1994) Lead isotopes systematics of granitoid weathering. *Geochimica et Cosmochimica Acta* **58**(23), 5299-5306.

Ganor J. and Lasaga A. C. (1994) The effects of oxalic acid on kaolinite dissolution rate. *Mineralogical magazine* **58A**, 315.

Givelet N., Le Roux G., Cheburkin A. K., Chen B., Frank J., Goodsite M. E., Kempter H., Krachler M., Noernberg T., Rausch N., Rheinberger S., Roos-Barraclough F., Sapkota A., Scholz C., and Shotyk W. (2004) Suggested protocol for collecting, handling and preparing peat cores and peat samples for physical, chemical, mineralogical and isotopic analyses. *Journal of Environmental Monitoring* **6**, 481-492.

Glooschenko W. A. (1986) Monitoring the atmospheric deposition of metals by use of bog vegetation and peat profiles. In *Toxics metals in the atmosphere* (ed. J. O. Nriagu and C. I. Davidson), pp. 507-533.

Glooschenko W. A., Holloway L., and Arafat N. (1986) The use of mires in monitoring the atmospheric deposition of heavy metals. *Aquatic Botany*(25), 179-190.

Gorham E., Bayley S. E., and Schindler D. W. (1984) Ecological effects of acid deposition upon peatlands: a neglected field in "acid rain" research. *Canadian Journal of Fisheries and Aquatic Science* **41**, 1256-1268.

Gorham E. and Tilton D. L. (1978) The mineral content of Sphagnum fuscum as affected by human settlement. *Canadian Journal of Botany* **56**, 2755-2759.

Göttlich K. (1990) Moor-und Torf-Kunde, pp. 529. E.Schweizerbart´sche Verlagsbuchhandlung.

Hamer M., Graham R. C., Amrhein C., and Bozhilov K. N. (2003) Dissolution of Ripidolite (Mg, Fe-Chlorite) in organic and inorganic acid solutions. *Soil Science Society of America Journal* **63**, 815-822.

Harlavan Y. and Erel Y. (2002) the release of Pb and REE from granitoids by the dissolution of accessory phases. *Geochimica et Cosmochimica Acta* **66**(5), 837-848.

Hodder A. P. W., De Lange P. J., and Lowe D. J. (1991) Dissolution and depletion of ferromagnesian minerals from Holocene tephra layers in an acid bog, New Zealand, and implications for tephra correlation. *Journal of Quaternary Science* **6**(3), 195-208.

Hölzer A. and Hölzer A. (1998) Silicon and titanium in peat profiles as indicators of human impact. *The Holocene* **8**(6), 685-696.

Huang W. H. and Keller W. D. (1971) Dissolution of clay minerals in dilute organic acids at room temperature. *American Mineralogist* **56**(6), 1082-1095.

Humphreys E. W. and Julien A. A. (1911) Local decomposition of rock by the corrosive action of pre-glacial peat-bogs. *Journal of geology*, 47-56.

Hunt T. S. (1875) *Chemical and Geological Essays*. Osgood.

Johnson S. W. (1866) *Peat and its uses, as fertilizer and fuel*. O.Judd.

Klaminder J., Renberg I., and Bindler R. (2003) Isotopic trend and background fluxes of atmospheric lead in northern Europe: analyses of three ombrotrophic bogs from south Sweden. *Global Biogeochemical Cycles* **17**(1).

Kolemikov Y. M. and Shestakov G. I. (1979) Lead isotope compositions for peat from the area of the Tungunska explosion of 1908. *Geokhimyia* **8**, 1202-1211.

Lewis Smith R. I. and Clymo R. S. (1984) An extraordinary peat-forming community on the Falkland Islands. *Nature* **1984**, 617-620.

Malmer N. (1986) Vegetational gradients in relation to environmental conditions in northwestern European mires. *Canadian Journal of Botany* **64**, 375-383.

Malmer N. (1988) Patterns in the growth and the accumulation in inorganic constituents in the Sphagnum cover on ombrotrophic bogs in Scandinavia. *Oikos* **53**.

Martini I. P. and Glooschenko W. A. (1985) Cold climate peat formation in Canada, and its relevance to lower Permian coal measures of Australia. *Earth-Science Reviews* **22**, 107-140.

Mattson S. and Koutler-Andersson E. (1954) Geochemistry of a raised bog. *Kungl. Lantbrushögskolans Annaler* **21**, 321-366.

McGlone M. S., Moar n. T., Wardle P., and Meurk C. D. (1997) Late-glacial and Holocene vegetation and environment of Campbell Island, far southern New Zealand. *The Holocene* **7**(1), 1-12.

McLennan S. M. (2001) Relationships between the trace element composition of sedimentary rocks and upper continental crust. *Geochemistry, Geophysics, Geosystems* **2**.

Niklas H. (1912) Untersuchungen über den Einfluss von Humustoffen auf der Verwiterrung der Silikate. *Int. Mitt. Bodenk.* **2**, 214-244.

Novak M., Adamova M., and Milicic J. (2003) Sulfur metabolism in polluted Sphagnum peat bogs: a combined 34S-35S-210Pb study. *Water, Air and Soil Pollution* **3**, 181-200.

Nriagu J. O. (1979) Global inventory of natural and anthropogenic emissions of trace metals to the atmosphere. *Nature* **279**, 409-411.

Nriagu J. O. (1989) A global assessment of natural sources of atmospheric trace metals. *Nature* **338**, 47-48.

Plummer L. N., Wigley T. M. L., and Parkhurst D. L. (1978) The kinetics of calcite dissolution in CO2-water system at 5° to 60°C and 0. to 1.0 atm CO2. *American Journal of Science* **278**(179-216).

Punning J.-M. and Alliksaar T. (1997) The trapping of fly-ash particles in the surface layers of Sphagnum-dominated peat. *Water, Air and Soil Pollution* **94**, 59-69.

Ramann E. (1895) Organogene Ablagerungen der Jetztzeit. *Neues Jahrbuch für Mineralogie, Geologie, und Paläontologie* **10**, 119-166.

Raymond R. J., Andrejko M. J., and Bardin S. W. (1983) Techniques for applying scanning electron microscopy to the study of mineral matter in peat. *Proceedings of workshop on mineral matter in peat: its occurrence, form and distribution*, 169-179.

Schütz L. (1989) Atmospheric mineral dust: properties and source markers. In *Paleoclimatology and Paleometeorology: Modern and Past Patterns of Global Atmospheric Transport* (ed. M. Leinen and M. Sarnthein), pp. 359-383.

Shearer J. C. (1997) Natural and anthropogenic influences on peat development in Waikato/Hauraki Plains restiad bogs. *Journal of the Royal Society of New Zealand* **27**(3), 295-313.

Shotyk W. (1988) Review of the Inorganic Geochemistry of Peats and Peatland Waters. *Earth Science Reviews*(25), 95-176.

Shotyk W. (1989) The geochemistry of peatland waters. *Water Quality Bulletin* **14**(2), 47-53+108.

Shotyk W. (1992) Organic Soils. In *Weathering, Soils, Paleosols* (ed. I. P. Martin and W. Chesworth), pp. 203-224. Elsevier.

Shotyk W. (1997) Atmospheric deposition and mass balance of major and trace elements in two oceanic peat bogs profiles, northern Scotland and the Shetland Islands. *Chemical Geology*(138), 55-72.

Shotyk W. (2001) Geochemistry of the peat bog at Etang de la Gruère, Jura Mountains, Switzerland, and its record of atmospheric Pb and lithogenic trace metals (Sc, Ti, Y, Zr, and REE) since 12,370 14C BP. *Geochimica et Cosmochimica Acta* **65**(14), 2337-2360.

Shotyk W., Krachler M., Martinez-Cortizas A., Cheburkin A. K., and Emons H. (2002) A peat bog record of natural, pre-anthropogenic erichments of trace elements in atmospheric aerosols since 12370 14C yr, and their variation with Holocene climate change. *Earth and Planetary Science Letters* **199**, 21-37.

Shotyk W. and Metson J. B. (1994) Secondary ion mass spectrometry (SIMS) and its application to chemical weathering. *Reviews of Geophysics* **32**(2).

Shotyk W., Weiss D., Appleby P. G., Cheburkin A. K., Frei R., Gloor M., Kramers J. D., Reese S., and Van Der Knaap W. O. (1998) History of atmospheric Lead Deposition since 12,730 14C yr BP from a Peat Bog, Jura Mountains, Switzerland. *Science* **281**, 1635-1640.

Siever R. (1962) Silica solubility, 0°C-200°C, and the diagenesis of siliceous sediments. *The Journal of Geology* **70**(2), 127-150.

Steinmann P. and Shotyk W. (1997a) Chemical composition, pH, and redox state of sulfur and iron in complete vertical profiles from two Sphagnum peat bogs, Jura Mountains, Switzerland. *Geochimica et Cosmochimica Acta* **61**(6), 1143-1163.

Steinmann P. and Shotyk W. (1997b) Geochemistry, mineralogy, and geochemical mass balance on major elements in two peat bog profiles (Jura Moutains, Switzerland). *Chemical Geology*(138), 25-53.

Stumm W., Wehrli B., and Wieland E. (1987) Surface complexation and its impact on geochemical kinetics. *Croatia Chemica Acta* **60**(429-456).

VanLoon G. W. and Duffy S. J. (2000) *Environmental Chemistry*. Oxford University Press.

Veski S., Heinsalu A., Kirsimäe K., Poska A., and Saarse L. (2001) Ecological catastrophe in connection with the impact of the Kaali meteorite about 800-400 B.C. on the island of Saaremaa, Estonia. *Meteoritic & Planetary Science* **36**, 1367-1375.

Von Bülow K. (1929) *Allgemeine Moorgeologie. Einführung in das Gesamtgebiet der Moorkunde*. Gerbruder Borntraeger.

Ward C. R. (2002) Analysis and significance of mineral matter in coal seams. *International Journal of Coal Geology* **50**, 135-168.

Wastegard S., Hall V. A., Hannon G. E., Van den Bogaard C., Pilcher J. R., Sigurgeisson M. A., and Hermanns-Audardottir M. (2003) Rhyolitic tephra horizons in northwestern Europe and Iceland from the AD 700s-800s: a potential alternative for dating first human impact. *The Holocene* **13**(2), 277-283.

Weiss D., Shotyk W., Rieley J., Page S., Gloor M., Reese S., and Martinez-Cortizas A. (2002) The geochemistry of major and selected trace elements in a forested peat bog, Kalimantan SE Asia, and its implications for past atmospheric dust deposition. *Geochimica et Cosmochimica Acta* **66**(13), 2307-2323.

Williams M. (1992) Evidence for the dissolution of magnetite in recent Scottish peats. *Quaternary Research* **37**, 171-182.

Wüst R. A. J., Ward C. R., Bustin M. R., and Hawke M. I. (2002) Characterization and quantification of inorganic constituents of tropical peats and organic-rich deposits from Tasek Bera (Peninsulaer Malaysia): implications for coals. *International Journal of Coal Geology* **49**, 215-249.

- Chapter 3.2 -

Fate of calcite, apatite and feldspars in an ombrotrophic peat bog[φ]

Gaël Le Roux, Emmanuel Laverret, William Shotyk

Institut für Umwelt Geochemie, Im Neuenheimer Feld 234-236, 69120 Heidelberg, Germany

Submitted to Geology

ABSTRACT:

The distribution of primary minerals was investigated using XRD in the upper ombrotrophic part of a peat bog dated using ^{210}Pb and ^{14}C. The main minerals present in the bog are the most abundant minerals in the local granite suggesting that the dust entering the bog is mainly of local origin. Apatite and calcite dissolve rapidly in the topmost 8 cm of the bog. The release of P by apatite dissolution is possibly the main source of plant-available P in the oligotrophic environment of the bog. Quartz and feldspars appear to be preserved for thousands of years despite the low pH and the high content of organic acids. This study suggests that dust deposition and apatite dissolution may affect peat accumulation rates, and that peat bogs could be valuable archives of aluminosilicate deposition since the Late Glacial.

[φ] Title taken from Bennett et al Bennett, P.C., Siegel, D.I., and Glaser, P.H., 1991, Fate of silicate minerals in a peat bog: Geology, v. 19, p. 328-331.

INTRODUCTION

Because of their low pH (3.5-4.5) and high abundance of organic acids, peat bogs have been suspected to be active agents of weathering for more than two centuries (Bischoff, 1854; Hunt, 1875). In addition to weathering of their substratum, the chemistry the bog waters could also affect the minerals being continually supplied to the bog surface via dust deposition. In fact, plants in ombrotrophic peat bogs are only fed by atmospheric deposition and the surface waters are therefore poor in nutrients. Nitrogen and P are thought to be the limiting nutrients for growth of bog vegetation (Dierssen and Dierssen, 2001; Verhoeven et al., 1990). Because the growth of the plants at the surface of a peat bog is limited by the low concentrations of plant-available nutrients in the aqueous phase, any release of elements by particle dissolution could influence the chemistry of the waters and therefore the growth of the plants. At this time, however, the main factors affecting nutrient availability and plant productivity in bogs is always poorly understood (Aerts et al., 1999). Sphagnum dominated peat bogs from the Northern hemisphere are a major carbon reservoir (Gorham, 1991) as well as a source of atmospheric methane (Smith et al., 2004) and understanding their growth has much wider environmental significance.

In addition, peat bogs have shown to be valuable environmental archives not only of pollen significance and fossil plant matter but also of trace elements. For example, there is much evidence that peat cores from raised bogs are valuable archives of atmospheric deposition of anthropogenic lead (Renberg et al., 2001; Shotyk, 2001; Weiss et al., 1999). While bogs appear to also record the changing rates of atmospheric dust deposition (Björck and Clemmensen, 2004; Dörfler, 1992; Shotyk et al., 2002; Vuorela, 1983), it is not yet clear which minerals are stable in acidic, anoxic bog waters, and which are not.

Few studies have investigated the distribution of minerals in Sphagnum-dominated bogs (Bennett et al., 1991; Finney and Farnham, 1968; Steinmann and Shotyk, 1997), because the concentrations of mineral matter are so low (typically < 2%). Whereas Bennett et al. (1991) suggested that alumino-silicates dissolve rapidly in peat bogs due to the complexation of aluminium with organic acids, Steinmannn and Shotyk (1997) found that the relative abundance of feldspars was constant in the uppermost 2 m of a peat bog in Switzerland. This finding suggested that feldspar dissolution was negligible during the past several thousand years.

In this study, we examine the abundance and distribution of primary minerals in an ombrotrophic peat bog located from Southern Germany. We focus on changes in the surface layers, which were precisely dated using ^{210}Pb and ^{14}C.

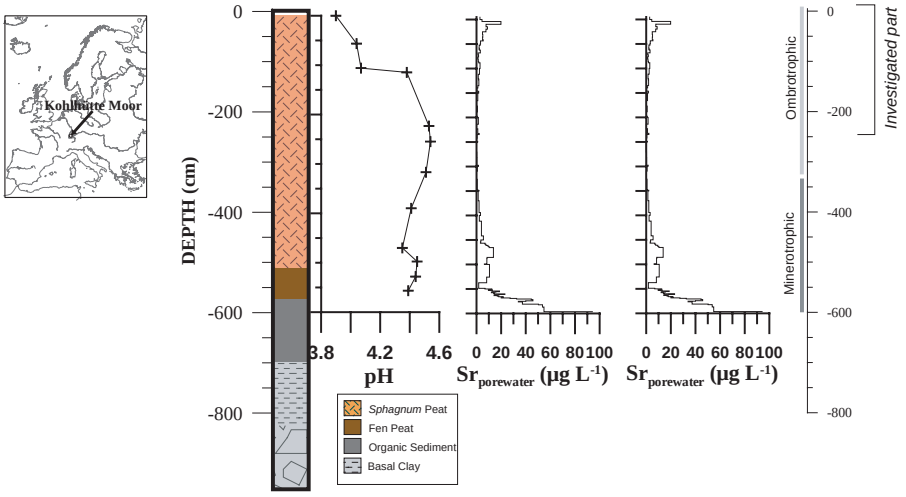

Figure 1: Status of the bog as described by the Sr concentration in the porewater and in the bulk peat samples. In this study, we only consider the samples where the minerals were entering the bog through atmospheric deposition.

STUDY AREA

Kohlhütte Moor is an ombrotrophic peat bog formed on glacial clays in the Black Forest, in the southern part of Germany (Fig.1). It is a *Sphagnum*-dominated bog where the main *Sphagnum* species are: *Augustifolium*, *Cuspidatum*, *Magellanicum*, and the main vascular plant *Eriophorum Vaginatum*. The complete flora is described in Dierssen and Dierssen (1984). This bog has accumulated more than 6m of peat in 10000 years (Fig.1 and Fig. DR1). The first five meters of peat accumulation are *Sphagnum* peat. The deeper samples are *Carex* peat underlain by organic-rich lake sediments on plastic clays (Fig.1). The average annual precipitation in this area is 1800 mm $year^{-1}$.

This bog is surrounded by soils derived from granite. The main minerals of this granite are quartz, plagioclase (An_{15-35}), K-feldspar and Ti-riched biotite (Sawatzki, 1992). Apatite is a common accessory mineral (<0.5 %).

METHODS

In Spring 2002, a complete peat profile including living *Sphagnum* was collected using a Wardnaar and a Belarussian corers as described by Le Roux et al. (2002) and by Givelet et al. (2004). Peat cores were cut precisely using stainless steel band saws.

Peat sub-samples were then dried and milled. Bulk peat chemistry was analysed directly using XRF on powders as well as using inductive coupled plasma optical emission spectrometry and mass spectrometry (ICP-OES and ICP-MS) after complete acid digestion (Krachler et al., 2002).

Sub-samples of wet peat were squeezed to obtain pore waters. After filtration (0.45 µm) with pre-cleaned filters, they were analysed using ICP-OES for major elements and Sr.

Strontium concentrations in bulk peat and porewaters (Fig.1) allow two distinct depositional environments to be distinguished: the deeper part (330 cm to 600 cm) with relatively high concentrations reflecting inputs of Sr from mineral weathering as well as atmospheric deposition. In contrast, the upper part (-330 cm, surface) contains lower Sr concentrations because this section of the core is supplied with Sr only by atmospheric inputs.

Selected peat samples from the upper part were also ashed at 550°C over night for ash. Mineralogical determinations were performed using X-ray diffraction (XRD) employing a Siemens D501 diffractometer with a step-scanning size from 2.5 to 70°, a step size of 0.02° and a counting time of 2s per step. Background stripping, indexation of the diffraction peaks, and mineral identification were carried out using MacDiff 4 Software (Petschick, 2005).

Radionuclides (^{210}Pb, ^{241}Am, ^{214}Pb, ^{137}Cs) were measured using low background gamma spectrometry (GCW4028, HPGE, Canberra). The maximum depth at which unsupported ^{210}Pb could be detected is 18 cm. The age-depth relationship was calculated using the ^{210}Pb CRS model (Appleby and Oldfield, 1978). For deeper samples, twenty-three ^{14}C AMS dates were performed at the ETH Zürich allowing the calculation of a robust age-depth model (C.I.).

Snow samples from a snow pack and the surface of the snow layer were collected at proximity from the coring point (3m) in the winter 2003 (Le Roux and Aubert, 2003). Samples after filtration with pre-cleaned filters (0.45µm) were measured for cations by ICP-OES and for anions by ion chromatography. Filters representing the particulate deposition in the bog were analysed using ICP-OES and ICP-MS after digestion with HNO_3.

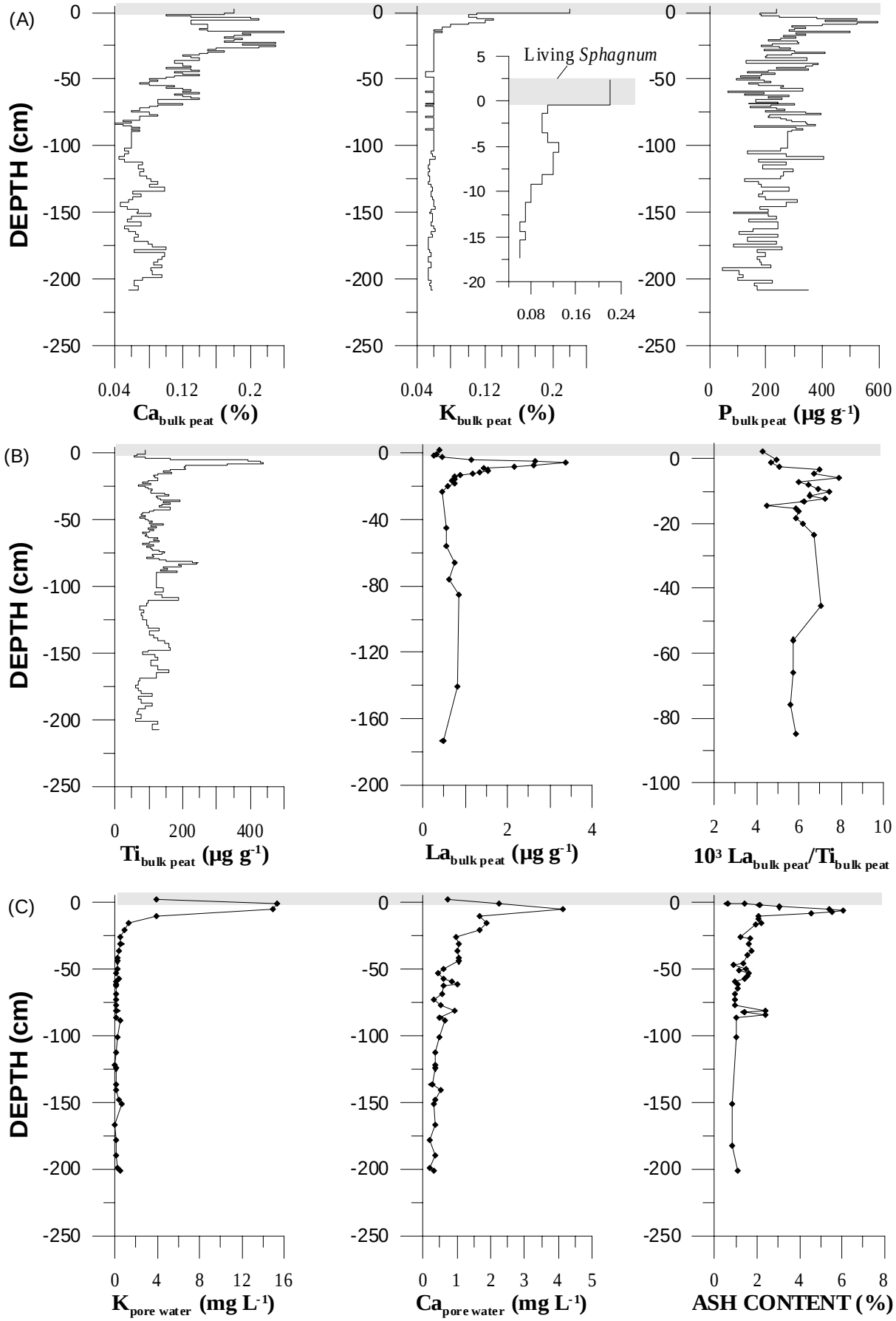

Figure 2: a) Ca, K, P, Ti, La concentrations in bulk peat (in grey: living moss, shaded: increase in ash)
b) Ti, La concentrations in bulk peat and La/Ti
c) K and Ca in the porewaters and ash content of the peat

Depth (cm)	Age Dating	Quartz	Calcite	Apatite	Feldspaths	Calcite Relative to Quartz	Apatite Relative to Quartz	Feldspars Relative to Quartz
+4.5 ; 0	*2002 A.D.*	X	XXX	XX	X	XXX	X	X
0 ; -1.7	*1991 A.D.*	X	XX	XX	XX	XX	XX	XXX
-1.7 ;-2.9	*1989 A.D.*	X	X	XX	(X)	X	X	X
-2.9 ;-4	*1983 A.D.*	XX	XX	XXX	X	XX	X	X
-4 ;-5	*1972 A.D.*	XXX	0	X	XXX	-	(X)	(X)
-5 ;-6.3	*1952 A.D.*	XXX	0	0	XXX	-	-	XX
-6.3 ;-7.6	*1927 A.D.*	XXXX	0	0	XXXX	-	-	X
-7.6 ;-8.7	*1906 A.D.*	XXX	0	0	XX	-	-	X
-9.6 ;-10.1	*1890 A.D.*	XXXX	0	0	XXX	-	-	X
-11.7 ;-12.2	1855 A.D.	XX	0	0	XX	-	-	XX
-15.8 ;-16.3	1820 A.D.	XX	0	0	XX	-	-	X
-41.4 ;-42.5	1400 A.D.	XX	0	0	(X)	-	-	(X)
-100 ; -101	750 A.D.	XX	0	0	X	-	-	X
-150 ; -151.8	200 A.D.	XXX	0	0	X	-	-	X
-200 ; -202.1	470 B.C.	XX	0	0	X	-	-	X

Table 1: Mineralogy of the samples using XRD, with age dating based on the combined ^{210}Pb CRS age model and the linear ^{14}C model. The relative intensity decreases in the order (XXXX,XXX,XX,X,(X)).

RESULTS

Calcium, potassium and phosphorus concentrations in the bulk peat are elevated in the topmost parts of the peat profile (Fig.2.a). Potassium and phosphorus are also enriched in the living plants (the 2 first samples) but also deeper at -5cm. This second peak is linked to a peak in the ash content and in conservative elements such as Ti, Al or REE (Fig.2b). Higher concentrations of potassium and calcium could be found in the surface samples.

The mineralogy of the ashed samples is given in the Table 1. Quartz is the main mineral found in the peat with feldspars also abundant. Using only the XRD pattern and because of the low intensity of the diffraction peaks, it is difficult to determine the relative proportions of plagioclase and K-feldspars because they have overlapping diffraction peaks. The abundance of quartz and feldspars follow the distribution of conservative elements (Ti, Al, La) with a peak at –5cm (Fig.2 b).

Apatite and calcite are only in the samples above - 4 cm corresponding to the living plants and the litter derived from them. The apatite was found to be mainly fluorapatite.

ORIGIN OF THE MINERALS

The main minerals present in the bog are the most abundant minerals in the granite. We therefore hypothesize that the dust entering the Black Forest bog is mainly of local origin. Biotite was not found in the peat ash samples, this may be because of reductive dissolution in the anoxic waters, or because the XRD analyses did not have sufficient sensitivity.

Calcite is also present. Its origin is not well determined; this mineral is present in weathering veins of the granite as secondary mineral but possibly comes from other sources such as remote sources like loess formations in the Rhine Valley or forest liming.

DISTRIBUTION OF THE MINERALS LINKED TO THE GEOCHEMISTRY OF THE BOG

Calcite and apatite are only present in the first cm of the peat core (Table 1). There are two hypothesis for this distribution patterns: (1) the composition of mineral dust entering the bog varied greatly with time with apatite and calcite being added only recently to the upper layer; (2) apatite and calcite are continuously supplied naturally to the bog by dust deposition but are dissolved under the acidic conditions of the bog. We examine the first hypothesis concerning apatite using the La concentration. Apatite is one of the main host mineral for REE (Aubert et al., 2002) and REE are thought to be immobile in the peat column (Krachler et al., 2003). If apatite

deposition increased during the past 20 years (Table 1), there should also be an increase in La concentrations and accumulation rates. However, this is not the case, and the ratio La/Ti is quite constant and do not increase in the topmost samples. We conclude that apatite is dissolving rapidly because of its small particle size and the low pH of the waters. It is difficult to assess whether the dissolution of apatite is progressive or if it is a very rapid but combined to the litter (i.e.: release of organic acids by moss decomposition). Assuming that the minerals are not physically moving in the acrotelm (Punning and Alliksaar, 1997), the life time of apatite is approximately 30 years.

With respect to calcite, there is no analogous trace metal (such as La) to independently monitor its input and fate. However given that the solubility of calcite is ca. two-three orders of magnitude greater than apatite (Kowaleski and Rimstidt, 2003; Plummer et al., 1978; Valsami-Jones et al., 1998), we suggest that calcite is subject to the same fate. Assuming a constant rate of supply calcite in atmospheric soil dust, the lifetime of calcite in acidic peat is ca. 20 years.

The presence of apatite one cm deeper than calcite is in agreement with slower experimental dissolution rate of apatite compared to calcite at pH ~ 4 (Kowaleski and Rimstidt, 2003).

The distribution of feldspars and quartz peaked around –5cm and this is correlated with a peak in ash and conservative elements. Potassium increased also at this depth (Fig.2a) Whereas the peak of potassium in the living mosses can be explained by plant retention (Malmer, 1988), the subsurface peak cannot. The distribution of K in the subsurface peats, therefore, is better explained by the distribution of minerals especially K-feldspars.

In contrast to the bog studied by Bennett et al. (1991), here we find no decrease in the abundance of feldspars relative to quartz. As suggested by Steinmannn and Shotyk (1997), the distribution of feldspars in the peat bog seems to be unaffected by low pH (4-4.5) and abundance of organic acids (e.g. 50 mg L^{-1}). As pointed out by Steinmannn and Shotyk (1997), the feldspar dissolution rate in peat is lower than those derived from experiment studies using HCl at pH 4 (Brantley, 2004). There are several possible reasons for the apparent differences in the silicate weathering rates presented here versus those published by Bennett et al. First, the Lost River Peatland (LRP), which was studied by Bennett et al. is not an ombrotrophic bog. Although bog plants at the surface dominate it, the peat column was assumed to be ombrotrophic, based on the stratigraphy of fossil plants (D.I. Siegel, personal communication). However, given the pH data, which they presented, the peat column, which they studied, appears to be mainly minerotrophic. Geochemical studies have shown that the botanical "bog/fen limit" may be several metres below the minerotrophic/ombrotrophic boundary (Shotyk, 1996). In fact, in the LRP, it may be that only the surface peat layer is truly ombrotrophic. Second, hydrological studies of the LRP have shown that it has a relatively high flushing rate; this process would have the effect of removing dissolved solutes from the porewaters, reducing the saturation state with respect to the dominant mineral phases, thereby promoting mineral dissolution.

Finally, the waters of LRP are much less acidic. Bennett et al. reported a loss of Si from the silicates, relative to Al. At low pH, it is the other way around. Experimental studies of plagioclase feldspar weathering at pH 4 have unambiguously shown that Al is depleted from the surface of the mineral, relative to Si (Correns and von Engelhardt, 1938, Shotyk and Metson, 1994).

ELEMENT	Particulate DEPOSITION (µg/g of solid)	Particulate DEPOSITION (ng/L of snow water)	WET DEPOSITION (ng/L)	Part./TOT(%) %
K	2250	3500	40000	8
Ca	950	1500	20000	7
P	550	850	<30	97

Table 2: typical values of the snow pack in Black Forest. Particulate deposition expressed as µg/g of solid and also as ng/L of snow water.

APATITE DISSOLUTION AS A SOURCE OF P FOR BOG PLANTS

The analyses of snow samples shows that most of the phosphorus being supplied to the bog arrives in the form of particles (Table 2). Apatite is one of the most important P-bearing primary minerals, and it has been identified in the surface layers of the bog. Apatite is not found in the deeper layers, suggesting that it dissolves rapidly in the acidic peat . Because P is probably one of the most important growth-limiting nutrient to bog plants (Small, 1972), the dissolution of apatite appears to be by far the most significant source of plant-available P to this unique plant community. Variations in rates of atmospheric deposition of soil dust containing apatite, therefore, might have an effect on the growth rate of bog plants, and therefore the accumulation rate of peat. As peatlands are an important carbon pool, the links between the dust deposition, mineral weathering, plant growth, and carbon accumulation, may be relevant to the global carbon cycle.

CONCLUSIONS

Ombrotrophic peat bogs receive mineral particles only from soil dust supplied by the atmosphere. Some of these minerals dissolve rapidly (calcite, apatite) whereas others appear to be preserved for thousands of years (quartz and feldspars). Fe-bearing minerals might be weathering rapidly due to reductive dissolution but this has not yet been clearly established. The most important factors governing mineral dissolution in peat appear to be pH, Eh, and the structure of the mineral. The low pH has an immediate effect on calcite and apatite, which dissolve readily; these minerals are relatively soluble and are quickly exhausted from the peat column. The anoxic conditions promote the reduction dissolution of Fe oxides, but Fe-bearing silicates probably suffer the same fate. In contrast, the silicates (quartz and feldspars) are well preserved, despite the low pH and the abundance of organic acids. The stability of quartz is to be expected given the solubility of quartz independently of pH below ca.pH 9 (Krauskopf, 1979).

The feldspars, however, are more complicated. In acidic solutions, experimental studies of the surface layers have shown that Al is removed, relative to Si, leaving behind a siliceous enriched layer. The rate of the layer is the rate-controlling step of feldspar dissolution, and it is unaffected by organic acids, and pH. We hypothesize that although feldspars might initially subject to surface attack, this process effectively stops as soon as a siliceous layer develops. An alternative hypothesis is that the surface layers become coated with humic acids (Ochs, 1996) or iron oxides (Nugent et al., 1998), which effectively shut down the dissolution process (Brantley, 2004).

The preservation of quartz and feldspars in ombrotrophic peat might make them useful archives of the changing rates of atmospheric dust deposition since the Last Glacial.

Acknowledgements

We would like to thank S. Person from the Regierungpräsidium Freiburg for coring permission, T. Noernberg (Ostende), A. Schleicher for her help with the XRD measurements, A. Cheburkin for the XRF measurements, P. Stille and D. Aubert for the ICP-MS measurements in Strasbourg and B. Kober for the original idea of the project. This work was funded by the Deutsche Forschung Gemeinschaft through the GRK 273 (www.geofluids.de).

BIBLIOGRAPHY:

Aerts, R., Verhoeven, J.T.A., and Whigham, D.F., 1999, Plant-mediated controls on nutrient cycling in temperate fens and bogs: Ecology, v. 80, p. 2170-2181.

Appleby, P.G., and Oldfield, F., 1978, The calculation of lead-210 dates assuming a constant rate of supply of unsupported 210Pb to the sediments: Catena, v. 5, p. 1-8.

Aubert, D., Stille, P., Probst, A., Gauthier-Lafaye, F., Pourcelot, L., and Del Nero, M., 2002, Characterization and migration of atmospheric REE in soils and surface waters: Geochimica et Cosmochimica Acta, v. 66, p. 3339-3350.

Bennett, P.C., Siegel, D.I., and Glaser, P.H., 1991, Fate of silicate minerals in a peat bog: Geology, v. 19, p. 328-331.

Bischoff, G., 1854, Elements of chemical and physical geology: London, Cavendish Society, 158 p.

Björck, S., and Clemmensen, L.B., 2004, Aeolian sediment in raised bog deposits, Halland, SW Sweden: a new proxy record of Holocene winter storminess variation in southern Scandinavia: The Holocene, v. 14, p. 677-688.

Brantley, S.L., 2004, Reaction kinetics of primary rock-forming minerals under ambient conditions, *in* Drever, J.I., ed., Fresh water geocemistry, weathering, and soils: Treatise on Geochemistry: Oxford, Pergamon Press, p. 73-118.

Dierssen, B., and Dierssen, K., 1984, Vegetation und Flora der Schwarzwaldmoore: Karlsruhe, Landesanstalt für Umweltschutz Baden-Württemberg, 512 p.

Dierssen, K., and Dierssen, B., 2001, Moore: Stuttgart, Ulmer, 230 p.

Dörfler, W., 1992, Radiography of peat profiles: a fast method for detecting human impact on vegetation and soils: Vegetation history and archaeobotany, v. 1, p. 93-100.

Finney, H.R., and Farnham, R.S., 1968, Mineralogy of the inorganic fraction of peat from two raised bgs in northern Minnesota, Third International Peat Congress, p. 102-108.

Givelet, N., Le Roux, G., Cheburkin, A.K., Chen, B., Frank, J., Goodsite, M.E., Kempter, H., Krachler, M., Noernberg, T., Rausch, N., Rheinberger, S., Roos-Barraclough, F., Sapkota, A., Scholz, C., and Shotyk, W., 2004, Suggested protocol for collecting, handling and preparing peat cores and peat samples for physical, chemical, mineralogical and isotopic analyses: Journal of Environmental Monitoring, v. 6, p. 481-492.

Gorham, E., 1991, Northern Peatlands: Role in the Carbon Cycle and Probable Responses to Climatic Warming: Ecological Applications, v. 1, p. 182-195.

Hunt, T.S., 1875, Chemical and Geological Essays: Boston, Osgood.

Kowaleski, M., and Rimstidt, J.D., 2003, Average lifetime and age spectra of detrital grains: toward a unifying theory of sedimentary particles: Journal of geology, v. 111, p. 427-439.

Krachler, M., Mohl, C., Emons, H., and Shotyk, W., 2002, Analytical procedures for the determination of selected trace elements in peat and plant samples by inductively coupled plasma spectrometry: Spectrochimica Acta Part B, v. 57.

—, 2003, Two thousand years of atmospheric rare earth element (REE) deposition as revealed by an ombrotrophic peat bog profile, Jura Mountains, Switzerland: Journal of Environmental Monitoring, v. 5, p. 111-121.

Krauskopf, K.B., 1979, Introduction to geochemistry, 617 p.

Le Roux, G., and Aubert, D., 2003, Post expedition field and Status report (http://cf.geocities.com/gwanach/fieldreportWINTER.pdf): Heidelberg, Institute of Environmental Geochemistry, p. 11.

Le Roux, G., Shotyk, W., and Kober, B., 2002, Post expedition field and Status report (http://cf.geocities.com/gwanach/fieldreport.pdf): Heidelberg, Institute of Environmental Geochemistry, p. 15.

Malmer, N., 1988, Patterns in the growth and the accumulation in inorganic constituents in the Sphagnum cover on ombrotrophic bogs in Scandinavia: Oikos, v. 53.

Nugent, M.A., Brantley, S.L., Pantano, C.G., and Maurice, P.A., 1998, The influence of natural mineral coatings on feldspar weathering: Nature, v. 395, p. 588-591.

Ochs, M., 1996, Influence of humified and non-humified natural organic compounds on mineral dissolution: Chemical Geology, v. 132, p. 119-124.

Petschick, R., 2005, MacDiff Software: Erlangen.

Plummer, L.N., Wigley, T.M.L., and Parkhurst, D.L., 1978, The kinetics of calcite dissolution in CO2-water system at 5° to 60°C and 0. to 1.0 atm CO2: American Journal of Science, v. 278.

Punning, J.-M., and Alliksaar, T., 1997, The traping of fly-ash particles in the surface layers of Sphagnum-dominated peat: Water, Air and Soil Pollution, v. 94, p. 59-69.

Renberg, I., Bindler, R., and Brännvall, M.-L., 2001, Using the historical atmospheric lead-deposition record as a chronological marker in sediments deposits in Europe: The Holocene, v. 11, p. 511-516.

Sawatzki, G., 1992, Erlaüterung zu Blatt 8214 St. Blasien: Stuttgart, Geologischen Landesamt Baden-Württemberg, 157 p.

Shotyk, W., 1996, Peat Bogs archives of atmospheric metal deposition: geochemical evaluation of peat profiles, natural variations in metal concentrations, and metal enrichment factors: Environmental Reviews, v. 4, p. 149-183.

—, 2001, Geochemistry of the peat bog at Etang de la Gruère, Jura Mountains, Switzerland, and its record of atmospheric Pb and lithogenic trace metals (Sc, Ti, Y, Zr, and REE) since 12,370 14C BP: Geochimica et Cosmochimica Acta, v. 65, p. 2337-2360.

Shotyk, W., Krachler, M., Martinez-Cortizas, A., Cheburkin, A.K., and Emons, H., 2002, A peat bog record of natural, pre-anthropogenic erichments of trace elements in atmospheric aerosols since 12370 14C yr, and their variation with Holocene climate change: Earth and Planetary Science Letters, v. 199, p. 21-37.

Shotyk, W., and Metson, J.B., 1994, Secondary ion mass spectrometry (SIMS) and its application to chemical weathering: Reviews of Geophysics, v. 32.

Small, E., 1972, Ecological significance of four critical elements in plants of raised Sphagnum peat bogs: Ecology, v. 53, p. 498-503.

Smith, L.C., MacDonald, G.M., Velichko, A.A., Beilman, D.W., Borisova, O.K., Frey, K.E., Kremenetski, K.V., and Sheng, Y., 2004, Siberian peatlands a net carbon sink and global methane source since the early Holocene: Science, v. 303, p. 353-356.

Steinmann, P., and Shotyk, W., 1997, Geochemistry, mineralogy, and geochemical mass balance on major elements in two peat bog profiles (Jura Moutains, Switzerland): Chemical Geology, p. 25-53.

Valsami-Jones, E., Ragnarsdottir, K.V., Putnis, A., Bosbach, D., Kemp, A.J., and Cressey, G., 1998, The dissolution of apatite in the presence of aqueous metal cations at pH 2-7: Chemical Geology, v. 151, p. 215-233.

Verhoeven, J.T.A., Maltby, E., and Schmitz, M.B., 1990, Nitrogen and phosphorus mineralization in fens and bogs: The Journal of Ecology, v. 78, p. 713-726.

Vuorela, I., 1983, Field erosion by wind as indicated by fluctuations in the ash content of Sphagnum peat: Bulletin of the Geological Society of Finland, v. 55, p. 25-33.

Weiss, D., Shotyk, W., Kramers, J.D., and Gloor, M., 1999, Sphagnum mosses as archives of recent and past atmosperic lead deposition in Switzerland: Atmospheric Environment, v. 33, p. 3751-3763.

DATA REPOSITORY MATERIAL:

FIGURE DR1: Age depth models

A) ^{14}C age depth model; B) ^{210}Pb CRS model and comparison with the upper end of the model based on ^{14}C dates (grey circles)

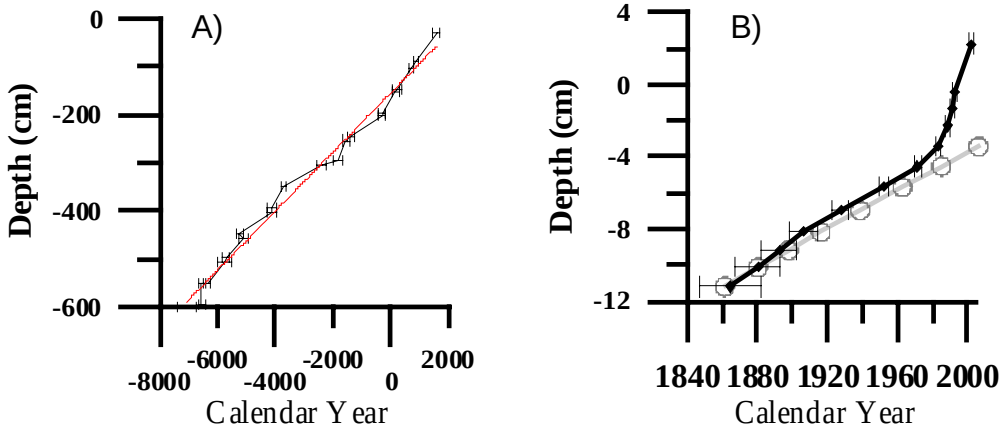

APPENDIXES

- Appendix 1 -

REE compositions of atmospheric deposition entering an ombrotrophic peat bog in Black Forest (SW Germany)

In collaboration with D. Aubert (University of Perpignan) and P. Stille (University of Strasbourg)

Introduction and objectives

Among trace metals, data for Rare Earth Elements (REE) in atmospheric precipitation are still very scarce (Freydier et al., 1998; Ikegawa et al., 1999; Aubert et al., 2002; Zhang and Liu, 2004) because these elements are often under the ng L^{-1} level, even in areas affected by human activities and therefore most of the time a pre-concentration procedure is required before analysis. Nevertheless, the problem of the REE behaviour at the atmosphere-soil interface is important because REE are more and more involved in industrial processes so that an increase of REE released in the environment could be expected (Krachler et al., 2003). Thus, recently there has been a growing interest in the use of REE as tracers of industrial processes, for example as tracer of petroleum refining (Olmez and Gordon, 1985). Moreover, understanding the behaviour of REE at the atmosphere-soil interface is important because the trivalent REE are considered as good analogues for the trivalent actinides (Johannesson et al., 1995; Stille et al., 2003) and because fission-derived REE and actinides can also be released into the atmosphere after serious nuclear accidents like in Chernobyl (Ukraine) in 1986.

Finally, because of their similar and conservative behaviours, the REE are characteristic of their sources in the environment. For example, REE could be used to trace the origin of dust (Krachler et al., 2003; Shotyk, 2001). However to our knowledge, no study have clearly evidenced that the REE atmospheric signal is preserved in the aggressive anoxic and acid environment of a peat bog. To our knowledge, it is only the fourth time that complete REE patterns are investigated in peat profiles (Akagi et al., 2002; Krachler et al., 2003; Yliruokanen and Lehto, 1995).

A vertical snow profile representing almost 2 months of deposition onto an ombrotrophic peat bog has been investigated. We compare the REE distributions in this snow pack with those of lichens and sphagnum mosses directly sampled in the same area and also with those collected at the first centimetres of a peat profile in order to know if it is possible to detect any variations in the REE distribution pattern within the snow pack representing a period of three months and also if the REE distribution in the precipitation (wet deposition and particles) is similar to the REE distribution in lichens and mosses.

The aim of this study is (1) to *assess the actual REE atmospheric deposition recorded in snow, lichens and Sphagnum mosses* (2) *to check the immobility of REE* in the profile and (2) *to determine the atmospheric REE deposition* during the past 400 years in Southern Germany.

Methods

Sampling

The vertical snow profile

The 19th of February 2003, a snow profile was dug in the 70 cm snow pack located on the ombrogenic part of the peat bog. The upper 50 centimetres consist of fresh and weakly snow. The lowermost 20 centimetres of the profile are characterized by two icy layers suggesting a melting of the snow during the second half of January. This seems to be confirmed by positive temperatures recorded at the neighbouring weather station. Each 10 cm layer was collected with PET gloves in sterile plastic bags previously "rinsed" three times with snow from the same level. Classical clean procedures to sample snow

were applied (Boutron, 1990; Nriagu et al., 1993). Three bags from every level were collected to obtain a sufficient amount of sample for measurements of major and trace elements measurements. Three additional bags were collected for snow samples at 0-10 cm, 20-30 cm and 60-70 cm in order to investigate REE concentrations. An additional snow sample was collected close to the road (about 500 m far from the snow profile) in order to evaluate the contribution of pollution directly coming from traffic and addition of salt (potash) during the winter season. Snow bags were kept frozen in an insulated box until their filtration in the Strasbourg laboratory. Snowmelt was realized at room temperature during the night. Meltwaters of the snow were filtered in an ultra-clean room using pre-cleaned 0.45 μm Millipore HAWP membranes. The filtered samples were conditioned in acid-cleaned polypropylene bottles and acidified with a sufficient amount of laboratory bi-distilled HNO_3 to reach a pH between 1 and 2. A non-acidified aliquot was preserved for pH determination and major elements analysis. The nine filtered meltwaters were then stored at 4°C.

Lichens

Two species of lichens were also sampled on trees located in the snow sampling area. These two species are *Usnea Fillipendula* commonly called "fishbone beard lichen" and *Evernia Prunastri* . The lichen samples were placed in clean plastic bags until air dry. No washing procedure of the lichens was done in order to avoid the leaching of soluble particles adsorbed on the thallus (e.g. Nimis et al., 1993). The *Evernia* species have been divided in two groups: two entire samples (evernia 1 and evernia 2) and the lichen branches extremities (evernia ext.) (2-3 mm) that are supposed to have grown recently and should have incorporated the most recent atmospheric derived material. Then lichens were crushed in a clean agate mortar before being digested 75 min at 240°C in a microwave autoclave with HNO_3 and HBF_4 as reagents, following the procedure described in Krachler et al. (2002).

Recent peat profile

In a previous sampling campaign (Le Roux et al., 2002), samples of peat from the ombrogenic part of the peat bog have been collected by a Wardnaar corer and sub-sampled in one cm slice following strictly the procedure described by Givelet et al. (2004). In this study, we considered the uppermost part of the peat bog representing ~400 years of peat accumulation estimated by ^{210}Pb age dating (Appleby and Oldfield, 1978) and ^{14}C age dating.

We also measured a deeper sample (346 cm depth) taken as a reference material characterizing the "pre-anthropogenic" period (3000 cal. B.C). The uppermost peat sample consists of living Sphagnum mosses. Peat samples were digested with the same procedure as for lichens (Krachler et al., 2002).

Analytical Methods

Chemical analyses were performed at the Centre de Géochimie de la Surface in Strasbourg and at the Institute of Environmental Geochemistry in Heidelberg.

Snow samples

pH was determined using a Meterlab PHM 210 instrument. Major cations have been determined by inductively coupled plasma-optical emission spectrometry (ICP-OES) both in Strasbourg and in Heidelberg whereas the ion chromatography (DIONEX) was applied to measure the anionic species. REE concentrations in snow samples are very low, under the ppt level (ng/l) for most of the REE. Therefore, a specific enrichment method was required. A liquid-liquid extraction technique using an organic phosphate solvent (HDEHP) was applied to enrich the REE by a factor of at least 100 (Shabani and Masuda, 1991; Tricca et al., 1999). Generally 1.5 to 3 liters of solution were necessary to achieve concentrations that could be measured by Inductively Coupled Plasma-Quadrupole Mass Spectrometer (ICP-QMS). The extraction yield of REE was checked 2 times (before the first sample extraction and after the last sample extraction) with a composite 0.01 ppb standard REE solution made using individual 1000 ppm RE standard solution from Specpure. The obtained extraction yields

for each rare earth were consistent with the average one determined by Tricca (1997).
REE and other elements were also determined in the dry deposition fraction, after dissolution of the particles previously removed from the filter by in ultrasonic bath, in bi-distilled concentrated HNO_3.
Peat and lichen samples
Peat and lichen compositions were determined using ICP-AES and ICP-QMS in Strasbourg. There is no available peat reference material with certified elemental concentrations. Therefore in addition to a lichen reference (IAEA-336 lichen, International Atomic Energy Agency, Vienna, Austria), several plant materials (GBW 07602, Bush Branches and Leaves, Institute of Geophysical and Geochemical Exploration, Langfang, China; SRM 1547, Peach Leaves, NIST; SRM 1573a, Tomato Leaves, NIST) with certified and information concentrations for REE and other trace elements were analysed in order to control the quality of digestion and analytical procedures (Table 1). These standard materials were digested in the same runs together with the Black Forest peat and lichens samples. Procedural blanks were also conducted and revealed no contamination from the reagents except for Tb. Measurements of the Reference Standards for all the elements are within the range of the certified values.

	Tomato leaves SRM 1573a		Bush Branches GBW 07602		Peach leaves SRM 1547		Lichen IAEA-336		
Elements ICP-AES	Std mes.	Certif. val. (inform. val.)	Std mes.	Certif. val. (inform. val.)	Std mes.	Certif. val. (inform. val.)	Mes 1.	Mes 2.	Rec. Val. 95% C.I. (inform. val.)
Al	466	598 ± 12	1850	2140 ± 70	237	249 ± 8	700	697	(680 ± 110)
Elements ICP-MS									
La	2.12	(2.3)	1.20	1.23 ± 0.07	9.33	(9)	0.61	0.57	0.66 ± 0.1
Ce	1.69	(2)	2.40	2.4 ± 0.19	10.53	(10)	1.27	1.21	1.28 ± 0.17
Pr	0.34	-	0.27	-	1.88		0.15	0.15	
Nd	1.28	-	1.04	(1.1)	7.41	(7)	0.59	0.59	(0.60 ± 0.18)
Sm	0.19	(0.19)	0.20	0.19 ± 0.01	1.15	(1)	0.113	0.113	0.106 ± 0.014
Eu	0.045	-	0.039	0.037 ± 0.002	0.21	(0.17)	0.024	0.025	(0.023 ± 0.004)
Gd	0.25	(0.17)	0.20	-	1.31	(1)	0.099	0.094	
Tb	0.018	-	0.020	(0.026)	0.13	(0.1)	0.011	0.012	(0.014 ± 0.002)
Dy	0.11	-	0.14	-	0.57		0.084	0.090	
Ho	0.023	-	0.027	-	0.10		0.016	0.016	
Er	0.064	-	0.080	-	0.27		0.047	0.049	
Tm	0.007	-	0.011	-	0.028		0.007	0.007	
Yb	0.045	-	0.072	0.063 ± 0.011	0.16	(0.2)	0.042	0.044	(0.037 ± 0.012)
Lu	0.006	-	0.011	-	0.021		0.0063	0.0066	(0.0066 ± 0.0024)

Table 1: Chemical analyses of the different certified materials used to validate the digestion procedure of the peat and lichen samples

Preliminary Results:

Distribution of REE in the snow (table 2)

To our knowledge, it is the first time that a snow pack profile has been investigated for the REE.
Rare Earth Elements (REE) concentrations in the dissolved fraction in the 4 selected snow samples (SBF road, SBF 0-10, SBF 20-30, SBF 60-70) are reported in the Table 2. SBF 20-30 and SBF 60-70 show almost the same REE concentrations and have lower concentrations compared to the surface snow samples and especially SBF road, which is supposed to be largely affected by traffic contamination.

REE concentrations are much higher in the dust sample from the SBF road (P.M. SBF road) than in SBF 0-10 collected on the peat bog (x 1.3 for Sm to 2.6 for Gd).
The dry/wet ratio in SBF 0-10 is on the order of 1/1, whereas in the SBF road the ratio dry/wet ratio is 10/1. This is not due to higher REE concentrations in PM SBF road but simply due to a higher particle load in the snow sample collected near the road. In addition, compared to the respective dissolved REE concentrations, both samples representing the particulate matter are HREE depleted with Yb/La close to 0.5.

Sample	*SBF Road*	*SBF 0-10*	*SBF 20-30*	*SBF 60-70*	**SBF Road P.M.**		**SBF 0-10 P.M.**	
	ng L^{-1}	*ng L^{-1}*	*ng L^{-1}*	*ng L^{-1}*	*µg g^{-1}*	*ng L^{-1}*	*µg g^{-1}*	*ng L^{-1}*
Depth (cm)	0-10	0-10	20-30	60-70	0-10		0-10	
La	10.31	6.53	1.63	1.05	26.25	56.00	3.34	5.22
Ce	18.93	11.97	2.426	2.337	42.79	91.28	6.34	9.92
Pr	1.97	1.35	0.254	0.280	4.79	10.21	0.69	1.07
Nd	8.26	5.00	1.008	1.000	15.82	33.75	2.51	3.92
Sm	1.60	0.95	0.177	0.194	2.79	5.94	0.45	0.70
Eu	0.25	0.22	0.034	0.033	0.67	1.42	0.09	0.14
Gd	1.99	1.16	0.238	0.207	3.29	7.01	0.47	0.74
Tb	0.29	0.12	0.029	0.035	0.46	0.98	0.05	0.07
Dy	1.41	0.79	0.187	0.154	1.75	3.73	0.28	0.43
Ho	0.28	0.15	0.032	0.035	0.46	0.99	0.05	0.08
Er	0.75	0.48	0.088	0.095	1.06	2.27	0.15	0.24
Tm	nd	nd	nd	nd	0.22	0.46	0.02	0.03
Yb	0.78	0.57	0.113	0.067	0.99	2.10	0.13	0.20
Lu	nd	nd	nd	nd	0.21	0.45	0.02	0.03

Table 2: Rare Earth Elements (REE) concentrations in the 4 selected snow meltwater samples (ng L^{-1}) and in the particles from the snow collected close to the road (SBF road P.M.) and from the surface snow (SBF 0-10 P.M.) (µg g^{-1} of particles and ng L^{-1} of bulk snow)

Comparison of the REE patterns of peat mosses, lichens and snow

A preliminary comparison between the different types of samples show that the REE patterns normalized to the post Archean average shale (PAAS, Mc Lennan, 1989) (taken as reference composition for dominantly terrigenous sediments and as used commonly in these REE studies on sedimentary rocks) have similar shapes with a slight increase in the middle rare earth elements.

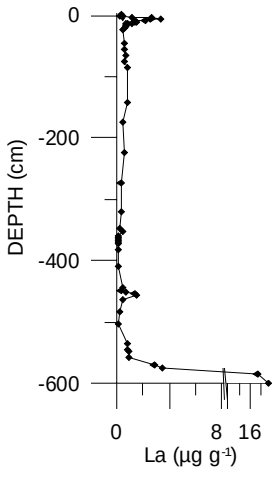

Figure 1: La concentration vs. depth in the peat profile, all the REE have the same distribution

These preliminary results are promising because:

1) the REE patterns between snow, lichen and surface peat sample are quite similar and therefore we can assume that REE distribution is preserved in the peat profile despite for example dissolution of apatite, a REE-hosting mineral (cf. Chap.3.1)
2) if the REE are not affected by mineral dissolution and other geochemical processes inside the peat profile, the REE patterns can be used as fingerprints of the sources of dust as suggested by Shotyk (2002) and Krachler (2003).

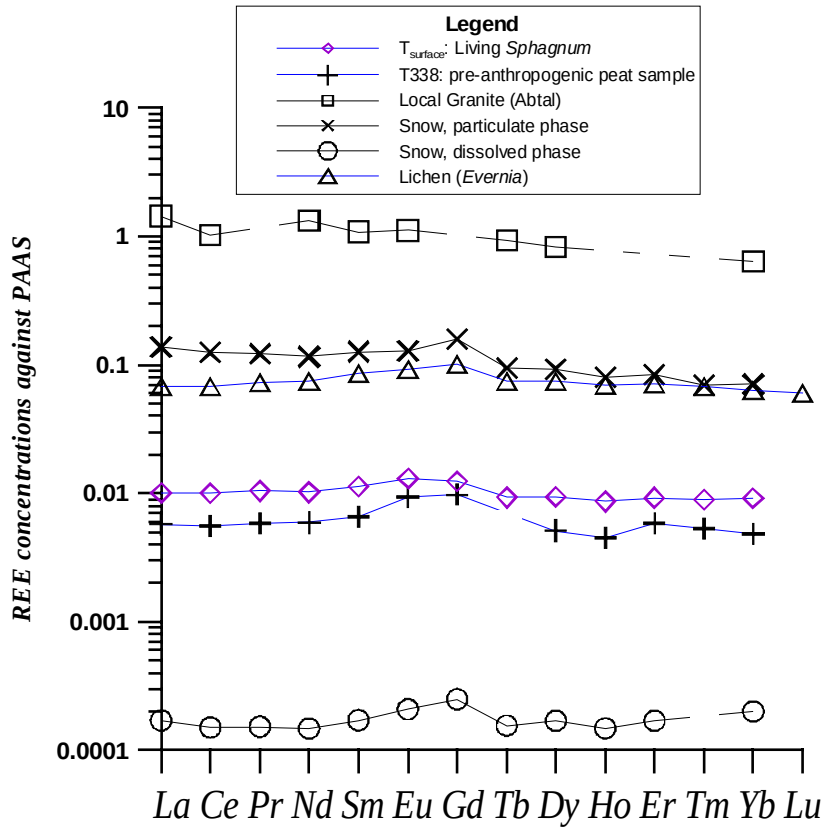

Figure 2: REE patterns normalised to the post Archean Australian shale (PAAS)

References

Akagi T., Feng-Fu F., and Yabuki S. (2002) Absence of Ce anomaly in the REE patterns of peat moss and peat grass in the Ozegahra peatland. *Geochemical Journal* 36, 113-118.

Appleby P. G. and Oldfield F. (1978) The calculation of lead-210 dates assuming a constant rate of supply of unsupported 210Pb to the sediments. *Catena* 5, 1-8.

Aubert D., Stille P., Probst A., Gauthier Lafaye F., Pourcelot L., Del Nero M. (2002)
Characterization and migration of atmospheric REE in soils and surface waters. *Geochim. Cosmochim. Acta*, 66, 3339-3350.

Boutron C.F.(1990) A clean laboratory for ultralow concentration heavy metal analysis.
Fresenius Journal of Analytical Chemistry (337), 482-491.

Freydier R., Dupré B., Lacaux J.P. (1998) Precipitation chemistry in intertropical Africa. *Atmos. Envir.*, 32, 4, 749-765.

Givelet N., Le Roux G., Cheburkin A. K., Chen B., Frank J., Goodsite M. E., Kempter H., Krachler M., Noernberg T., Rausch N., Rheinberger S., Roos-Barraclough F., Sapkota A., Scholz C., and Shotyk W. (2004) Suggested protocol for collecting, handling and preparing peat cores and peat samples for physical,

chemical, mineralogical and isotopic analyses. *Journal of Environmental Monitoring* 6, 481-492.

Ikegawa M., Kimura M., Honda K., Akabane I., Makita K., Motoyama H., Fujii Y., Itokawa Y. (1999) Geographical variations of major and trace elements in East Antarctica. *Atmos. Envir*., 33, 1457-1467.

Johannesson K.H., Stetzenbach K.J., Hodge V.F. (1995) Speciation of the rare earth element neodymium in groundwaters of the Nevada Test Site and Yucca Mountain and implications for actinide solubility. *App. Geochem.*, 10, 5, 565-572.

Krachler M., Mohl C., Emons H., Shotyk W. (2003) Two thousand years of atmospheric rare earth element (REE) deposition as revealed by an ombrotrophic peat bog profile, Jura Mountains, Switzerland. *J. Environ. Monit*., 5, 111-121.

Krachler M., Mohl C., Emons H., Shotyk W. (2002) Influence of digestion procedures on the determination of rare earth elements in peat and plant samples by USN-ICP-MS. *J. Anal. At. Spectrom*., 17, 844-851.

McLennan T.M. (1989) Rare earth elements in sedimentary rocks: Influence of provenance and sedimentary processes. In: *Reviews in Mineralogy. Geochemistry and mineralogy of rare earth elements* (Eds B.R. Lippin and G.A. McKay), 21, 169-200.

Nimis L., Castello M., Perotti M. (1993) Lichens as bioindicators of heavy metal pollution: a case study at La Spezia (N Italy). In: *Plants as biomonitors. Indicators for heavy metals in the terrestrial environment.* (Ed. Bernd Markert), Weinheim, New York, Basel, Cambridge, 644 p.

Nriagu J.O., Lawson G., Wong H.K.T., Azcue J. M. (1993) A protocol for minimizing contamination in the analysis of trace metals in great lakes waters. *Journal of Great Lakes Research* 19(1), 175-182.

Olmez I., Gordon G.E. (1985) Rare earths: atmospheric signature for oil-fired power plants and refineries. *Science*, 229, 966-968.

Shabani M.B., Masuda A. (1991) Sample introduction by on-line two-stage solvent extraction and back-extraction to eliminate matrix interference and to enhance sensitivity in the determination of rare earth elements with inductively coupled plasma spectrometry. *Anal. Chem.* 63, 2099-2105.

Shotyk W., Weiss D., Kramers J.D., Frei R., Cheburkin A.K., Gloor M., Reese S. (2001) Geochemistry of the peat bog at Etang de la Gruère, Jura Mountains, Switzerland, and its record of atmospheric Pb and lithogenic trace metals (Sc, Ti, Y, Zr, and REE) since 12,370 ^{14}C yr BP. *Geochim. Cosmochim. Acta*, 65, 2337-2360.

Shotyk W., Krachler M., Martinez-Cortizas A., Cheburkin A. K., and Emons H. (2002) A peat bog record of natural, pre-anthropogenic erichments of trace elements in atmospheric aerosols since 12370 14C yr, and their variation with Holocene climate change. *Earth and Planetary Science Letters* 199, 21-37.

Stille P., Gauthier-Lafaye F. Jensen K.A., Salah S., Bracke G., Ewing R.C., Louvat D., Million D. (2003) REE mobility in groundwater proximate to the natural fission reactor at Bangombé (Gabon). *Chem. Geol*., 198, 3-4, 289-304.

Tricca A. (1997) Transport mechanisms of trace elements in surface and ground water: Sr, Nd, U and Rare Earth Elements evidence. *PhD Thesis*, Univ. Louis Pasteur, Strasbourg, 234 p. + appendix.

Tricca A., Stille P., Steinmann M., Kiefel B., Samuel J., Eikenberg J. (1999) Rare earth elements and Sr and Nd compositions of dissolved and suspended loads from small river systems in the Vosges Mountains (France), the river Rhine and the groundwater. *Chem. Geol*. 160, 139-158.

Yliruokanen I. and Lehto S. (1995) The occurence of rare earth elements in some finnish mires. *Bulletin of the Geological Society of Finland*, 27-38.

Zhang J., Liu C.Q. (2004) Major and rare earth elements in rainwaters from Japan and East China Sea: Natural and anthropogenic sources. *Chem. Geol.*, 209, 315-326.

- Appendix 2 -

Geochimica et Cosmochimica Act, Vol. 69, No. 1 pp. 1-17, 2005

Accumulation rates and predominant atmospheric sources of natural and anthropogenic Hg and Pb on the Faroe Islands

W. Shotyk,[1,*] M. E. Goodsite,[2,†] F. Roos-Barraclough,[3,‡] N. Givelet,[3,§] G. Le Roux,[1] D. Weiss,[4] A. K. Cheburkin,[1] K. Knudsen,[5] J. Heinemeier,[6] W. O. van Der Knaap,[7] S. A. Norton,[8] and C. Lohse,[5]

[1]Institute of Environmental Geochemistry, University of Heidelberg, INF 236, D-69120 Heidelberg, Germany
[2]Department of Atmospheric Environment, National Environmental Research Institute of Denmark, Frederiksborgvej 399, P. O. Box 358, DK-4000 Roskilde, Denmark
[3]Institute of Geological Sciences, University of Berne, Baltzerstrasse 1-3, CH-3012 Berne, Switzerland
[4]Earth Science and Engineering, Imperial College, RSM Building, Prince Consort Road, London SW7 2BP England
[5]Environmental Chemistry Research Group, Department of Chemistry, University of Southern Denmark, Odense University, Campusvej 55, Odense M, Denmark
[6]AMS 14C Dating Laboratory, IFA, Aarhus University, Aarhus, Denmark
[7]Institute of Plant Sciences, University of Berne, Altenbergrain 21, CH-3013 Berne, Switzerland
[8]Department of Earth Sciences, Bryand Global Sciences Center University of Maine, Orono, Maine 04469-5790 USA

(*Received July* 24, 2003; *accepted in revised form June* 3, 2004)

Abstract—A monolith representing 5420 ^{14}C yr of peat accumulation was collected from a blanket bog at Myrarnar, Faroe Islands. The maximum Hg concentration (498 ng/g at a depth of 4.5 cm) coincides with the maximum concentration of anthropogenic Pb (111 μg/g). Age dating of recent peat accumulation using ^{210}Pb (CRS model) shows that the maxima in Hg and Pb concentrations occur at AD 1954 ± 2. These results, combined with the isotopic composition of Pb in that sample (^{206}Pb/^{207}Pb = 1.1720 ± 0.0017), suggest that coal burning was the dominant source of both elements. From the onset of peat accumulation (ca. 4286 BC) until AD 1385, the ratios Hg/Br and Hg/Se were constant (2.2 ± 0.5 × 10^{-4} and 8.5 ± 1.8 × 10^{-3}, respectively). Since then, Hg/Br and Hg/Se values have increased, also reaching their maxima in AD 1954. The age date of the maximum concentrations of anthropogenic Hg and Pb in the Faroe Islands is consistent with a previous study of peat cores from Greenland and Denmark (dated using the atmospheric bomb pulse curve of ^{14}C), which showed maximum concentrations in AD 1953.

The average rate of atmospheric Hg accumulation from 1520 BC to AD 1385 was 1.27 ± 0.38 μg/m^2/yr. The Br and Se concentrations and the background Hg/Br and Hg/Se ratios were used to calculate the average rate of *natural* Hg accumulation for the same period, 1.32 ± 0.36 μg/m^2/yr and 1.34 ± 0.29 μg/m^2/yr, respectively. These fluxes are similar to the preanthropogenic rates obtained using peat cores from Switzerland, southern Greenland, southern Ontario, Canada, and the northeastern United States. Episodic volcanic emissions and the continual supply of marine aerosols to the Faroe Islands, therefore, have not contributed significantly to the Hg inventory or the Hg accumulation rates, relative to these other areas. The maximum rate of Hg accumulation was 34 μg/m^2/yr. The greatest fluxes of *anthropogenic* Hg accumulation calculated using Br and Se, respectively, were 26 and 31 μg/m^2/yr. The rate of atmospheric Hg accumulation in 1998 (16 μg/m^2/yr) is comparable to the values recently obtained by atmospheric transport modeling for Denmark, the Faroe Islands, and Greenland.

1. INTRODUCTION

There is concern about the concentrations and chemical speciation of Hg in the food chain of the Faroe Islands, and their possible impacts on human health. Marine foods constitute an important part of the Faroese diet, including meat and blubber from pilot whales. Muscle tissue of these whales contain on average 3.3 μg/g Hg, half of which is potentially toxic methylmercury (Weihe et al., 1996). The average dietary intake of Hg approaches the Provisional Temporary Weekly Intake of 0.3 mg (Weihe et al., 1996). In one of eight human births, Hg concentrations in maternal hair exceed the limit of 10 μg/g, the threshold of neurobehavioural dysfunction for the fetus; Hg concentrations in umbilical cord blood have similar implications (Weihe et al., 1996). Correlations occur between cord-blood Hg concentrations and deficits in language, attention, and memory, while fine motor function deficits correlate with maternal hair Hg (Grandjean et al., 1997).

It is unclear how much of the present day Hg flux to the Faroe Islands is from anthropogenic sources (Larsen and Dam, 1999; Mikkelsen et al., 2002). As volcanic and mantle degassing are thought to be important natural sources of Hg to the global atmosphere (Rasmussen, 1994; Nriagu and Becker, 2003), Icelandic emissions represent a potentially important natural source of atmospheric Hg to the Faroe Islands, only 450 km to the SE (Fig. 1). If the natural fluxes of atmospheric Hg to the Faroes are high, local inhabitants may have been exposed

* Author to whom correspondence should be addressed (shotyk@ugc.uni-heidelberg.de).
† *Present address:* Environmental Chemistry Research Group, Department of Chemistry, University of Southern Denmark, Odense University, Odense M, Denmark.
‡ *Present address:* Zentralstrasse 68, 8212-Neuhausen am Rheinfall, Switzerland.
§ *Present address:* Institute of Environmental Geochemistry, University of Heidelberg, INF 236, D-69120 Heidelberg, Germany.

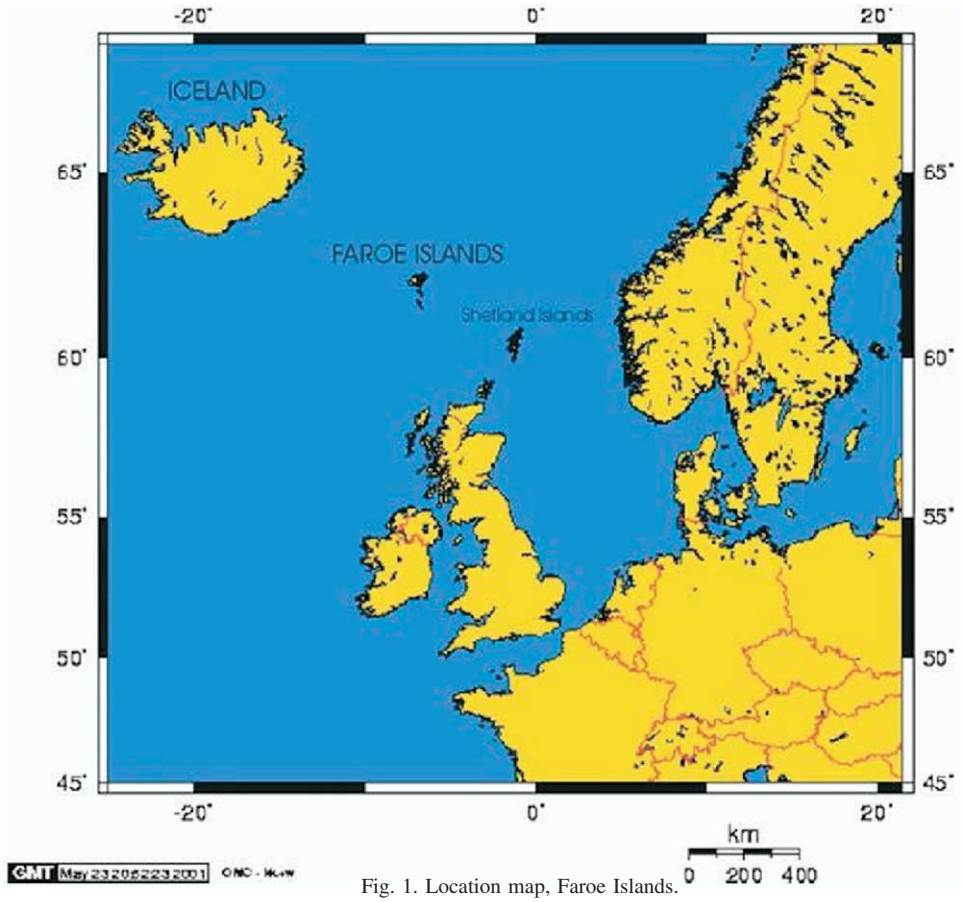

Fig. 1. Location map, Faroe Islands.

to elevated Hg ever since settlement began in the sixth to ninth centuries AD (Hannon and Bradshaw, 2000).

The rates of atmospheric Hg accumulation and their temporal variation can be obtained using archival records. Ombrotrophic bogs are the only archive on the Faroe Islands that can provide a long-term record of Hg supplied exclusively by the atmosphere. Peat is an excellent medium for strongly adsorbing and complexing Hg^{2+} (Oechsle, 1982; Lodenius, 1983), and ombrotrophic bogs have been studied extensively as archives of the changing rates of atmospheric Hg deposition (Boyarkina et al., 1980; Pheiffer-Madsen, 1981; Jensen and Jensen, 1991; Norton et al., 1997; Benoit et al., 1998; Martinez-Cortizas et al., 1999; Biester et al., 2002; Bindler, 2003). A peat core from the Swiss bog at Etang de la Gruère (EGR) has been used to reconstruct in detail the record of atmospheric Hg accumulation extending back 14,500 calendar yr (Roos-Barraclough et al., 2002). A subsequent study from a nearby bog yielded a very similar chronology of atmospheric Hg accumulation for the past two millenia (Roos-Barraclough and Shotyk, 2003). Using the same approach, peat cores from ombrotrophic bogs have also been used for high resolution reconstruction of atmospheric Hg deposition in Denmark and Greenland (Shotyk et al., 2003), as well as southern Ontario, Canada (Givelet et al., 2003).

The main objectives of the present study were to (1) quantify net rates of atmospheric Hg accumulation on the Faroe Islands using a) recent peats dated using ^{210}Pb and b) preindustrial peats dated using ^{14}C; (2) separate the Hg inventory into its natural and anthropogenic components using Br and Se as reference elements; and (3) identify the predominant anthropogenic sources of Hg using stable Pb isotopes (Shotyk et al., 2003).

Unlike continental ombrotrophic bogs, maritime blanket bogs from the Faroe Islands are expected to be rich in volcanic ash particles (Persson, 1971) as well as oceanogenic elements derived from marine aerosols (Shotyk, 1997). In the acidic, anoxic, organic-rich peat environment, there is considerable potential for mineral weathering and chemical diagenesis to affect the distribution of a range of major and trace elements. A detailed geochemical description of the peat profile studied is essential, therefore, to establish that the Hg and Pb in the peat column have been supplied exclusively by atmospheric deposition, and that these elements have been faithfully preserved over time (Shotyk, 1996).

2. MATERIALS AND METHODS

Several Faroe Island peat bogs have been studied in detail for their tephrachronological records (Persson, 1971; Mangerud et al., 1986; Dugmore and Newton, 1998; Wastegård et al., 2001). Approximately 4 km northeast of Vestmannahavn, on Streymoy (Fig. 2), the peat deposit at Myrarnar was described by Persson (1971): he found 125 cm of peat and volcanic ash layers at depths of 20 to 23 cm and 73 to 87 cm; these

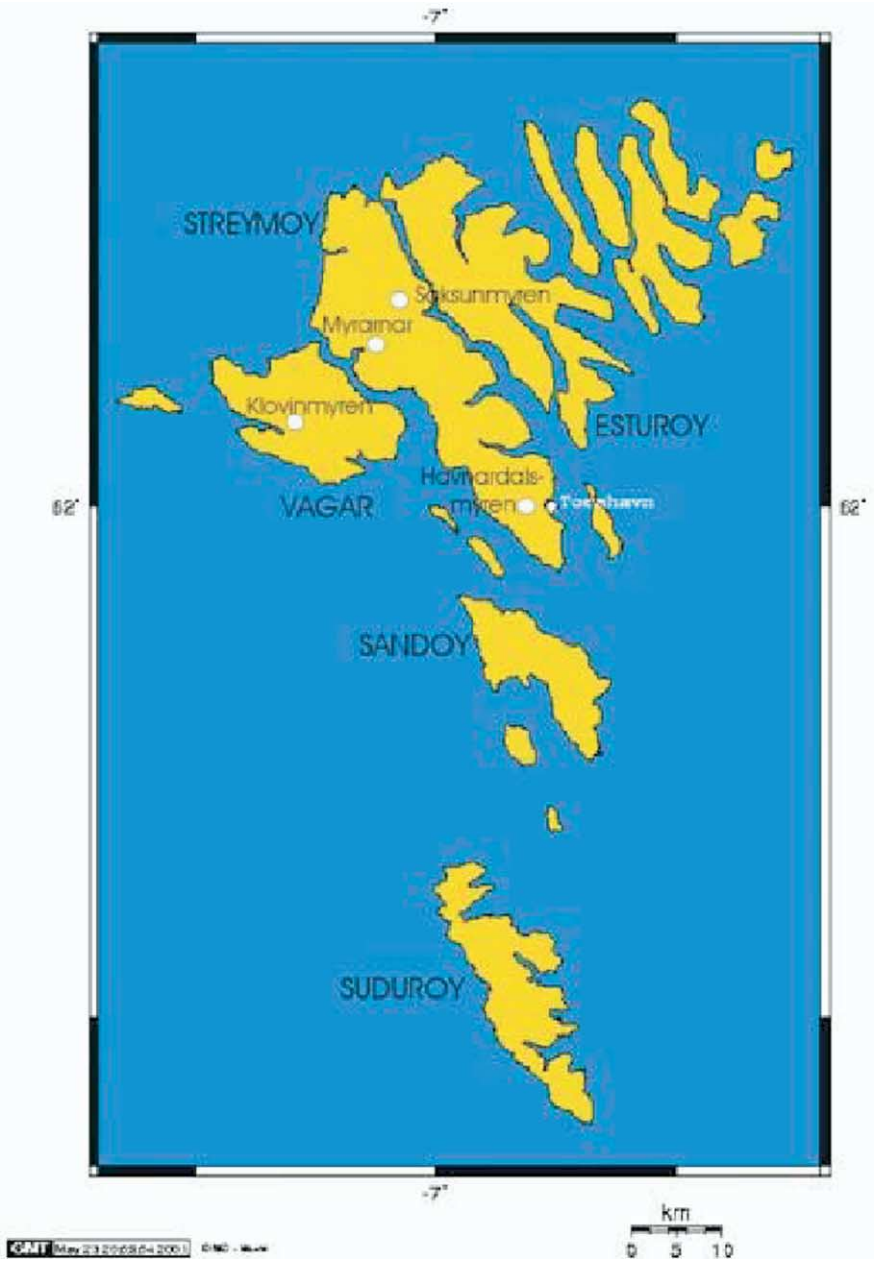

Fig. 2. Location of Myrarnar peat bog, Streymoy, Faroe Islands.

were dated using ^{14}C to AD 1050 ± 120 and ca. 1500 BC, respectively. We collected the MYR2 core in May of 2000 at a site intermediate between small hummocks and hollows using a Wardenaar corer (Wardenaar, 1987) made of titanium. All of the peat was very decomposed except for the surface layer. Roots similar to those of *Scirpus* or *Trichophorum* were visible throughout the core. A summary of our field work activities, detailed descriptions, and photos of the sites, are available as a .pdf file from the senior author. Local inhabitants indicated that there was no peat cutting in recent history. Average annual precipitation at Torshavn (1961–1990) was 1284 mm and average annual temperature was 7.0°C (Danish Meteorological Institute, Technical Report 98-14).

2.1. Sample Preparation

The core was cut while frozen at −18°C into 1 cm slices using a stainless steel band saw (Givelet et al., 2004). A Plexiglas template was used to allow the outside edges of each peat slice to be trimmed away using a Ti knife, and discarded. Individual slices were subsampled, prepared, and measured for bulk density and humification (Givelet et al., 2003).

2.2. Trace Element Determinations

One gram of dried, milled peat was analyzed for selected trace elements using the EMMA XRF spectrometer (Cheburkin and Shotyk, 1996). The accuracy and precision of the trace metal measurements were given by Cheburkin and Shotyk (1996), and the Br and Se quality control data summarised by Givelet et al. (2003). Titanium was quantified using the NASTIA XRF spectrometer (Shotyk et al., 2002a).

Subsamples for Hg determination were obtained, prepared, and analyzed using the LECO AMA 254 (Givelet et al., 2003). The accuracy and precision of these measurements were determined by mea-

Table 1. AMS ^{14}C dating of plant macrofossils and peat fractions from MYR peat core from Myrarnar, Faroe Islands.

Lab. nr. AAR-	Average depth (cm)	Material dated	$\delta^{13}C$ (‰)	Conv. ^{14}C age (BP)	Calibrated age (68% confidence intervals)
8006	5.5	*Sphagnum*	−26.48	255 ± 65	AD: 1510–1680; 1760–1810; 1930–1950
8007-2	13.5	*Peat fraction <0.2 mm*	−28.00	510 ± 44	AD: 1330–1440
8008	20.5	*Sphagnum*	−28.10	1184 ± 37	AD: 780–890
8009-1	29.5	*Sphagnum*	−26.32	1725 ± 39	AD: 250–390
8009-2	29.5	*Peat fraction <0.2 mm*	−28.08	2532 ± 47	BC: 800–540
8010	36.5	*Selaginella*	−25.40	1770 ± 50	AD: 130–350
8011	39.5	*Selaginella*	−25.07	2217 ± 43	BC: 370–200
8012	52.5	*Sphagnum*	−26.22	3260 ± 55	BC: 1610–1450
8013	57.5	*Selaginella*	−24.94	5104 ± 47	BC: 3970–3800
7802	13.5	*Plant root*	−25.33	−44 ± 38	AD 1955? (needs bomb calibration)
7803	20.5	*Plant root*	−25.12	105 ± 36	AD: 1690–1730; 1810–1920
7804	29.5	*Plant root*	−25.55	126 ± 36	AD: 1680–1740; 1800–1890; 1910–1950
7805	36.5	*Plant root*	−25.03	229 ± 38	AD: 1640–1680; 1760–1810; 1930–1950
7806	39.5	*Plant root*	−25.00	119 ± 39	AD: 1680–1740; 1800–1890; 1910–1950
7807	52.5	*Plant root*	−24.54	534 ± 41	AD: 1330–1440
7808	57.5	*Plant root*	−24.97	29 ± 36	AD: 1951

suring a certified standard reference material after every 10th sample, either NIST 1547 Peach Leaves (certified value 31 ± 7 ng/g; measured value 30.9 ± 0.9 ng/g, n = 12) or NIST 1515 Apple Leaves (certified value 44 ± 4 ng/g; measured value 42.8 ± 0.6 ng/g; n = 12). The mean relative standard deviation of Hg within a peat slice was 7.4% (n = 3).

As an independent check on the validity of the analytical method described above, Hg concentrations were measured in eleven selected subsamples using hydride generation atomic fluorescence, following acid dissolution, at the University of Maine, Orono. Samples were dried at 40°C and a 0.4 to 0.5 g aliquot digested using a microwave-assisted acid digestion. Mercury was brought into solution through leaching with nitric and hydrochloric acids and closed vessel heating by microwave, followed by oxidation with permanganate/persulfate solutions. Hydroxylamine hydrochloride was added to the digestate, which was then brought to 100 mL with deionized water. The solutions were filtered and analyzed using cold vapor atomic absorption with a flow injection mercury system (FIMS). Precision and accuracy were routinely checked with standard reference material (SRM) analyses, blanks, duplicate analyses, replicate samples, spike recoveries, and periodic checks of standards during a run. One SRM and one duplicate were digested per 10 samples, a blank was prepared every 10 samples, and 1 of every 10 samples was a replicate.

2.3. Age Dating Using ^{210}Pb

Dried milled samples from the uppermost ca. 20 cm were age dated using ^{210}Pb as described previously (Appleby et al., 1997).

2.4. Age Dating Using ^{14}C

Plant macrofossils were ^{14}C dated with Accelerator Mass Spectrometry (AMS). The macrofossils were taken from the centers of selected one-cm slices at the Institute of Plant Science, University of Berne, where they were also cleaned and dried at 60°C. Within one week from selection they were processed using a standard procedure for plant material (washed, acid-base-acid treatment) at the Dating Laboratory, University of Aarhus. A sample from the bottom slice (72 cm+) was dried, milled, and homogenized, then age dated using ^{14}C AMS (ETH Zurich) at 5415 ± 60 ^{14}C yr BP (ETH-23508). The calibrated age of this sample (4359 to 4212 cal yr BC) implies a long-term, average rate of peat accumulation of ~72 cm/6286 yr = 0.012 cm/yr.

2.5. Stable Pb Isotopes

Selected samples were evaporated in Savillex beakers after acid HNO_3-HBF_4-H_2O_2 microwave digestion (Krachler et al., 2002). Dried samples were redissolved in 2.4N HCl. Lead was consequently separated using 3 to 4 μL EiChrom Sr-resin and 6N HCl elution in the clean laboratory in Heidelberg (Weiss et al., 2004). Lead isotope ratios were determined using an Isoprobe multi-collector ICP-MS at the Imperial College/Natural History Museum Joint Analytical Facility (JAF), London. Mass fractionation was corrected using NBS 997 Tl as an internal standard (Rehkämper and Mezger, 2000). The Pb/Tl ratios were kept constant and above 2 to avoid possible peak overlaps of the dopant. The $^{205}Tl/^{203}Tl$ ratio used for mass bias correction was optimised daily using repeated measurements of spiked NBS 981 Pb solutions and the values of Galer and Abouchami (1998). Long-term reproducibility determined over a five-month period (n = 42) was 263 ppm for $^{206}Pb/^{204}Pb$, 322 ppm for $^{207}Pb/^{204}Pb$, 314 ppm for $^{208}Pb/^{204}Pb$, 222 ppm for $^{207}Pb/^{206}Pb$, and 263 ppm for $^{208}Pb/^{206}Pb$ (Weiss et al., 2003). Procedural blanks were insignificant compared to the total amount of Pb in the samples. No blank correction was necessary. Baseline correction was done using an on peak zeroing procedure. Interference contributions by Hg on ^{204}Pb were corrected using ^{200}Hg but were well below 0.1% for all measurements. One additional sample (Myr Neo 11) was measured by classical thermal ionisation mass spectrometry (TIMS) on a MAT Finnigan 261 in Heidelberg (Kober et al., 1999) after the same resin extraction (Table 4).

3. RESULTS

3.1. Development of an Age-Depth Model

The ^{210}Pb age dates were used to calculate peat accumulation rates for the top 9.5 cm (Table 3), and the ^{14}C ages were used from 13.5 cm to 52.5 cm (Table 1). The peat accumulation rates obtained using the ^{210}Pb chronology are listed in Table 3. The six ^{14}C age dates between 13.5 cm (AD 1385) and 52.5 cm (1530 BC) plotted against depth yields a linear peat accumulation rate of 0.014 cm/yr (r^2 = 0.877).

The rate of peat accumulation recorded by the MYR2 core is approximately one third the long-term rate of peat accumulation at Etang de la Gruère (Shotyk et al., 2001). Also, the MYR2 peat accumulation rates are approximately one fifth the long-term peat accumulation rates found in blanket peat bogs from NW Scotland and the Island of Foula in Shetland (Shotyk, 1996). The rate of peat accumulation between 52.5 cm (1530 BC) and 57.5 cm (3885 BC) is particularly low (0.002 cm/yr).

3.2. Geochemistry of the Peat Profile

3.2.1. Volcanic ash particles

The peat core contained abundant white to gray mineral grains ~0.5 to 3 mm in diameter. These grains were particu-

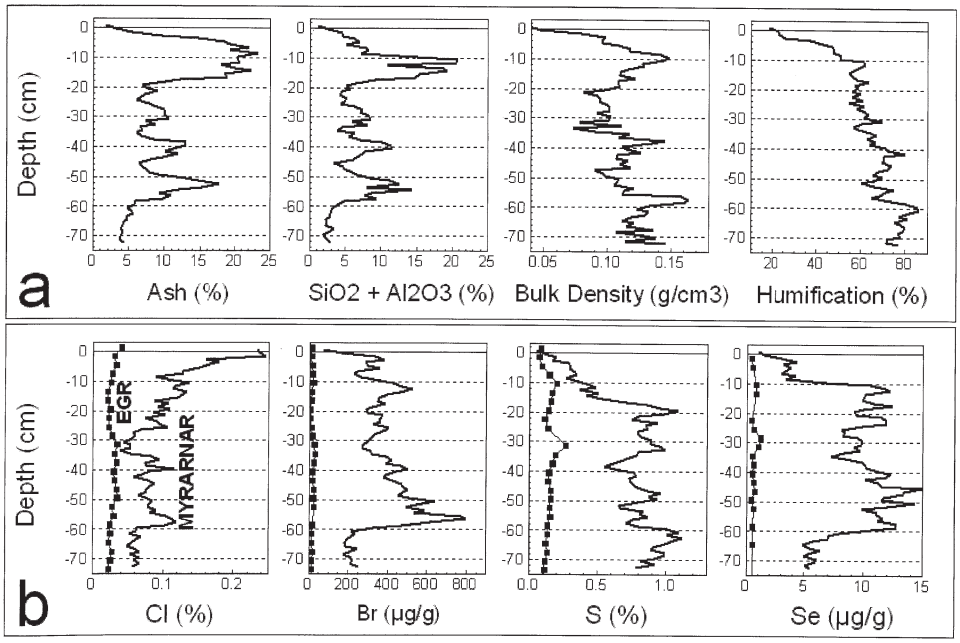

Fig. 3. (a) Ash content (%), concentrations of SiO_2 + Al_2O_3 (%), dry bulk density (g/cm^3), and peat humification (%) in the MYR 2 peat core; and (b) concentrations of Cl (%), Br (μg/g), S (%), and Se (μg/g). Concentrations of Cl, Br, Se and Se in the continental, ombrotrophic peat bog at EGR are indicated for comparison.

larly abundant in the samples from 3 to 9, 10 to 20, 23 to 32, 34 to 43, and 56 to 59 cm, and less common from 45 to 46, 47 to 48, and 53 to 54 cm. Grains from depths of 12 to 13, 30 to 31, 41 to 42 and 56 to 57 cm were examined using an optical microscope as well as SEM/EDAX. The particles were either gray ashy masses, or almost pure white. Some grains had fresh surfaces (41–42 cm) whereas others were highly pitted (56–57 cm). Gas vesicles were obvious in the grains from the 30 to 31 cm and 41 to 42 cm slices. An EDAX analysis of a grain selected from 12 to 13 cm showed that Si, Al, Fe, and Ca are the dominant elements, followed by Ti and Na. Analyses of individual grains using the EMMA microXRF analyser (Cheburkin et al., 1997) indicated that Rb and Sr were the most abundant trace elements.

3.2.2. Ash content, bulk density, and humification

The ash content of the peat profile (Fig. 3a) reflects the abundance and distribution of the volcanic particles. Despite the abundance of mineral grains and the elevated ash contents, the bulk density of the peat samples is within the typical range for ombrotrophic peats (Fig. 3a). The topmost 10 cm are poorly decomposed, compared to deeper underlying layers (Fig. 3a).

3.2.3. Marine derived elements: Cl, Br, S, and Se

Chlorine, Br, S, and Se are strongly enriched relative to the continental *Sphagnum* bog at EGR (Fig. 3b), reflecting the importance of marine aerosols to the MYR2 profile. The average concentration of Cl^- in the pore waters at Myrarnar is ca. 18 mg/L, comparable with the long-term average rainwater value (ca. 21 mg/L) for this area (Danish Meteorological Institute, Technical Report 98-14). For comparison, the concentrations of Cl^- in the pore waters at EGR and in precipitation at Payerne in western Switzerland is 0.3 mg/L (Steinmann and Shotyk, 1997a). Given the similar levels of precipitation (1300 mm per yr in the Jura Mountains and 1280 mm per yr on the Faroe Islands), the differences in chloride concentrations in the pore waters (0.3 at EGR vs. 18 mg/L at Myrarnar) indicate that inputs of marine aerosols to Myrarnar via wet deposition are ~60 times higher than in the continental peat bog.

3.2.4. Conservative lithogenic elements: Ti, Ga, Y, Zr

Concentrations of Ti, Ga, Y, and Zr are greatest at discrete depths, in particular at ca. 10, 31, 39, and 52 cm (Fig. 4a), indicating episodic supply. Zirconium is the most conservative of the four elements during chemical weathering (Goldich, 1938); this element is used as a surrogate for the distribution of mineral matter in the peat core. The concentrations of Ti, Ga, Y, and Zr are far higher in the MYR2 profile compared with EGR, indicating that volcanic sources of mineral matter dominate inputs to the MYR2 peat profile.

3.2.5. Mobile lithogenic elements: Ca, Sr, Mn, Fe

The distributions of Sr and Mn (Fig. 4b) generally follow the conservative elements Ti and Zr (Fig. 4a), which suggests that Sr and Mn are also supplied primarily by volcanic sources. The Ca/Sr and Ca/Ti ratios (Fig. 5a), however, show that the peat samples below 58 cm are enriched in Ca, relative to overlying peat; this probably reflects groundwater inputs of Ca from chemical weathering of the bedrock and soil under the peat. Thus, the MYR2 profile is truly ombrotrophic only to a depth of 58 cm, below which it becomes increasingly minerotrophic.

The average concentration of Fe in MYR2 (1.3%) is approx-

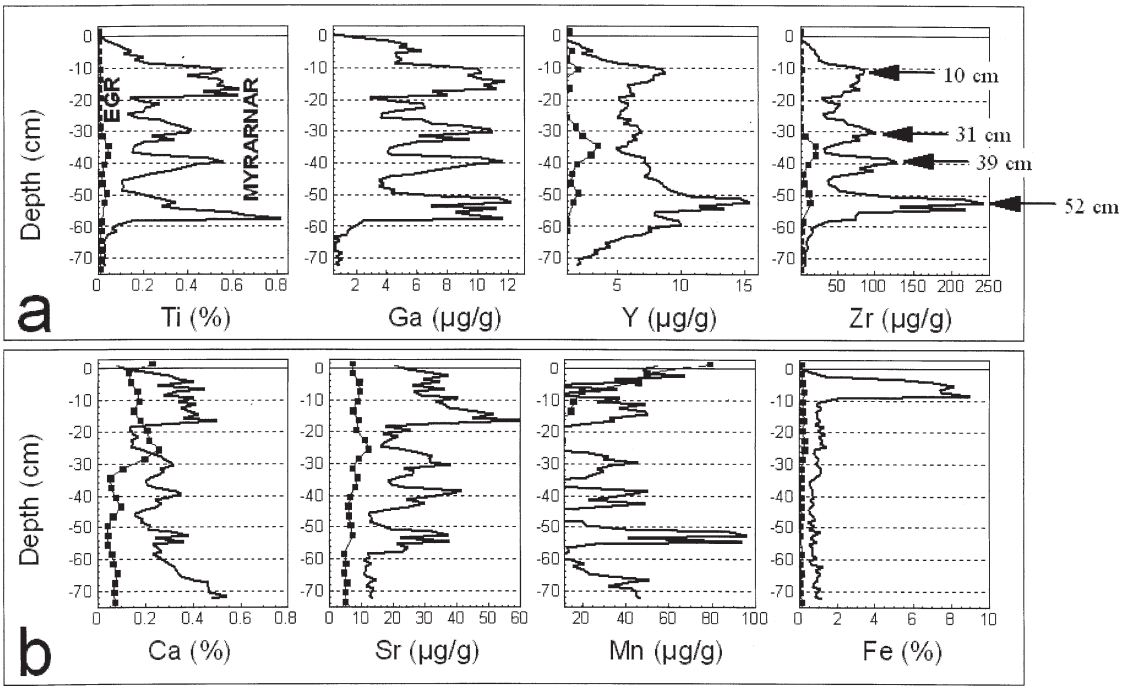

Fig. 4. (a) Concentrations of Ti (%), Ga (μg/g), Y (μg/g), and Zr (μg/g) in the MYR 2 peat core. The arrows indicate the depths at which the maximum concentrations of volcanic ash particles are found (10, 31, 39, and 52 cm); and (b) concentrations of Ca (%), Sr (μg/g), Mn (μg/g), and Fe (%). Concentrations of these elements in the continental, ombrotrophic peat bog at EGR are indicated for comparison.

imately a factor of ten greater than in typical ombrotrophic peats. Iron concentrations reach ~9% at a depth of 7.5 cm (Fig. 4b). The Fe/Zr ratio and the percentage of Fe in the ash fraction (Fig. 5b) shows that Fe is enriched in the peat immediately above the peaks in ash content.

3.2.6. Fallout radionuclides ^{137}Cs, ^{210}Pb, ^{241}Am

The radionuclide concentrations are given in Table 2. Unsupported ^{210}Pb was not detected in samples below a depth of 10 cm (Fig. 6a). The maximum concentrations of ^{137}Cs and ^{241}Am occur at 3 to 4 and 4 to 5 cm, respectively (Fig. 6a). The Constant Rate of Supply model was used to calculate the ^{210}Pb ages (Fig. 6b). The position of AD 1963 was determined using the ^{137}Cs stratigraphy.

3.2.7. Hg

The Hg concentrations obtained using AAS (LECO AMA 254) are shown along with the selected samples (diamonds) measured using AFS, the volumetric Hg concentrations and selected ^{14}C age dates, calibrated to calendar years (Fig. 7). The depths of maximum Zr concentrations (solid black arrows) are interpreted as volcanic ash inputs. The peak in volcanic ash at 39 cm has a corresponding peak in Hg concentration and the ash peak at 10 cm has a corresponding Hg shoulder; the other volcanic ash peaks (31 cm and 52 cm) do not have corresponding peaks in Hg (Fig. 7). The largest peak in Hg concentrations in the profile (4 to 5 cm and dated as AD 1954 $\pm$ 2), does not have a corresponding peak in volcanic ash.

3.3. Nonatmospheric Sources of Hg and Pb to the Peat Profile

The Ca/Sr and Ca/Ti ratios (Fig. 5a) suggest that the peat above 58 cm is ombrotrophic, whereas it is minerotrophic below. In contrast, Hg (Fig. 7) and Pb (Fig. 8) concentrations do not increase with depth in the peat samples below 58 cm. Therefore, unlike Ca, which is also supplied to the deeper peat layers by terrestrial/aquatic sources, Hg and Pb have been supplied exclusively by atmospheric deposition since peat accumulation began ca. 4286 BC

3.4. Chemical Diagenesis of Hg and Pb Within the Peat Profile

Mercury may become adsorbed onto Fe and Mn oxides, which are formed when Fe (II) and Mn (II) in the anoxic zone of sediments diffuse upward and become oxidized (Gobeil et al., 1999). Peatlands may have a thin oxic zone, depending on the seasonally dependent depth-to-water table (Shotyk, 1988). The strong Fe enrichment at MYR2 (Fig. 4b) and the highly variable Fe/Zr ratio (Fig. 5b) may have been caused by the reductive dissolution of Fe-bearing minerals, upward migration of dissolved ferrous Fe, and oxidation and precipitation as Fe hydroxide in the surface layer (Steinmann and Shotyk, 1997b). Compared to the peaks in Zr concentration at 52, 39, 31, and 10 cm (original inputs of mineral matter), there are overlying peaks in Fe/Zr (diagenetic formation of Fe hydroxides) at 47, 35, 25, and 5.5 cm (Fig. 9a). Therefore, there have been a number of periods of Fe diagenesis that are preserved as peaks

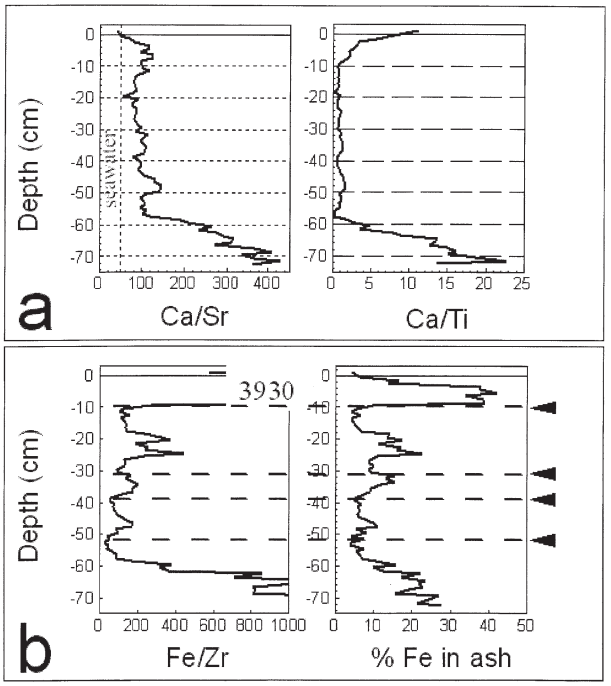

Fig. 5. (a) Ca/Sr and Ca/Ti in the MYR 2 peat core; and (b) Fe/Zr and Fe concentration in the ash fraction (%) of the MYR2 peat core. Black arrows and dashed horizontal lines indicate the depths at which the maximum concentrations of volcanic ash particles are found.

in Fe/Zr. However, none of the ancient peaks in Fe/Zr (65, 47, 35, 25, and 21 cm) have a corresponding Hg peak.

In the near-surface peat layer, Fe concentrations increase from 1.1% Fe (10.5 cm) to 8.9% Fe (8.5 cm) over a distance of only 2 cm (Fig. 9b). The zone of greatest Fe enrichment is broad, with all samples from 3 to 9 cm containing more than 5% Fe. Mercury concentrations, on the other hand, reach their maximum concentration at 4 to 5 cm. In addition, the increase in Hg concentrations begins at a depth of ~20 cm, which is 10 cm below the increase in Fe (Fig. 9b). Also, the increase in Hg concentration predates the Fe peak; the start of the increase in Hg concentrations (ca. 20 cm) dates to AD 779–893 (Table 1), whereas the increase in Fe concentration (ca. 10 cm) dates to approximately AD 1812 (Table 3). Finally, we note that Hg concentrations increase by a factor of three from ca. 20 cm to 10 cm, while there is no change in Fe concentrations over the same depth (Fig. 9b). Therefore, even though there has been considerable diagenesis of Fe, these processes and reactions do not appear to have affected the Hg concentration profile.

Increasing concentrations of anthropogenic Pb also predate the changes in Fe concentrations (Fig. 9b). In addition, the isotopic composition of Pb (Fig. 8) shows a pronounced change beginning 5 cm below the peat surface; if Pb had been migrating upward in the profile and adsorbed by Fe hydroxides, the change in isotopic composition would not be as sharp.

3.5. Effects of Organic Matter Decay on the Apparent Rates of Hg Accumulation

Biester et al. (2003) suggested that bulk density is not an adequate parameter to express changes in peat humification and that Hg accumulation rates should be corrected for humification. In Figure 10, the changes in volumetric Hg concentrations, Hg/Br, bulk density, and humification are shown for the top 30 cm of the MYR2 peat profile. These graphs emphasise the fact that volumetric Hg concentrations, the Hg/Br ratio, and the Hg/Se ratio (not shown) achieve their maxima at a depth of 4 to 5 cm. In contrast, bulk density and humification increase from the top of the core to reach their maxima at 9 to 10 and 10 to 11 cm, respectively (Fig. 10). The maximum Hg concentration and Hg/Br and Hg/Se ratios, therefore, are independent of the maximum in bulk density and humification. Whereas the maximum Hg concentration by weight and volume, Hg/Br, and Hg/Se date from AD 1954, the maximum in bulk density dates to AD 1812 ± 16 (Table 3), and the maximum in peat humification predates this. Thus, the maximum extent of Hg enrichment cannot be explained by decay processes. Moreover, these data suggest that the effect of organic matter decomposition is adequately considered if the rate of atmospheric Hg accumu-

Table 2. Fallout radionuclide concentrations in Myranar core MYR2.

Depth		^{210}Pb						^{137}Cs		^{241}Am	
		Total		Unsupported		Supported					
cm	g cm^{-2}	Bq kg^{-1}	±	Bq kg^{-1}	±	Bq kg^{-1}	±	Bq kg^{-1}	±	Bq kg^{-1}	±
0.5	0.04	1159.4	24.4	1141.0	24.5	18.3	2.7	176.3	5.0	0.0	0.0
1.5	0.12	1102.2	34.7	1095.2	35.0	6.9	4.1	256.8	7.4	0.0	0.0
2.5	0.21	1361.1	28.4	1350.8	28.6	10.3	2.7	431.8	7.5	4.0	1.8
3.5	0.32	1227.7	31.7	1221.0	31.9	6.7	3.4	482.3	8.4	6.3	1.8
4.5	0.44	929.2	24.3	912.3	24.5	16.9	2.8	403.8	7.6	10.0	1.5
5.5	0.54	537.6	21.2	526.5	21.4	11.2	2.8	246.9	6.0	7.0	1.5
6.5	0.64	346.9	23.6	330.0	23.9	16.9	3.5	156.9	5.9	0.0	0.0
7.5	0.75	163.5	17.6	151.3	17.8	12.3	3.1	107.7	4.5	0.0	0.0
8.5	0.89	75.8	8.6	62.2	8.8	13.6	1.8	68.6	2.9	0.0	0.0
9.5	1.05	37.3	5.7	24.1	5.9	13.2	1.6	52.0	2.1	0.0	0.0
10.5	1.22	6.8	9.9	−8.9	10.2	15.7	2.2	53.1	2.5	0.0	0.0
12.5	1.53	9.9	5.2	−3.3	5.4	13.2	1.5	40.2	1.6	0.0	0.0
16.5	2.06	11.6	6.8	−3.1	7.1	14.6	2.1	42.7	2.6	0.0	0.0
20.5	2.52	11.6	6.8	−3.3	7.1	14.9	2.1	22.5	2.4	0.0	0.0

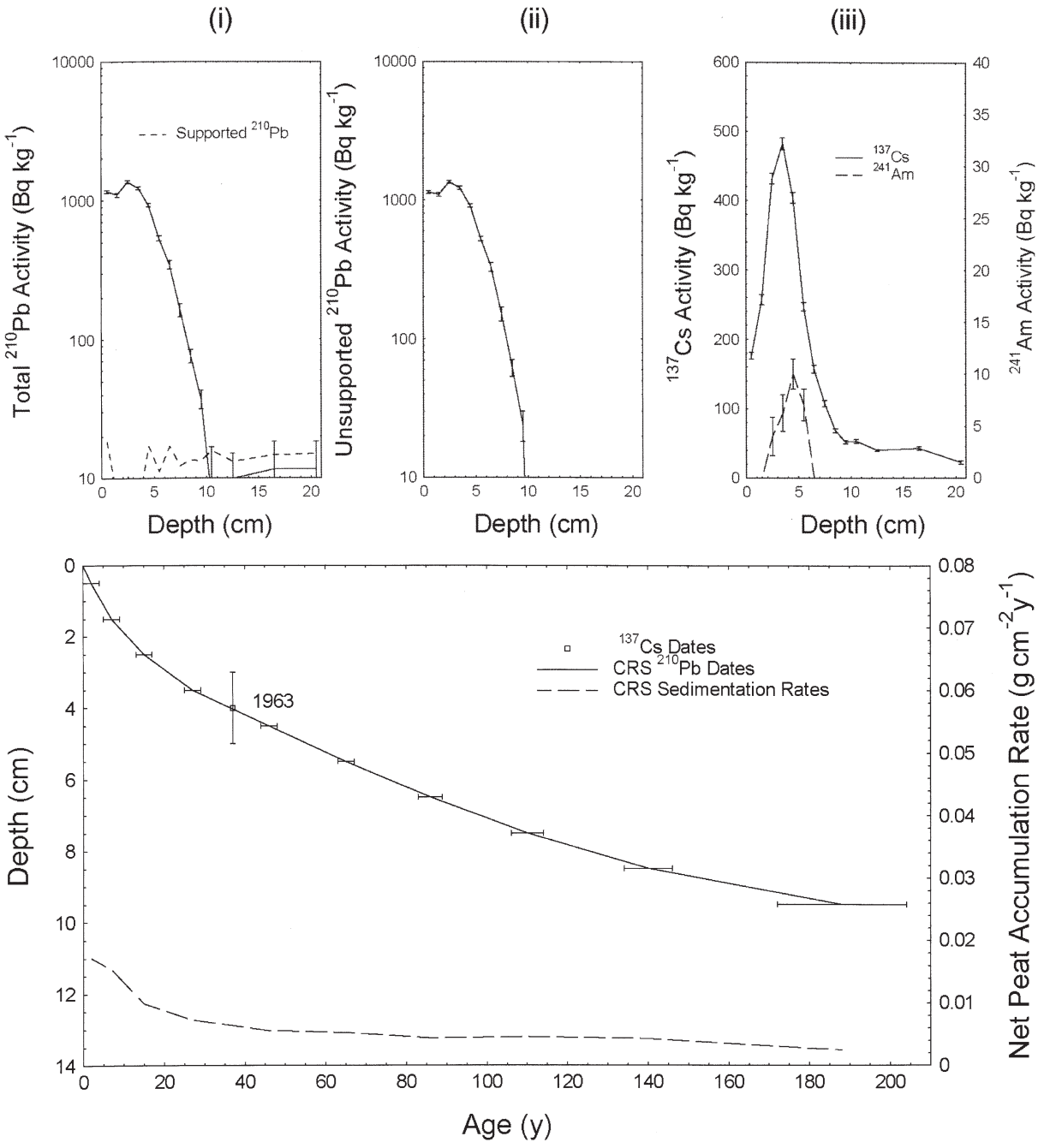

Fig. 6. (a) Activities of fallout radionuclides: total and supported and unsupported ^{210}Pb, ^{137}Cs, and ^{241}Am; and (b) radiometric chronology of MYR2 showing the CRS model ^{210}Pb dates and sedimentation rates together with the 1963 depth determined from the ^{137}Cs and ^{241}Am stratigraphies.

lation is calculated as the product of the volumetric Hg concentrations [ng/cm^3] and the peat accumulation rate [cm/yr]. Increases in bulk density are apparently compensated by decreases in peat accumulation rate.

4. DISCUSSION

The MYR2 profile has received Pb and Hg exclusively from the atmosphere, even though the basal peat layers are minerotrophic. This finding is consistent with several recent studies describing Pb and Hg accumulation in minerotrophic peats. For example, at EGR in Switzerland, even though Ca, Sr, Fe, and Mn are clearly elevated in the minerotrophic fen peats because of the chemical weathering of calcareous basal sediments, this process has neither contributed significantly to the inventory of Pb (Shotyk et al., 2001) nor Hg (Roos-Barraclough et al., 2002). Even at the predominately minerotrophic peatland of Tourbière des Genevez in the Swiss Jura, both Pb (Shotyk, 2002) and Hg (Roos-Barraclough and

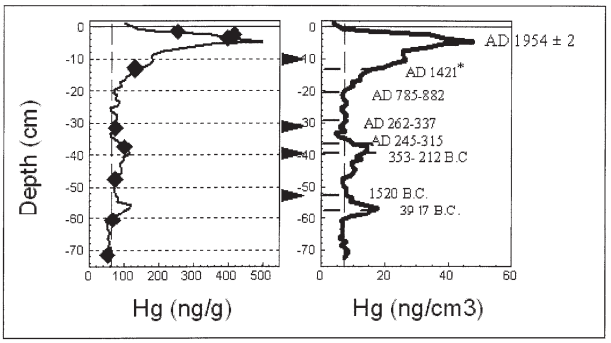

Fig. 7. Gravimetric (ng/g) and volumetric (ng/cm^3) Hg concentrations. The values indicated by the solid lines were obtained using AAS of solid samples, and the concentrations indicated by the diamonds using AFS following acid digestion (see text for details). Black arrows and dashed horizontal lines indicate the depths at which the maximum concentrations of volcanic ash particles are found. Selected ^{14}C age dates are shown (from Table 1). The age date of AD 1954 ± 2 was determined using ^{210}Pb (Table 3).

Shotyk, 2003) are supplied exclusively by atmospheric deposition.

The data presented here also argue that Pb and Hg are well retained in the peat profile. There is a growing body of information suggesting that Pb is immobile in ombrotrophic peat (Vile et al., 1995; Shotyk et al., 1996; Bränvall et al., 1997; Farmer et al., 1997; Kempter et al., 1997; MacKenzie et al., 1997; Martinez-Cortizas et al., 1997; Norton et al., 1997; Shotyk et al., 1997; MacKenzie et al., 1998; Shotyk et al., 1998; Kempter and Frenzel, 1999; Vile et al., 1999; Weiss et al., 1999a; Weiss et al., 1999b; Kempter and Frenzel, 2000; Vile et al., 2000; Shotyk et al., 2001; Martinez-Cortizas et al., 2002; Nieminen et al., 2002; Renberg et al., 2002; Shotyk, 2002; Shotyk et al., 2002b; Weiss et al., 2002; Givelet et al., 2003; Klaminder et al., 2003; Novak et al., 2003; Givelet et al., 2004; Le Roux et al., 2004). Taking Pb to represent an immobile reference element, the coincidence of the Hg (Fig. 7) and Pb (Fig. 8) concentration peaks suggests that Hg also is very well retained by the peat profile.

The maximum Hg concentration in the MYR2 core occurred at AD 1954 ± 2, which is not significantly different from the date of the Hg peak in the Storelung bog in Denmark (AD 1953 ± 2), and in the minerotrophic peat core from Tasiusaq in southern Greenland (AD 1953 ± 2), both of which were age dated using the atmospheric bomb pulse curve of ^{14}C (Shotyk et al., 2003). The occurrence of synchronous peaks in atmospheric Hg accumulation in these different geochemical settings suggests that the dominant changes in Hg concentration are not the result of chemical diagenesis, but rather due to the changing rates of atmospheric Hg deposition. In other words, the peat cores from these mires are faithful archives of atmospheric Hg inputs.

4.1. Distinguishing Between Natural and Anthropogenic Pb Using Ti

The Pb concentrations can be separated into "lithogenic" and "anthropogenic" components as follows (Shotyk et al., 2001):

$$[\mathrm{Pb}]_{\mathrm{lithogenic}} = [\mathrm{Ti}]_{\mathrm{sample}} \times (\mathrm{Pb/Ti})_{\mathrm{background}}$$

where the "background" Pb/Ti ratio was determined using the samples below 39.5 cm; these samples predate the Roman Period. We assume that the average Pb/Ti in these samples (0.001) represents the natural value. "Anthropogenic" Pb is then calculated as

$$[\mathrm{Pb}]_{\mathrm{anthropogenic}} = [\mathrm{Pb}]_{\mathrm{total}} - [\mathrm{Pb}]_{\mathrm{lithogenic}}$$

The elevated Pb concentrations in the uppermost layers of the MYR2 peat profile are predominately anthropogenic, with the maximum concentration of anthropogenic Pb (115 μg/g) dating to AD 1954 ± 2. A second peak in anthropogenic Pb occurs at a depth of 36 to 37 cm. This sample dates to AD 130–350 and is most likely due to long range transport of atmospheric Pb contamination from Roman Pb mining and smelting (Hong et al., 1994; Shotyk et al., 1998; Le Roux et al., 2004).

4.2. Distinguishing Between Natural and Anthropogenic Hg Using Br and Se

The ratio of Hg/Br in peat dating from preanthropogenic time varies over a narrow range. The Br concentrations and the

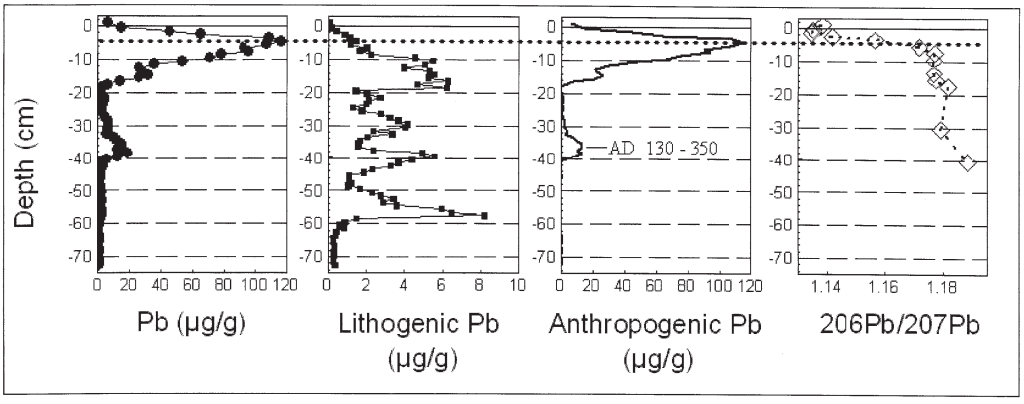

Fig. 8. Concentrations (μg/g) of total Pb, lithogenic Pb, and anthropogenic Pb (see text for description of the calculation), and isotopic composition of Pb (summarised as the ratio ^{206}Pb/^{207}Pb). The peak in anthropogenic Pb at a depth of 36 cm dates to the Roman Period.

Table 3. ^{210}Pb chronology of Myranar core MYR2.

Depth		Chronology			Sedimentation rate		
cm	g cm^{-2}	Date AD	Age y	±	g cm^{-2} y^{-1}	cm y^{-1}	± (%)
0.0	0.00	2000	0				
0.5	0.04	1998	2	2	0.017	0.25	3.2
1.0	0.08	1996	4	2	0.016	0.20	3.6
1.5	0.12	1993	7	2	0.015	0.14	4.1
2.0	0.16	1989	11	2	0.013	0.13	3.8
2.5	0.21	1985	15	2	0.010	0.10	3.6
3.0	0.26	1979	21	2	0.0086	0.083	3.9
3.5	0.32	1973	27	2	0.0073	0.067	4.2
4.0	0.38	1964	36	2	0.0064	0.053	4.5
4.5	0.44	1954	46	2	0.0056	0.053	4.8
5.0	0.49	1945	55	2	0.0054	0.053	5.7
5.5	0.54	1935	65	2	0.0053	0.050	6.6
6.0	0.59	1925	75	2	0.0049	0.048	8.4
6.5	0.64	1914	86	3	0.0044	0.043	10.2
7.0	0.70	1902	98	3	0.0045	0.042	12.8
7.5	0.75	1890	110	4	0.0046	0.037	15.5
8.0	0.82	1875	125	5	0.0044	0.033	18.9
8.5	0.89	1860	140	6	0.0043	0.026	22.3
9.0	0.97	1836	164	11	0.0034	0.021	26.2
9.5	1.05	1812	188	16	0.0025	0.021	30.0

"background" Hg/Br ratio can be used to calculate "natural" concentrations of Hg in peat (Roos-Barraclough et al., 2002; Givelet et al., 2003; Roos-Barraclough and Shotyk, 2003). The ratio of Hg to Se in peat dating from preanthropogenic times also has varied over a limit range, and this parameter too can be used to calculate "natural Hg" (Givelet et al., 2003). "Excess"

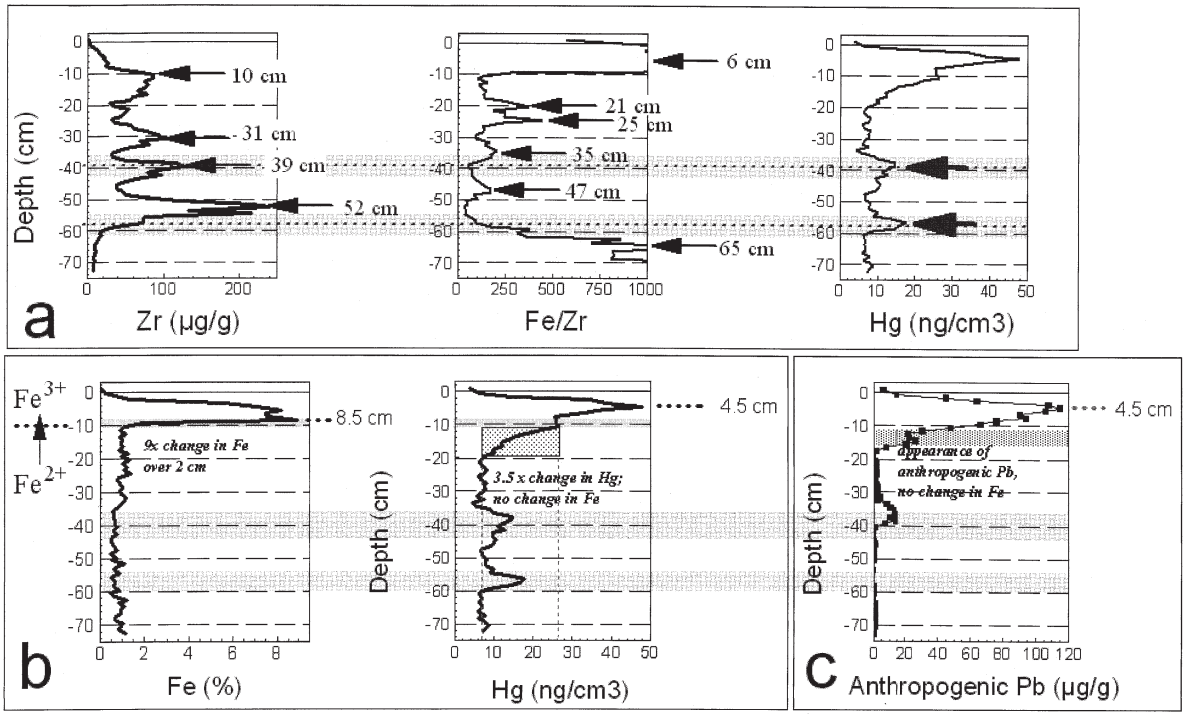

Fig. 9. (a) Comparison of Zr concentrations (μg/g) with Fe/Zr and volumetric Hg concentrations (ng/cm^3). Notice that two of the peaks in Zr concentration have corresponding peaks in Hg concentration. Peaks in Fe/Zr tend to overlie the peaks in Zr, indicating diagenetic Fe mobilisation. However, the peaks in Fe/Zr do not have corresponding peaks in Hg concentrations; and (b) concentrations of Fe (%), volumetric Hg concentrations (ng/cm^3), and anthropogenic Pb (μg/g). There is a threefold change in Hg concentrations that precede and predate the ninefold changes in Fe concentrations. The appearance of anthropogenic Pb (15.5 cm) and the maximum in anthropogenic Pb (4.5 cm) are much greater, and vertically more extensive, than the changes in Fe concentration (ninefold over a distance of only 2 cm).

Table 4. Isotopic composition of selected peat samples, Myr2 core, Faroe Island.

Depth (cm)	Sample ID	$^{206}Pb/^{204}Pb$	$^{207}Pb/^{204}Pb$	$^{208}Pb/^{204}Pb$	$^{207}Pb/^{206}Pb$	$^{206}Pb/^{207}Pb$	$^{208}Pb/^{206}Pb$	[Pb] μg/g
1	Myr Neo 01	17,738	15,583	37,606	0,8785	1,1383	2,1201	*6*
−0,5	Myr Neo 02	17,688	15,582	37,577	0,8809	1,1352	2,1244	*14,8*
−1,5	Myr Neo 03	17,657	15,562	37,503	0,8813	1,1346	2,1239	*45,3*
−2,5	Myr Neo 04	17,774	15,567	37,651	0,8759	1,1417	2,1184	*65*
−3,5	Myr Neo 05	18,043	15,599	38,004	0,8645	1,1567	2,1063	*109*
−5,5	Myr Neo 07	18,307	15,621	38,326	0,8533	1,1719	2,0936	*107,4*
−7,5	Myr Neo 09	18,383	15,616	38,348	0,8495	1,1772	2,0860	*95,9*
−9,5	Myr Neo 11*	18,423	15,655	38,463	0,8496	1,1770	2,0880	*70,1*
−13,5	Myr Neo 15	18,404	15,637	38,443	0,8496	1,1770	2,0888	*28,1*
−15,5	Myr Neo 17	18,396	15,620	38,381	0,8491	1,1777	2,0864	*26*
−17,5	Myr Neo 19	18,470	15,629	38,505	0,8462	1,1818	2,0848	*6,2*
−30,5	Myr Neo 32	18,428	15,626	38,452	0,8480	1,1793	2,0867	*6,4*
−40,5	Myr Neo 42	18,557	15,614	38,600	0,8414	1,1885	2,0800	*5,4*
	Reproducibility (ppm)	263	322	314	222		263	

* Was measured by TIMS.

Hg is the difference between total Hg concentrations and natural Hg. Excess Hg may be either volcanic (sharp peaks in Hg concentrations from preanthropogenic time) or "anthropogenic" Hg (much larger and broader peaks in peat dating from Industrial times). At Myrarnar, the Hg/Br and Hg/Se ratios (Fig. 11) were fairly constant for thousands of years: Hg/Br = $2.2 \pm 0.5 \times 10^{-4}$ and Hg/Se = $8.5 \pm 1.8 \times 10^{-3}$ (n = 54). Considering the different geochemical behaviour of Br and Se, the constancy in these ratios is remarkable. However, the Hg/Br and Hg/Se ratios increase dramatically within the Industrial Period (Fig. 11), reflecting anthropogenic contributions. Excess Hg is similar using both approaches, and a linear regression yields [Excess Hg (Se)] = 1.081 * [Excess Hg (Br)] + 4.69 (r^2 = 0.956, n = 74).

Bromine has been found to play a role in the scavenging of atmospheric Hg (Lindberg et al., 2002; Skov et al., 2004). If Br and Se are deposited as marine aerosols, efficiently retained by the peat (or at least retained at a rate proportional to deposition), and are conserved during chemical diagenesis, the Hg/Br and Hg/Se profiles suggest that both Br and Se are useful reference elements for quantifying the changing rates and sources of atmospheric Hg.

4.3. Rates of Atmospheric Hg Deposition From Natural and Anthropogenic Sources

The rate of atmospheric Hg accumulation is calculated using the total Hg concentrations, the bulk density, and the rates of peat accumulation (Fig. 12). The average rate of atmospheric Hg accumulation from 1520 BC to AD 1385 was 1.27 ± 0.38 μg/m^2/yr (n = 39), with much higher accumulation rates in modern peat samples (Fig. 12). The natural fluxes of Hg are calculated in the same way, but substituting "natural Hg" concentrations, which are calculated as the product of the Hg/Br and Hg/Se ratios and the Br and Se concentrations, respectively. The average rate of natural Hg accumulation from 1520 BC to AD 1385 was 1.32 ± 0.36 μg/m^2/yr and 1.34 ± 0.29 μg/m^2/yr using Br and Se, respectively (Fig. 12). The agreement between the "background" Hg accumulation rates calculated using these three approaches indicates that both the Hg/Br and Hg/Se ratios are good predictors of natural Hg concentrations. The difference between "natural" Hg accumulation rates and the total Hg flux is attributed to anthropogenic contributions (Fig. 12). The rate of natural Hg accumulation calculated using Br is clearly elevated at the top of the peat core; this

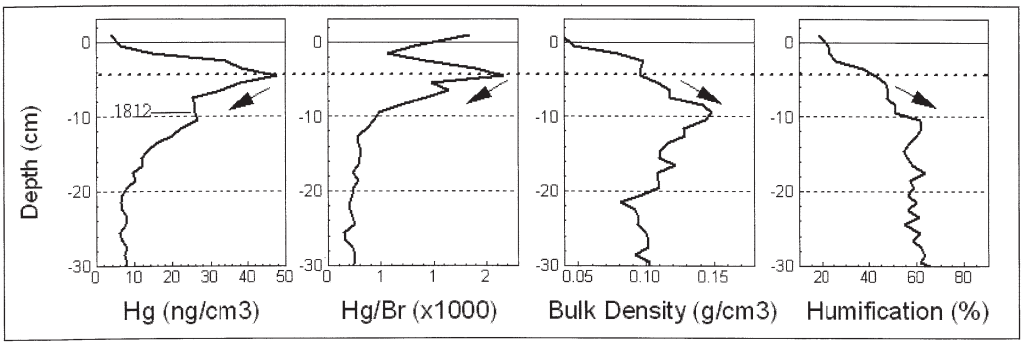

Fig. 10. Comparison of volumetric Hg concentrations (ng/cm^3), Hg/Br (x1000), peat bulk density, and humification (%). Notice that the changes in Hg concentrations and Hg/Br ratio within the top 10 cm of the profile do not correspond to the changes in bulk density or humification.

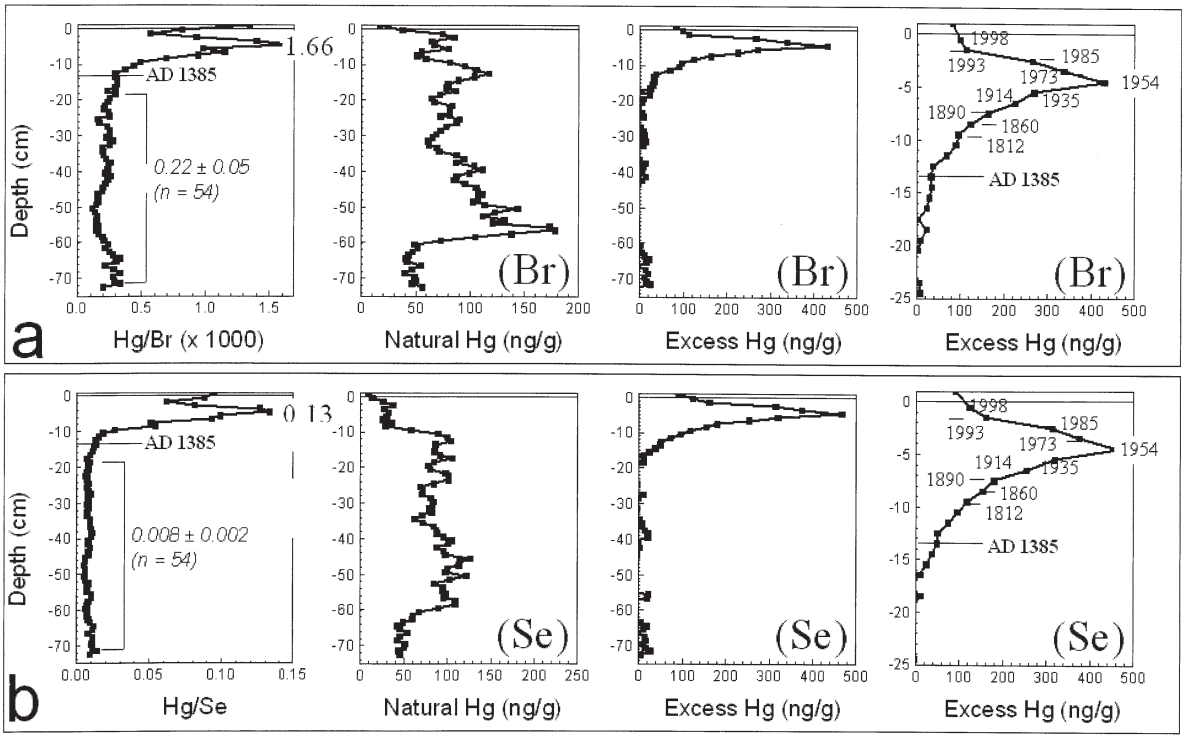

Fig. 11. (a) Hg/Br ratio and concentrations of natural and excess Hg (ng/g) calculated using Br concentrations and the "background" Hg/Br ratio (see text); and (b) Hg/Se ratio and concentrations of natural and excess Hg (ng/g) calculated using Se concentrations and the "background" Hg/Se ratio (see text).

is true also of Se, but to a lesser extent (Fig. 12). Anthropogenic Br has been emitted to the atmosphere as scavengers for Pb in gasoline additives, and Se from coal combustion and metal refining. If Br (or Se) deposition has a signficant anthropogenic component, anthropogenic Hg is underestimated.

For comparison with the background values, the maximum rate of total Hg accumulation is 34 $\mu g/m^2/yr$; this value exceeds the average Hg accumulation rate from 1520 BC to AD 1385 by 27 times. The greatest fluxes of anthropogenic Hg accumulation are 26 and 31 $\mu g/m^2/yr$ calculated using Br and Se, respectively (Fig. 12); these exceed the average rate of natural Hg accumulation (Br, Se) by 26 and 31 times, respectively. The rate of atmospheric Hg accumulation in 1998 (16 $\mu g/m^2/yr$) provided by the peat core is comparable to the 1995 values obtained by atmospheric transport modelling for Denmark, the Faroe Islands, and Greenland of 18, 10 and 12 $\mu g/m^2/yr$, respectively (Heidam et al., 2004).

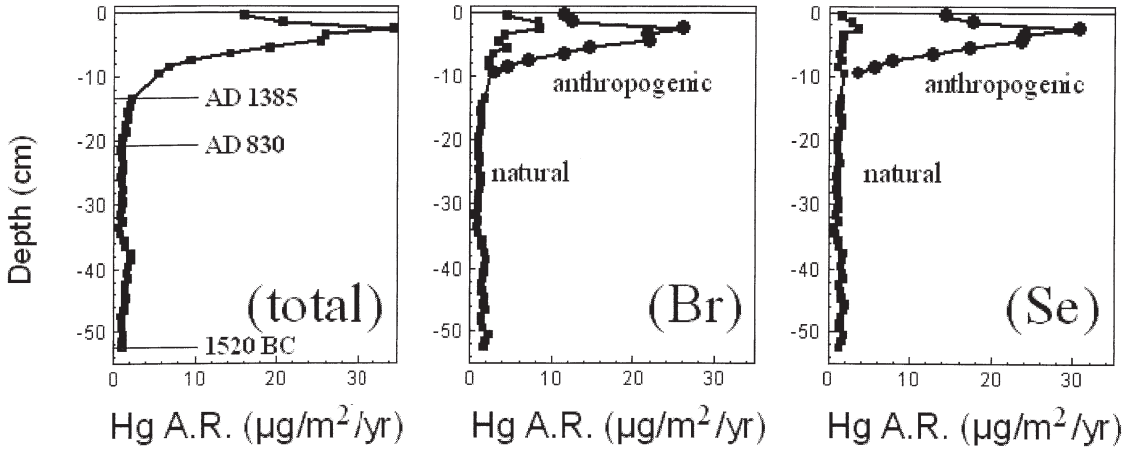

Fig. 12. Accumulation rates of atmospheric Hg ($\mu g/m^2/yr$): total, natural, and anthropogenic. Natural and anthropogenic fluxes of Hg calculated using Br and Se concentrations, and Hg/Br and Hg/Se ratios, as described in the text.

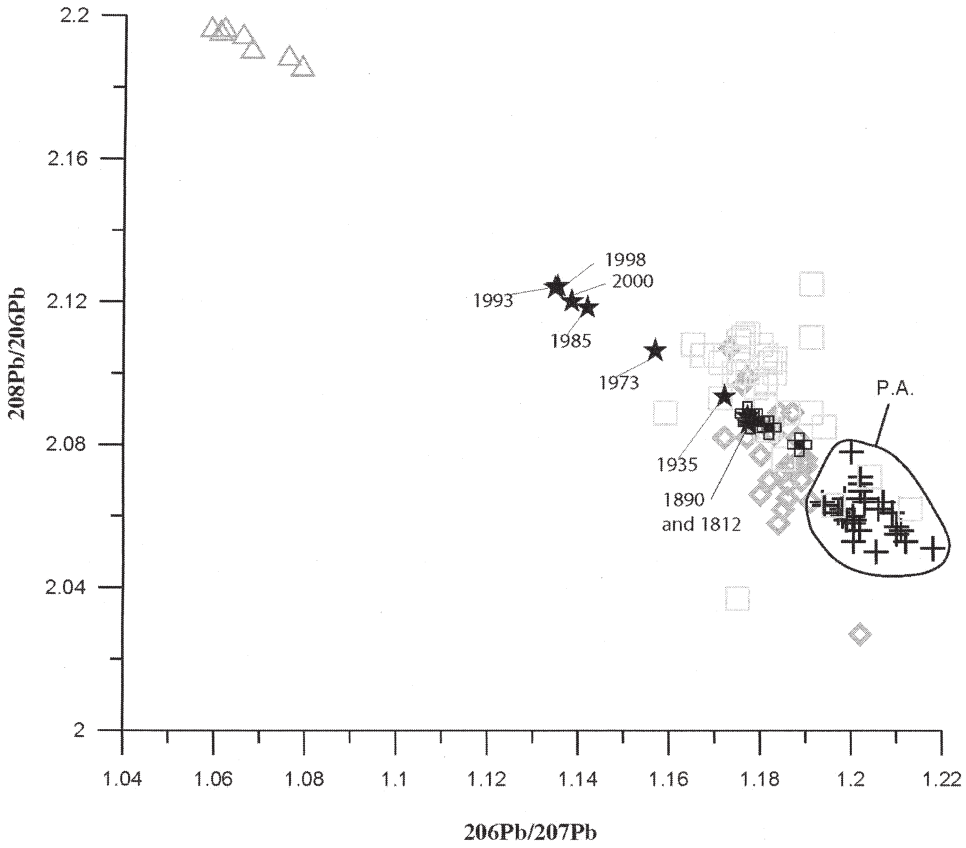

Fig. 13. Three isotope plot ($^{208}Pb/^{206}Pb$ vs. $^{206}Pb/^{207}Pb$) diagram with the least radiogenic samples (triangles) corresponding to leaded gasoline from England in 1995 (Monna et al., 1997) and the most radiogenic samples (+) representing values for sediments from "preanthropogenic" (PA) time (Sun, 1980; Shotyk et al., 2001). Values for UK coals from Farmer et al. (1999) are from England (diamonds) and Scotland (squares). Peat samples dating from the 19th century and the early part of the 20th century most closely resemble UK coal, whereas the most recent peat samples (past 30 yr) can only be explained by the addition of Pb-bearing aerosols derived from the combustion of leaded gasoline.

4.4. Determining the Predominant Source of Anthropogenic Pb and Hg Using Pb Isotopes

The predominant sources of atmospheric Pb to the peat core can be identified by comparing the $^{208}Pb/^{206}Pb$ ratio with the $^{206}Pb/^{207}Pb$ ratio (Fig. 13). The deepest sample measured (MYR Neo 42) shows the most radiogenic signature. Samples since AD 1812 contain significant concentrations of anthropogenic Pb (Fig. 8) and are less radiogenic than the underlying peats (Fig. 13). However, these highly contaminated samples fall into two categories. First, the lowest $^{206}Pb/^{207}Pb$ ratios occur in peat samples dating from 1993 to 1998 (Fig. 13). The data shown in Figure 13 indicates that these Pb isotope ratios can only be explained by the introduction of aerosols from leaded gasoline combustion. Second, the samples predating 1973 are more radiogenic, with $^{206}Pb/^{207}Pb$ ratios (1.1712 to 1.1770 from AD 1812 to AD 1935) comparable to British coals (Fig. 13). In this group of samples, therefore, coal combustion was the predominant source of anthropogenic Pb. In fact, much of the anthropogenic Pb in the MYR2 core predates, by a considerable margin, the introduction of leaded gasoline (in North America) in 1923 (Nriagu, 1990). The $^{206}Pb/^{207}Pb$ ratio (Fig. 8) shows that Pb became much less radiogenic *after* the maximum concentration of anthropogenic Pb was achieved. Similar results have been reported for peat cores from Switzerland (Shotyk et al., 2002a) and Denmark (Shotyk et al., 2003) and indicate that the maximum extent of atmospheric Pb contamination in Europe *predates* the maximum impact of Pb emissions from the use of leaded gasoline.

The maximum concentration of anthropogenic Pb dates to 1954 (Fig. 8), and this Pb was supplied primarily by coal-burning (Fig. 13). The maximum concentration of anthropogenic Pb (Fig. 8), however, also corresponds with the maximum concentration of Hg (Fig. 9) and the maximum Hg/Br and Hg/Se ratios (Fig. 10). Taken together, the Hg and Pb concentrations, the Hg/Br and Hg/Se ratios, and the Pb isotope data show that the predominant source of anthropogenic Hg to the peat core was coal burning, and this source reached its maximum strength in AD 1954.

4.5. Implications for the Global Atmospheric Hg Cycle

The results presented here are in general agreement with the history of global primary production of Hg over the last 500 yr as reported by Hylander and Meili (2003). This is a good indication of the global character and long residence time of elemental Hg in the atmosphere, and why similar chronologies

and accumulation rates are found in archives collected from areas with no significant local or regional source. The MYR2 peat core, however, provides poor temporal resolution and cannot be compared quantitatively with annual mercury production records (Hylander and Meili, 2003). For example, while the maximum Hg accumulation rate is found in peat dating from AD 1954, the overlying peat slice dates from AD 1973 ± 2, and the underlying segment from AD 1935 ± 2 (Table 3). Hylander and Meili (2003) indicate that approximately one half of the mercury produced during the past five centuries has been used to recover silver and gold. The appearance of anthropogenic Hg dating from medieval times in peat bogs from Spain (Martinez-Cortizas et al., 1999), Switzerland (Roos-Barraclough et al., 2002; Roos-Barraclough and Shotyk, 2003), and the Faroe Islands (this study) is probably a consequence of metallurgical uses of mercury.

Nriagu and Becker (2003) have estimated the total global flux of Hg from volcanic emissions at ~100 t/yr. In contrast, emissions of Hg from coal burning worldwide were estimated at 3000 t/yr (Joensuu, 1971); this estimate was based on global coal consumption of 3×10^9 t/yr, but coal consumption today exceeds 4×10^9 t/yr. The peat core at MYR2 confirms that Hg emissions from coal burning have been quantitatively more important than volcanic emissions, but also that they declined since the mid-1950s. The age of the maximum concentrations of anthropogenic Hg and Pb in the Faroe Islands is consistent with peat cores from Greenland and Denmark, which showed maximum concentrations in AD 1953 (Shotyk et al., 2003). In addition, peat cores from three bogs in southern Ontario, Canada, show maximum Hg accumulation rates between AD 1956 and 1959 (Givelet et al., 2003). The decline in Hg accumulation rates since the 1950's appears to be inconsistent with the progressive increase in coal consumption worldwide and the potential mobilisation of Hg from coal burning. However, the development and introduction of pollution control technologies, with their emphasis on removal of fly ash particles and SO_2, may have caused a shift in the kind of Hg that is being emitted from these facilities, with a decrease in the relative proportion of particulate Hg that is readily scavenged by precipitation.

The preindustrial flux recorded by the MYR2 core is ~1 $\mu g/m^2/yr$, which is also the minimum Hg accumulation rate recorded by the peat bog at EGR (Roos-Barraclough et al., 2002), as well as peat cores from Greenland (Shotyk et al., 2003), southern Ontario (Givelet et al., 2003), and northeastern USA. The elevated inputs of volcanic materials and marine aerosols to the peat profile at Myrarnar, therefore, have not measurably influenced the natural rate of atmospheric Hg accumulation relative to these other areas. Natural rates of atmospheric Hg accumulation recorded by peat bogs in Sweden (Bindler, 2003) and by alpine glacial ice in Wyoming, USA (Schuster et al., 2002) are also on the order of 1 $\mu g/m^2/yr$. In contrast, the preindustrial annual flux of Hg to the continents has been estimated at 4 Mmoles (Lamborg et al., 2002). Considering the area represented by the continental land mass (147×10^6 km^2), an average preindustrial flux of 5.5 $\mu g/m^2/yr$ is implied. The preindustrial flux calculated by Lamborg et al. (2002), therefore, may be too large by a factor of five. Thus, the true impact of human activities on the emissions of Hg to the global atmosphere may have been underestimated by the same extent.

Compared to the "natural background" rate of atmospheric Hg accumulation recorded by the peat cores we have studied, the maximum rate of atmospheric Hg accumulation in Switzerland, Denmark, Greenland, southern Ontario, and northeastern USA are as much as 30 to 50 times greater. The difference between the long-term rate of atmospheric Hg accumulation and the maximum rates of Hg accumulation provide quantitative insight into the true impact of human activities on the atmospheric Hg cycle.

5. CONCLUSIONS

The geochemical data presented here shows that there are considerable atmospheric inputs to the peatland at Myrarnar, Faroe Islands, from Icelandic volcanoes (Si, Al, Ga, Ti, Y, Zr) and marine aerosols (S, Cl, Br, Se). The preindustrial rate of atmospheric Hg accumulation recorded by the peat core is ~1 $\mu g/m^2/yr$. This value is comparable to those obtained from peat bogs in Switzerland (Roos-Barraclough et al., 2002; Roos-Barraclough and Shotyk, 2003), southern Greenland (Shotyk et al., 2003), southern Ontario (Givelet et al., 2003), and northeastern USA. Therefore, natural inputs of Hg from volcanoes and marine aerosols are no more important to the peat deposits of the Faroe Islands than they are to these other sites.

The maximum rate of total Hg accumulation (34 $\mu g/m^2/yr$) was found in peat dating from AD 1954, but the accumulation rates have since declined by ca. 50%. Bromine and selenium are useful reference elements for Hg because they too are supplied to the peat only by the atmosphere, and because the ratios Hg/Br and Hg/Se are constant in peat dating from preanthropogenic times. Using the measured Br and Se concentrations and the "natural" Hg/Br and Hg/Se ratios, "anthropogenic Hg" in peat can be easily calculated. The Pb isotope data indicates that coal burning was the single most important source of anthropogenic Hg (and Pb) to the bog.

Acknowledgments—For financial support we are grateful to the International Arctic Research Centre, Fairbanks, Alaska (grant to W. Shotyk, H. F. Schöler, and S. A. Norton), and DANCEA (Danish Cooperation for Environment in the Arctic) grant to M. E. Goodsite, W. Shotyk, and G. Asmund. Additional financial support from the Swiss National Science Foundation (grants to W. Shotyk), the Carlsberg Foundation (to C. Lohse), as well as the Danish EPA Project "Arctic Mercury on the Faroe Islands", to H. Skov (NERI-ATMI) and a Copenhagen Global Change Initiative (COGCI) Ph.D. graduate research assistantship to M. E. Goodsite. "Fate of Mercury in the Arctic," funded by the Danish Research Agency and NERI-ATMI, is gratefully acknowledged. The authors thank in Denmark the Danish Polar Centre Journal (Nr. 502-68); The National Environmental Research Institute, Department of Atmospheric Environment, Henrik Skov, Gary Geernaert and Prof. Ole John Nielsen, Department of Chemistry, University of Copenhagen; The University of Southern Denmark (Odense), Department of Chemistry (especially, P. B. Hansen, B. Daugaard, E. Dons, P. W. Jensen and F. Jensen). In Switzerland the authors thank Mr. H.-P. Bärtschi and the late A. Werthemann. We thank Prof. Esbern Warncke, Department of Plant Ecology, Aarhus University, for identification of the modern plant samples and Prof. P. G. Appleby for the radionuclide data and ^{210}Pb age dating. In the Faroe Islands, we thank the Faroe Islands Food and Environmental Agency (especially Jacob Pauli, Maria Dam, Jóhanna Olsen, and Katrin Hoydal); Dorete Bloch of the Museum of Natural History; Tummas í Niðristovu of Vestmanna, and Olivur Poulsen, Vatnsoyrar. Goods and services were provided by Atlantic Airways (special thanks to Frode Hansen and David Ormston);

Avis car rental, Thorshavn; Kodak Switzerland, Lausanne; LECO Instruments GmbH, Germany; Mountain Equipment Co-Op; Canada; Pentax Switzerland; Swissair Cargo; Victorinox, Switzerland; and Zarges, Germany. The clarity of this manuscript was considerably improved with the helpful comments of the Associate Editor and three anonymous reviewers. Special thanks from W.S. to Dr. Bernd Kober for making it possible for G.L. to use the TIMS in Heidelberg, and the usual message to Beth Haas.

Associate editor: M. Novak

REFERENCES

Appleby P. G., Shotyk W., and Fankhauser A. (1997) ^{210}Pb age dating of three peat cores in the Jura Mountains, Switzerland. *Water, Air, & Soil Pollution* **100,** 223–231.

Benoit J. M., Fitzgerald W. F., and Damman A. W. H. (1998) The biogeochemistry of an ombrotrophic bog: evaluation of use as an archive of atmospheric mercury deposition. *Environmental Research, Section A* **78,** 118–133.

Biester H., Kilian R., Hertel C., Woda C., Mangini A., and Schöler H. F. (2002) Elevated mercury concentrations in peat bogs of South Patagonia, Chile-an anthropogenic signal. *Earth and Planetary Science Letters* **201,** 609–620.

Biester H., Martinez-Cortizas A., Birkenstock S., and Kilian R. (2003) Historic mercury records in peat bogs. The role of peat decomposition and mass losses *Environmental Science and Technology* **37,** 32–39.

Bindler R. (2003) Estimating the natural background atmospheric deposition rate of mercury utilizing ombrotrophic bogs in south Sweden. *Environmental Science and Technology* **37,** 40–46.

Boyarkina A. P., Vasil'ev N. V., Glukhov G. G., Rezchikov V. I., and Tyulyupo E. B. (1980) Gold and mercury levels in *Sphagnum* peats. *Byull. Pochv. Inst. im. V. V. Dokuchaeva.* **24,** 24–24-5.

Bränvall M. L., Bindler R., Emteryd O., Nilsson M., and Renberg I. (1997) Stable isotope and concentration records of atmospheric lead pollution in peat and lake sediments in Sweden. *Water, Air, & Soil Pollution* **100,** 243–252.

Cheburkin A. K. and Shotyk W. (1996) An Energy-dispersive Miniprobe Multielement Analyzer (EMMA) for direct analysis of Pb and other trace elements in peats. *Fresenius J. of Analytical Chemistry* **354,** 688–691.

Cheburkin A. K., Frei R., and Shotyk W. (1997) An Energy-dispersive Miniprobe Multielement Analyzer (EMMA) for direct analysis of trace elements and chemical age dating of single mineral grains. *Chem. Geology* **135,** 75–87.

Dugmore A. J. and Newton A. J. (1998) Holocene tephra layers in the Faroe Islands. *Frooskaparrit* **46,** 191–204.

Farmer J. G., Mackenzie A. B., Sugden C. L., Edgar P. J., and Eades L. J. (1997) A comparison of the historical lead pollution records in peat and freshwater lake sediments from central Scotland. *Water, Air, & Soil Pollution* **100,** 253–270.

Farmer J. G., Eades L. J., and Graham M. C. (1999) The lead content and isotopic composition of Br coals and their implications for past and present releases of lead to the U.K. environment *Environmental Geochemistry and Health* **21,** 257–272.

Galer S. J. G. and Abouchami W. (1998) Practical application of lead spiking for correction of instrumental mass discrimination. *Mineralogical Magazine* **62A,** 491–492.

Givelet N., Roos-Barraclough F., and Shotyk W. (2003) Rates and predominant anthropogenic sources of atmospheric Hg accumulation in southern Ontario recorded by peat cores from three bogs: comparison with natural "background" values (past 8,000 years). *J. of Environmental Monitoring* **5,** 935–949.

Givelet N., Le Roux G., Cheburkin A. K., Chen B., Goodsite M. E., Frank J., Kempter H., Krachler M., Nørnberg T., Rausch N., Rheinberger S., Roos-Barraclough F., Sapkota A., Scholz C., and Shotyk W. (2004) Protocol for collecting, handling and preparing peat cores and peat samples for physical, chemical, mineralogical and isotopic analyses. *J. of Environmental Monitoring* **6,** 481–492.

Gobeil C., Macdonald R. W., and Smith J. N. (1999) Mercury profiles in sediments of the Arctic Ocean basins. *Environmental Science and Technology* **33,** 4194–4198.

Goldich S. S. (1938) A study in rock-weathering *J. of Geology* **46,** 17–58.

Grandjean P., Weihe P., White R. F., Debes F., Araki S., Murata K., Sørensen N., Dahl D., Yokoyama K., and Jørgensen P. J. (1997) Cognitive deficit in 7-year-old children with prenatal exposure to methylmercury. *Neurotoxicology Teratology* **19,** 417–28.

Hannon G. E. and Bradshaw R. H. W. (2000) Impacts and timing of the first human settlement on vegetation of the Faroe Islands. *Quat. Res.* **54,** 404–413.

Heidam N. Z., Christensen J., Wåhlin P., and Skov H. (2004) Arctic atmospheric contaminants in Greenland: levels, variations, origins, transport, transformations and trends 1990 to 2001. *Science of the Total Environment* (in press).

Hong S., Candelone J.-P., Patterson C. C., and Boutron C. F. (1994) Greenland ice evidence of hemispheric lead pollution two millenia ago by Greek and Roman civilizations. *Science* **265,** 1841–1843.

Hylander L. D. and Meili M. (2003) 500 years of mercury production: global annual inventory by region until 2000 and associated emissions. *Science of the Total Environment* **304,** 13–27.

Jensen A. and Jensen A. (1991) Historical rates of mercury in Scandinavia estimated by dating and measurement of mercury in cores of peat bogs. *Water, Air, & Soil Pollution* **56,** 769–777.

Joensuu O. (1971) Fossil fuels as a source of mercury pollution. *Science* **172,** 1027–1028.

Kempter H. and Frenzel B. (1999) The local nature of anthropogenic emission sources on the elemental content of nearby ombrotrophic peat bogs, Vulkaneifel, Germany. *Science of the Total Environment* **241,** 117–128.

Kempter H. and Frenzel B. (2000) The impact of early mining and smelting on the local tropospheric aerosol detected in ombrotrophic peat bogs in the Harz, Germany. *Water, Air, & Soil Pollution* **121,** 93–108.

Kempter H., Görres M., and Frenzel B. (1997) Ti and Pb concentrations in rainwater-fed bogs in Europe as indicators of past anthropogenic activities. *Water, Air, & Soil Pollution* **100,** 367–377.

Klaminder J., Renberg I., Bindler R., and Emteryd O. (2003) Isotopic trends and background fluxes of atmospheric lead in northern Europe: Analyses of three ombrotrophic bogs from south Sweden. *Global Biogeochemical Cycles* **17** (*1*), 1019, doi:10.1029/2002GB001921.

Kober B., Wessels M., Bollhöfer A., and Mangini A. (1999) Pb isotopes in sediments of Lake Constance, Central Europe constrain the heavy metal pathways and the pollution history of the catchment, the lake and the regional atmosphere. *Geochim. Cosmochim. Acta* **63,** 1293–1303.

Krachler M., Mohl C., Emons H., and Shotyk W. (2002) Analytical procedures for the determination of selected trace elements in peat and plant samples by inductively coupled plasma spectrometry. *Spectrochimica Acta B* **57,** 1277–1289.

Lamborg C. H., Fitzgerald W. F., O'Donnell J., and Torgersen T. (2002) A non-steady state compartmental model of global-scale mercury biogeochemistry with interhemispheric atmospheric gradients. *Geochim. Cosmochim. Acta* **66,** 1105–1118.

Larsen R. B. and Dam M. (1999) AMAP Phase 1. The Faroe Islands *Faroe Islands Food and Environmental Agency Report,* **1999,** 119.

Le Roux G., Weiss D., Grattan J., Givelet N., Krachler M., Cheburkin A. K., Rausch N., Kober B., and Shotyk W. (2004) Identifying the sources and timing of ancient and medieval atmospheric metal pollution in England by a peat profile. *J. of Environmental Monitoring* **6,** 502–510.

Lindberg S. E., Brooks S., Lin, C.-J., Scott K. J., Landis M. S., Stevens R. K., Goodsite M. E., and Richter A. (2002) Dynamic oxidation of gaseous mercury in the Arctic troposphere at polar sunrise. *Environmental Science and Technology* **36,** 1245–1256.

Lodenius M., Seppänen A., and Uusi-Rauva A. (1983) Sorption and mobilization of mercury in peat soil. *Chemosphere* **12,** 1575–1581.

MacKenzie A. B., Farmer J. G., and Sugden C. L. (1997) Isotopic evidence of the relative retention and mobility of lead and radiocaesium in Scottish ombrotrophic peats. *Science of the Total Environment* **203,** 115–127.

MacKenzie A. B., Logan E. M., Cook G. T., and Pulford I. D. (1998) Distributions, inventories and isotopic composition of lead in ^{210}Pb-dated peat cores from contrasting biogeochemical environments: Implications for lead mobility. *Science of the Total Environment* **223,** 25–35.

Mangerud J., Furnes H. and Johansen J. (1986) A 9000-year old ash bed on the Faroe Islands. *Quat. Res.* **26,** 262–265.

Martinez-Cortizas A., Pontevedra Pomba X., Novoa Munoz J. C., and Garcia-Rodeja E. (1997) Four thousand years of atmospheric Pb, Cd and Zn deposition recorded by the ombrotrophic peat bog of Penido Vello (northwestern Spain). *Water, Air, & Soil Pollution* **100,** 387–403.

Martinez-Cortizas A. M., Pontevedra Pomba X., Garcia-Rodeja E., Novoa Munoz J. C., and Shotyk W.. (1999) Mercury in a Spanish peat bog: archive of climate change and atmospheric metal deposition. *Science* **284,** 939–942.

Martinez-Cortizas A., Garcia-Rodeja E., Pontevedra Pomba X., Novoa Munoz J. C., Weiss D., and Cheburkin A. K. (2002) Atmospheric Pb deposition in Spain during the last 4600 years recorded by two ombrotrophic peat bogs and implications for the use of peat as archive. *Science of the Total Environment* **292,** 33–44.

Mikkelsen B., Hoydal. K., Dam M., and Danielsen J. (2002) Føroya Umhvørvi I Tølum 2001 (in Faroese). *Heilsurfrøoðiliga Starvstovan, rapport nr.* **1,** Torshavn, Faroe Islands.

Monna F., Lancelot J., Croudace I. W., Cundy A. B., and Lewis J. T. (1997) Pb isotopic composition of airborne particulate material from France and the southern United Kingdom: Implications for Pb pollution sources in urban areas. *Environmental Science and Technology* **31,** 2277–2286.

Nieminen T., Ukonmaanaho L., and Shotyk W. (2002) Enrichment of Cu, Ni, Zn, Pb and As in an ombrotrophic peat bog near a Cu-Ni smelter in SW Finland. *Science of the Total Environment* **292,** 81–89.

Norton S. A., Evans G. C., and Kahl J. S. (1997) Comparison of Hg and Pb fluxes to hummocks and hollows of ombrotrophic Big Heath Bog and to nearby Sargent Mt. Pond, Maine, USA *Water, Air, & Soil Pollution* **100,** 271–286.

Novak M., Emmanuel S., Vile M. A., Erel Y., Veron A., Paces T., Wieder R. K., Vanecek M., Stepanova M., Brizova E., Hovorka J. (2003) Origin of lead in eight Central European Peat Bogs determined from isotope ratios, strengths and operation times of regional pollution sources. *Environmental Science and Technology* **37,** 437–445.

Nriagu J. O. (1990) The rise and fall of leaded gasoline. *The Science of the Total Environment* **92,** 13–28.

Nriagu J. O. and Becker C. (2003) Volcanic emissions of mercury to the atmosphere: regional and global inventories. *Science of the Total Environment* **304,** 1–12.

Oechsle D. (1982) *Untersuchungen zur Mobilität vonq Uecksilber-Spezies in Hochmooren und Möglichkeiten zu ihrer analytische Trennung and Bestimmung*. Ph.D. Thesis, Universität Stuttgart.

Persson C. (1971) Tephrochronological investigation of peat deposits in Scandinavia and on the Faroe Islands. *Sveriges Geologiska Undersökning, Ser C* **65,** 3–34.

Pheiffer-Madsen P. (1981) Peat bog records of atmospheric mercury deposition. *Nature* **293,** 127–129.

Rasmussen P. E. (1994) Current methods of estimating atmospheric mercury fluxes in remote areas. *Environmental Science and Technology* **28,** 2233–2241.

Rehkämper M. and Mezger K. (2000) Investigation of matrix effects for Pb isotope ratio measurements by multiple collector ICP-MS: verification and application of optimized protocols. *J. of Analytical Atomic Spectrometry* **15,** 1451–1460.

Renberg I., Brännvall M.-L., Bindler R., and Emteryd O. (2002) Stable isotopes and lake sediments- a useful combination for the study of atmospheric lead pollution history. *Science of the Total Environment* **292,** 45–54.

Roos-Barraclough F. and Shotyk W. (2003) Millennial-scale records of atmospheric mercury deposition obtained from ombrotrophic and minerotrophic peat from the Swiss Jura Mountains. *Environmental Science and Technology* **37,** 235–244.

Roos-Barraclough F., Martinez-Cortizas A., Garcia-Rodeja E., and Shotyk W. (2002) A 14,500 year record of the accumulation of atmospheric mercury in peat: volcanic signals, anthropogenic influences and a correlation to bromine accumulation. *Earth and Planetary Science Letters* **202,** 435–451.

Schuster P. F., Krabbenhoft D. P., Naftz D. L. O., Cecil D., Olson M. L., Dewild J. F., Susong D. F., Green J. R., and Abbott M. L. (2002) Atmospheric mercury deposition during the last 270 years: a glacial ice core record of natural and anthropogenic sources. *Environmental Science and Technology* **36,** 2303–2310.

Shotyk W. (1988) Review of the inorganic geochemistry of peats and peatland waters. *Earth-Science Rev.* **25,** 95–176.

Shotyk W. (1996) Peat bog archives of atmospheric metal deposition: Geochemical assessment of peat profiles, natural variations in metal concentrations and metal enrichment factors. *Environmental Rev.* **4,** 149–183.

Shotyk W. (1997) Atmospheric deposition and geochemical mass balance of major elements and trace elements in two oceanic blanket bogs, northern Scotland and the Shetland Islands. *Chem. Geology* **138,** 55–72.

Shotyk W. (2002) The chronology of anthropogenic, *atmospheric* Pb deposition recorded by peat cores in 3 *minerotrophic* peat deposits from Switzerland. *Science of the Total Environment* **292,** 19–31.

Shotyk W., Cheburkin A. K., Appleby P. G., Fankhauser A., and Kramers J. D. (1996) Two thousand years of atmospheric arsenic, antimony and lead deposition recorded in a peat bog profile, Jura Mountains, Switzerland. *Earth and Planetary Science Letters* **145,** E1–E7.

Shotyk W., Cheburkin A. K., Appleby P. G., Fankhauser A., and Kramers J. D. (1997) Lead in three peat bog profiles, Jura Mountains, Switzerland: enrichment factors, isotopic composition and chronology of atmospheric deposition. *Water, Air, & Soil Pollution* **100,** 297–310.

Shotyk W., Weiss D., Appleby P. G., Cheburkin A. K., Frei R., Gloor M., Kramers J. D., Reese S., and van der Knaap W. O. (1998) History of atmospheric lead deposition since 12,370 ^{14}C yr BP recorded in a peat bog profile, Jura Mountains, Switzerland. *Science* **281,** 1635–1640.

Shotyk W., Weiss D., Kramers J. D., Frei R., Cheburkin A. K., Gloor M., and Reese S. (2001) Geochemistry of the peat bog at Etang de la Gruère, Jura Mountains, Switzerland and its record of atmospheric Pb and lithogenic trace elements (Sc, Ti, Y, Zr, Hf and REE) since 12,370 ^{14}C yr BP. *Geochim. Cosmochim. Acta* **65,** 2337–2360.

Shotyk W., Weiss D., Heisterkamp M., Cheburkin A. K., and Adams F. C. (2002a) A new peat bog record of atmospheric lead pollution in Switzerland: Pb concentrations, enrichment factors, isotopic composition and organolead species. *Environmental Science and Technology* **36,** 3893–3900.

Shotyk W., Krachler M., Martinez-Cortizas A., Cheburkin A. K., and Emons H. (2002b) A peat bog record of natural, pre-anthropogenic enrichments of trace elements in atmospheric aerosols since 12,370 ^{14}C yr BP and their variation with Holocene climate change. *Earth and Planetary Science Letters* **199,** 21–37.

Shotyk W., Goodsite M. E., Roos-Barraclough F., Heinemeier J., Frei R., Asmund G., Lohse C., and Stroyer T. H. (2003) Anthropogenic contributions to atmospheric Hg, Pb and As deposition recorded by peat cores from Greenland and Denmark dated using the ^{14}C ams "bomb pulse curve". *Geochim. Cosmochim. Acta* **67,** 3991–4011.

Skov H., Christensen J., Goodsite M., Heidam N. Z., Jensen B., Wåhlin P., and Geernaert G. (2004) Fate of elemental mercury in the Arctic during atmospheric mercury depletion episodes and the load of atmospheric mercury to the Arctic. *Environmental Science and Technology* **38,** 2373–2382.

Steinmann P. and Shotyk W. (1997a) The pH, redox chemistry and speciation of Fe and S in pore waters from two contrasting *Sphagnum* bogs, Jura Mountains, Switzerland. *Geochim. Cosmochim. Acta* **61,** 1143–1163.

Steinmann P. and Shotyk W. (1997b) The geochemistry of major elements in peats from two contrasting *Sphagnum* bogs, Jura Mountains, Switzerland. *Chem. Geology* **138,** 25–53.

Sun S. S. (1980) Lead isotopic study of young volcanic rocks from mid-ocean ridges, ocean islands and islands arcs. *Philosophical Transactions of the Royal Society of London* **A297,** 409–445

Vile M. A., Novak M. J., Brizova E., Wieder R. K., and Schell W. R. (1995) Historical rates of atmospheric Pb deposition using ^{210}Pb dated peat cores: corroboration, computation and interpretation. *Water, Air, & Soil Pollution* **79,** 89–106.

Vile M. A., Wieder R. K., and Novak M. (1999) Mobility of Pb in *Sphagnum*-derived peat. *Biogeochemistry* **45,** 35–52.

Vile M. A., Wieder R. K., and Novak M. (2000) 200 years of Pb deposition throughout the Czech Republic: patterns and sources. *Environmental Science and Technology* **34,** 12–20.

Wardenaar E. C. P. (1987) A new hand tool for cutting peat profiles. *Canadian J. of Botany* **65,** 1772–1773.

Wastegård S., Björck S., Grauert M., and Hannon G. E. (2001) The Mjáuvøtn Tephra and other Holocene tephra horizons from the Faroe Islands: a potential link between the Icelandic source region, the Nordic Seas and the European continent. *The Holocene* **11,** 101–109.

Weihe P., Grandjean P., Debes F., and White R. (1996) Health implications for Faroe Islanders of heavy metals and PCBs from pilot whale. *Science of the Total Environment* **186,** 141–148.

Weiss D., Shotyk W., Appleby P. G., Cheburkin A. K., and Kramers J. D. (1999a) Atmospheric Pb deposition since the Industrial Revolution recorded by five Swiss peat profiles: enrichment factors, fluxes, isotopic compositon and sources. *Environmental Science and Technology* **33,** 1340–1352.

Weiss D., Shotyk W., Gloor M., and Kramers J. D. (1999b). Herbarium specimens of *Sphagnum* moss as archives of recent and past atmospheric Pb deposition in Switzerland: isotopic composition and source assessment. *Atmospheric Environment* **33,** 3751–3763.

Weiss D., Shotyk W., Boyle E. A., Kramers J. D., Appleby P. G., and Cheburkin A. K. (2002) Constraining lead sources to the North Atlantic Ocean: Recent atmospheric lead deposition recorded by two ombrotrophic peat bogs in Scotland and Eastern Canada. *Science of the Total Environment* **292,** 7–18.

Weiss D. J., Kober B., Gallagher K., Dolgopolova A., Mason T. F. D., Coles B. J., Kylander M., LeRoux G., and Spiro B. (2004) Accurate and precise Pb isotope measurements in environmental samples using MC-ICP-MS. *Intern. J. Mass Spectrom.* **232,** 205–215.1

- Appendix 3-

Comparison of atmospheric deposition of copper, nickel, cobalt, zinc and cadmium recorded by peat cores from three ombrotrophic bogs in Finland with monitoring data and emission records

Nicole Rausch[1], Tiina Nieminen[2], Liisa Ukonmaanaho[2], Gaël Le Roux[1], Michael Krachler[1], Andriy K. Cheburkin[1], Georges Bonani[3], William Shotyk*,[1]

[1]Institute of Environmental Geochemistry, University of Heidelberg, Im Neuenheimer Feld 236, 69120 Heidelberg, Germany; [2]Finnish Forest Research Institute, Box 18, 01301 Vantaa, Finland, [3]Institute for Particle Physics, ETH Zuerich, Switzerland

*Corresponding author phone: +48-6221-544801; fax: +48-6221-545228; e-mail: shotyk@ugc.uni-heidelberg.de;

Submitted to Environmental Science and Technology

Abstract

This study aims to determine the extent to which the accumulation rates of Cu, Ni, Co, Zn and Cd in peat cores agree with established histories of atmospheric emission from local point sources. Metals accumulating in three Finnish peat cores with known metal deposition histories have been measured using sector field inductively coupled plasma-mass spectrometry. Samples were age-dated using both ^{210}Pb and ^{14}C (bomb pulse curve). At the Outokumpu (Out) site as well as the low-background site Hietajärvi (HJ), ^{210}Pb age dates are in excellent agreement with the ^{14}C bomb pulse curve method, and the precision is between one and ten years for most of the samples; at the Harjavalta site, precision is greater than 6 years. Mean regional "background" concentrations have been calculated from deeper peat layers of the HJ site (µg g^{-1}): Cu 1.3 ± 0.2 (n=62), Co 0.25 ± 0.04 (n=71), Cd 0.08 ± 0.01 (n=23), and Zn 4 ± 2 (n=40). For layers accumulated within the last 100 years, accumulation rates (ARs) have been calculated. In sites with <0.06 g m^{-2} cumulative Ni inventory (HJ and Out), ARs of Cu and Co trace the known metal deposition histories very well. Slight mobility of Cu and Co occurred at Har, where 0.9 g m^{-2} Ni has accumulated. ARs of Zn were between three and 30 mg m^{-2} yr^{-1}, and of Cd between 24 and 140 µg m^{-2} yr^{-1} at all sites, and are independent of the chronology of their inputs from the atmosphere.

KEYWORDS: Cu; Ni; Co; Zn; Cd; atmospheric deposition; ombrotrophic peat bogs; mining; smelting

Introduction

Ombrotrophic peat cores have recently proved to be meaningful archives of recent as well as ancient atmospheric metal deposition, especially for Pb [1-3] and Hg [4-7]. In contrast, there are far fewer studies on the distribution and fate of Cu [8-14], Ni [13,15], Co [12], Cd [8,10] or Zn [8,10-12,14,16-18] in ombrotrophic peat bogs. While some studies have provided evidence that Cu concentrations may reflect the history of ancient mining and smelting [9,16], Zn is thought to be rather mobile in peat and to be readily redistributed by plants [8,10,12,14,16-18]. In general, however, previous work on these trace metals in ombrotrophic peat tends to suffer either from poor temporal resolution, uncertain analytical data, a lack of characterisation of the background metal concentration and its natural variation, inaccurate or insufficient age dating, or poorly constrained peat accumulation rates.

Here, peat cores were collected from bogs which had already been subjected to preliminary study [19,20]. Replicate cores were frozen and precisely cut into 1 cm slices, and age dated using both ^{210}Pb and ^{14}C (including the atmospheric "bomb pulse curve"[21]). This approach has been used successfully for atmospheric deposition of Pb and Hg [22,23] and offers the promise of detailed, high resolution reconstructions of atmospheric trace metal deposition which can be compared with the known metal emission histories of the three sites: Harjavalta, nearby a Cu-Ni smelter, Outokumpu, near the famous Cu-Ni mine, and Hietajärvi, a "low background" control site which receives atmospheric trace metals predominantly from long range transport. The main goal of the study is to determine the extent to which the accumulation rates of Cu, Ni, Co, Zn and Cd in the peat cores agree with the established histories of atmospheric emission from these point sources. If there is disagreement between the metal accumulation rates in the bogs and the emission histories, the second goal is to determine whether these are due to the uncertainty in the age dating methods, or whether physical, chemical, or biological processes in the bogs might be responsible for redistributing the metals, subsequent to their deposition from the air.

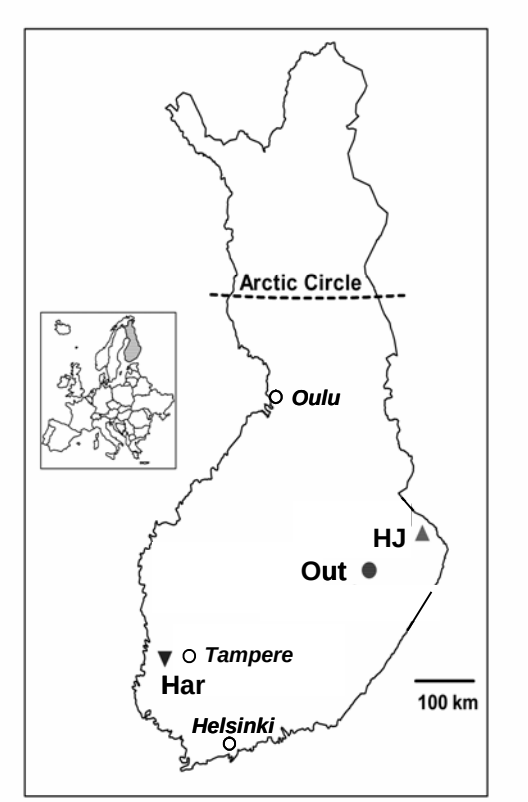

FIGURE 1. Map of Finland with the location of the sampling sites indicated. HJ: Hietajärvi; Out: Outokumpu; Har: Harjavalta.

Materials and Methods

Study sites. Peat cores were taken from undisturbed, *Sphagnum*-dominated ombrotrophic peat bogs at Hietajärvi (HJ), Outokumpu (Out) and Harjavalta (Har) (Figure 1). The surface waters have a pH of ~ 4 which is typical of ombrotrophic bogs. A detailed description of the sampling sites is given elsewhere [19,20] and summarized here. The HJ site is located in the Patvinsuo National Park, Eastern Finland. As there are no agricultural activities or roads in the vicinity, and no point sources of atmospheric metal pollution within a radius of tens of kilometers, the predominant source of contaminants is from long range transport [24]. The Out sampling site is located in the Viurusuo mire complex in eastern Finland, 8 km SW of the town of Outokumpu. A Cu-Ni mine and concentration plant operated at

Outokumpu from 1910 until the 1980s, and a small smelter from 1913 until 1929 [25]. At the Har site, peat samples were taken from a peat bog in the Pyhäsuo mire complex, 6 km northeast of Harjavalta, SW Finland, where a Cu smelter has been operating since 1945 and a Ni smelter since 1959 [25].

Sampling. Each site was sampled using a titanium Wardenaar corer. The cores were immediately frozen and shipped to the lab where they were sectioned into 1 cm slices with a stainless steel band saw. The edges of each slice were removed, the residual peat dried at 105° C in Teflon bowls, and milled with a Titanium centrifugal mill equipped with 0.25 mm sieve. Details of the sample collection and preparation protocol are given elsewhere [26].

Representativeness. The distribution of Cu, Ni and Zn in the Out and Har cores is similar to the distribution in the replicate cores described elsewhere [19]. Other studies also found replicate cores recording similar metal concentrations [6,9,11,16,27].

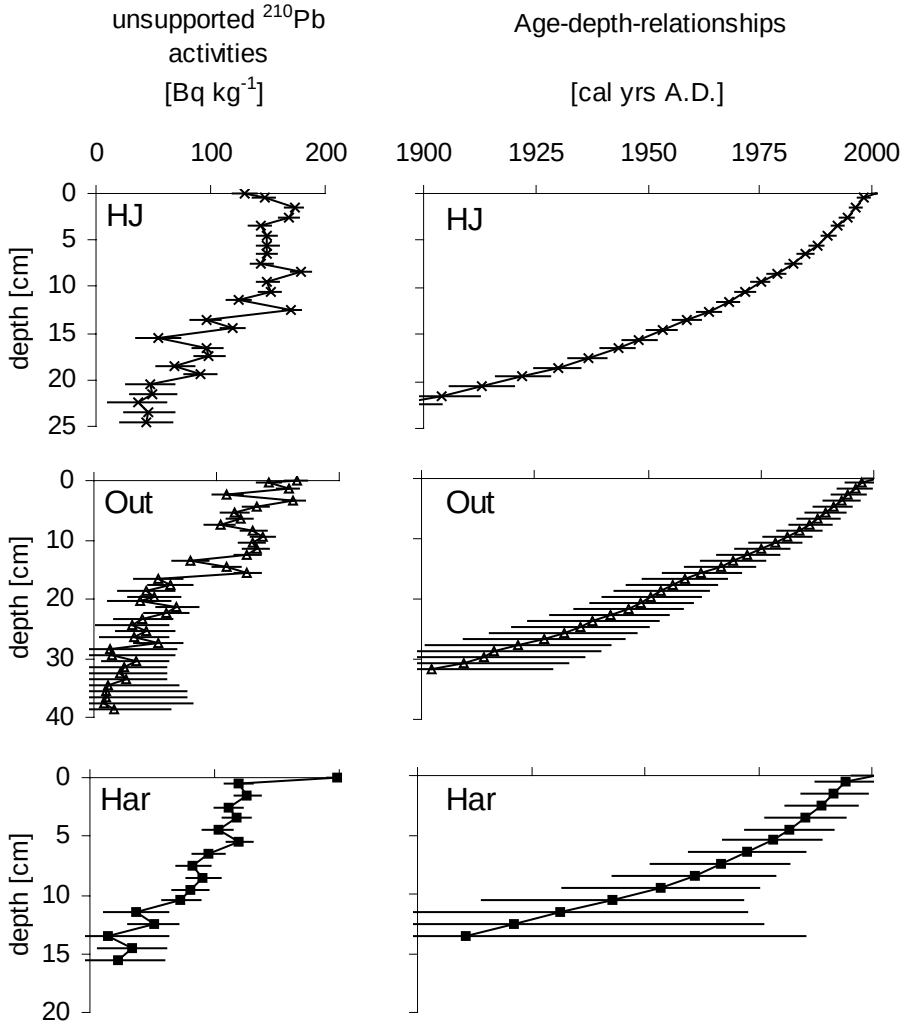

FIGURE 2. Age dating using ^{210}Pb: Unsupported ^{210}Pb activities and age-depth-relationships of the HJ, Out and Har cores.

Age dating. Recent peat samples were age dated using ^{210}Pb (CRS model) [28]. The activities of ^{210}Pb were determined in bulk samples of peat powder using low background gamma spectroscopy (GCW 4028, HPGE, Canberra). Estimated errors in ^{210}Pb age dates are based on error propagation of ^{210}Pb counting errors and density variability. As an independent check on the ages obtained using ^{210}Pb, the atmospheric

bomb pulse of ^{14}C was used to date five samples more recent than AD 1950 selected from each peat core. Ages of older peat samples were obtained using conventional ^{14}C age dating. All ages given in the text, except where noted, were obtained using ^{210}Pb.

Macrofossils of *Sphagnum* moss were identified in selected slices using optical microscopy, carefully removed, prepared using a standard procedure for plant material [29] and then age dated (^{14}C) using accelerator mass spectrometry (AMS) at the ETH Zürich. In two highly decomposed samples where no *Sphagnum* could be identified, *Carex* fibres were selected (Table 1). For dating using the bomb pulse curve (b.p.c.), ages were graphically evaluated using the calibrated ^{14}C b.p.c. of the northernmost northern hemisphere [30]. For samples older than 1800, calibrated (bomb-corrected) radiocarbon ages were presented as 2σ-ranges (95% confidence limit) and calculated using the program CalibETH [31].

Trace metal analyses. Powdered samples were digested in duplicate using a microwave-heated high-pressure autoclave (ultraCLAVE II, MLS) employing high-purity reagents (subboiled HNO_3, H_2O_2 and HBF_4) as described elsewhere [15]. Sector field ICP MS (SF-ICP-MS, Element2, Thermo Electron) was used to determine Cd, Co, Cu, Ni and Sc concentrations in the HJ and Out core, while ICP-OES (Vista MPX, Varian Inc.) was used to determine these elements in the Har core. For SF-ICP-MS measurements, digests with a dilution factor of ~500 were spiked with 1 µg L^{-1} In as internal standard element, and primed by a self-aspirating inert sampling introduction system (Micro-Flow PFA-100 nebulizer and Scott-type spray chamber made of PFA). For ICP-OES analysis, digests with a dilution factor of ~50 were measured using an inert Sturman-Masters cyclone spray chamber and V-slit nebulizer using Sc as internal standard element for the Cu, Ni, Co and Cd analysis. Method detection limits for ICP-OES analysis, referring to solid samples, were as follows: Cu 0.03 µg g^{-1}, Ni 0.05 µg g^{-1}, Co 0.05 µg g^{-1}, Cd 0.006 µg g^{-1}. Cobalt concentrations approached the limit of detection of ICP-OES in the Har samples below of 30 cm.

Quality control and inter-method comparison. Plant reference materials were digested in duplicate with every batch of samples and analyzed together with samples, to ensure both the completeness of digestion and the accuracy of the analysis. For SF-ICP-MS measurements, NIST SRM 1573 A Tomato Leaves and CTA-OTL-1 Oriental Tobacco Leaves were used. For ICP-OES measurements, CTA-VTL-2 Virginia Tobacco Leaves was used. Results obtained for Cd, Co, Cu, Ni and Sc were within the certified range. An inter-method comparison based on regression analysis of ten Har peat samples showed excellent correlation ($r \geq 0.99$; $n=10$) between SF-ICP-MS and ICP-OES measurements for all elements, with relative systematic errors of ≤3% for Cd, Co, Cu and Ni and 13% for Sc concentrations.

Further analyses. Zinc and Sr were determined using an energy-dispersive miniprobe X-ray fluorescence multi-element analyzer as described elsewhere [32]. For Ca, a new X-ray fluorescence spectrometer was used [33]. Percentage light absorption of NaOH extracts (8%) of peat samples was determined using a UV-VIS spectrometer (λ=550 nm) as a proxy of peat decomposition as described elsewhere [34]. Density was calculated after determining the thickness (± 0.1 mm) and dry weight of three single plugs with defined area.

depth (cm)	Mat. ^{210}Pb dated	Date ^{210}Pb yr A.D.	Mat. ^{14}C dated	^{14}C AMS	Lab. No.	Date ^{14}C yr B.P.	δ^{13}C (‰)	Date Cal yr A.D. (B.C.)
HJ 6.5	*Bulk*	1985 ± 2	*Sph*	^{14}C b.p.c.	ETH-28610	-2230±40	-28.0	1979 ± 1
7.5	*Bulk*	1982 ± 2						
8.5	*Bulk*	1979 ± 2						
9.5	*Bulk*	1975 ± 2	*Sph*	^{14}C b.p.c.	ETH-28611	-2885±40	-24.8	1973 ± 1
10.5	*Bulk*	1972 ± 2						
11.5	*Bulk*	1968 ± 2	*Sph*	^{14}C b.p.c.	ETH-28612	-4155±40	-28.8	1967 ± 1 1963 ± 1
12.5	*Bulk*	1964 ± 3	*Sph*	^{14}C b.p.c.	ETH-28613	-3460±40	-31.9	1963 ± 1
13.5	*Bulk*	1959 ± 3	*Sph*	^{14}C b.p.c.	ETH-28614	-785±40	-30.8	1957 ± 1
44.5			*Sph*	Convent. ^{14}C	ETH-28660	955±45	-25.4	1000-1164 (95%) 1167-1188 (5%)
54.5			*Sph*	Convent. ^{14}C	ETH-28661	1145±45	-25.6	778-986 (100%)
74.5			*Carex*	Convent. ^{14}C	ETH-28662	2480±50	-28.2	(BC 779-479) (87%) (BC 470-446) (5%) (BC 444-411) (8%)
Out 7.5	*Bulk*	1986 ± 5	*Sph*	^{14}C b.p.c.	ETH-28605	-1470±40	-28.5	1986 ± 1
8.5	*Bulk*	1984 ± 5						
9.5	*Bulk*	1981 ± 5						
10.5	*Bulk*	1978 ± 6						
11.5	*Bulk*	1975 ± 6	*Sph*	^{14}C b.p.c.	ETH-28606	-2825±40	-27.3	1973 ± 1
12.5	*Bulk*	1972 ± 7						
13.5	*Bulk*	1969 ± 7						
14.5	*Bulk*	1966 ± 8	*Sph*	^{14}C b.p.c.	ETH-28607	-4435±40	-27.1	1964 ± 1
16.5	*Bulk*	1962 ± 9	*Sph*	^{14}C b.p.c.	ETH-28608	-4710±40	-28.6	1964 ± 1 1965 ± 1
17.5	*Bulk*	1958 ± 10	*Sph*	^{14}C b.p.c.	ETH-28609	-3015±40	-27.2	1963 ± 1
49.5			*Sph*	Convent. ^{14}C	ETH-28656	415±45	-25.6	1420-1525 (76%) 1557-1630 (24%)
69.5			*Sph*	Convent. ^{14}C	ETH-28657	945±45	-26.3	1017-1192 (100%)
79.5			*Carex*	Convent. ^{14}C	ETH-28658	1505±45	-25.6	471-479 (5%) 531-622 (89%) 630-637 (4%)
Har 3.5	*Bulk*	1985 ± 9	*Sph*	^{14}C b.p.c.	ETH-28615	-1335±40	-30.2	1988 ± 1
4.5	*Bulk*	1982 ± 10						
6.5	*Bulk*	1978 ± 11	*Sph*	^{14}C b.p.c.	ETH-28616	-3355±40	-30.0	1971 ± 1
7.5	*Bulk*	1973 ± 13						
8.5	*Bulk*	1967 ± 15	*Sph*	^{14}C b.p.c.	ETH-28617	-1735±40	-28.9	1982 ± 1
9.5	*Bulk*	1961 ± 18	*Sph*	^{14}C b.p.c.	ETH-28618	-3840±40	-28.9	1962 ± 1
10.5	*Bulk*	1954 ± 22	*Sph*	^{14}C b.p.c.	ETH-28619	-2540±40	-29.0	1962 ± 1
39.5			*Sph*	Convent. ^{14}C	ETH-28664	560±45	-25.2	1302-1370 (53%) 1381-1435 (47%)
59.5			*Sph*	Convent. ^{14}C	ETH-28665	830±45	-25.6	1055-1088 (6%) 1121-1139 (4%) 1156-1282 (88%)
69.5			*Sph*	Convent. ^{14}C	ETH-28666	875±45	-23.1	1038-1143 (45%) 1149-1255 (55%)

Table 1: Age dates of ^{210}Pb, ^{14}C bomb pulse curve and conventional ^{14}C of the HJ, Out and Har core obtained from bulk peat samples and macrofossils. *Sph*: *Sphagnum* species

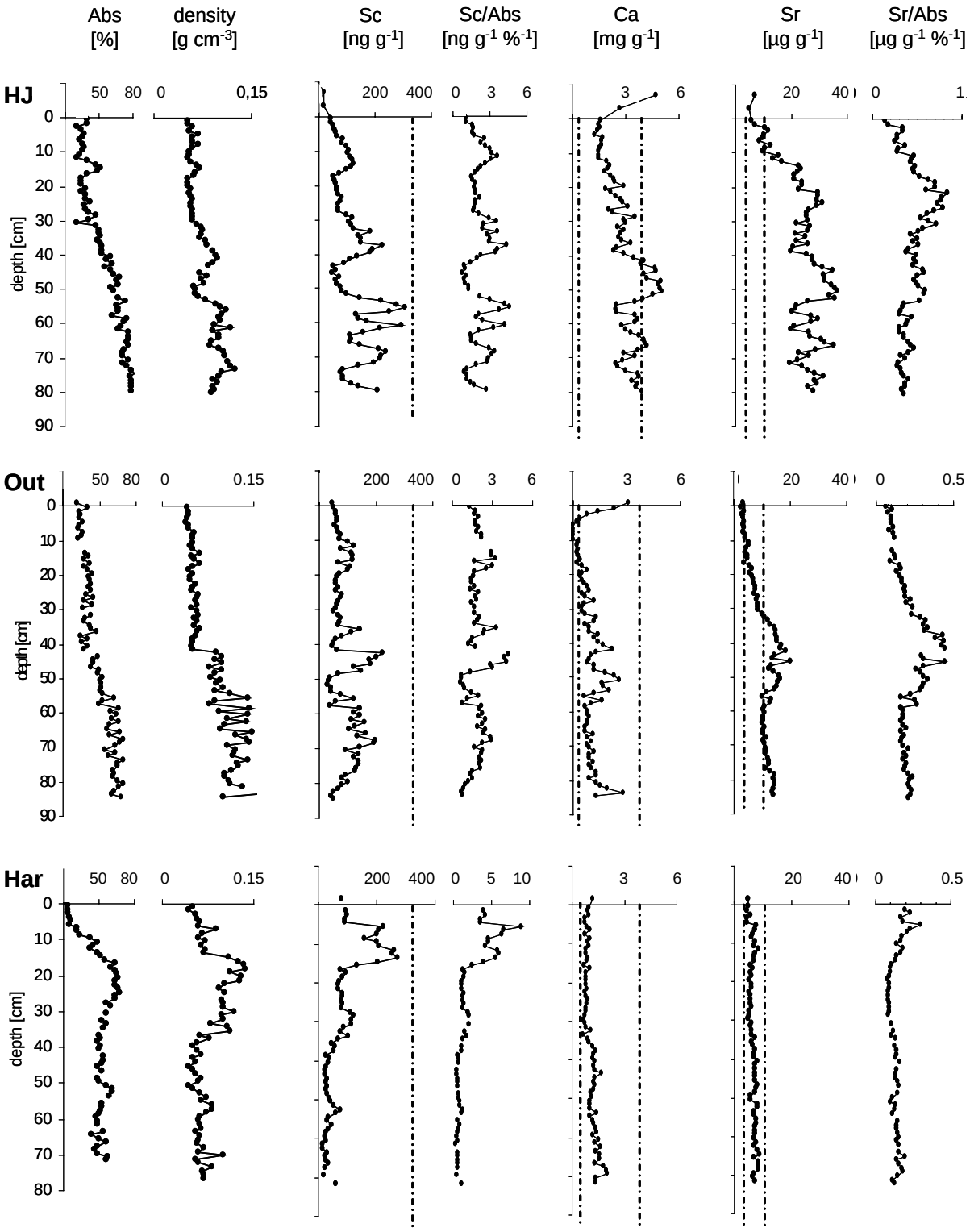

FIGURE 3. Depth profiles of absorption, density, Sc, Sc/absorption, Ca, Sr, Sr/absorption for HJ, Out and Har. Dashed lines indicate typical values of ombrotrophic bogs from Switzerland.

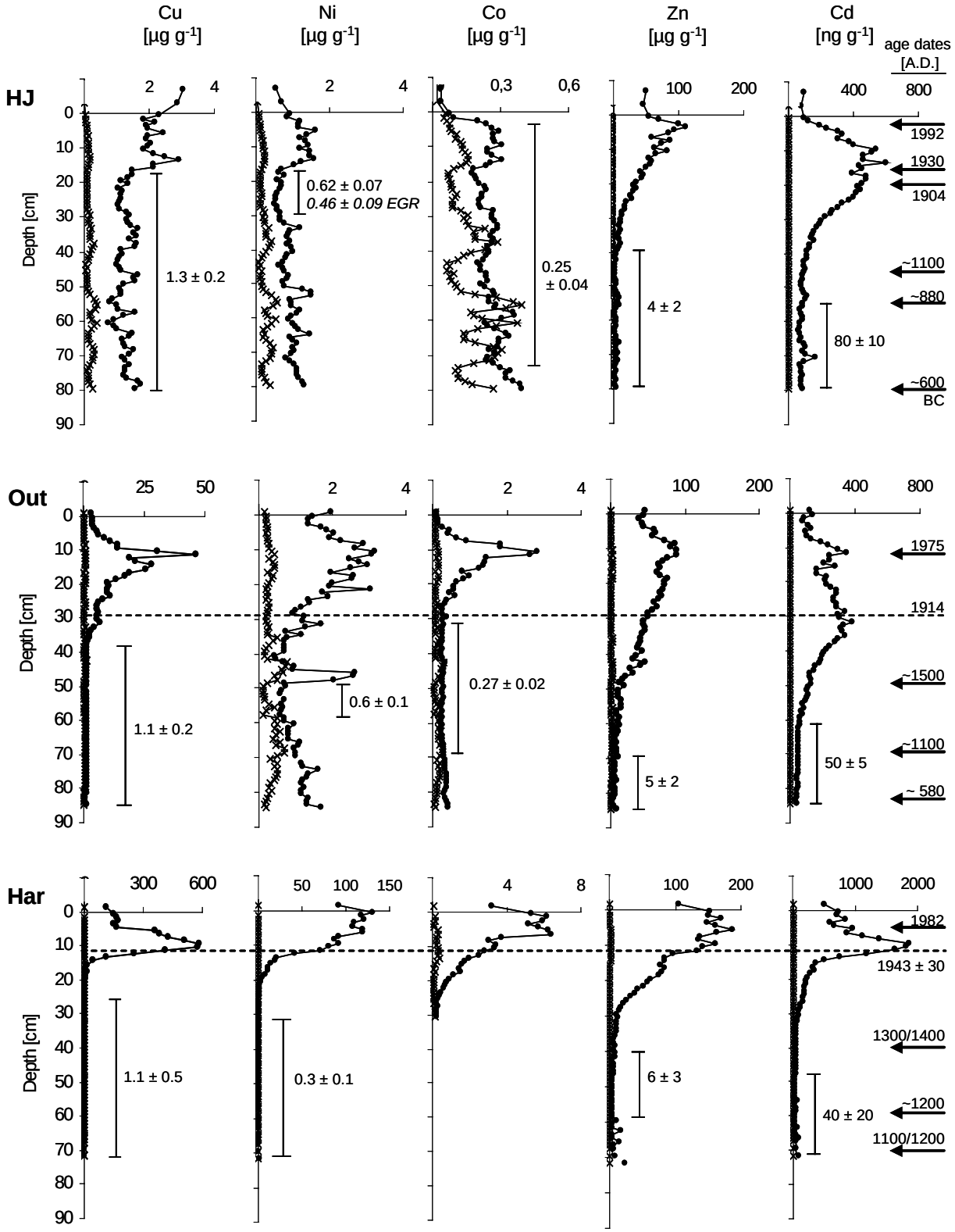

FIGURE 4. Concentrations of Cu, Ni, Co, Zn and Cd (solid dots), and calculated concentrations of lithogenic Cu, Ni, Co, Zn and Cd concentrations (crosses) at the HJ, Out and Har cores. For layers of constant metal concentrations, mean values are given. The horizontal dashed line refers to the onset of mining (Out) and smelting (Har), as derived from the ^{210}Pb chronologies.

Results and Discussion

Evaluation of ^{210}Pb age dating. Activities of unsupported ^{210}Pb decline toward zero below approximately 40 cm in the Out core, and below approximately 15 and 25 cm at Har and HJ core, respectively (Figure 2). Due to the lower activities of unsupported ^{210}Pb and the greater variations in density, the mathematical error in the ^{210}Pb ages is higher for the Har samples (± 6 to 75 years for the last century) than for the Out (± 3 to 30 years) and HJ (± 1 to 8 years) samples. The ^{210}Pb activities were determined in bulk peat samples which are representative of the entire peat slice which is 1 cm thick [26]. In contrast, the age dates obtained using the b.p.c. of ^{14}C requires a measurement of the percent modern carbon (PMC), relative to A.D. 1950, in a single plant macrofossil which has been removed from the peat slice and weighs but a few mg. A plant macrofossil which was obtained toward the top of the peat slice might have an age younger than the average ^{210}Pb age, and one taken near the bottom of the slice an older age, depending on the length of time represented by the slice. Good agreement between the two dating methods means that the ^{14}C age falls within the range of ^{210}Pb age and this should be the case if the macrofossil was obtained from the centre of the plug removed from the slice for subsampling. Good agreement is found in the HJ and Out samples (Table 1). Due to the greater error of the ^{210}Pb dating of the Har samples, the ^{14}C AMS b.p.c. age dates generally fall within the range of ^{210}Pb dates, too, although some samples show a high bias to the ^{14}C b.p.c. age. However, the samples in ten and eleven cm depth have similar ^{14}C b.p.c. age dates, suggesting that macrofossils may not have originated from the centre of these slices. Additionally, the ^{14}C b.p.c. age of the sample from 9 cm is much older than the overlying sample. In the peat core at Har, therefore, although the ^{14}C b.p.c. dates do not constrain the ^{210}Pb ages, this reflects sub-sampling difficulties rather than a problem with the age dates themselves. Because the ^{210}Pb age dates are consistent with the ^{14}C b.p.c. (HJ, Out), and because they were obtained using bulk samples representing the entire peat slice, all dates referred to in the text are those obtained using ^{210}Pb.

Peat accumulation. Age dating using ^{210}Pb allows continuous dating of peat layers accumulated within the last 150 years thereby allowing the age-depth-relationship of the core to be reconstructed (Figure 1) and yielding the accumulation rates of the elements of interest. The age-depth models show that peat accumulation is non-linear. Moreover, bogs which are situated close together, such as HJ and Out may exhibit very different growth rates.

Regarding the last 100 years, growth rates are low at Har (0.15 cm yr^{-1}), compared to Out (0.32 cm yr^{-1}) and HJ (0.22 cm yr^{-1}). If the last 1000 years are considered using calibrated ^{14}C age dates (Table 1), greater growth rates are found at Har and Out (0.080 cm yr^{-1}) than at HJ (0.057 cm yr^{-1}). These differences highlight the importance of detailed age dating for each peat core. The HJ core covers a much longer time period (until ~ 630 B.C.) than either the Har or Out cores (until ~ 1100 A.D.).

Trophic status of the cores. Given that the thickness of the ombrotrophic peat layer depends to some extent on the overall depth of the peat deposit as well as the mineralogical composition of the underlying substrate, the possible importance of trace metal migration into the peat profile from mineral weathering at the peat-sediment interface needs to be considered. Calcium and Sr are two of the most dynamic elements in peat in the sense that they are readily supplied to the porewaters in the basal peat layer from mineral weathering, and because they will rapidly diffuse upward into the peat column from that interface [1,35]. The concentrations of Ca found in all three peat cores are well within the range reported for continental ombrotrophic peat bogs (Figure 3). At Har, the Sr concentrations are typically between 6 and 8 µg g^{-1} which are similar to the average value for Sr (7 µg g^{-1}) at a continental, ombrotrophic peat bog in Switzerland (EGR). At HJ and Out the values in the surface layers are comparable with the values from EGR,

but somewhat higher below 10 and 30 cm, respectively. However, the Sr concentrations normalized to absorbance are constant below 30 cm which shows that variations in dust deposition and decay of organic matter, not upward migration from basal sediments, control the Sr concentration profile.

Natural "background" concentrations. The HJ site is situated within a National Park in an area which is mainly forested, which further reduces emissions of local soil dust. Furthermore, the HJ core includes very old peat layers (up to 630 B.C. cal. ^{14}C yrs), which pre-date anthropogenic contributions from long range transport. For these reasons, the HJ core is well suited to determine the natural "mean regional background" concentrations (MRB) for metals in these peat bogs. In fact, the constantly low concentrations of Cu, Co, Cd and Zn in the deeper layers of the HJ core provide the following MRB values (µg g^{-1}): Cu 1.3 ± 0.2 (n=62), Co 0.25 ± 0.04 (n=71), Cd 0.08 ± 0.01 (n=23), and Zn 4 ± 2 (n=40) (Figure 4). The Cu, Co, Cd and Zn concentrations in the deeper parts of both the Har and Out cores are constantly at these MRB values, which confirms that the MRB values presented here are representative for Southern Finland. Furthermore, in the aforementioned peat bog EGR from Switzerland, the lowest Cu, Co, Cd and Zn concentrations are in good agreement with the Finnish MRB values [10], which suggests that they might have an even broader validity. In contrast, Ni concentrations slightly increase downwards in the HJ profile, so that reliable MRBs could not be calculated. However, the lowest Ni concentrations found in very old (> 5320 ^{14}C yr B.P.) layers of the Swiss peat bog average 0.46 ± 0.09 µg g^{-1} Ni (n=18) [15]. This value fits very well with the lowest concentrations of Ni found in the middle part of the HJ core and is used here for the MRB value.

Enrichment of Cu, Ni, Co, Zn and Cd in upper peat layers. The greatest concentrations of all metals of interest are found within the upper layers of the Har core (Figure 4), corresponding to the beginning of smelting activity (1945). Peaks of Cu and Cd concentrations occur in layers slightly below those of Ni, Co and Zn. At the Out site, elevated concentrations are found in layers corresponding to mining activities, with sharp, distinct peaks for Cu and Co. In contrast, Ni, Zn and Cd show broad peaks, and even though these elements are strongly enriched in the Out ores (Table 2), their maximum values at best slightly exceed the maximum concentrations at HJ. At the HJ site, Cu and Ni are slightly enriched (1.9 and 3.5 times, respectively) in the uppermost peat layers compared to MRB values, while Cd and Zn are enriched up to 7 and 28 times in the upper part of the core.

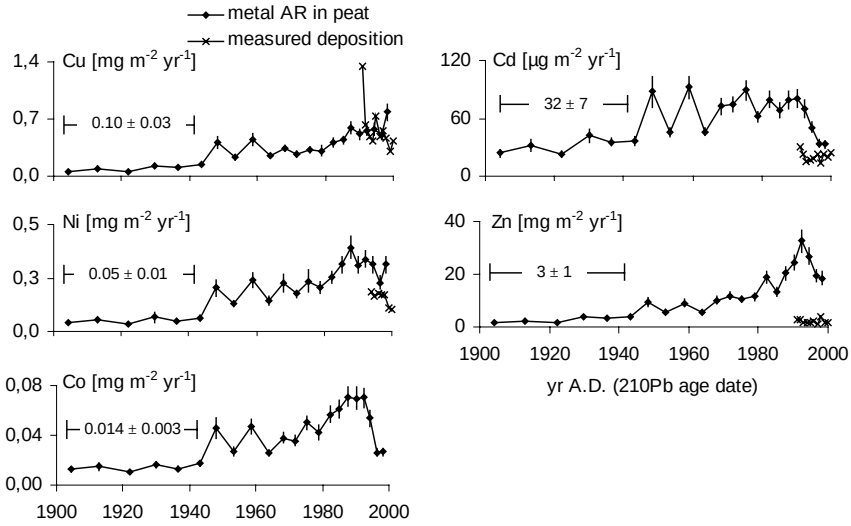

FIGURE 5. ARs of Cu, Ni, Co, Zn and Cd in peat (HJ) and atmospheric bulk deposition (wet+dry) at open area as monitored at HJ.

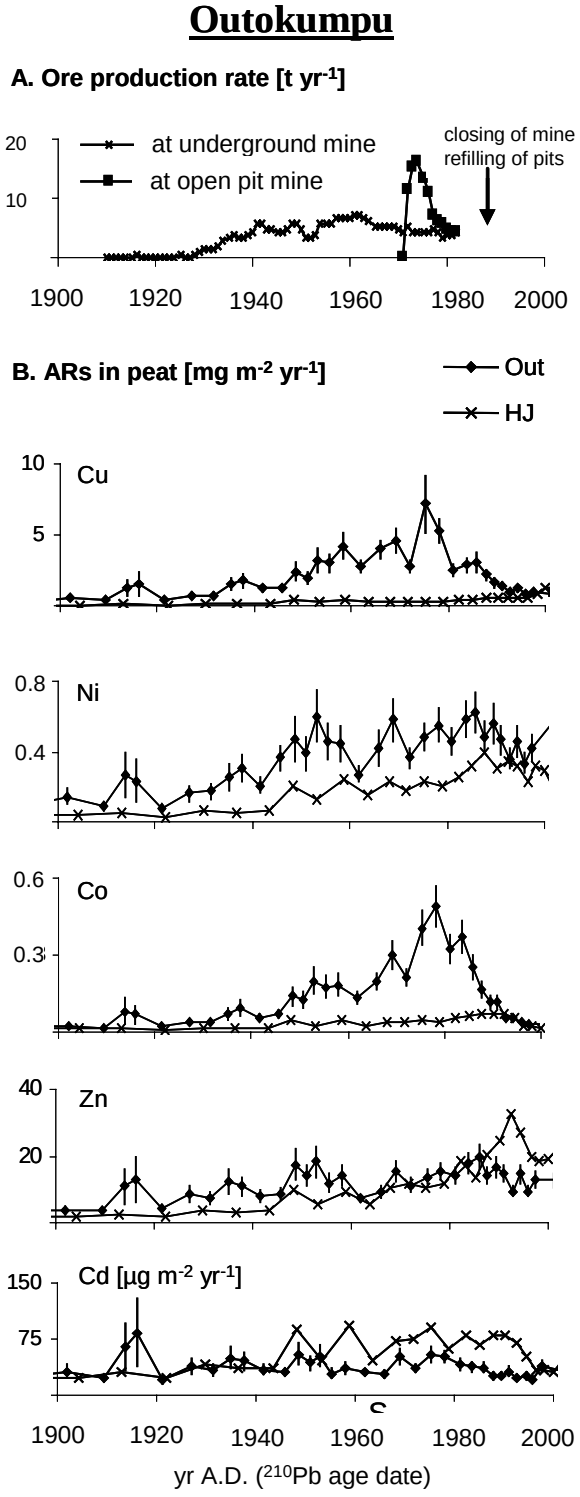

FIGURE 6. A. Ore production rates at the Outokumpu mines. B. ARs of Cu, Ni, Co, Zn and Cd in peat.

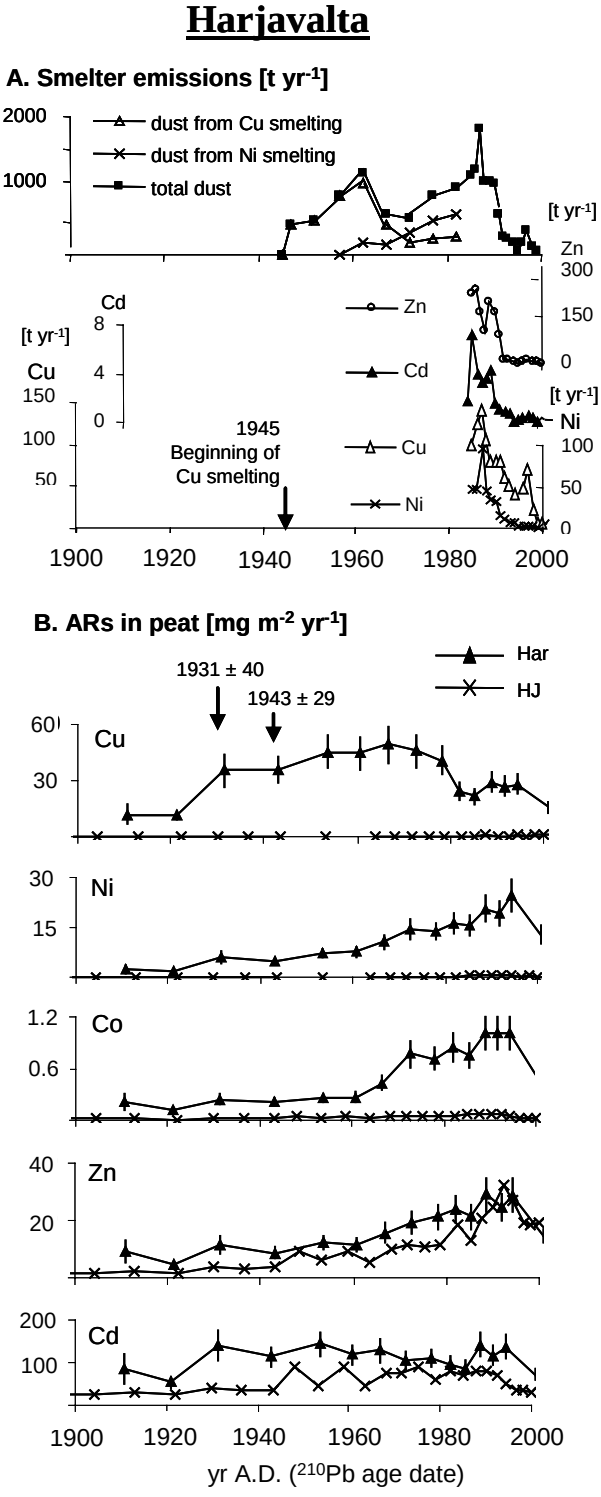

FIGURE 7. A. Emissions at the Harjavalta smelter. B. ARs of Cu, Ni, Co, Zn and Cd in peat. See text for explanations.

Influence of mineral matter abundance on the trace metal distribution. The concentration of Sc can be taken as an indicator of the abundance of mineral material in the peat cores, consisting mainly of silicates and derived primarily from atmospheric soil dust [1]. Assuming that for pre-industrial times the input of natural soil dust determines the Cu, Ni, Co, Zn and Cd distribution, the "lithogenic" fraction of these metals can be estimated using the product of Sc concentrations and the metal/Sc ratio of the natural dust. As there are strong regional differences in the "soil dust" composition between the three sites, the metal/Sc ratios of local tills [36] were taken instead of average crustal values. However, the lithogenic fractions at most account for ca. 50% of total Co, 40% of Ni, 20% of Zn, 15% of Cu, and <1% of Cd in the pre-industrial layers of the HJ core (Figure 4); in peat layers below 50 cm (> 880 A.D.), the profiles of lithogenic and total metals are more similar. Similar results were found by Erisman [37], who showed that in remote areas, Cu is predominantly deposited in dissolved form (88% of total deposition), while Ni is mainly deposited as solid particles (62%). Therefore, either there are other significant natural sources of these metals, or the dust inputs have varied in composition with time.

Influence of organic matter decay on the trace metal distribution. In the cores from HJ and Out, the peat layers where trace metals are most enriched (Figure 4) are poorly decomposed (Figure 2). At Har, too, the greatest absorbance values clearly underlie the peaks in metal concentration. Therefore, the decomposition of organic matter, which would lead to a relative enrichment of solid particles due to mass loss, cannot explain the variations in trace metals concentrations. We note further that peat density and absorbance profiles show similar variations. Peat density therefore compensates for variations in the degree of humification of the peats when calculating metal accumulation rates.

Influence of deposition history on the trace metal distribution. If the elements are retained by the peat column, subsequent to their deposition, the elevated concentrations in the upper peat layers should reflect increases in rates of atmospheric supply. In fact, if the elements are well preserved in the profiles and if the cores are accurately age dated, then the chronology of accumulation of these elements should match the chronology of their emissions. As noted earlier, atmospheric deposition has been monitored at the low-background site HJ for some time, and the emissions of metals from the Out mine and the Harjavalta smelter can be reconstructed from historical records of mining and smelting. The metal accumulation rates (ARs) for the upper peat layers can be calculated using the product of metal concentration and peat accumulation rate of each sample [4]. The precision of the ARs is calculated by error propagation of mass accumulation rates of peat and of metal concentrations (standard deviation of double digestions). Moreover, the use of ARs instead of absolute concentrations or enrichment factors allows direct comparisons between the cores, as differences in peat growth rate and density (humification) are taken into account.

	UCC* $\mu g\ g^{-1}$	Outokumpu ore† wt-%	Vuonos Cu ore‡ wt-%	Vuonos Ni ore‡ wt-%	Harjavalta emissions§ t $year^{-1}$
Cu	25	3.8	2.45	0.07	6-140
Ni	56	0.1	0.13	0.33	0.6-96
Co	24	0.2	0.16	0.05	n.a.
Cd	0.1	n.a.	n.a.	n.a.	0.02-7.1
Zn	65	0.8	1.6	0.06	0.9-232

* after [38]; † after [39];‡ after [40]; § range of annual emissions for the period 1985 to 1999 [20]; n.a. no data available

TABLE 2. Characterization of the Upper Continental Crust (UCC) and of main sources of trace elements at Outokumpu and Harjavalta

.**Metal accumulation rate vs. deposition history at Hietajärvi.** Copper, Ni, and Co ARs were low at the beginning of the 19th century, and increased considerably from ~1945 onwards (Figure 5). The greatest ARs of all metals of interest occur during the 1990s, except Cd which has elevated ARs since 1968. Monitoring of annual bulk deposition only started in 1990 in the vicinity of the coring site [41-50]. Prior to this, there were various possible trace metal sources for this area (including settlement, forest fires, paper and pulp production, as well as long range transport of pollutants. In the absence of deposition data prior to 1990, it is not possible to interpret the earlier part of the HJ record. However, the HJ record is a valuable reference site for comparison with the other sites (see below).

Monitored Cu deposition varies between 0.3 and 0.74 mg m^{-2} yr^{-1}, which is in good agreement with the Cu ARs for this period. Despite this, there is one outlier in measured Cu deposition (1.3 mg m^{-2} yr^{-1} in 1991) which doesn't fit with Cu ARs. Due to the limited monitoring data it is not possible to decide if this value is an outlier, or if it reflects a general trend of decreasing Cu deposition at this remote site. Accumulation rates of Ni slightly exceed the monitored deposition of these metals, suggesting that the deposition ra s (obtained by monitoring) may have underestimated the true inputs. Studies of Erisman [51] showed that the *effective* atmospheric deposition to a given ecosystem is strongly dependent on roughness and wetness of the surface. For example, living *Sphagnum* plants with their raised stems can effectively filter solid particles from the air stream, whereas bulk deposition samplers represent an aerodynamic obstacle causing wind streams to divert from the opening as well as creating turbulent flow. As Ni (and Co) seem to be mainly deposited as solid particles in remote areas (see above), effective deposition might be higher for these elements than for metals like Cu, which are predominantly deposited in dissolved form at remote sites [37]. The retention of Co in the peat layers cannot be assessed, as monitoring data for Co is lacking. Zinc ARs are decoupled from true deposition, suggesting that post-depositional processes are responsible for the distribution of Zn in peat, as suggested by others [8,10,12,14,16-18]. Cadmium ARs of uppermost samples are in the same range than monitored deposition; however, in deeper layers, Cd ARs were much greater. Although there are no deposition records available for comparison, monitoring studies based on forest mosses showed that Cd deposition from long-range transport was ca. 3 times higher in 1985 than in 2000 [52]; the decline in Cd AR at HJ is consistent with this trend.

Metal accumulation rate vs. emission history at Outokumpu. The area was fairly inaccessible until the discovery of the ore deposit lead to the foundation of the town of Outokumpu. Two different ore bodies can be distinguished: the Cu-rich "Outokumpu" ore body, which was excavated by means of a underground mine from 1912 to 1989, and the "Vuonos" ore body with two different ore types, mined between 1972 and 1982, both underground and by open pit [40,53]. These ore bodies not only differ from each other in their chemical composition (Table 2), but are also inhomogeneous. The ores were further processed by milling and concentrating, and tailings were stored in open waste heaps. During the first 20 years these tailings still contained considerable concentrations of metals due to an inefficient concentrator process; additionally, a test plant refined small amounts of Cu until 1929 [25]. All things considered, the ore production rate (Figure 6) is only an approximate guide to local metal emissions.

During the early years of the 20th century, ARs of Cu and Ni slightly exceed the ARs at HJ, while ARs of Co and Cd are similar to the low-background site (Figure 6). From 1931 ± 17 onwards, ARs of Cu and Co strongly increase, corresponding to the increasing production of Cu/Co rich ores at underground mines. The greatest ARs of Cu and Co occur in peat layers accumulated during the period of additional open pit mining (1975/78). The continuously decreasing Cu and Co ARs since 1986 ± 5 coincide with the decline of mining

industry since 1983, and subsequent re-filling of the open pit. In summary, the Cu and Co ARs obtained by the peat core provide an accurate reflection of the known history of production of these metals. Slight differences between Cu and Co ARs from 1975 ± 6 onwards could be due to the changeover to separate grinding grades for different ore types in 1977 [54]. Nickel ARs increase slightly with the beginning of the mining industry at the Outokumpu ore body. However, in contrast to Cu and Co, there is no peak resulting from open pit at Vuonos. This is even more remarkable considering that the ore of Vuonos contains three times more Ni than the Out ore. In addition, Ni ARs recorded by the Out core are twice that of the low-background site, while Cu and Co ARs are up to 23 and 10 times higher. Clearly, the Ni ARs obtained using the peat core are not an accurate reflection of the local Ni emission history. Zinc ARs are very similar to ARs at HJ, regarding both absolute values as well as the temporal trend. Therefore, the distribution of Zn seems to be more dependent on natural processes operating within the peat bog rather than the local deposition history. Similarly, Cd ARs do not reflect mining impacts, and overall variations in Cd ARs are small.

Metal accumulation rate vs. emission history at Harjavalta. At Harjavalta, a copper smelter has been operating since 1945 and a Ni smelter since 1959. From the beginning of smelting operations until 1984, estimations of dust emissions based on production data have been available [20]; since 1985, the company has monitored the emissions of Cu, Ni, Zn and Cd (Figure 7). Emissions from other metal and chemical industrial companies in the industrial area of Harjavalta or surrounding towns should be of minor importance compared to the substantial emissions from the smelter stack. The slag produced during smelting is stored in basins at the plant site. The granulated Ni slag (together with Cu slag until 1990), is piled in uncovered heaps and could act as an additional source of dust emission [19,20].

The Cu ARs are considerably enhanced from 1931 ± 40 to 1978 ± 11, and from 1989 ± 8 to 1994 ± 7. Despite the large uncertainties of the ^{210}Pb age dates of the Har core (see above), the ARs trace the high Cu emissions in the early years of smelting and in the late 1980s quite well (Figure 7). However, considering only the average values of ^{210}Pb age dates, the increase in Cu AR in "1931" pre-dates the true beginning of Cu smelting at Har in 1945 by approximately 14 years. However, the spatial difference between the sample accumulated in "1931" and the overlying sample accumulated in "1943" is only one centimeter. Therefore, the difference (14 yrs) between the increase in Cu ARs (peat) and the known beginning of smelting activity is a consequence of the great uncertainties in the ^{210}Pb age dates and the time-resolution between adjacent samples, rather than downward Cu migration. Similar to Cu, the timing of the beginning of increasing Ni ARs cannot be determined with sufficient reliability. Nickel ARs are enhanced during the early period of Cu smelting, probably due to the Ni impurities (together with Co and Zn) in the Cu concentrates used at the Harjavalta smelter [55]. With the beginning of Ni smelting, Ni ARs increase until a maximum value in 1994 ± 7. A similar shape in ARs is obtained for Co, implying that Co is enriched in Ni concentrates. In summary, Cu, Ni and Co reflect the general trends in deposition history. Zinc and Cd ARs do not reflect smelting impacts: Zn and Cd ARs at Har are similar to those at HJ.

Comparison of the three cores. Regarding peat samples pre-dating the beginning of smelting activity (1911/1920), ARs of Cu, Ni and Co are up to 120, 40 and 20 times greater at Har than at HJ and Out. Although the region around Har was settled and industrialized much earlier, the most likely reason for the elevated ARs are a slight downward migration of these metals, subsequent to their release from the smelter and deposition on the bog surface, in the range of a few centimeters (Figure 4). Cumulative metal inventories (see supplementary information) show, that the peat bog at Har has been severely impacted

by atmospheric Cu, Ni and Co contamination, with up to 60 (Cu), 30 (Ni) and 7 (Co) times greater inventories than at the low background site (HJ). In contrast, inventories of Zn and Cd at Har are only twice those of HJ. The cumulative inventory of the Ni, which is known to have a delaterious effect to lower plants such as mosses [56], has reached 0.9 g m^{-2} Ni at Har. Even though there has been some slight metal migration, most of the Ni is concentrated within the topmost 15 cm. It is not yet known what effect the high Ni input would have had in the ability of the bog to preserve a chronology of atmospheric metal deposition; however, this might explain the slight mobility of Cu and Co (together with Ni) at Har compared to the excellent retention of Cu and Co at Out and HJ, where the cumulative Ni inventory is <0.06 g m^{-2}.

Acknowledgments

Financial support was provided by the German Research Foundation (grant SH 89/1-1 to W.S. and M.K.) and the Finnish Forest Research Institute. We thank K. Taimi, K. Lyytikäinen, W. Roberts and L. Hirvisaari for their assistance in the field work, C. Scholz for help with ICP-OES measurements, H. Wild for the humification measurements, M. Väliranta and N. Schnyder for the macrofossil separations, P. Van der Knaap for additional help, and special thanks to H. Kempter and N. Givelet for very useful discussions.

REFERENCES

(1) Shotyk, W.; Weiss, D.; Kramers, J. D.; Frei, R.; Cheburkin, A. K.; Gloor, M.; Rees, S. Geochemistry of the peat bog at Etang de la Gruère, Jura Mountains, Switzerland, and its record of atmospheric Pb and lithogenic trace metals (Sc, Ti, Y, Zr, and REE) since 12,370 ^{14}C yr BP. *Geochim. Cosmochim. Acta* **2001**, *65*, 2337-2360.

(2) Vile, M. A.; Wieder, R. K.; Novak, M. Mobility of Pb in Sphagnum-derived peat. *Biogeochem.* **1999**, *45*.

(3) Weiss, D.; Shotyk, W.; Kramers, J. D.; Gloor, M. Sphagnum mosses as archives of recent and past atmospheric lead deposition in Switzerland. *Atmos. Environ.* **1999**, *33*, 3751-3763.

(4) Givelet, N.; Roos-Barraclough, F.; Shotyk, W. Predominant anthropogenic sources and rates of atmospheric mercury accumulation in southern Ontario recorded by peat cores from three bogs: comparison with natural "background" values (past 8000 years). *J. Environ. Monit.* **2003**, *5*, 935-949.

(5) Roos-Barraclough, F.; Shotyk, W. Millennial-scale records of atmospheric mercury deposition obtained from ombrotrophic and minerotrophic peatlands in the Swiss Jura Mountains. *Environ. Sci. Technol.* **2003**, *37*, 235-244.

(6) Benoit, J. M.; Fitzgerald, W. F.; Damman, A. W. H. The biogeochemistry of an ombrotrophic bog: evaluation of use as an archive of atmospheric mercury deposition. *Environ. Res. A* **1998**, *78*, 118-133.

(7) Pheiffer Madsen, P. Peat bog records of atmospheric mercury deposition. *Nature* **1981**, *293*, 127-130.

(8) Monna, F.; Petit, C.; Guillaumet, J.-P.; Jouffroy-Bapicot, I.; Blanchot, C.; Dominik, J.; Losno, R.; Richard, H.; Leveque, J.; Chateau, C. C. History and Environmental impact of mining activity in Celtic Aeduan Territory recorded in a peat bog (Morvan, France). *Environ. Sci. Technol.* **2004**, *38*, 665-673.

(9) Mighall, T. M.; Abrahams, P. W.; Grattan, J. P.; Hayes, D.; Timberlake, S.; Forsyth, S. Geochemical evidence for atmospheric pollution derived from prehistoric copper mining at Copa Hill, Cwmystwyth, mid-Wales, UK. *Sci. Tot. Environ.* **2002**, *292*, 69-80.

(10) Shotyk, W.; Krachler, M.; Martinez-Cortizas, A.; Cheburkin, A. K.; Emons, H. A peat bog record of natural, pre-anthropogenic enrichments of trace elements in atmospheric aerosols since 12,370 14C yr BP, and their variation with Holocene climate change. *Earth Planet. Sci. Lett.* **2002**, *199*, 21-37.

(11) Kettles, I. M.; Bonham-carter, G. F. Modelling dispersal of metals from a copper smelter at Rouyn-Noranda (Québec, Canada) using peatland data. *Geochem Expl. Environ. Anal.* **2002**, *2*, 99-110.

(12) MacKenzie, A. B.; Logan, E. M.; Cook, G. T.; Pulford, I. D. A historical record of atmospheric depositional fluxes of contaminants in west-central Scotland derived from an ombrotrophic peat core. *Sci. Tot. Environ.* **1998**, *222*, 157-166.

(13) Holynska, B.; Ostachowicz, B.; Ostachowicz, J.; Samek, L.; Wachniew, P.; Obidowicz, A.; Wobrauschek, P.; Streli, C.; Halmetschlager, G. Characterisation of 210Pb dated peat core by various X-ray fluorescence techniques. *Sci. Tot. Environ.* **1998**, *218*, 239-248.

(14) Livett, E. A.; Lee, J. A.; Tallis, J. H. Lead, zinc and copper analyses of British blanket peats. *J. Ecol.* **1979**, *67*, 865-891.

(15) Krachler, M.; Mohl, C.; Emons, H.; Shotyk, W. Atmospheric deposition of V, Cr, and Ni since the late glacial: Effects of climatic cycles, human impacts, and comparison with crustal abundances. *Environ. Sci. Technol.* **2003**, *37*, 2658-2667.

(16) Kempter, H.; Frenzel, B. The impact of early mining and smelting on the local tropospheric aerosol detected in ombrotrophic peat bogs in the Harz, Germany. *Water Air Soil Poll.* **2000**, *121*, 93-108.

(17) Espi, E.; Boutron, C. F.; Hong, S.; Pourchet, M.; Ferrari, C.; Shotyk, W.; Charlet, L. Changing

concentrations of Cu, Zn, Cd and Pb in a high altitude peat bog from Bolivia during the past three centuries. *Water Air Soil Poll.* **1997**, *100*, 289-296.
(18) Sugden, C. L.; Farmer, J. G.; MacKenzie, A. B. Isotopic ratios of lead in contemporary environmental materials from Scotland. *Environ Geochem Health* **1993**, *15*, 59-65.
(19) Ukonmaanaho, L.; Nieminen, T.; Rausch, N.; Shotyk, W. Heavy metal and arsenic profiles in ombrogenous peat cores from four differently loaded areas in Finland. *Water Air Soil Poll.* **2004**, *158*, 261-277.
(20) Nieminen, T. M.; Ukonmaanaho, L.; Shotyk, W. Enrichment of Cu, Ni, Zn, Pb and As in an ombrotrophic peat bog near a Cu-Ni smelter in southwest Finland. *Sci. Tot. Environ.* **2002**, *292*, 81-89.
(21) Jungner, H.; Sonninen, E.; Possnert, G.; Tolonen, K. Use of bomb-produced C-14 to evaluate the amount of CO_2 emanating from 2 peat bogs in Finland. *Radiocarbon* **1995**, *37*, 567–573.
(22) Shotyk, W.; Goodsite, M. E.; Roos-Barraclough, F.; Givelet, N.; Le Roux, G.; Weiss, D.; Cheburkin, A. K.; Knudsen, K.; Heinemeier, J.; Van der Knaap, W. O.; Norton, S. A.; Lohse, C. Accumulation rates and predominant atmospheric sources of natural and anthropogenic Hg and Pb on the Faroe Islands since 5420 ^{14}C yr BP recorded by a peat core from a blanket bog. *Geochim. Cosmochim. Acta* **2005**, *69*, 1-17.
(23) Shotyk, W.; Goodsite, M. E.; Roos-Barraclough, F.; Frei, R.; Heinemeier, J.; Asmund, G.; Lohse, C.; Hansen, T. S. Anthropogenic contributions to atmospheric Hg, Pb and As deposition recorded by peat cores from southern Greenland and Denmark dated using the ^{14}C "bomb pulse curve". *Geochim. Cosmochim. Acta* **2003**, *67*, 3991-4011.
(24) Ukonmaanaho, L.; Starr, M.; Mannio, J.; Ruoho-Airola, T. Heavy metal budgets for two headwater forested catchments in background areas of Finland. *Environ. Poll.* **2001**, *114*, 63-75.
(25) Kuisma, M. *Kuparikaivoksesta suuryhtiöksi, Outokumpu 1910-1985*; Forssan kirjapaino Oy: Forssa, 1985.
(26) Givelet, N.; Le Roux, G.; Cheburkin, A.; Chen, B.; Frank, J.; Goodsite, M. E.; Kempter, H.; Krachler, M.; Noernberg, T.; Rausch, N.; Rheinberger, S.; Roos-Barraclough, F.; Sapkota, A.; Scholz, C.; Shotyk, W. Suggested protocol for collecting, handling and preparing peat cores and peat samples for physical, chemical, mineralogical and isotopic analyses. *J. Environ. Monit.* **2004**, *6*, 481-492.
(27) Kempter, H.; Frenzel, B. Zur Bedeutung von ombrotrophen Mooren als Archive der atmosphärischen Deposition. *Telma* **1997**, *27*, 107-130.
(28) Appleby, P. G.; Oldfield, F. The calculation of lead-210 dates assuming a constant rate of supply of unsupported ^{210}Pb to the sediments. *Catena* **1978**, *5*, 1-8.
(29) Shore, J. S.; Bartley, D. D.; Harkness, D. D. *Quart. Sci. Rev.* **1995**, *14*, 373.
(30) Goodsite, M. E.; Rom, W.; Heinemeier, J.; Lange, T.; Ooi, S.; Appleby, P. G.; Shotyk, W.; van der Knaap, W. O.; Lohse, C.; Hansen, T. S. High-resolution AMS ^{14}C Dating of post-bomb peat archives of atmospheric pollutants. *Radiocarbon* **2001**, *43*, 453.
(31) Niklaus, T. R.; Bonani, G.; Simonius, M.; Suter, M.; Wolfli, W. CalibETH - an Interactive Computer-Program for the Calibration of Radiocarbon-Dates. *Radiocarbon* **1992**, *34*, 483-492.
(32) Cheburkin, A. K.; Shotyk, W. An energy-dispersive miniprobe multielement analyzer (EMMA) for direct analysis of Pb and other trace elements in peats. *Fresenius. J. Anal. Chem.* **1996**, *354*, 688-691.
(33) Cheburkin, A. K.; Shotyk, W. Energy-dispersive XRF spectrometer for Ti determination (TITAN). *X-Ray Spectrom.* **2005**, *34*, 73-79.
(34) Blackford, J. J.; Chambers, F. M. Determining the degree of peat decomposition for peat-based palaeoclimatic studies. *Int. Peat J.* **1993**, *5*, 7-24.
(35) Steinmann, P.; Shotyk, W. Chemical composition, pH, and redox state of sulfur and iron in complete vertical porewater profiles from two *Sphagnum* peat bogs, Jura Mountains, Switzerland. *Geochim. Cosmochim. Acta* **1997**, *61*, 1143-1163.
(36) Koljonen, T., Ed. *The Geochemical Atlas of Finland. Part 2: Till*; Geological Survey of Finland: Espoo, 1992.
(37) Erisman, J. W. *Towards development of a deposition monitoring network for air pollution in Europe*. National Institute of Public Health and the Environment, 1996.
(38) Leinonen, L.; Juntto, S. *Ilmanlaatumittauksia - Air quality measurements 1991*. Finnish Meteorological Institute, 1992.
(39) Leinonen, L. *Ilmanlaatumittauksia - Air quality measurements 1992*. Finnish Meteorological Institute, 1993.
(40) Leinonen, L. *Ilmanlaatumittauksia - Air quality measurements 1993*. Finnish Meteorological Institute, 1994.
(41) Leinonen, L. *Ilmanlaatumittauksia - Air quality measurements 1994*. Finnish Meteorological Institute, 1996.
(42) Leinonen, L. *Ilmanlaatumittauksia - Air quality measurements 1995*. Finnish Meteorological Institute, 1997.
(43) Leinonen, L. *Ilmanlaatumittauksia - Air quality measurements 1996*. Finnish Meteorological Institute, 1998.
(44) Leinonen, L. *Ilmanlaatumittauksia - Air quality measurements 1998*. Finnish Meteorological Institute, 1999.

(45)Leinonen, L. *Ilmanlaatumittauksia - Air quality measurements 1997*. Finnish Meteorological Institute, 1999.
(46)Leinonen, L. *Ilmanlaatumittauksia - Air quality measurements 1999*. Finnish Meteorological Institute, 2000.
(47)Leinonen, L. *Ilmanlaatumittauksia - Air quality measurements 2000*. Finnish Meteorological Institute, 2001.
(48)Erisman, J. W.; Mennen, M. G.; Fowler, D.; Flechard, C. R.; Spindler, G.; Grüner, A.; Duyzer, J. H.; Ruigrok, W.; Qyers, G. P. Deposition monitoring in Europe. *Environ. Monit. Assess.* **1998**, *53*, 279-295.
(49)Poikolainen, J.; Kubin, E.; Piispanen, J.; Karhu, J. Atmospheric heavy metal deposition in Finland during 1985-2000 using mosses as bioindicators. *Sci. Tot. Environ.* **2004**, *318*, 171-185.
(50)Parkkinen, J.; Reino, J. Nickel occurrences of the Outokumpu type at Vuonos and Keretti. *Bull. Geol. Survey Finland* **1985**, *333*, 178-188.
(51)Laznicka, P. *Precambrian empirical metallogeny - precambrian lithologic associations and metallic ores*; Elsevier Science Ltd: Amsterdam, 1993; Vol. 2 a.
(52)Kauppinen, H. Vuonoksen kuparimalmityypit ja rikastamon syötteet. Summary: The copper ore types and concentrator feeds in Vuonos. *Vuoriteollisuus* **1978**, *36*, 16-21.
(53)Pongrácz, E., Ed. *Proceedings of the Waste Minimization and Resources Use Optimization Conference*; Oulu University Press: Oulu, 2004.
(54)Tyler, G. *Critical concentrations of heavy metals in the mor horizon of Swedish forests*. Swedish Environmental Protection Agency, 1992.
(55)Wedepohl, K. H. The composition of the continental crust. *Geochim. Cosmochim. Acta* **1995**, *59*, 1217-1232.
(56)Mäkinen, E. Die Kupfererzlagerstätte Outokumpu in Finnland und ihre Verwertung. *Metall und Erz* **1938**, *2*, 25-33.

Mass accumulation rates [kg m^{-2} yr^{-1}]

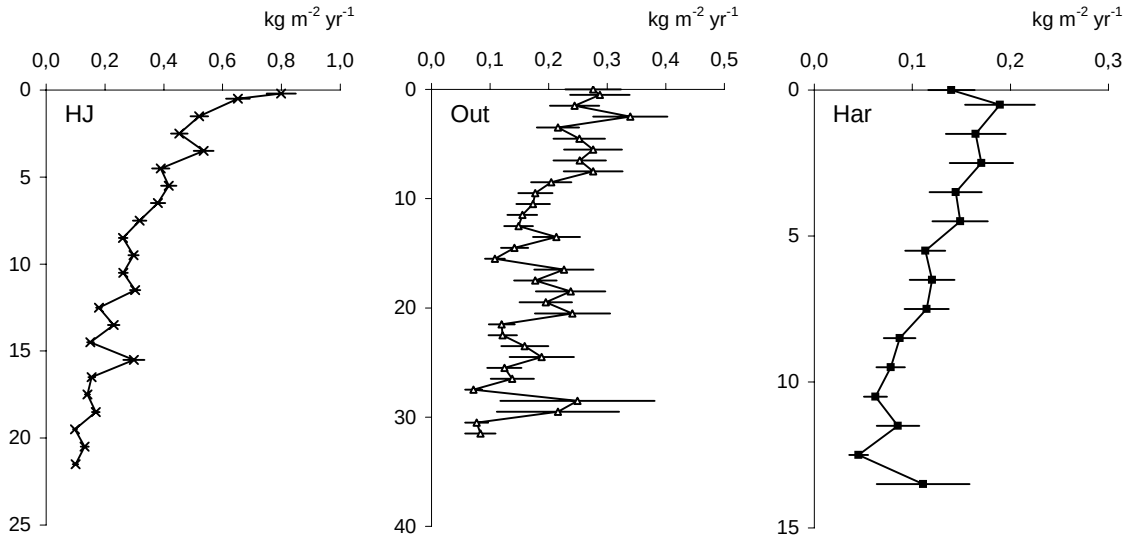

Cumulative metal inventory (peat layers accumulated since 1100 A.D.)

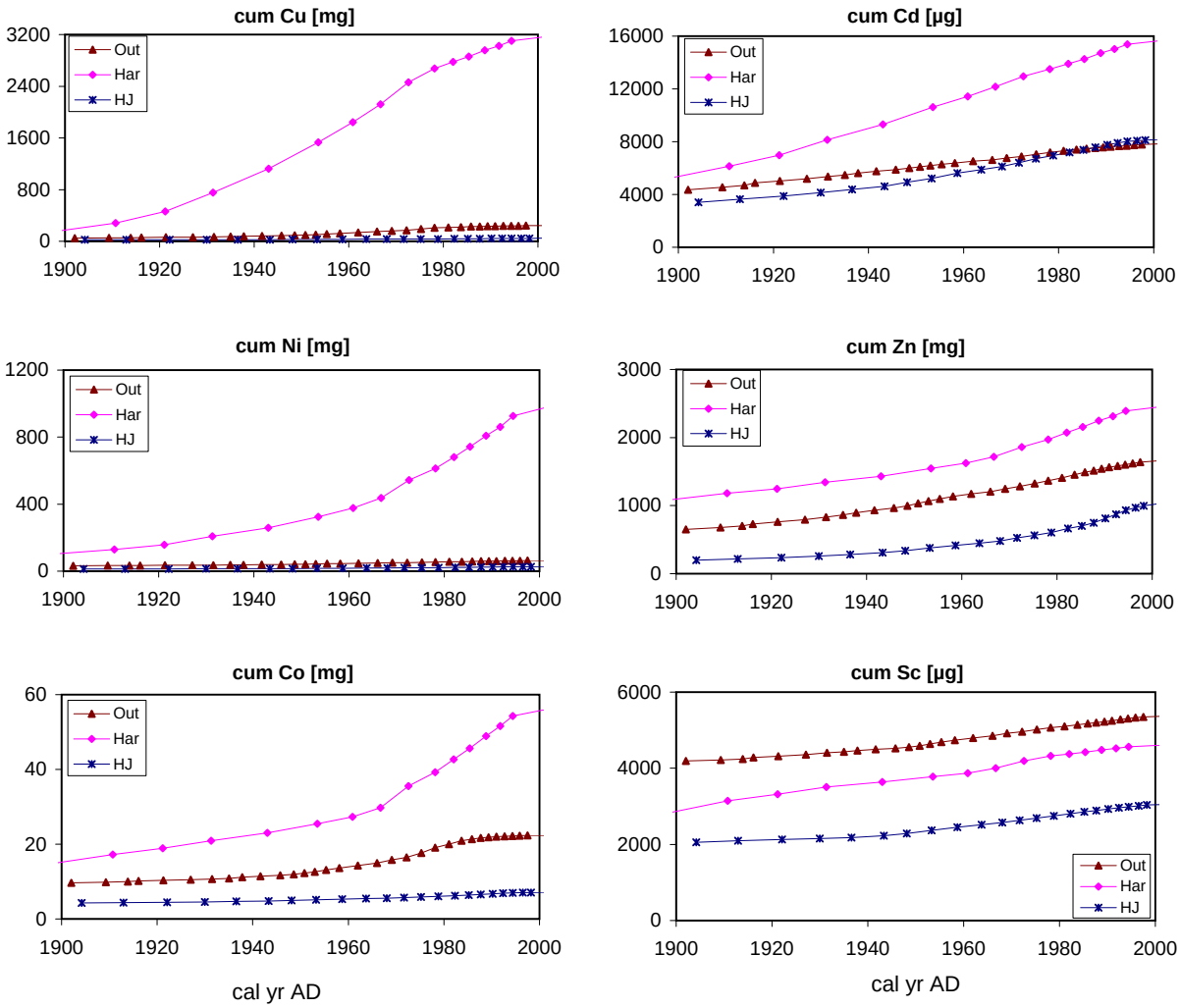

-Appendix 4-

Surface distribution of ^{137}Cs in the Kohlhütte Moor

Introduction and objectives

^{137}Cs is an artificial isotope emitted by nuclear accidents and nuclear weapon tests. ^{137}Cs has the insidious property of being mistaken for potassium, entering this way into the food chain and has an intermediate half-life of 30.2 years.

We investigated the ^{137}Cs distribution in the bog ecosystem using *Sphagnum* specimens collected at the surface of the bog.

Methods

On the 21st of October, we collected the 21st October 2002 along a transect in KM approximately every twenty meters a set of specimens of *Sphagnum Angustifolium* by hand using PET gloves. Each set of samples were sub-sampled as follows: each plant specimen was picked out of the set and cut individually across the stem into two parts : one visibly green ("living sample") and one brown (more decomposed, "dead part"). These samples were dried overnight at 105°C and then pulverised in a Ti-mill.

Samples were measured for ^{137}Cs (20 hours) using a low background gamma spectrometer. The instrument was calibrated using peat internal standards kindly given by Dr. Laurent Pourcelot (IRSN, CEA, Cadarache, France).

Results

First, the ^{137}Cs activity in the brown part is always lower than in the living part of the *Sphagnum* (Fig.1). Malmer (1988) shows that K was also enriched in the living Sphagnum because they is bio-recycling of K from the litter (i.e: plant uptake). Because ^{137}Cs has the same behaviour, it is obviously the cause of the enrichment of ^{137}Cs in the living part.

As illustrated by the figure 1, the ^{137}Cs in the Sphagnum decreases from the centre of the bog to the lagg.

Reference:

Malmer, N., 1988, Patterns in the growth and the accumulation in inorganic constituents in the Sphagnum cover on ombrotrophic bogs in Scandinavia: *Oikos*, **53**, 105-120

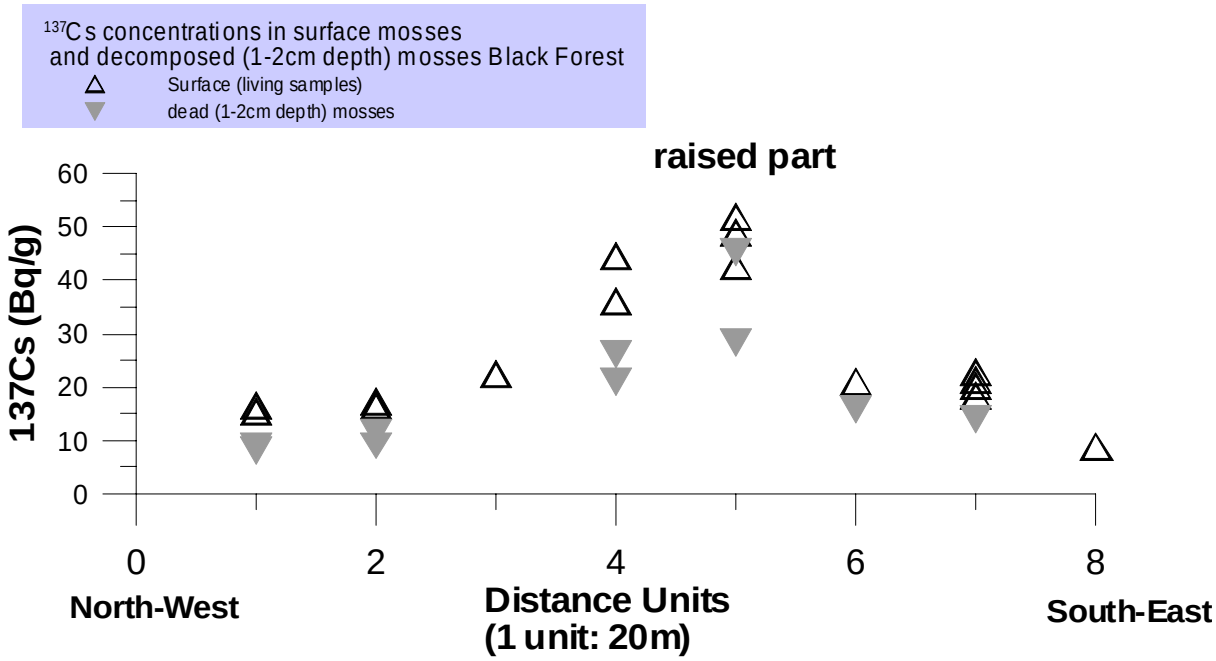

Figure 1: distribution of the ^{137}Cs activity in Sphagnum specimens along a transect NW-SE in KM

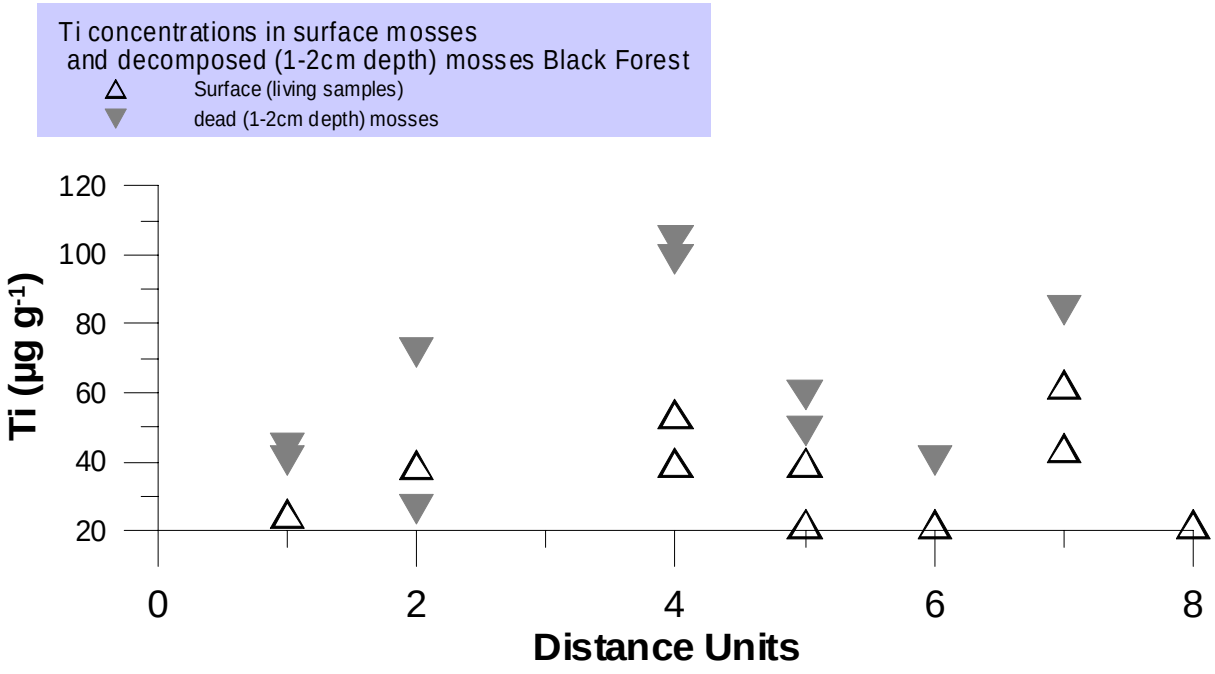

Figure 2: distribution of Ti in Sphagnum specimens along a transect NW-SE in KM

-Appendix 5-

Microbial distribution in the deeper layers of a peat bog

In collaboration with M. Gommeau (CEA, Cadarache)

Introduction and objectives

The aim of the study was to investigate the bacterial distribution in the deeper layers of Kohlhütte Moor.

Methods

Sub-samples from the Kohlhütte Moor peat profile were selected:

(1) one sample corresponding to a anoxic layer of peat (z = 4.75m)
(2) and one sample corresponding to the basal sediment layer (z = 5.75m).

The samples were sent frozen to Cadarache.

There, each sample was diluted with a KCl solution (8,5 g L^{-1}):

(1) Peat sample :79,8 mg in 720 µL KCl
(2) Sediment : 76,1 mg in 685 µL KCl.

After vortex mixing of the initial suspension (D0) and an additional 30 s to allow for particles to settle, successive tenfold dilutions were made in KCl (D1 to D5) without decantation.

For bacterial counts, Petri dishes containing tenfold-diluted Tryptic Soy Agar were divided in four sectors. Four repeats of each dilution were inoculated on the surface of the nutritive agar medium (40 µl). The plates were incubated for two days at 30°C before colonies were counted

For species determination, PCR (polymerase chain reaction) was performed using Hot GoldStar kit (EuroGenTec). For that, fragments of bacterial colonies was taken and homogenized in 200 µl of water. 3 µl was used as PCR template. The results were checked by electrophoresis using agarose gel stained with ethidium bromide.

Results

Different types of microbe morphology can be distinguished with the microscope or visible to the naked eye:

(1) for the peat, one “pink” morphotype accounts for most colony-forming units (~ $3.5\ 10^6$ $CFU \cdot g^{-1}$ of wet sediment). A minority of “yellow”colonies is present (8000 $CFU \cdot g^{-1}$);
(2) for the sediment, mainly a so-called “small white” ($1.8\ 10^6$ $CFU \cdot g^{-1}$ of wet peat) but also $4.1\ 10^5$ $CFU \cdot g^{-1}$ of “big white” and $2.3\ 10^4$ $CFU \cdot g^{-1}$ of “pink”.

At this time, only two bacterial species from the sediment are identified. The “pink” morphotype from the sediment belongs to the species *Methylobacterium fujisawaense*. The “big white” belongs to the genus *Mycobacterium* species *mucogenicum* or *Rhodesiae*.

Acknowledgements

Firstly I would like to thank **Bill Shotyk**, my PhD supervisor. His enthusiasm is and was always a source of new (re)motivation. He also improved the quality of the manuscripts by critical reading. Field trips with him in Germany, Switzerland and England were always "learning adventures", especially, the very long Lindow coring day…
My greatest thanks also to my co-supervisors: **Bernd Kober**, **Michael Krachler** and **Andriy Cheburkin**.
Thanks to Dominique Aubert, Peter Stille, Dominik Weiss, John Grattan, Emmanuel Laverret, Maxime Gommeau, Nicolas Givelet and Nicole Rausch: this work won't have been done without you!
A general Merci to all friends, colleagues and professors from the "archives" group, the Environmental Geochemistry and the Geosciences Faculty.
I would like to thank especially Stefan, Christian, Didi, Torsten, Tanja and Roswitha.
Merci à la French Connection et associés (Nico, Thierry, Dom´, Manu, Thomas, Fabio) pour leur soutien moral lors de soirées et voyages mémorables pas uniquement de labeur.
Merci à **Nicolas Givelet** pour son premier mail, il y a 4 ans me suggérant de contacter Bill et pour les discussions passionnées sur les tourbières.
Merci à **Dominique Aubert** pour le travail effectué ensemble, sa disponibilité malgré un projet de post-doc qui lui prenait tout son temps et son enthousiasme…
Ich danke auch Luca, Verena, Rahel, Anja, Anne und all meinen Freunde, die mich erlaubt haben, aus der Arbeit zu „flüchten".
Merci à ma famille pour leur soutien permanent, là-bas baignée dans les embruns...

Merci à **Amélie**.

Erklärung.

- Hiermit erkläre ich, Gaël Le Roux (geb. 03.02.1978 in Paris, Frankreich), an Eides statt, dass ich die vorlegte Dissertation selbst verfasst und mich dabei keiner anderen als der von mir ausdrücklich bezeichneten Quellen und Hilfen bedient habe.

- Ich, Gaël Le Roux (geb. 03.02.1978 in Paris, Frankreich), erkläre zudem an Eides statt, dass ich an keiner anderen Stelle ein Prüfungsverfahren beantragt habe, dass ich die Dissertation nicht in dieser Form oder anderer Form bereits anderweitig als Prüfungsarbeit verwendet habe und dass ich sie an keiner anderen Fakultät als Dissertation vorgelegt habe.

  Heidelberg, den 8.03.2005